Protein subcellular trafficking during the oxidative stress response in plants

Protein subcellular trafficking during the oxidative stress response in plants

Annelies Inzé

Annelies Inzé

PROMOTOR
Prof. Dr. Frank Van Breusegem

UNIVERSITEIT GENT
FWO VLAANDEREN
Plant Systems Biology

Ghent University
Faculty of Sciences
Department of Plant Biotechnology and Bioinformatics

Protein subcellular trafficking during the oxidative stress response in plants

Annelies Inzé

Thesis submitted in partial fulfillment of the requirements
for the degree of Doctor (Ph.D.) in Sciences, Biotechnology
Academic year: 2011-2012

Promoter:
Prof. Dr. Frank Van Breusegem

VIB Department of Plant Systems Biology
Oxidative Stress and Cell Death Group
Technologiepark 927, 9052, Belgium

This work was conducted in the department Plant Systems Biology of the Flanders Institute for Biotechnology (VIB).

This work was supported by funding from Fonds Wetenschappelijk Onderzoek – Vlaanderen (FWO).

Het langverwachte moment is aangebroken… Het schrijven van het allerlaatste deel van deze thesis: het dankwoord! Dit wil zeggen dat het einde van het doctoraat écht is aangebroken.

Vooreerst gaat mijn dank uit naar mijn promotor Frank om mij de kans te geven deel uit te maken van de Oxidatieve Stress en Celdood groep. Frank, bedankt voor het vertrouwen en alle kansen die je mij de afgelopen jaren geboden hebt.

Thanks to the members of the jury for reading the manuscript and for valuable comments. I would further like to thank Prof. Dr. Krupinska and Dr. Marc Bots for their enthusiasm and advice.

Mijn dank gaat uit naar alle voormalige en huidige leden van de Oxidatieve Stress en Celdood groep. Inge, je was een zeer fijne collega met wie ik met veel plezier samenwerkte. Bedankt voor de zeer goede vriendschap en jouw steun. Sandy, bedankt voor de vele nuttige tips, de hulp en de verbeteringen. Silke, bedankt voor de leuke babbels, jouw spontaniteit en humor zijn onvergetelijk! Brigitte en Michaël, bedankt voor de excellente technische ondersteuning. Verder wil ik alle andere groepsleden bedanken voor de leuke momenten samen.

Bedankt aan alle collega's van PSB, in het bijzonder iedereen van Support, Carine en Els voor de vele Arabidopsis transformaties, Griet en Stijn voor de maïs transformaties, Riet en Dana voor de zorgvuldige uitvoering van het IEM experiment en Evelien en Daniel voor het beantwoorden van mijn vele vragen over de confocale microscoop.

Bedankt Astrid, je bent in eerste plaats een zeer goede vriendin bij wie ik alles kwijtkan. We hebben al heel wat biotechnologische wateren doorzwommen! Bedankt voor alle steun, de goede gesprekken, kortom voor een goede vriendin te zijn.

Verder gaat mijn dank ook uit naar Prof. Dr. Bruno Cammue en Dr. Janick Mathys van de Universiteit Leuven. Bedankt voor jullie interesse, expertise en uitstekende samenwerking. Delphine, ik vond het zeer leuk om met jou samen te werken hier in Gent!

Verder wil ik mijn familie ontzettend bedanken voor hun onvoorwaardelijke steun en vertrouwen. Lieve ouders, bedankt dat ik steeds op jullie kon rekenen en dat jullie altijd voor me klaarstonden. Jullie hebben me altijd gesteund en steeds aangemoedigd om in mezelf te geloven. Papa, jouw gedrevenheid en passie voor wetenschap zijn absoluut bewonderenswaardig! Bedankt aan mijn broer Andries, samen met Kim, voor de vriendschap en de vele plezierige ontspanningsavonden.

Ten laatste wil ik mijn lieve man Koen bedanken. Jouw steun, luisterend oor maar vooral je liefde waren onmisbaar tijdens dit doctoraat! Ook bedankt voor het maken van de cover en steeds voor me klaar te staan als Word me weer in de steek gelaten had. Maar vooral om er steeds voor me te zijn, ik dank je voor alles en nog veel meer!

Annelies

Exam Commission

Prof. Dr. Ann Depicker (Chair)

Faculty of Sciences, Department of Plant Biotechnology and Bioinformatics, Ghent University

Prof. Dr. Frank Van Breusegem (Promoter)

Faculty of Sciences, Department of Plant Biotechnology and Bioinformatics, Ghent University

Prof. Dr. Karin Krupinska[*]

Botanisches Insitut und Botanischer Garten, Abt. Biologie der Planzenzelle, Christian-Albrechts-Universität zu Kiel

Prof. Dr. Bruno Cammue

Centre of Microbial and Plant Genetics, K.U. Leuven

Prof. Dr. Monica Höfte[*]

Faculty of Bioscience Engineering, Department of Crop Protection, Ghent University

Prof. Dr. Geert De Jaeger

Faculty of Sciences, Department of Plant Biotechnology and Bioinformatics, Ghent University

Prof. Dr. Alain Goossens[*]

Faculty of Sciences, Department of Plant Biotechnology and Bioinformatics, Ghent University

Dr. Daniel Van Damme[*]

Faculty of Sciences, Department of Plant Biotechnology and Bioinformatics, Ghent University

Dr. Marc Bots

Bayer BioScience N.V., Ghent, Belgium

[*] Members of the reading committee

Table of Contents

List of Abbreviations

ABA	abscisic acid
ABRE	ABA response element
AGI	Arabidopsis Genome Initiative
AMP	antimicrobial peptide
AOX	alternative oxidase
APX	ascorbate peroxidase
At	*Arabidopsis thaliana*
BLAST	basic local alignment search tool
bp	base pair
BTH	benzothiadiazole
CaMV	cauliflower mosaic virus
CAT	catalase
CDS	coding sequence
cDNA	complementary DNA
Col	*Arabidopsis thaliana* Columbia ecotype
CRF	cytokinin response factor
cTP	chloroplast targeting peptide
DNA	deoxyribonucleic acid
dpi	days post inoculation
ER	endoplasmatic reticulum
ERF	ethylene response factor
ET	ethylene
ETC	electron transport chain
FC	fold change
GA	gibberellic acid
gDNA	genomic DNA
GFP	green fluorescent protein
GO	gene ontology
GUS	β-glucuronidase
HIG	hydrogen peroxide-induced gene
HL	high light
H_2O_2	hydrogen peroxide
HR	hypersensitive response
HS	heat shock
HSF	heat shock transcription factor
HSG	heat shock granule
HSP	heat shock protein
HSR	heat shock response
JA	jasmonic acid
kb	kilobase
kDa	kilodalton

KO	knock-out
LTP	lipid-transfer protein
LRR	leucine-rich repeat
MAPK	mitogen-activated protein kinase
MeJA	methyl jasmonate
MV	methyl viologen
mRNA	messenger RNA
mTP	mitochondrial targeting peptide
NAC	No Apical Meristem, Arabidopsis ATAF1/2 and CUC
NADPH	nicotinamide adenine dinuclotide phosphate
NES	nuclear export signal
NLS	nuclear localization signal
NTL	NAC WITH TRANSMEMBRANE MOTIF1-LIKE
$^1O_2$	singlet oxygen
$O_2^{\bullet-}$	superoxide radical
OE	overexpression
$OH^{\bullet}$	hydroxyl radical
ORF	open reading frame
PA	proteome analyst
PCR	polymerase chain reaction
PDF	plant defensin
PR	pathogenesis-related
PS	photosystem
qRT-PCR	quantitative reverse transcriptase-PCR
RIP	regulated intramembrane proteolysis
RNA	ribonucleic acid
ROS	reactive oxygen species
SA	salicylic acid
SE	standard error
SOD	superoxide dismutase
TAIR	The Arabidopsis Information Resource
T-DNA	transfer-DNA
WT	wild type
ZF	Zinc Finger

SCOPE AND OBJECTIVES

Due to their sessile lifestyle, plants are permanently exposed to a variety of adverse environmental conditions leading to the accumulation of reactive oxygen species (ROS). Although initially considered as harmful byproducts of aerobic metabolism reacting in high concentrations with all cellular components, ROS are generally accepted as key signaling molecules that coordinate a broad range of environmental and developmental processes.

At the beginning of my Ph.D., significant progress has been made in the description of oxidative stress-dependent gene expression, but the regulation of the complex ROS signal transduction network remains largely unknown. The functional analysis of proteins that are encoded by genes that rapidly respond to ROS can therefore give novel insights into the early signaling steps triggered by a sudden increase in intracellular ROS. During adverse environmental conditions, the regulation of dynamic protein trafficking is an important intracellular signaling strategy to elicit a fast defense response. The aim of this project was to identify and characterize proteins that relocalize during oxidative stress. Therefore, we first made a comprehensive inventory of hydrogen peroxide (H_2O_2)-induced genes by comparing H_2O_2-related expression data sets and selected in a well-considered manner 85 candidate genes for further functional studies. We focussed our selection on genes encoding transcription factors and proteins of unknown function. To identify proteins with a potential dynamic behaviour during oxidative stress, we employed two medium-throughput localization screens of green fluorescent protein (GFP)-tagged proteins by transient expression in *Nicotiana benthamiana* and by stable expression in transgenic *Arabidopsis thaliana* lines. Transgenic *Arabidopsis* plants with perturbed levels of interesting candidate genes were assayed for altered tolerance to abiotic and biotic stress. The identification of proteins that dynamically relocalize during stress conditions, together with a detailed understanding of the mechanisms behind the identified oxidative stress-induced relocalizations, will provide a better understanding of stress response signaling.

Part I

Protein subcellular trafficking during the oxidative stress response in plants

1

Dynamic protein trafficking during the oxidative stress response in plants

Annelies Inzé and Frank Van Breusegem

AUTHOR CONTRIBUTIONS

A.I. wrote the manuscript with help of F.V.B and S.V.

ABSTRACT

The regulation of signal transduction is highly dynamic over time and space and involves active trafficking of signaling components. Adverse environmental conditions influence the spatiotemporal dynamics of proteins in which the tightly regulated production of reactive oxygen species (ROS) at different subcellular compartments plays a key role. During biotic and abiotic stresses, oxidative stress-induced protein relocalizations are an important intracellular signaling strategy that neither requires transcription nor translation steps, allowing a fast initiation of the stress response. Several mechanisms that affect protein subcellular trafficking under oxidative stress have been described. Together with the understanding of the tight regulation of ROS homeostasis, abiotic stress-triggered relocalizations of signal transduction components can provide more insights into how ROS are perceived, transduced and how they eventually activate the appropriate response.

INTRODUCTION

Although reactive oxygen species (ROS) were initially considered as toxic byproducts of aerobic metabolism, it is now generally accepted that ROS are key signaling molecules (Apel and Hirt, 2004). ROS are continuously produced at sites with a high metabolic rate or intense electron flow, such as mitochondria, chloroplasts and peroxisomes, by the excitation or incomplete reduction of molecular dioxygen (O_2) (Box 1). To control steady-state levels of ROS, plants have evolved a complex gene network encoding both ROS-producing and ROS-scavenging enzymes. The different components of this antioxidant system are diversified in their scavenging capacity not only in terms of specificity and affinity towards the different ROS species, but also by their distinct subcellular location in the vicinity of ROS production sites (Mittler *et al.*, 2004). Hence, the fine-tuned balance between ROS production and ROS-scavenging enabled plants to highly control ROS levels and to use ROS as signaling molecules in the control and regulation of different biological processes, such as defense responses and cell death (Apel and Hirt, 2004; Gadjev *et al.*, 2006; Van Breusegem and Dat, 2006). During abiotic stress conditions, ROS homeostasis is perturbed leading to a sudden increase in intracellular ROS which can cause significant cellular damage at high concentrations, but can initiate defense responses by controlling gene expression at low concentrations (Suzuki *et al.*, 2011a). Importantly, the subcellular location of ROS signals is tightly controlled and limited to certain subcellular compartments (i.e. cytosol, chloroplasts, mitochondria and peroxisomes) or areas (apoplast) by both compartment-specific non-enzymatic antioxidants and by the ROS gene network enzymes, making ROS accumulation highly specific but also very complex (Mittler *et al.*, 2011). Previous studies have illustrated that the chemical identity of ROS, the signal intensity and their subcellular production sites greatly influence the type of response (Gadjev *et al.*, 2006; Gechev *et al.*, 2006). The generation of mutants lacking important compartment-specific ROS-scavenging enzymes, the identification of the conditional fluorescent (*flu*) mutant and treatments with ROS-generating agents have tremendously increased our knowledge about ROS-specific signaling (Gadjev *et al.*, 2006).

There has been much debate on how a ROS signal can be specific for a certain stimulus (Mittler *et al.*, 2011). One possible explanation is that each cellular (sub)compartment could have its own set of receptors that directly perceive stress-induced ROS that, in turn, can convey the signal through other signaling networks, such as protein kinase networks, calcium signaling networks, metabolic pathways and redox responses, to initiate an appropriate response (Mittler *et al.*, 2011). The identification of a true sensor for ROS signal transduction would be of great importance for the ROS signaling research community, but remains largely elusive. However, different components of the ROS signaling network have been identified, including kinases, phosphatases and ROS-responsive transcription factors. ROS

might interact selectively with specific target molecules, such as redox-sensitive proteins/transcription factors that thereby sense and translate the elevated ROS levels into a transcriptional response (Apel and Hirt, 2004). In addition, oxidized peptides generated from the proteolytic breakdown of oxidatively damaged proteins are proposed to act as secondary ROS signaling molecules generated in a compartment-specific manner by different types of ROS (Møller and Sweetlove, 2010). Moreover, oxidative stress can affect the subcellular distribution of proteins. Oxidative stress-triggered relocalizations can ensure a rapid adaptive response to environmental stimuli as this does not require transcription and/or translation.

Here, we focus on the dynamic behavior of proteins during abiotic stress. First, we discuss several mechanisms that affect protein subcellular trafficking under oxidative stress. Next, we focus on the currently known relocalizations during abiotic stress conditions such as low and high temperature stresses, high salinity stress and hypoxia. A detailed understanding of stress-triggered relocalizations could enhance the knowledge of how ROS are perceived, transduced and how they initiate an appropriate response.

Box 1. Generation of different ROS

ROS are either formed by transfer of electrons or energy to ground state triplet molecular dioxygen (O_2) and are easily converted from one type into another (Halliwell, 2006). The first reduction step of O_2 leads to the formation of superoxide ($O_2^{\bullet-}$) or hydroperoxide ($HO_2^{\bullet-}$) radicals (Figure 1). Further reduction leads to the production of hydrogen peroxide (H_2O_2), a relatively stable molecule that can freely diffuse between subcellular compartments and even neighboring cells (Henzler and Steudle, 2000; Bienert *et al.*, 2006). $O_2^{\bullet-}$ can either be spontaneously converted to H_2O_2 or enzymatically by superoxide dismutase (SOD). In the presence of transition metals such as copper and iron, H_2O_2 can give rise to the highly reactive hydroxyl radicals ($OH^{\bullet}$) through the so-called Haber-Weiss mechanism (Kehrer, 2000). $OH^{\bullet}$ are considered as the most toxic ROS because of their extreme reactivity with virtually all biological molecules, such as nucleic acids, proteins and lipids (Halliwell, 2006). Consequently, cells do not possess an enzymatic detoxification mechanism against these radicals. When an electron of O_2 is elevated to a higher energy orbital leading to spin reversal, the highly reactive singlet oxygen ($^1O_2$) is produced (Laloi *et al.*, 2006). This energy transfer predominantly occurs with photo-excited triple-state chlorophyll (Chl) that is formed though insufficient energy dissipation during photosynthesis (Laloi *et al.*, 2006). When $^1O_2$ is not rapidly quenched by β-carotene, α-tocopherol or plastoquinone, it can virtually damage all components of the photosynthetic machinery, in particular photosystem (PS) I and II.

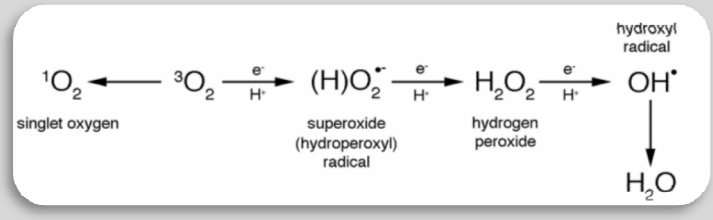

Figure 1. Generation of ROS by excitation or reduction of molecular dioxygen.

Dynamic behavior of proteins during oxidative stress in plants

The regulation of signal transduction is highly dynamic over time and space in which protein trafficking can play an important role. Protein transport can be categorized into two classes: non-mediated and mediated transport. While non-mediated transport is merely simple diffusion, mediated transport can either be facilitated transport (diffusion from high to low concentration) or active transport (against the concentration gradient) which is often guided through interacting proteins (Miyawaki, 2011).

Developmental and/or environmental (biotic and abiotic) stimuli actively influence the spatiotemporal dynamics of proteins to trigger an appropriate response. An important aspect of oxidative stress-triggered protein relocalizations is the subcellular localization of the protein where the oxidative stress is initially sensed. Each subcellular compartment generates its own specific set of ROS molecules each with different molecular properties that could give rise to different protein modifications (Box 2). Several mechanisms have been described for oxidative stress-regulated protein relocalizations such as (i) redox-based relocalizations, (ii) phosphorylation-dependent trafficking by ROS-activated kinases, (iii) stress-induced release of membrane-anchored transcription factors, (iv) sequestration and stress-triggered release and (v) relocalizations mediated by a nuclear retention factor (Figure 3).

Redox-based relocalizations

The redox status of cytosolic proteins can be reversibly or irreversibly modified by intracellular ROS that, in turn, can dynamically affect the protein's subcellular localization and function. These oxidative modifications predominantly occur when proteins are in close proximity with the ROS production site. The most common and best studied redox modification is oxidation of cysteine residues that might further lead to other redox-based post-translational modifications, such as disulphide formation that can trigger conformational changes in the protein. For instance, redox modifications can initiate mono/multimerization as is the case for the redox-regulated dynamic subcellular localization of NPR1 (NONEXPRESSOR OF PATHOGENESIS-RELATED (PR) GENES1), the master regulator of salicylic acid (SA)-dependent defense gene expression (Dong, 2004). During normal conditions, disulphide-linked oligomers of NPR1 are localized in the cytosol. During pathogen infection, SA levels increase leading to the thioredoxin-mediated NPR1 disulphide reduction that results in the release of NPR1 monomers that are redirected to the nucleus to regulate defense gene expression (Dong, 2004).

Box 2. Subcellular ROS-producing and ROS-scavenging sites.

In plants, ROS are continuously produced throughout the cell particularly at sites with a high metabolic rate or intense electron flow such as the peroxisomes, the chloroplasts and the mitochondria (Dat *et al.*, 2000; Figure 2). **Abiotic stress** conditions, such as high light, drought, low and high temperature, perturb the equilibrium between ROS production and ROS-scavenging leading to a rapid accumulation of ROS (Suzuki *et al.*, 2011a). In **chloroplasts**, reduced components of the photosynthetic machinery, such as triplet Chl, the electron transport chain (ETC), PSI and PSII, are major production sites of ROS, in particular $O_2^{\bullet-}$, $^1O_2$, and H_2O_2 (Asada, 2006). When the ETC is overloaded, a part of the electron flow is diverted from Ferredoxin (Fd) to O_2 (Mehler reaction) leading to the formation of $O_2^{\bullet-}$ that is readily converted to H_2O_2 by SOD. In turn, H_2O_2 is detoxified by ascorbate peroxidase (APX) with ascorbate (AsA) as electron donor. AsA is first oxidized to the monodehydroascorbate radical (MDA$^{\bullet}$) and to dehydroascorbate (DHA) before it is recycled in the Halliwell-Asada pathway which involves monodehydroascorbate reductase (MDHAR), Fd, dehydroascorbate reductase (DHAR), glutathione reductase (GR) and the non-enzymatic antioxidants glutathione (GSH [reduced] and GSSG [oxidized]). The highly toxic $^1O_2$ molecules are formed from energy transfer between O_2 and triple-state Chl in PSII (Laloi *et al.*, 2006; Box 1). Other major ROS production sites are the **peroxisomes**, where H_2O_2 accumulates during photorespiration, a process that is tightly linked with photosynthesis (del Río *et al.*, 2006). During low CO_2 availability, the oxygenase activity of the chloroplastic ribulose-1,5-biphosphate carboxylase/oxygenase (Rubisco) is increased leading to the release of glycolate that is transported to the peroxisomes to become oxidized by glycolate oxidase thereby producing large amounts of H_2O_2 that are readily scavenged by catalase (CAT) (del Río *et al.*, 2006). In **mitochondria**, the respiratory ETC is a major ROS source, in particular $O_2^{\bullet-}$ and H_2O_2 (Møller, 2001). Mitochondrial ROS producing sites are NADH dehydrogenases, ubiquinone radicals and complex I and III. Other important ROS ($O_2^{\bullet}$, H_2O_2)-generating sites are the **plasma membrane** (PM) and the **apoplast** by the presence of NAD(P)H oxidases and peroxidases, respectively (Sagi and Fluhr, 2006). H_2O_2 can freely diffuse from the different subcompartments into the **cytosol** which is further facilitated by specialized aquaporins, called peroxyporins. Cytosolic H_2O_2 is scavenged by various peroxidases or may be transported into the vacuole (Gould *et al.*, 2002; Bienert *et al.*, 2006). Elevated levels of ROS induces several signaling cascades including mitogen-activated protein kinases (MAPK) cascades, Ca^{2+} and hormone signaling pathways and activates redox-sensitive transcription factors, leading to stress-responsive gene expression.

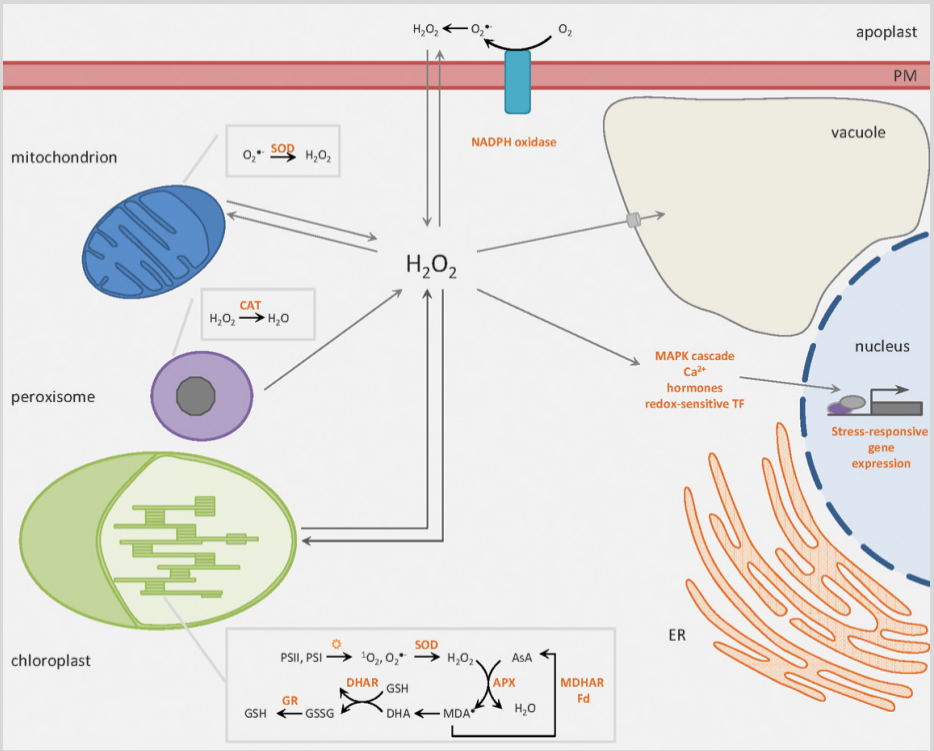

Figure 2. Subcellular ROS production sites. Adapted from Gechev *et al.*, 2006. See text for explanation.

Phosphorylation-dependent trafficking during oxidative stress

The mitogen-activated protein kinase (MAPK) cascade is a well known ROS-activated signaling network that triggers dynamic protein trafficking by protein phosphorylation. The plant MAPK cascades usually consist of a MAPK kinase kinase (MAPKKK) that phosphorylates and activates a MAPKK which then, in turn, phosphorylates a MAPK. These MAPK cascades have been shown to be involved in a number of biotic and abiotic stress responses and include the ROS-responsive MEKK1, MPK4 and MPK6 (Mittler *et al.*, 2011). The activation of MAPK by phosphorylation is often accompanied by relocalization to the nucleus where they are involved in controlling gene expression (Treisman, 1996; Ligterink *et al.*, 1997; Cobb and Goldsmith, 2000; Ahlfors *et al.*, 2004). For instance during ozone stress, AtMPK3 and AtMPK6 are activated by phosphorylation by a still unknown MAPKK and subsequently translocated to the nucleus where they activate ozone-responsive genes (Ahlfors *et al.*, 2004).

Stress-induced release of membrane-anchored transcription factors

Another area that has seen much progress in recent years is the dynamic trafficking of membrane-anchored transcription factors. During incoming environmental stimuli, these transcription factors are proteolytically activated and retargeted to the nucleus to control defense responses (reviewed by Seo *et al.*, 2008). A genome-wide screen identified 85 membrane-anchored transcription factors in *Arabidopsis thaliana* comprising members of all major transcription factor families (Kim *et al.*, 2010). Several bZIP (basic leucine zipper) and NAC (NAM, ATAF and CUC2) transcription factors anchored by a transmembrane domain to respectively the endoplasmatic reticulum (ER) membrane or plasma membrane have been shown to be proteolytically activated and subsequently imported into the nucleus upon abiotic stress stimuli (reviewed by Seo *et al.*, 2008; see also further). In plants, membrane-anchored transcription factors seem to be activated by a regulated intramembrane proteolysis (RIP) mechanism that is governed by site-1 proteases (S1P and S2P), calpain proteases or metalloproteases (Seo *et al.*, 2008).

Sequestration and stress-triggered release

Another strategy is the sequestration of proteins by interaction with other proteins that are modified during oxidative stress. An interesting example is the interaction of WRKY40 with the magnesium-protoporphyrin IX chelatase H subunit (CHLH/ABAR), a chloroplast-localized intracellular abscisic acid (ABA) receptor that also plays a key role in mediating plastid-to-nucleus retrograde signaling (Shang *et al.*, 2010). Interestingly, ABAR is an outer chloroplast envelope-localized transmembrane protein with both its N- and C-terminus exposed to the cytosol. Under normal physiological concentrations of ABA, WRKY40 is present in the nucleus where it represses ABA-responsive genes, such as *ABI5*. Upon

increasing ABA concentrations, WRKY40 translocates by an unknown mechanism from the nucleus to the cytosol where it interacts with the C-terminus of ABAR at the chloroplast periphery (Shang *et al.*, 2010). Similar is the cytosolic retention of AtbZIP10 by interacting with LSD1 (LESION SIMULATING DISEASE RESISTANCE1) that is involved in the regulation of basal defense and cell death during pathogen infection (Kaminaka *et al.*, 2006). LSD1 is a cytosolic plant-specific Zinc Finger (ZF) protein that is a negative regulator of programmed cell death (Dietrich *et al.*, 1994; Jabs *et al.*, 1996; Dietrich *et al.*, 1997; Mateo *et al.*, 2004). AtbZIP10 actively shuttles between the nucleus and the cytosol presumably mediated by the nuclear export factor EXPORTIN1 (AtXPO1). In the absence of endogenous or environmental signals, LSD1 retains AtbZIP10 in the cytosol by interacting with its C-terminal domain that likely blocks the nuclear localization signal (NLS). After perception of a ROS-derived signal, AtbZIP10 dissociates from LSD1 and translocates to the nucleus to induce hypersensitive response- and basal defense-related gene expression (Kaminaka *et al.*, 2006).

Relocalization mediated by a nuclear retention factor

Several reports have described the redistribution of proteins mediated by a stress-induced interaction with a nuclear retention factor. In tomato (*Lycopersicon esculentum*), heat stress triggers the interaction of LpHSFA2 with LpHSFA1a that guides LpHSFA2 to the nucleus to induce heat stress-responsive genes (Scharf *et al.*, 1998; Heerklotz *et al.*, 2001; see further). In *Arabidopsis*, a ROF1-HSP90.1 complex relocalizes to the nucleus by the heat stress-induced interaction with AtHSFA2 (Meiri and Breiman, 2009; see further). Another interesting example is the tobacco stress-induced1 (Tsi1)-interacting protein1 (Tsip1), a DnaJ-type ZF protein that cooperatively enhances the transcriptional activity of Tsi1, an EREBP/AP2-type transcription factor (Ham *et al.*, 2006). Tsip1 is associated with the outer chloroplast surface that is mediated by the presence of an N-terminal chloroplast transit peptide. Upon treatment with SA, Tsip1 dissociates from the chloroplasts by an unknown mechanism and is released into the cytosol where it forms a protein complex with Tsi1. Subsequently, this protein complex is redirected to the nucleus by Tsi1-mediated nuclear translocation. Once in the nucleus, Tsip1 functions as a transcriptional enhancer of Tsi1 to activate stress-responsive genes (Ham *et al.*, 2006)

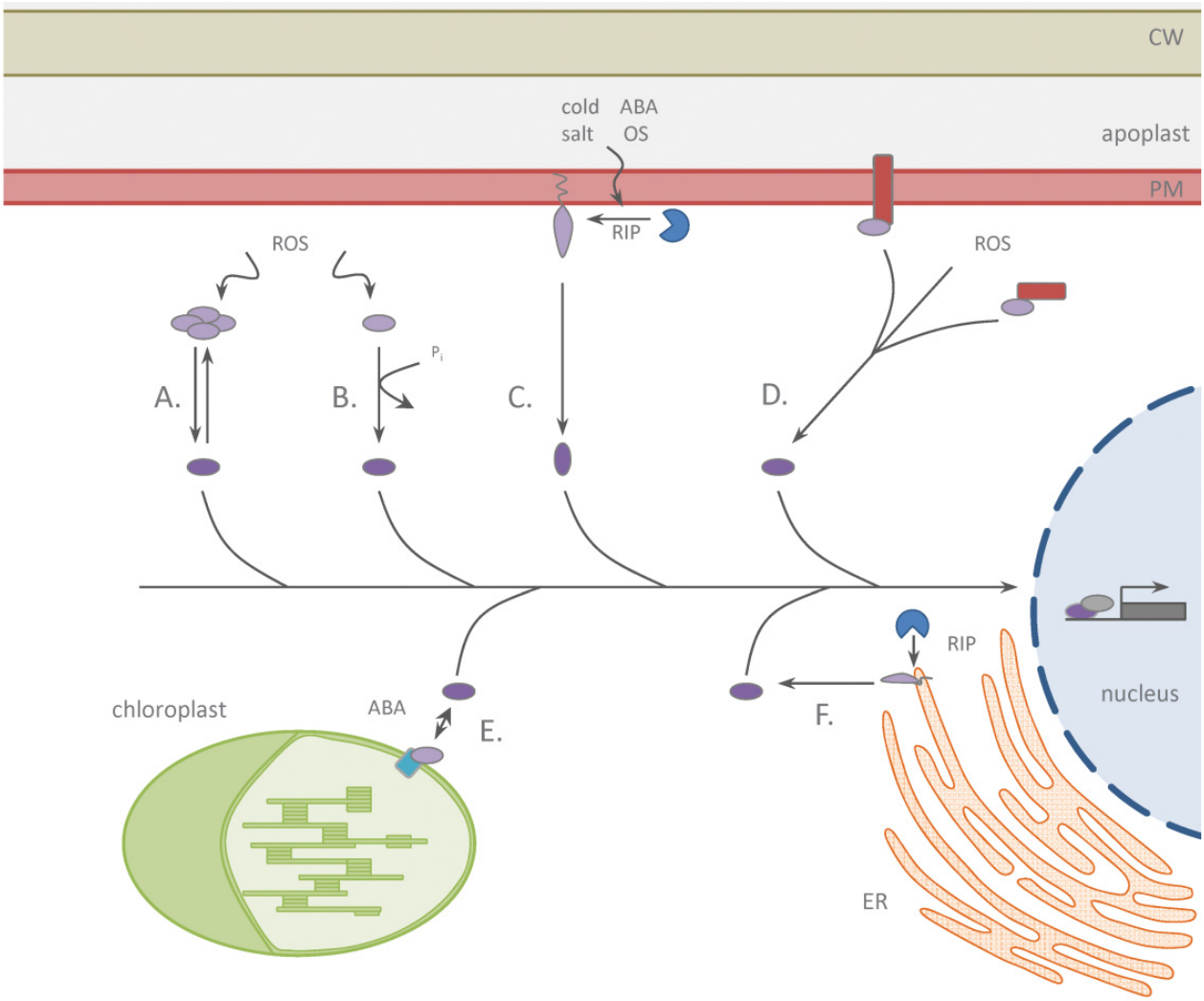

Figure 3. Mechanisms of known oxidative stress-induced relocalizations.

Proteins in their 'native' subcellular localization are indicated in light purple. Proteins that redistribute to another compartment by an oxidative stress-triggered relocalization mechanism are indicated in dark purple. The different mechanisms are indicated by capital letters. (A) Oxidative stress-induced monomerization. Proteins are organized in oligomers that dissociate into monomers by protein oxidation during oxidative stress. These monomers are subsequently imported into the nucleus. (B) ROS-induced phosphorylation cascades. A ROS-activated kinase directly (or indirectly through another kinase) phosphorylates a target protein leading to a conformational change that results in the retargeting of the protein. (C, F) During abiotic stress conditions such as cold and high salinity, dormant plasma membrane-associated (C) or ER-anchored (F) transcription factors are activated by their release from the membrane (via regulated intramembrane proteolysis (RIP)) into to cytosol and subsequently redirected to the nucleus. (D) Oxidative stress-induced release of sequestered proteins. During normal conditions, proteins are retained in the cytosol by interaction with membrane-associated proteins or cytosolic proteins. During oxidative stress, this interaction is abolished leading to the redistribution to another subcellular compartment directed by a targeting signal. (E) Oxidative stress-induced sequestration from the nucleus to the chloroplast periphery by binding to a chloroplast envelope protein. ABA, abscisic acid; CW, cell wall; ER, endoplasmatic reticulum; OS, osmotic stress; ROS, reactive oxygen species.

Abiotic stress-triggered relocalizations

Heat stress

High temperature stress (HS) is the best documented abiotic stress that triggers protein relocalizations. The heat stress response (HSR) is a well conserved defense mechanism that is characterized by the production of heat shock proteins (HSPs) that act as molecular chaperones to prevent the denaturation and aggregation of proteins, a major consequence of thermal denaturation. HSPs are also involved in the refolding, intracellular distribution and degradation of many proteins (Sun *et al.*, 2002). HSPs are classified according to their molecular weight into different families, such as HSP100, HSP90, HSP70, HSP60 and the small HSPs (sHSPs; 12-43 kDa; Baniwal *et al.*, 2004). In plants, sHSPs are found in many subcellular compartments: nucleus and cytosol, ER, chloroplasts, mitochondria and peroxisomes (Scharf *et al.*, 2001; Ma *et al.*, 2006). Cytosolic plant sHSPs are characterized by the formation of highly ordered chaperone complexes. At normal temperatures, sHSPs form homo-oligomers of 200 to 350 kDa (Lee *et al.*, 1995; Helm *et al.*, 1997). During HS, these oligomers dissociate leading to the exposition of their hydrophobic binding sites that govern the interaction with denatured substrates (Bova *et al.*, 1997; Lee *et al.*, 1997; Ehrnsperger *et al.*, 1999; Haslbeck *et al.*, 1999). Subsequently, these complexes are further reassembled into a larger complex that, in turn, can lead to the formation of large cytosolic multichaperone complexes, called heat stress granules (HSGs) that are unique to plants (Nover *et al.*, 1983, 1989; Kirschner *et al.*, 2000).

In plants, the HSR is regulated by a complex network of HS transcription factors (HSFs; Kotak *et al.*, 2007) in which the dynamic subcellular distribution of HSFs and HSF-interacting proteins play a key role. HSFs are comprised of a conserved N-terminal DNA-binding domain that interacts with highly conserved heat shock elements (HSE) in the promoters of HS-inducible genes, an oligomerization domain with an adjacent NLS, and a C-terminal activation motif. In most cases, HSFs also contain a strong nuclear export signal (NES), indicating that their subcellular localization is regulated by nucleocytoplasmic partitioning (Heerklotz *et al.*, 2001). An important step in the activation of HSFs in response to stress is the formation of homo- or heterotrimers influencing their subcellular distribution. The balance between nuclear import and export together with the trimerization of a large variety of HSFs leads to a complex HSR response. For instance in tomato, the onset of an appropriate HSR is mediated by the interaction of two key HSFs, LpHSFA1a and LpHSFA2, and is dependent on the intracellular redistribution of both proteins. LpHSFA1a, also considered as the master regulator of the HSR in tomato (Mishra *et al.*, 2002), is constitutively expressed and is predominantly cytosolic at normal temperatures, due to an efficient nuclear export and a masked NLS. During HS, LpHSFA2 is rapidly synthesized upon LpHSFA1a-dependent expression. LpHSFA2 fails to be imported into the nucleus by

itself, presumably by the presence of a strong NES. During HS, LpHSFA2 forms a hetero-oligomeric complex with LpHSFA1a that acts as a nuclear retention factor and guides LpHSFA2 into the nucleus to function as a transcriptional activator (Scharf *et al.*, 1998; Heerklotz *et al.*, 2001). During recovery, LpHSFA2 is repressed and redirected to the cytosol through interaction of its C-terminal activator domain with HSP17.4-CII (Port *et al.*, 2004). Prolongation of the HS leads to the incorporation of LpHSFA2, together with HSP17 and other cytosolic sHSPs, into cytosolic HSGs (Scharf *et al.*, 1998; Bharti *et al.*, 2000).

Within the 21 HSFs present in Arabidopsis, no master HSF has been identified; the HS-triggered production of AtHSFA2 is nor dependent on AtHSF1a or AtHSF1b (Busch *et al.*, 2005) and neither is the HS-induced nuclear localization of AtHSFA2 (Kotak *et al.*, 2004). Several HS-induced relocalizations that are dependent on interaction with HSFs have been described in Arabidopsis (Meiri and Breiman, 2009; Hsu *et al.*, 2010). For example ROF1, also known as AtFKBP62 (FK506-binding protein), is a peptidyl prolyl *cis/trans* isomerase with chaperone activity that relocalizes during HS. Under normal conditions, ROF1 binds to HSP90.1 in the cytosol. Upon HS, AtHSF2A is synthesized, together with other proteins such as ROF1, HSP90.1, sHSPs and ROF2 (see further). In the first stages of HS recovery, AtHSFA2 interacts with HSP90.1 that forms, together with ROF1, a complex that is subsequently targeted to the nucleus mediated by the HS-induced nuclear translocation of AtHSF2A. Possibly, the interaction between ROF1-HSP90.1 and AtHSFA2 stabilizes AtHSFA2 to ensure high levels of AtHSFA2-dependent synthesis of sHSPs during the recovery from HS (Meiri and Breiman, 2009). Only one year later, it was found that ROF2 (AtFKBP65), a ROF1 homologue that is produced during HS, also associates with the ROF1-HSP90.1-AtHSFA2 complex via a heterodimeric interaction with ROF1 (Meiri *et al.*, 2010). Interestingly, ROF2 also relocalizes to the nucleus, but only during the recovery period where it abrogates the transcriptional activity of AtHSFA2. Meiri and coworkers proposed that ROF2 acts as a sensor for the accumulation of sHSPs by a negative feedback regulatory mechanism that inhibits AtHSFA2 activity (Meiri *et al.*, 2010). Another HSF-binding protein, AtHSBP, was identified as a negative regulator of HSR that is translocated from the cytosol to the nucleus during HS (Hsu *et al.*, 2010). At normal temperatures, AtHSBP is predominantly cytosolic, whereas faint fluorescent nuclei appeared after one hour of HS. After one hour of recovery, a clear nucleocytosolic localization was observed, while after two hours of recovery, AtHSBP was again exclusively cytosolic, which is concomitant with the attenuation of HSR (Hsu *et al.*, 2010). AtHSBP interacts with itself and with the trimerization domain of HSFs that is presumably governed by its C-terminal coiled-coil region. Further studies are necessary to unravel the mechanism of the HS-induced AtHSBP relocalization (Hsu *et al.*, 2010). Another HS-induced relocalization was demonstrated for MBF1c (MULTIPROTEIN BRIDGING FACTOR1c), a highly conserved protein that is induced upon both biotic and abiotic

stresses such as heat, salinity and drought, and functions as a key transcriptional regulator of thermotolerance in Arabidopsis (Suzuki *et al.*, 2008). At normal conditions, MBF1c is a cytosolic protein but relocalizes rapidly to nuclei upon HS to regulates a novel HSR regulon (Suzuki *et al.*, 2008; Suzuki *et al.*, 2011b).

Cold stress

The physical status of the plasma membrane is in close relation with cold perception and signaling (Murata and Los, 1997; Örvar *et al.*, 2000; Browse and Xin, 2001; Vígh *et al.*, 2007). Recently, a link between cold stress and the induction of the pathogen defense response governed by the relocalization of a membrane-tethered NAC transcription factor has been demonstrated (Seo *et al.*, 2010a). During cold stress, the dormant plasma membrane–anchored NTL6 (NTM1 (NAC WITH TRANSMEMBRANE MOTIF1)-LIKE6) is cleaved by a metalloprotease upon cold-induced changes in membrane fluidity (Seo *et al.*, 2010a; Seo *et al.*, 2010b). In turn, the transcriptionally active form is released into the cytosol and subsequently redirected to the nucleus where it binds consensus sequences in the promoters of several of cold-inducible *PR* genes to confer a cold-induced resistance that might be important against (psychrophilic) pathogens that are capable of growing and reproducing at cold temperatures. Accordingly, overexpression of the transcriptionally active form of NTL6 leads to an enhanced pathogen resistance (Seo *et al.*, 2010a; Seo *et al.*, 2010b).

OXIDATIVE STRESS2 (OXS2) was originally identified in an Arabidopsis expression library screen in yeast (*Saccharomyces cerevisiae*) to discover genes that confer oxidative stress tolerance (Blanvillain *et al.*, 2011). OXS2 belongs to the ZF family with one C_2H_2 and two C_3H ZFs, in addition to two ankyrin repeat motifs, and is regulated by several abiotic stress treatments, such as cold, salt, ABA and osmotic stress. While OXS2 is cytosolic under normal conditions, it relocalized to the nucleus upon treatment with cold, ABA or leptomycin B - a covalent inhibitor of AtXPO1 (Kudo *et al.*, 1998). Due to the absence of a NLS and because deletions in the ankyrin motifs reduced nuclear accumulation, it is postulated that the ankyrin motifs play a role in the stress-induced relocalization of OXS2 by interacting with a yet unidentified carrier protein (Blanvillain *et al.*, 2011). The authors suggest a dual function of OXS2 that is dependent on its subcellular localization; while the cytosolic localization of OXS2 during normal growth conditions promotes vegetative growth by a yet unknown mechanism, the oxidative stress-induced nuclear accumulation of OXS2 leads to the activation of a defense response. When stress conditions are sustained this response may trigger reproduction through the activation of the floral integrator genes (Blanvillain *et al.*, 2011).

Another example of a cold stress-induced nucleocytoplasmatic partitioning is in the case of HOS1 (HIGH EXPRESSION OF OSMOTIC RESPONSIVE1), a C_3HC_4-type RING finger protein

that was originally identified as a negative regulator of cold signaling pathways (Ishitani *et al.*, 1998; Lee *et al.*, 1999). *hos1* mutants are characterized by a high induction of cold-responsive marker genes, such as *RD29A*, *COR47*, *COR15A*, *KIN1* and *ADH* (Ishitani *et al.*, 1998). Although the *hos1* mutation decreases freezing tolerance in non-acclimated plants, no significant differences were obvious after cold acclimation. Moreover, *hos1* mutants display a constitutive vernalization response (Ishitani *et al.*, 1998) that was linked to the reduced threshold induction of cold stress-responsive genes. In addition, *hos1* mutants have decreased expression levels of *FLC* (*FLOWERING LOCUS C*) that correlated with the early flowering phenotype. At normal growth temperatures, HOS1 is located in the cytosol, while during cold stress HOS1 is completely redirected to the nucleus by a yet unknown mechanism. When plants are subsequently returned to normal growth temperatures, HOS1-GFP fluorescence disappeared (Lee *et al.*, 2001). Later, it was found that HOS1 functions as an E3 ligase that is required for the cold stress-induced ubiquitination and, thus, degradation of ICE1 (INDUCER OF CBF (C-REPEAT (CRT)-BINDING FACTOR) EXPRESSION1), a transcription factor that controls the induction of *CBF3* (Dong *et al.*, 2006).

Salt stress

Salt stress can be subdivided into either osmotic stress or ionic stress by the perturbation of ion homeostasis leading to an increase of toxic Na^+ ions and a decrease in essential ions such as K^+ (Munns and Tester, 2008). Numerous salt stress-induced relocalizations acting through different mechanisms have been reported. Interestingly, many of these relocalizations involve membrane proteins. One of the most important pathways to cope with high salinity stress is the salt-overly-sensitive (SOS) pathway that is responsible for Na^+ homeostasis in plants (Zhu, 2002). SOS1, a plasma membrane-localized Na^+/H^+ antiporter, functions in the extrusion of intracellular Na^+ and is essential for plant salt tolerance (Shi *et al.*, 2000). Upon salt and oxidative stress, SOS1 interacts through its cytosolic tail with RCD1 (RADICAL-INDUCED CELL DEATH1), an important transcriptional regulator of oxidative stress responses (Katiyar-Agarwal *et al.*, 2006). While RCD1 is a nuclear protein under normal conditions, RCD1 is partially sequestered to the cytosol through interaction with SOS1 during stress (Katiyar-Agarwal *et al.*, 2006). The mechanism behind this nucleus-to-cytoplasm relocalization of RCD1 is yet unknown.

Another interesting example of a salt stress-triggered relocalization is in the case of NTL8, a membrane-bound NAC transcription factor that regulates gibberellic acid (GA)-mediated salt signaling during seed germination (Kim *et al.*, 2008). Under normal conditions, inactive NTL8 is bound with a C-terminal transmembrane domain to the plasma membrane. During salt stress, NTL8 is processed by a yet unknown protease thereby releasing the active form of NTL8 into the cytosol. From there, NTL8 is

redirected to the nucleus by NLS-mediated import to control nuclear gene expression that reduces GA-stimulated seed germination (Kim *et al.*, 2008). Furthermore, it was also shown that NTL8 could play a role in the regulation of salt-responsive flowering (Kim *et al.*, 2007).

Salt stress is not only sensed at the plasma membrane, but also at the ER by the generation of an ER stress response. During conditions that inhibit normal protein folding and secretion, misfolded or unfolded proteins accumulate in the ER that, in turn, activate the unfolded protein response signaling pathway (Urade, 2007, 2009; Liu and Howell, 2010b). In Arabidopsis, the ER stress signal is transduced by ER-bound transcription factors that are activated by proteolytic cleavage and which are redirected to the nucleus under environmental stress conditions. AtbZIP17, an ER-localized membrane-bound bZIP transcription factor, was the first protein reported with an ER stress-induced relocalization caused by salt stress (Liu *et al.*, 2007b). During salt stress, improperly folded proteins accumulate leading to the retargeting of AtbZIP17 to the Golgi apparatus where it is cleaved by site-1 protease (AtS1P; Liu *et al.*, 2008). Subsequently, AtbZIP17 is released into the cytosol, from where it relocates to the nucleus. Besides salt stress, other environmental conditions such as pathogen attack, drought and heat stress can lead to ER stress-triggered relocalizations of ER-bound transcription factors such as AtbZIP28 (Liu *et al.*, 2007a; Liu and Howell, 2010a; Gao *et al.*, 2008) and AtbZIP60 (Iwata *et al.*, 2008).

Besides membrane-to-nucleus relocalizations, several examples are known of salt stress-induced nucleocytoplasmic partitioning of proteins. For instance, AtbZIP24 acts as a negative transcriptional regulator of the salt stress acclimation response and is regulated by nucleocytoplasmic partitioning (Yang *et al.*, 2009). During control conditions, AtbZIP24 homodimers are present in both the cytosol and the nucleus. However in salt-stressed plants, cytoplasmic AtbZIP24 levels were decreased whereas the amount of nuclear AtbZIP24 had increased (Yang *et al.*, 2009).

Several examples exist of osmotic stress-induced relocalizations. For instance, polyethylene glycol (PEG) treatment, that induces osmotic stress, triggers the proteolytic cleavage of NTL9, a plasma membrane-anchored NAC transcription factor, thereby releasing a transcriptionally active form into the cytosol that is subsequently imported in the nucleus to regulate leaf senescence (Yoon *et al.*, 2008). Another important example is the stress-induced dynamic redistribution of aquaporins that facilitate the diffusion of water across biological membranes. In *Mesembryanthemum crystallinum* (Iceplant) cells, mannitol-induced osmotic stress leads to the redistribution of a tonoplast intrinsic protein (TIP) subfamily aquaporin to a putative endosomal compartment, possibly to maintain the osmotic balance of the cytosol (Vera-Estrella *et al.*, 2004). In Arabidopsis, the plasma membrane intrinsic protein (PIP)-type aquaporins (PIP1;2 and PIP2;1) are internalized upon salt treatment (Boursiac *et al.*, 2005). In addition, the Arabidopsis vacuolar TIP1;1 relocalizes upon salt stress to vacuolar invaginations possibly to affect the tonoplast water uptake capacity (Boursiac *et al.*, 2005; Li *et al.*, 2011). Later, it was found that also

treatment with SA and H_2O_2 markedly induced the intracellular accumulation of PIPs (Boursiac *et al.*, 2008a) through protein phosphorylation (Boursiac *et al.*, 2008b).

Hypoxia

Prolonged flooding alters the physicochemical properties of the soil, including the availability of O_2. During hypoxic conditions, the reduction in available O_2 becomes a limiting factor for ATP production through oxidative phosphorylation, depleting thus the ATP pool (Dat *et al.*, 2004). One strategy to cope with hypoxia is to suppress major energy-consuming processes. For instance, hypoxia induces the inhibition of protein synthesis through a block in gene translation. The DEAD box protein eIF4a-III, a putative anchor protein of the exon junction complex that is involved in mRNA biogenesis, is an ATPase that in response to hypoxia relocalizes from the nucleoplasm to the nucleolus and to splicing speckles (Koroleva *et al.*, 2009). This relocalization results from the inhibition of respiration whereby the depletion of ATP is sensed by eIF4A-III: because ATP binding provokes a conformational change that provides a binding site for mRNA ribonucleotides, ATP deficiency impairs mRNA binding that, in turn, might be a signal for mRNA storage in nuclear speckles (Koroleva *et al.*, 2009).

CONCLUSION AND PERSPECTIVES

Although significant progress has been made in the description of oxidative stress-dependent gene expression, the regulation of the complex ROS signaling transduction network remains largely unknown. Protein activation and trafficking play an important role in rendering signal transduction highly dynamic over time and space. During adverse environmental conditions, the regulation of dynamic protein trafficking is key to stress signaling involving post-translational modifications. Therefore, the identification of oxidative stress-induced post-translationally modified proteins could provide novel candidates for stress-triggered relocalization studies. However, proteomic studies to identify ROS-modified proteins remain scarce, are often gel-based, lack sensitivity and do not reflect the whole proteome. With the current development of the combined fractional diagonal chromatography™ (COFRADIC™) technology (Gevaert *et al.*, 2002), differential proteome studies can be performed to identify oxidative stress-induced proteins. Moreover, post-translational protein modifications that occur during oxidative stress conditions, such as tyrosine nitration (Ghesquière *et al.*, 2009; Ghesquière *et al.*, 2011a) and methionine oxidation (Ghesquière *et al.*, 2011b) can be studied on a proteome-wide basis. Although redox regulation and ROS metabolism in the different subcellular compartments are tightly interconnected (e.g. the chloroplasts and the mitochondria), different types of abiotic stresses seem to affect certain subcellular compartments more which, in turn, produce compartment-specific ROS. Thus, the mechanism of an abiotic stress-induced relocalization is often correlated with the type of abiotic stress and the subcellular compartment. Moreover, extensive cross-talk between divergent ROS signals from different organelles takes place in the cytosol (Suzuki *et al.*, 2011a) making it an important site where oxidative stress-triggered protein relocalizations initiate. Future integration of ROS-modified protein datasets with subcellular localization studies and the visualization of compartment-specific ROS (see below) will provide a comprehensive view on the protein modifications and/or relocalizations that occur during stress.

Importantly, identifying novel oxidative stress-induced relocalizations is experimentally demanding and requires a detailed understanding of several parameters, such as the physicochemical properties of the protein of interest, its subcellular localization during non-stressed conditions (membrane-bound vs. non-membrane-bound, organellar vs. cytosolic), the potential interactors, the spatiotemporal dynamics of both the protein of interest and ROS, and the involved abiotic stress pathway. In addition, protein relocalization experiments often require rigorous optimization steps to determine the correct timing and the exact abiotic stress stimulus.

To increase our knowledge about the complex timing and location of abiotic stress-triggered ROS production, several tools can be used to quantify real-time changes in ROS levels *in vivo* (Swanson

et al., 2011). Although several techniques, such as two-photon fluorescence microscopy, matrix-assisted laser desorption/ionization mass spectrometry (MALDI-MS) imaging, atomic force microscopy and optical tweezers force spectroscopy have been valuable tools for measuring the level of ROS in different organisms, their use in plants remains limited (Mittler *et al.*, 2011). In plants, ROS imaging studies are predominantly based on using ROS-specific dyes, luciferase assays and redox-sensitive GFP (roGFP). The selective targeting of GFP-based biosensors using compartment-specific targeting sequences will allow to monitor ROS levels in a broad range of subcellular compartments (Swanson *et al.*, 2011). Currently, protein relocalizations experiments are predominantly based on imaging of tagged proteins with a fluorescent fluorophore or measuring protein abundancies by western blot. However, more quantitative methods to easily determine the shift in protein distribution from one compartment to another are required.

In conclusion, protein relocalization during oxidative stress is an important intracellular signaling strategy to deliver the ROS-derived signal from one location to another to ultimately elicit a fast defense response. A detailed understanding of oxidative stress-triggered relocalizations together with the tight spatiotemporal control of ROS levels at the different subcellular compartments under abiotic stress conditions will provide a better understanding of stress response signaling.

REFERENCES

Ahlfors, R., Macioszek, V., Rudd, J., Brosché, M., Schlichting, R., Scheel, D. and Kangasjärvi, J. (2004) Stress hormone-independent activation and nuclear translocation of mitogen-activated protein kinases in *Arabidopsis thaliana* during ozone exposure. *Plant J.*, **40**, 512-522.

Apel, K. and Hirt, H. (2004) Reactive oxygen species: metabolism, oxidative stress, and signal transduction. *Annu. Rev. Plant Biol.*, **55**, 373-399.

Asada, K. (2006) Production and scavenging of reactive oxygen species in chloroplasts and their functions. *Plant Physiol.*, **141**, 391-396.

Baniwal, S., Bharti, K., Chan, K., Fauth, M., Misra, S., Nover, L., Port, M. and Scharf, K.D. (2004) Heat stress response in plants: a complex game with chaperones and more than twenty heat stress transcription factors. *J. Biosci.*, **29**, 471-487.

Bharti, K., Schmidt, E., Lyck, R., Heerklotz, D., Bublak, D. and Scharf, K.-D. (2000) Isolation and characterization of HsfA3, a new heat stress transcription factor of *Lycopersicon peruvianum*. *Plant J.*, **22**, 355-365.

Bienert, G.P., Schjoerring, J.K. and Jahn, T.P. (2006) Membrane transport of hydrogen peroxide. *Biochim. Biophys. Acta*, **1758**, 994-1003.

Blanvillain, R., Wei, S., Wei, P., Kim, J.H. and Ow, D.W. (2011) Stress tolerance to stress escape in plants: role of the OXS2 zinc-finger transcription factor family. *EMBO J.*, **30**, 3812-3822.

Boursiac, Y., Boudet, J., Postaire, O., Luu, D.-T., Tournaire-Roux, C. and Maurel, C. (2008a) Stimulus-induced downregulation of root water transport involves reactive oxygen species-activated cell signalling and plasma membrane intrinsic protein internalization. *Plant J.*, **56**, 207-218.

Boursiac, Y., Chen, S., Luu, D.-T., Sorieul, M., van den Dries, N. and Maurel, C. (2005) Early effects of salinity on water transport in *Arabidopsis* roots. Molecular and cellular features of aquaporin expression. *Plant Physiol.*, **139**, 790-805.

Boursiac, Y., Prak, S., Boudet, J., Postaire, O., Luu, D.-T., Tournaire-Roux, C., Santoni, V. and Maurel, C. (2008b) The response of *Arabidopsis* root water transport to a challenging environment implicates reactive oxygen species- and phosphorylation-dependent internalization of aquaporins. *Plant Signal. Behav.*, **3**, 1096-1098.

Bova, M.P., Ding, L.-L., Horwitz, J. and Fung, B.K.-K. (1997) Subunit exchange of αA-crystallin. *J. Biol. Chem.*, **272**, 29511-29517.

Browse, J. and Xin, Z. (2001) Temperature sensing and cold acclimation. *Curr. Opin. Plant Biol.*, **4**, 241-246.

Busch, W., Wunderlich, M. and Schöffl, F. (2005) Identification of novel heat shock factor-dependent genes and biochemical pathways in *Arabidopsis thaliana*. *Plant J.*, **41**, 1-14.

Cobb, M.H. and Goldsmith, E.J. (2000) Dimerization in MAP-kinase signaling. *Trends Biochem. Sci.*, **25**, 7-9.

Dat, J., Vandenabeele, S., Vranová, E., Van Montagu, M., Inzé, D. and Van Breusegem, F. (2000) Dual action of the active oxygen species during plant stress responses. *Cell. Mol. Life Sci.*, **57**, 779-795.

Dat, J.F., Capelli, N., Folzer, H., Bourgeade, P. and Badot, P.-M. (2004) Sensing and signalling during plant flooding. *Plant Physiol. Biochem.*, **42**, 273-282.

del Río, L.A., Sandalio, L.M., Corpas, F.J., Palma, J.M. and Barroso, J.B. (2006) Reactive oxygen species and reactive nitrogen species in peroxisomes. Production, scavenging, and role in cell signaling. *Plant Physiol.*, **141**, 330-335.

Dietrich, R.A., Delaney, T.P., Uknes, S.J., Ward, E.R., Ryals, J.A. and Dangl, J.L. (1994) *Arabidopsis* mutants simulating disease resistance response. *Cell*, **77**, 565-577.

Dietrich, R.A., Richberg, M.H., Schmidt, R., Dean, C. and Dangl, J.L. (1997) A novel Zinc Finger protein is encoded by the *Arabidopsis LSD1* gene and functions as a negative regulator of plant cell death. *Cell*, **88**, 685-694.

Dong, C.-H., Agarwal, M., Zhang, Y., Xie, Q. and Zhu, J.-K. (2006) The negative regulator of plant cold responses, HOS1, is a RING E3 ligase that mediates the ubiquitination and degradation of ICE1. *Proc. Natl. Acad. Sci. USA*, **103**, 8281-8286.

Dong, X. (2004) NPR1, all things considered. *Curr. Opin. Plant Biol.*, **7**, 547-552.

Ehrnsperger, M., Lilie, H., Gaestel, M. and Buchner, J. (1999) The dynamics of Hsp25 quaternary structure. *J. Biol. Chem.*, **274**, 14867-14874.

Gadjev, I., Vanderauwera, S., Gechev, T.S., Laloi, C., Minkov, I.N., Shulaev, V., Apel, K., Inzé, D., Mittler, R. and Van Breusegem, F. (2006) Transcriptomic footprints disclose specificity of reactive oxygen species signaling in *Arabidopsis*. *Plant Physiol.*, **141**, 436-445.

Gao, H., Brandizzi, F., Benning, C. and Larkin, R.M. (2008) A membrane-tethered transcription factor defines a branch of the heat stress response in *Arabidopsis thaliana*. *Proc. Natl. Acad. Sci. USA*, **105**, 16398-16403.

Gechev, T.S., Van Breusegem, F., Stone, J.M., Denev, I. and Laloi, C. (2006) Reactive oxygen species as signals that modulate plant stress responses and programmed cell death. *BioEssays*, **28**, 1-11.

Gevaert, K., Van Damme, J., Goethals, M., Thomas, G.R., Hoorelbeke, B., Demol, H., Martens, L., Puype, M., Staes, A. and Vandekerckhove, J. (2002) Chromatographic isolation of methionine-containing peptides for gel-free proteome analysis. *Mol. Cell. Proteomics*, **1**, 896-903.

Ghesquière, B., Colaert, N., Helsens, K., Dejager, L., Vanhaute, C., Verleysen, K., Kas, K., Timmerman, E., Goethals, M., Libert, C., Vandekerckhove, J. and Gevaert, K. (2009) *In vitro* and *in vivo* protein-bound tyrosine nitration characterized by diagonal chromatography. *Mol. Cell. Proteomics*, **8**, 2642-2652.

Ghesquière, B., Helsens, K., Vandekerckhove, J. and Gevaert, K. (2011a) A stringent approach to improve the quality of nitrotyrosine peptide identifications. *Proteomics*, **11**, 1094-1098.

Ghesquière, B., Jonckheere, V., Colaert, N., Van Durme, J., Timmerman, E., Goethals, M., Schymkowitz, J., Rousseau, F., Vandekerckhove, J. and Gevaert, K. (2011b) Redox proteomics of protein-bound methionine oxidation. *Mol. Cell. Proteomics*, **10**, In Press.

Gould, K.S., McKelvie, J. and Markham, K.R. (2002) Do anthocyanins function as antioxidants in leaves? Imaging of H_2O_2 in red and green leaves after mechanical injury. *Plant Cell Environ.*, **25**, 1261-1269.

Halliwell, B. (2006) Reactive species and antioxidants. Redox biology is a fundamental theme of aerobic life. *Plant Physiol.*, **141**, 312-322.

Ham, B.-K., Park, J.M., Lee, S.-B., Kim, M.J., Lee, I.-J., Kim, K.-J., Kwon, C.S. and Paek, K.-H. (2006) Tobacco Tsip1, a DnaJ-type Zn Finger protein, is recruited to and potentiates Tsi1-mediated transcriptional activation. *Plant Cell*, **18**, 2005-2020.

Haslbeck, M., Walke, S., Stromer, T., Ehrnsperger, M., White, H.E., Chen, S., Saibil, H.R. and Buchner, J. (1999) Hsp26: a temperature-regulated chaperone. *EMBO J.*, **18**, 6744-6751.

Heerklotz, D., Döring, P., Bonzelius, F., Winkelhaus, S. and Nover, L. (2001) The balance of nuclear import and export determines the intracellular distribution and function of tomato heat stress transcription factor HsfA2. *Mol. Cell. Biol.*, **21**, 1759-1768.

Helm, K.W., Lee, G.J. and Vierling, E. (1997) Expression and native structure of cytosolic class II small heat-shock proteins. *Plant Physiol.*, **114**, 1477-1485.

Henzler, T. and Steudle, E. (2000) Transport and metabolic degradation of hydrogen peroxide in *Chara corallina*: model calculations and measurements with the pressure probe suggest transport of H_2O_2 across water channels. *J. Exp. Bot.*, **51**, 2053-2066.

Hsu, S.-F., Lai, H.-C. and Jinn, T.-L. (2010) Cytosol-localized heat shock factor-binding protein, AtHSBP, functions as a negative regulator of heat shock response by translocation to the nucleus and Is required for seed development in *Arabidopsis*. *Plant Physiol.*, **153**, 773-784.

Ishitani, M., Xiong, L., Lee, H., Stevenson, B. and Zhu, J.-K. (1998) *HOS1*, a genetic locus involved in cold-responsive gene expression in *Arabidopsis*. *Plant Cell*, **10**, 1151-1162.

Iwata, Y., Fedoroff, N.V. and Koizumi, N. (2008) *Arabidopsis* bZIP60 is a proteolysis-activated transcription factor involved in the endoplasmic reticulum stress response. *Plant Cell*, **20**, 3107-3121.

Jabs, T., Dietrich, R. and Dangl, J. (1996) Initiation of runaway cell death in an *Arabidopsis* mutant by extracellular superoxide. *Science*, **273**, 1853-1856.

Kaminaka, H., Nake, C., Epple, P., Dittgen, J., Schutze, K., Chaban, C., Holt, B.F., Merkle, T., Schafer, E., Harter, K. and Dangl, J.L. (2006) bZIP10-LSD1 antagonism modulates basal defense and cell death in *Arabidopsis* following infection. *EMBO J.*, **25**, 4400-4411.

Katiyar-Agarwal, S., Zhu, J., Kim, K., Agarwal, M., Fu, X., Huang, A. and Zhu, J.-K. (2006) The plasma membrane Na^+/H^+ antiporter SOS1 interacts with RCD1 and functions in oxidative stress tolerance in *Arabidopsis*. *Proc. Natl. Acad. Sci. USA*, **103**, 18816-18821.

Kehrer, J.P. (2000) The Haber–Weiss reaction and mechanisms of toxicity. *Toxicology*, **149**, 43-50.

Kim, S.-G., Kim, S.-Y. and Park, C.-M. (2007) A membrane-associated NAC transcription factor regulates salt-responsive flowering via *FLOWERING LOCUS* in *Arabidopsis*. *Planta*, **226**, 647-654.

Kim, S.-G., Lee, A.-K., Yoon, H.-K. and Park, C.-M. (2008) A membrane-bound NAC transcription factor NTL8 regulates gibberellic acid-mediated salt signaling in *Arabidopsis* seed germination. *Plant J.*, **55**, 77-88.

Kim, S.-G., Lee, S., Seo, P.J., Kim, S.-K., Kim, J.-K. and Park, C.-M. (2010) Genome-scale screening and molecular characterization of membrane-bound transcription factors in *Arabidopsis* and rice. *Genomics*, **95**, 56-65.

Kirschner, M., Winkelhaus, S., Thierfelder, J.M. and Nover, L. (2000) Transient expression and heat-stress-induced co-aggregation of endogenous and heterologous small heat-stress proteins in tobacco protoplasts. *Plant J.*, **24**, 397-412.

Koroleva, O.A., Calder, G., Pendle, A.F., Kim, S.H., Lewandowska, D., Simpson, C.G., Jones, I.M., Brown, J.W.S. and Shaw, P.J. (2009) Dynamic behavior of *Arabidopsis* eIF4A-III, putative core protein of exon junction complex: fast relocation to nucleolus and splicing speckles under hypoxia. *Plant Cell*, **21**, 1592-1606.

Kotak, S., Larkindale, J., Lee, U., von Koskull-Döring, P., Vierling, E. and Scharf, K.-D. (2007) Complexity of the heat stress response in plants. *Curr. Opin. Plant Biol.*, **10**, 310-316.

Kotak, S., Port, M., Ganguli, A., Bicker, F. and Von Koskull-Döring, P. (2004) Characterization of C-terminal domains of *Arabidopsis* heat stress transcription factors (Hsfs) and identification of a new signature combination of plant class A Hsfs with AHA and NES motifs essential for activator function and intracellular localization. *Plant J.*, **39**, 98-112.

Kudo, N., Wolff, B., Sekimoto, T., Schreiner, E.P., Yoneda, Y., Yanagida, M., Horinouchi, S. and Yoshida, M. (1998) Leptomycin B inhibition of signal-mediated nuclear export by direct binding to CRM1. *Exp. Cell Res.*, **242**, 540-547.

Laloi, C., Przybyla, D. and Apel, K. (2006) A genetic approach towards elucidating the biological activity of different reactive oxygen species in *Arabidopsis thaliana*. *J. Exp. Bot.*, **57**, 1719-1724.

Lee, G.J., Pokala, N. and Vierling, E. (1995) Structure and *in vitro* molecular chaperone activity of cytosolic small heat shock proteins from pea. *J. Biol. Chem.*, **270**, 10432-10438.

Lee, G.J., Roseman, A.M., Saibil, H.R. and Vierling, E. (1997) A small heat shock protein stably binds heat-denatured model substrates and can maintain a substrate in a folding-competent state. *EMBO J.*, **16**, 659-671.

Lee, H., Xiong, L., Gong, Z., Ishitani, M., Stevenson, B. and Zhu, J.-K. (2001) The *Arabidopsis HOS1* gene negatively regulates cold signal transduction and encodes a RING finger protein that displays cold-regulated nucleo–cytoplasmic partitioning. *Genes Dev.*, **15**, 912-924.

Lee, H., Xiong, L., Ishitani, M., Stevenson, B. and Zhu, J.-K. (1999) Cold-regulated gene expression and freezing tolerance in an *Arabidopsis thaliana* mutant. *Plant J.*, **17**, 301-308.

Li, X., Wang, X., Yang, Y., Li, R., He, Q., Fang, X., Luu, D.-T., Maurel, C. and Lin, J. (2011) Single-molecule analysis of PIP2;1 dynamics and partitioning reveals multiple modes of *Arabidopsis* plasma membrane aquaporin regulation. *Plant Cell*, **23**, 3780-3797.

Ligterink, W., Kroj, T., Nieden, U.z., Hirt, H. and Scheel, D. (1997) Receptor-mediated activation of a MAP kinase in pathogen defense of plants. *Science*, **276**, 2054-2057.

Liu, J.-X. and Howell, S.H. (2010a) bZIP28 and NF-Y transcription factors are activated by ER stress and assemble into a transcriptional complex to regulate stress response genes in *Arabidopsis*. *Plant Cell*, **22**, 782-796.

Liu, J.-X. and Howell, S.H. (2010b) Endoplasmic reticulum protein quality control and its relationship to environmental stress responses in plants. *Plant Cell*, **22**, 2930-2942.

Liu, J.-X., Srivastava, R., Che, P. and Howell, S.H. (2007a) An endoplasmic reticulum stress response in *Arabidopsis* is mediated by proteolytic processing and nuclear relocation of a membrane-associated transcription factor, bZIP28. *Plant Cell*, **19**, 4111-4119.

Liu, J.-X., Srivastava, R., Che, P. and Howell, S.H. (2007b) Salt stress responses in *Arabidopsis* utilize a signal transduction pathway related to endoplasmic reticulum stress signaling. *Plant J.*, **51**, 897-909.

Liu, J.-X., Srivastava, R., Che, P. and Howell, S.H. (2008) Salt stress signaling in *Arabidopsis thaliana* involves a membrane-bound transcription factor AtbZIP17 as a signal transducer. *Plant Signal. Behav.*, **3**, 56-57.

Ma, C., Haslbeck, M., Babujee, L., Jahn, O. and Reumann, S. (2006) Identification and characterization of a stress-inducible and a constitutive small heat-shock protein targeted to the matrix of plant peroxisomes. *Plant Physiol.*, **141**, 47-60.

Mateo, A., Mühlenbock, P., Rustérucci, C., Chang, C.C.-C., Miszalski, Z., Karpinska, B., Parker, J.E., Mullineaux, P.M. and Karpinski, S. (2004) LESION SIMULATING DISEASE 1 is required for acclimation to conditions that promote excess excitation energy. *Plant Physiol.*, **136**, 2818-2830.

Meiri, D. and Breiman, A. (2009) *Arabidopsis* ROF1 (FKBP62) modulates thermotolerance by interacting with HSP90.1 and affecting the accumulation of HsfA2-regulated sHSPs. *Plant J.*, **59**, 387-399.

Meiri, D., Tazat, K., Cohen-Peer, R., Farchi-Pisanty, O., Aviezer-Hagai, K., Avni, A. and Breiman, A. (2010) Involvement of *Arabidopsis* ROF2 (FKBP65) in thermotolerance. *Plant Mol. Biol.*, **72**, 191-203.

Mishra, S.K., Tripp, J., Winkelhaus, S., Tschiersch, B., Theres, K., Nover, L. and Scharf, K.-D. (2002) In the complex family of heat stress transcription factors, HsfA1 has a unique role as master regulator of thermotolerance in tomato. *Genes Dev.*, **16**, 1555-1567.

Mittler, R., Vanderauwera, S., Gollery, M. and Van Breusegem, F. (2004) Reactive oxygen gene network of plants. *Trends Plant Sci.*, **9**, 490-498.

Mittler, R., Vanderauwera, S., Suzuki, N., Miller, G., Tognetti, V.B., Vandepoele, K., Gollery, M., Shulaev, V. and Van Breusegem, F. (2011) ROS signaling: the new wave? *Trends Plant Sci.*, **16**, 300-309.

Miyawaki, A. (2011) Proteins on the move: insights gained from fluorescent protein technologies. *Nat. Rev. Mol. Cell Biol.*, **12**, 656-668.

Møller, I.M. (2001) Plant mitochondria and oxidative stress: electron transport, NADPH turnover, and metabolism of reactive oxygen species. *Annu. Rev. Plant Physiol. Plant Mol. Biol.*, **52**, 561-591.

Møller, I.M. and Sweetlove, L.J. (2010) ROS signaling – specificity is required. *Trends Plant Sci.*, **15**, 370-374.

Munns, R. and Tester, M. (2008) Mechanisms of salinity tolerance. *Annu. Rev. Plant Biol.*, **59**, 651-681.

Murata, N. and Los, D.A. (1997) Membrane fluidity and temperature perception. *Plant Physiol.*, **115**, 875-879.

Nover, L., Scharf, K.D. and Neumann, D. (1983) Formation of cytoplasmic heat shock granules in tomato cell cultures and leaves. *Mol. Cell. Biol.*, **3**, 1648-1655.

Nover, L., Scharf, K.D. and Neumann, D. (1989) Cytoplasmic heat shock granules are formed from precursor particles and are associated with a specific set of mRNAs. *Mol. Cell. Biol.*, **9**, 1298-1308.

Örvar, B.L., Sangwan, V., Omann, F. and Dhindsa, R.S. (2000) Early steps in cold sensing by plant cells: the role of actin cytoskeleton and membrane fluidity. *Plant J.*, **23**, 785-794.

Port, M., Tripp, J., Zielinski, D., Weber, C., Heerklotz, D., Winkelhaus, S., Bublak, D. and Scharf, K.-D. (2004) Role of Hsp17.4-CII as coregulator and cytoplasmic retention factor of tomato heat stress transcription factor HsfA2. *Plant Physiol.*, **135**, 1457-1470.

Sagi, M. and Fluhr, R. (2006) Production of reactive oxygen species by plant NADPH oxidases. *Plant Physiol.*, **141**, 336-340.

Scharf, K.-D., Heider, H., Höhfeld, I., Lyck, R., Schmidt, E. and Nover, L. (1998) The tomato Hsf system: HsfA2 needs interaction with HsfA1 for efficient nuclear import and may be localized in cytoplasmic heat stress granules. *Mol. Cell. Biol.*, **18**, 2240-2251.

Scharf, K.D., Siddique, M. and Vierling, E. (2001) The expanding family of *Arabidopsis thaliana* small heat stress proteins and a new family of proteins containing α-crystallin domains (Acd proteins). *Cell Stress Chaperones*, **3**, 225-237.

Seo, P.J., Kim, M.J., Park, J.-Y., Kim, S.-Y., Jeon, J., Lee, Y.-H., Kim, J. and Park, C.-M. (2010a) Cold activation of a plasma membrane-tethered NAC transcription factor induces a pathogen resistance response in *Arabidopsis*. *Plant J.*, **61**, 661-671.

Seo, P.J., Kim, M.J., Song, J.-S., Kim, Y.-S., Kim, H.-J. and Park, C.-M. (2010b) Proteolytic processing of an *Arabidopsis* membrane-bound NAC transcription factor is triggered by cold-induced changes in membrane fluidity. *Biochem. J.*, **427**, 359-367.

Seo, P.J., Kim, S.-G. and Park, C.-M. (2008) Membrane-bound transcription factors in plants. *Trends Plant Sci.*, **13**, 550-556.

Shang, Y., Yan, L., Liu, Z.-Q., Cao, Z., Mei, C., Xin, Q., Wu, F.-Q., Wang, X.-F., Du, S.-Y., Jiang, T., Zhang, X.-F., Zhao, R., Sun, H.-L., Liu, R., Yu, Y.-T. and Zhang, D.-P. (2010) The Mg-chelatase H subunit of *Arabidopsis* antagonizes a group of WRKY transcription repressors to relieve ABA-responsive genes of inhibition. *Plant Cell*, **22**, 1909-1935.

Shi, H., Ishitani, M., Kim, C. and Zhu, J.-K. (2000) The *Arabidopsis thaliana* salt tolerance gene *SOS1* encodes a putative Na^+/H^+ antiporter. *Proc. Natl. Acad. Sci. USA*, **97**, 6896-6901.

Sun, W., Van Montagu, M. and Verbruggen, N. (2002) Small heat shock proteins and stress tolerance in plants. *Biochim. Biophys. Acta*, **1577**, 1-9.

Suzuki, N., Bajad, S., Shuman, J., Shulaev, V. and Mittler, R. (2008) The transcriptional co-activator MBF1c is a key regulator of thermotolerance in *Arabidopsis thaliana*. *J. Biol. Chem.*, **283**, 9269-9275.

Suzuki, N., Koussevitzky, S., Mittler, R.O.N. and Miller, G.A.D. (2011a) ROS and redox signalling in the response of plants to abiotic stress. *Plant Cell Environ.*, doi: 10.1111/j.1365-3040.2011.02336.x.

Suzuki, N., Sejima, H., Tam, R., Schlauch, K. and Mittler, R. (2011b) Identification of the MBF1 heat-response regulon of *Arabidopsis thaliana*. *Plant J.*, **66**, 844-851.

Swanson, S.J., Choi, W.-G., Chanoca, A. and Gilroy, S. (2011) *In vivo* Imaging of Ca^{2+}, pH, and reactive oxygen species using fluorescent probes in plants. *Annu. Rev. Plant Biol.*, **62**, 273-297.

Treisman, R. (1996) Regulation of transcription by MAP kinase cascades. *Curr. Opin. Cell Biol.*, **8**, 205-215.

Urade, R. (2007) Cellular response to unfolded proteins in the endoplasmic reticulum of plants. *FEBS J.*, **274**, 1152-1171.

Urade, R. (2009) The endoplasmic reticulum stress signaling pathways in plants. *Biofactors*, **35**, 326-331.

Van Breusegem, F. and Dat, J.F. (2006) Reactive oxygen species in plant cell death. *Plant Physiol.*, **141**, 384-390.

Vera-Estrella, R., Barkla, B.J., Bohnert, H.J. and Pantoja, O. (2004) Novel regulation of aquaporins during osmotic stress. *Plant Physiol.*, **135**, 2318-2329.

Vígh, L., Török, Z., Balogh, G., Glatz, A., Piotto, S. and Horváth, I. (2007) Membrane-regulated stress response. In *Molecular aspects of the stress response: chaperones, membranes and networks* (Csermely, P. and Vígh, L. eds): Springer New York, pp. 114-131.

Yang, O., Popova, O.V., Süthoff, U., Lüking, I., Dietz, K.-J. and Golldack, D. (2009) The *Arabidopsis* basic leucine zipper transcription factor AtbZIP24 regulates complex transcriptional networks involved in abiotic stress resistance. *Gene*, **436**, 45-55.

Yoon, H.-K., Kim, S.G., Kim, S. and Park, C.-M. (2008) Regulation of leaf senescence by NTL9-mediated osmotic stress signaling in *Arabidopsis*. *Mol. Cells*, **25**, 438-445.

Zhu, J.-K. (2002) Salt and drought stress signal transduction in plants. *Annu. Rev. Plant Biol.*, **53**, 247-273.

2

A subcellular localization compendium of hydrogen peroxide-induced proteins

Annelies Inzé, Sandy Vanderauwera, Frank A. Hoeberichts, Brigitte van de Cotte, Michaël Vandorpe, Tim Van Gaever and Frank Van Breusegem

AUTHOR CONTRIBUTIONS

A.I. conceived and designed the experiments; A.I. performed the majority of the experiments. A.I. wrote the manuscript with help of F.V.B. and S.V.

ABSTRACT

The signal transduction mechanisms of the oxidative stress response in plants remain largely unexplored. Previously, increased levels of cellular hydrogen peroxide (H_2O_2) had been shown to drastically affect the plant transcriptome. Genome-wide transcriptome analyses allowed us to build a comprehensive inventory of H_2O_2-induced genes in plants. Here, the primary objective was to determine the subcellular localization of these genes and to assess potential trafficking during oxidative stress. After high-throughput cloning in Gateway-derived vectors, the subcellular localization of 49 proteins fused to the green fluorescent protein (GFP) was identified in a transient assay in tobacco (*Nicotiana benthamiana)* by means of agro-infiltration and confirmed for a selection of genes in transgenic *Arabidopsis thaliana* plants. Whereas eight of the GFP-tagged proteins are exclusively localized in the nucleus, 23 reside both in the nucleus and cytosol, in which several classes of known transcription factors and proteins of unknown function can be recognized. In this study, the mapping of the subcellular localization of H_2O_2-induced proteins paves the way for future research to unravel the H_2O_2 responses in plants. Furthermore, the effect of increased H_2O_2 levels on the subcellular localization of a subset of proteins was assessed.

A modified version of this chapter has been published in **Plant, Cell and Environment**, **35**, **308-320**, February 2012 by **Inzé, A., Vanderauwera, S., Hoeberichts, F.A., Vandorpe, M., Van Gaever, T. and Van Breusegem, F.** under the title **"A subcellular localization compendium of hydrogen peroxide-induced proteins"**

INTRODUCTION

Because of their sessile lifestyle, plants are permanently exposed to adverse environmental conditions that promote the accumulation of reactive oxygen species (ROS). These harmful by-products of aerobic metabolism react with all cellular components. Accordingly, ROS are considered toxic molecules that cause irreparable cellular damage (Gechev *et al.*, 2006). ROS levels are highly balanced and tightly coordinated by a network of at least 152 genes encoding both ROS-producing and ROS-scavenging enzymes (Mittler *et al.*, 2004). By controlling the ROS toxicity, plants have been able to use ROS as signaling molecules to coordinate a broad range of environmental and developmental processes. For instance, ROS play a major role during growth and development by triggering cell division and cell death, and are also involved in the signal transduction during the response against biotic and abiotic factors (Apel and Hirt, 2004; Van Breusegem and Dat, 2006). Although the signaling function of ROS is now generally accepted, little is known on how these signals are perceived, transmitted and how they finally provoke a specific response. Because many enzymatic components of the antioxidant system of plants are well characterized, perturbation of this scavenging system is an excellent strategy to investigate ROS signaling (Gadjev *et al.*, 2006). As peroxisomal catalases are major scavengers of H_2O_2, reduction of their levels allows *in planta* modulation of the H_2O_2 concentration. Under photorespiration-promoting conditions, such as high light (HL), the subcellular production of ROS is substantially elevated and scavenged readily by a variety of antioxidant systems. In contrast, catalase-deficient plants accumulate photorespiratory H_2O_2, which, in turn, leads to an elaborate transcriptional response (Vandenabeele *et al.*, 2003; Vandenabeele *et al.*, 2004; Vanderauwera *et al.*, 2005). Previous studies with the catalase-deficient model system (Dat *et al.*, 2001) and analysis of four independent genome-wide expression studies in *Arabidopsis thaliana* and *Nicotiana tabacum* have led to an inventory of genes that are responsive to elevated levels of photorespiratory H_2O_2 in leaves (Vandenabeele *et al.*, 2003; Vandenabeele *et al.*, 2004; Vanderauwera *et al.*, 2005; Vanderauwera *et al.*, 2011; Hoeberichts *et al.,* unpublished results). The functional analysis of proteins that are encoded by genes that rapidly respond to H_2O_2 can give novel insights into the early signaling steps triggered by an abrupt increase in H_2O_2 availability.

Although little is known on how cells perceive ROS, different mechanisms are plausible, such as unidentified receptor proteins, direct inhibition of phosphatases by ROS, and redox-sensitive transcription factors (Apel and Hirt, 2004; Mittler *et al.*, 2004). In general, the status of proteins with redox-sensitive amino acids, such as cysteines and methionines, can be oxidized or reduced during oxidative stress in a rapid and dose-dependent manner. Differential subcellular localization caused by redox regulation can be governed conceivably by various processes (Chapter 1). For instance, oxidative modification(s) can set off (i) conformational changes that, in turn, could expose a targeting sequence of

a different subcellular compartment; (ii) multimerization and/or monomerization (Kinkema *et al.*, 2000) by which interacting proteins can be altered and sequester the targeting signals, leading to a differential localization of the target under oxidative stress conditions (Kaminaka *et al.*, 2006; Katiyar-Agarwal *et al.*, 2006); (iii) activation or inhibition of modifying enzymes, such as kinases and phosphatases, which under oxidative stress modify the subcellular localization of their targets; and (iv) elicitation of membrane-bound transcription factors by regulated intramembrane proteolysis (RIP), releasing dormant membrane-anchored transcription factors into the cytosol that subsequently enter the nucleus to regulate the expression of target genes (Seo *et al.*, 2008).

Here, we provide a survey in which the subcellular localization of 49 H_2O_2-induced proteins was systematically determined and their potential subcellular trafficking was assessed during oxidative stress.

RESULTS AND DISCUSSION

Photorespiratory hydrogen peroxide-dependent gene expression

First, we compared the available microarray data sets that profiled the Arabidopsis transcriptome during elevated photorespiratory H_2O_2 levels. Perturbation of catalase activities, by mutation or gene silencing, results in decreased H_2O_2-scavenging during HL stress or low CO_2 availability in C_3 plants (Willekens *et al.*, 1997; Noctor *et al.*, 2002). Catalase loss-of-function mutants are an ideal *in planta* model system to examine the consequences of increased levels of endogenous H_2O_2, because disturbance in H_2O_2 homeostasis can be sustained over time, no invasive techniques are needed and physiologically relevant H_2O_2 levels are obtained (Dat *et al.*, 2001). In three independent studies, the transcriptome of HL-stressed transgenic Arabidopsis leaves perturbed in the most predominant catalase (CAT2) was assessed by three different microarray platforms: Affymetrix GeneChip ATH1, CATMA microarray v2 and Agilent Arabidopsis v3 oligonucleotide array. By monitoring different time points after HL exposure, the dynamics of the transcriptional response could be investigated (Table S1; Vanderauwera *et al.*, 2005; Vanderauwera *et al.*, 2011; Hoeberichts *et al.,* unpublished results). These genome-wide transcriptome analyses allowed us to build a comprehensive inventory of H_2O_2-induced genes (HIGs) in Arabidopsis. To make a robust selection of HIGs for further functional studies, the induction of each transcript was studied in all three experiments. To understand the early signaling steps triggered by an abrupt change in H_2O_2 availability, we selected genes that responded within 1 to 8 h after shifting the catalase-deficient lines to higher irradiance. For a cross-platform comparison, a fold change-dependent threshold was used as selection criterion for differential gene expression (see Materials and Methods). A total of 783 transcripts had a modified expression in response to elevated levels of photorespiratory H_2O_2 and were

designated HIGs. An assessment of overrepresented gene ontology (GO) terms within these 783 HIGs by means of the BiNGO tool (Maere *et al.*, 2005) revealed that the majority of the genes were associated with stress responses (Table S3a). The most significant GO term was 'response to stimulus'. Pairwise comparisons of the three data sets indicated that approximately 20% of the transcripts were induced in at least two experiments (Figure S1a). This intersection was significantly enriched in transcripts belonging to the 'response to heat' GO term (Table S3b), which is in accordance with the well-established relationship between the oxidative and heat stress responses (Miller and Mittler, 2006). Many small heat shock proteins (sHSPs), together with other HSPs and heat shock factors (HSFs), are substantially up-regulated by photorespiratory H_2O_2. In fact, 11% of all heat shock-responsive genes are up-regulated by H_2O_2 in catalase-deficient plants (Vanderauwera *et al.*, 2005). A total of 24 H_2O_2-responsive genes are common for all three data sets and are enriched in genes belonging to the GO molecular function 'oxidoreductase activity' (Table S3c).

Selection of hydrogen peroxide-induced proteins for localization study

The subcellular localization is a key functional characteristic of eukaryotic proteins. To properly execute their biological functions, proteins must be targeted to or retained in the correct subcellular compartments or organelles in time or during a particular stimulus. To obtain a first indication of the subcellular localization, we used the publicly available and high-throughput *in silico* prediction program Proteome Analyst (PA). PA adopts features calculated with PSI-BLAST (Altschul *et al.*, 1997) against the Swiss-Prot database and employs a Naive Bayes algorithm to assign a protein in different subcellular compartments: nucleus, cytosol, chloroplast, mitochondrion, endoplasmic reticulum (ER), Golgi apparatus, lysosome, peroxisome, vacuole and plasma membrane (Szafron *et al.*, 2004). *In silico* prediction of subcellular localizations is an asset in the era of generating large-scale proteomic, transcriptomic and genomic data. However, it still remains a cumbersome task, especially in plants for which the nature or sequence characteristics of many targeting signals are largely elusive.

Of the 783 HIGs, PA assigned 483 proteins to a specific compartment of which the majority was predicted to reside in the nucleus (123) and cytosol (110) (Figure S1b). For 85 transcripts, we initiated an experimental validation of the subcellular location. The selection of these 85 transcripts was based on three criteria, namely, PA-based computational predictions, functional category and responsiveness towards various abiotic stresses. To focus on the most strongly H_2O_2-responsive transcripts of the 783 HIGs, we retained only transcripts with at least a fivefold increase in expression (20% was induced at least 10-fold; Figure S2). We selected predominantly proteins that were (i) predicted to reside in the nucleus or cytosol and omitted chloroplastic or vacuolar predicted proteins (48) and (ii) categorized as (putative) transcription factors and/or nucleic acid-binding proteins and genes of unknown function

(Table S4). In addition, we assessed the responsiveness of the selected transcripts under abiotic stress conditions with the AtGenExpress abiotic stress time series (Kilian *et al.*, 2007) and the UV-A and UV-B light series (Peschke and Kretsch, 2011), and retained only those transcripts that were induced by multiple abiotic stresses. In total, 85 transcripts were obtained by these consecutive selection steps and their abiotic stress response profiles and subcellular localization (both *in silico* and *in vivo*) are presented (Figure 1).

Because our future objective is to identify regulators within H_2O_2-dependent signaling networks, these proteins are primary candidates for possible shuttling between the nucleus and cytosol under oxidative stress conditions. When the co-expression patterns for the 85 HIGs were considered (based on pairwise correlation analyses with the AtGenExpress abiotic stress compendium) by means of the web tool CORNET, almost all genes were part of one or two tightly co-regulated networks (Figure S3). Besides providing insights into the co-expression networks based on transcriptome data, CORNET also integrates the protein interactome, localization data (both *in silico* and experimental) and functional information of Arabidopsis.

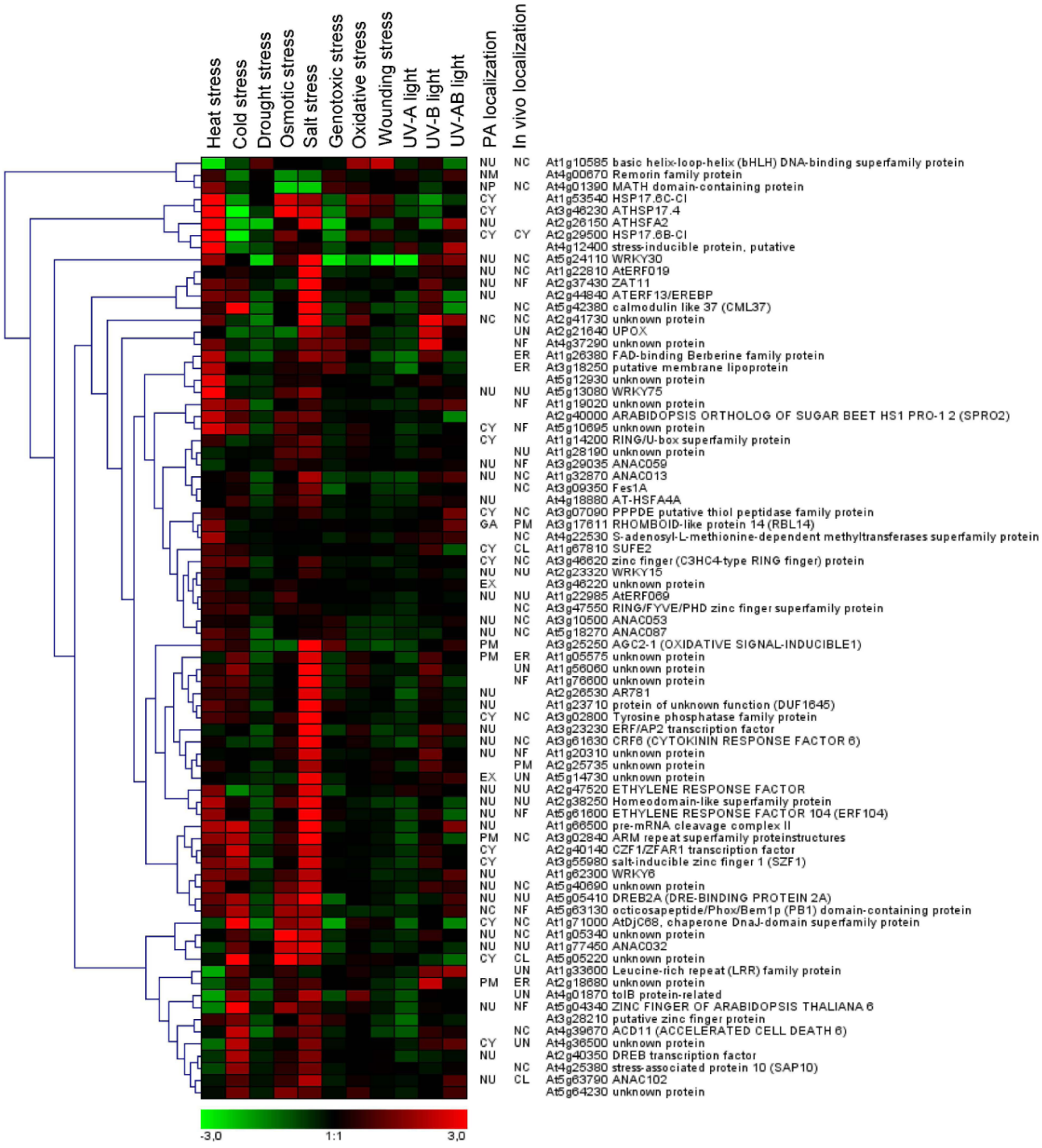

Figure 1. Hierarchical average linkage clustering of the response profiles of 85 HIGs to various abiotic stress conditions. *In silico* predicted subcellular localizations, AGI codes and annotations are indicated. Expression data were obtained with GENEVESTIGATOR (Zimmermann *et al.*, 2004; Zimmermann *et al.*, 2005) and clustered with GENESIS (Sturn *et al.*, 2002). HIG, H_2O_2-induced gene; NU, nucleus; CY, cytosol; NC, nucleus and cytosol; CL, chloroplast; PM, plasma membrane; NM, nucleus and plasma membrane; NP, nucleus and peroxisome; ER, endoplasmic reticulum; EX, extracellular; GA, Golgi apparatus; NF, not GFP fluorescent; UN, undetermined.

Subcellular localization of GFP-tagged hydrogen peroxide-induced proteins

For these 85 H_2O_2-induced proteins, the aim was to fuse the open reading frames (ORFs) to GFP both at the N- and C-terminal ends under the control of the constitutive CaMV35S promoter with Gateway-compatible plant transformation vectors (Karimi *et al.*, 2007). We successfully obtained 52 GFP-ORF and 37 ORF-GFP fusion constructs that were subsequently used in a protein localization assay in abaxial epidermis cells of tobacco leaves via *Agrobacterium*-mediated transient expression. Both the simplicity of the Gateway cloning and the transient infiltration assay provided the desired throughput necessary for such screening. The subcellular localization could be rapidly determined *in situ* in photosynthetically active leaves, which corresponded to tissues in which the HIGs originally had been identified. This technique results in a high transformation frequency in comparison with mesophyll cell transfection or biolistic bombardment of cell cultures in Arabidopsis (Sparkes *et al.*, 2006).

The subcellular localization for each construct was analysed 2 d after *Agrobacterium* infiltration in at least two independent transformation events. From 68 constructs in total, localization data were obtained for 49 different proteins, but for the remaining ones no detectable GFP signal was observed (11) or the construction of GFP fusions was unsuccessful (25). Whereas eight GFP-tagged proteins were exclusively located in the nucleus, 23 resided both in the nucleus and cytosol. As expected, nearly all nucleus-localized proteins were transcription factors or nucleic acid-binding proteins. An exclusively cytosolic localization was seen only for two sHSPs. Three proteins displayed a chloroplastic localization, including unexpectedly a petunia No Apical Meristem, Arabidopsis ATAF1/2 and CUC (NAC) transcription factor. Of six proteins present in the endomembrane compartment, two had distinct plasma membrane localizations. For seven proteins, the subcellular localization could not be assigned to a particular subcellular compartment (Table 1). Comparison between the *in silico* predictions and our experimental data revealed the strength of PA for nucleus-predicted proteins (Figure 2). Almost all members belonging to the functional category 'transcription factor/nucleic acid-binding protein' were predicted to be nuclear. These proteins show a nuclear or nucleocytosolic localization *in vivo*, thereby confirming the *in silico* nuclear predictions. In addition, the majority of the proteins with an unknown function predicted to be nuclear or cytosolic were also confirmed *in vivo*. However, it is important to keep in mind that the prediction of a subcellular localization of a protein cannot replace experimental data, because factors other than the presence of a targeting sequence can define its subcellular localization. For instance, interacting partners can sequester the protein to another subcellular compartment and some proteins have a dynamic localization depending on the plant's developmental stage or environmental stimuli encountered (Chapter 1). Although fluorescent tagging of a protein can provide insights into the *in vivo* (dynamic) subcellular localization, some considerations have to be taken into account. Firstly, the position of the fluorescent tag can alter the location of the native protein. For

example, interactions with other proteins can be abrogated and misfolding can occur. Secondly, constitutive overproduction of the tagged protein can saturate interaction partners and organellar import machineries, leading to protein misfolding and aggregation. Thirdly, in contrast, transgenic production of fusion proteins under the control of the native promoter often generates a very weak signal that, in turn, might limit the throughput of the assay. Notwithstanding these considerations, the strategy used here allows a fast generation of data in a relatively small time frame.

The localizations of WRKY75, DREB2A, RHOMBOID-LIKE 14 (AtRBL14), SUFE2 and AtFes1A have recently been described and confirm our observations (Sakuma *et al.*, 2006; Devaiah *et al.*, 2007; Murthy *et al.*, 2007; Kmiec-Wisniewska *et al.*, 2008; Zhang *et al.*, 2010), whereas the localizations of CYTOKININ RESPONSE FACTOR6 (CRF6) and UPREGULATED BY OXIDATIVE STRESS (UPOX) differed from previously published localizations and will be discussed next.

To validate our findings of the transient expression assay, we produced stably transformed transgenic Arabidopsis plants to allow homologous gene expression and examination of different cell types. In addition, the overall impact of overproduction of the fusion proteins on plant development and the adaptability towards environmental stimuli can be assessed (see further). With the same constructs as those in the transient assay, stable transgenic Arabidopsis plants were obtained for 30 of the 49 proteins. At least two independent transgenic lines per construct were analyzed. Except for two proteins [HSP17.6B-CI (At2g29500) and HYPOXIA-RESPONSIVE ERF2 (HRE2; At2g47500)], the tobacco subcellular localization of all fusion proteins was confirmed in Arabidopsis (Figure 3 and Figures S4-S6).

Table 1. *In vivo* subcellular localizations.

AGI code	Protein description	*In vivo* localization	*N*	*C*	PA	ATH1[a]	CATMA[b]	Agilent[c]
Transcription factors and DNA-binding proteins								
At1g32870	ANAC013 – NTL1	NC	x		NU	2.45	2.57	1.48
At1g77450	ANAC032	NU	x	x	NU	5.03		19.92
At3g10500	ANAC053 – NTL4	NC	x	-	NU			10.43
At5g18270	ANAC087	NC	x	x	NU	4.10	6.33	
At5g63790	ANAC102	CL	x*	x	NU	3.25		28.14
At1g10585	bHLH transcription factor	NC	x		NU	85.12		
At3g61630	CRF6	NC	x	x	NU	1.96	2.18	
At5g05410	DREB2A	NU	x		NU	8.01		96.44
At1g22810	AtERF019	NC	x		NU	24.15		271.18
At1g22985	AtERF069 (CRF7)	NU	x	x	NU	5.64		
At2g38250	Homeodomain-like superfamily protein	NU	x	x	NU	4.98		7.58
At2g47520	HRE2	NU	x*	x	NU	12.99		
At3g47550	RING/FYVE/PHD Zinc Finger	NC	x					6.74
At4g25380	Stress-associated protein 10 (SAP10)	NC	x	x		132.39		
At2g23320	WRKY15	NU		x	NU			16.35
At5g24110	WRKY30	NC	x		NU	14.80		142.00
At5g13080	WRKY75	NU	x		NU	5.69		
At3g46620	C_3HC_4-type RING finger family protein	NC		x	CY			7.17
Proteins of unknown function								
At3g02840	ARM repeat superfamily protein	NC	x		PM	3.43		48.52
At5g42380	Calmodulin-like 37 (CML37)	NC	x			7.61		74.86
At2g21640	UPOX	UD	-	x		4.86	6.64	
At1g26380	FAD-binding berberine family protein	ER	x*	x		26.32		35.44
At4g39670	Glycolipid transfer protein (GLTP), ACDH11	NC	x	x		11.86		
At5g19230	Glycoprotein membrane precursor GPI- anchored	UD	x		PM			11.45
At1g33600	Leucine-rich repeat family protein	UD	x			3.97		10.45
At4g01390	MATH domain-containing protein	NC	x	x	NP	-3.94		1.51
At3g07090	PPPDE putative thiol peptidase	NC	x	x	CY	4.66	5.95	
At3g18250	Putative membrane lipoprotein	ER	x			2.15	9.05	1.23
At3g17611	RHOMBOID-like protein 14 (RBL14)	PM	x		GA	8.36		3.55
At4g22530	SAM-dependent methyltransferase	NC	x	x		12.73		
At4g01870	TolB protein-related	UD	x			43.38		
At5g05220	Unknown protein	CL	-	x	CY	6.35		
At1g05575	Unknown protein	ER		x	PM	7.92		
At1g05340	Unknown protein	NC	x		NU	7.34		
At2g25735	Unknown protein	PM	x	-				17.76
At2g18680	Unknown protein	ER		x	PM	5.21		
At1g28190	Unknown protein	NU	x			3.01		50.46
At5g40690	Unknown protein	NC	x	x	NU	7.86		
At2g41730	Unknown protein	NC	x		NU	27.27		
At5g36925	Unknown protein	NC	x					22.12
At1g56060	Unknown protein	UD	x	x		4.30		
At4g36500	Unknown protein	UD	x	-	CY			13.34
At5g14730	Unknown protein	UD	x		EX	23.18		144.77
Miscellaneous functions								
At1g71000	Chaperone DnaJ-domain superfamily protein	NC	x		CY	17.29		43.72
At3g09350	Fes1A	NC	x	x		15.21	23.81	14.26
At2g29500	HSP17.6B-CI	CY	x	-	CY	3.93	173.87	60.17
At1g07400	HSP17.8-CI	CY	x	-	CY		69.55	13.28
At1g67810	SUFE2	CL	x	x	CY	8.49		
At3g02800	Tyrosine phosphatase	NC		x	CY	6.16		57.79

For 49 HIGs, the *in vivo* subcellular localization was determined. PA-predicted localization, availability of GFP constructs and fold changes in each H_2O_2-related experiment (ATH1, CATMA and Agilent) are indicated.

HIG, H_2O_2-induced gene; NU, nucleus; CY, cytosol; NC, nucleus and cytosol; CL, chloroplasts; NP, nucleus and peroxisome; PM, plasma membrane; ER, endoplasmic reticulum; EX, extracellular; GA, Golgi apparatus; UD, undetermined. *N*, N-terminal GFP fusion; *C*, C-terminal GFP fusion; x, construct available; hyphen, no fluorescence; asterisk, differences in localization patterns (discussed in the text); FC, fold change; WT, wild type; HL, high light.

[a] relative FC in *cat2* mutant versus WT plants after 3 h of HL exposure (Vanderauwera *et al.,* 2005).

[b] relative FC in *cat2* mutant versus WT plants after 8 h of HL irradiation (Hoeberichts *et al.,* unpublished results).

[c] relative FC in *cat2* mutant versus WT plants after 1 h of HL irradiation (Vanderauwera *et al.*, 2011).

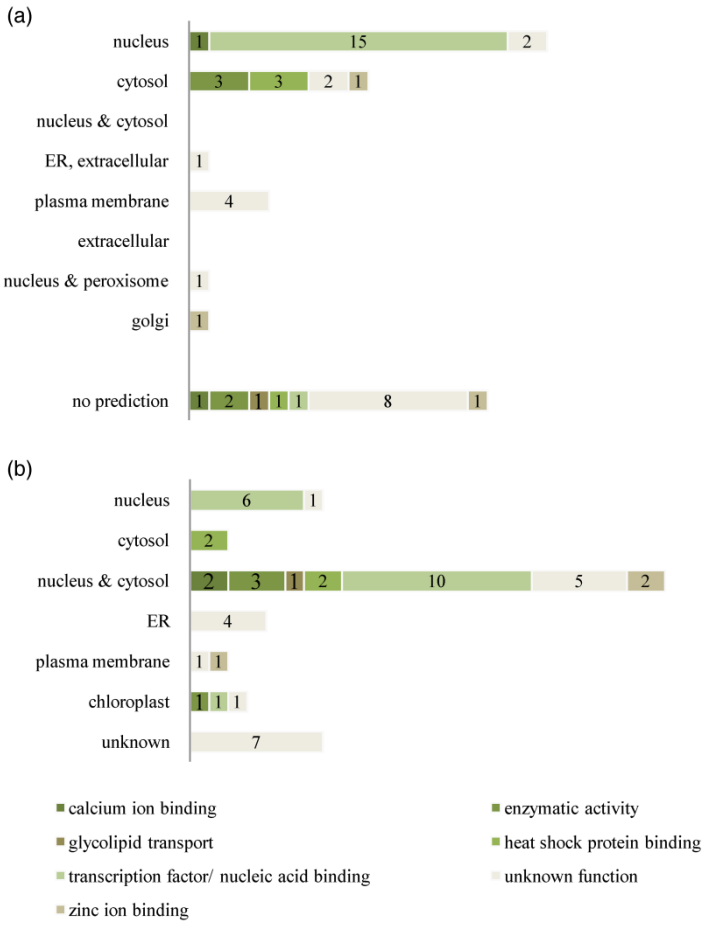

Figure 2. Comparison between *in silico* and *in vivo* localizations of 49 proteins.

(a) Computational prediction of the subcellular localization and functional categorization of 49 H_2O_2-induced proteins. Predictions were obtained with PA (Szafron *et al.,* 2004) and functional categories were defined based on TAIR7 annotation. Numbers of genes in each category are indicated.

(b) *In vivo* subcellular localization was determined by transient expression of N- and/C-terminal GFP fusions in tobacco by means of agro-infiltration. Numbers of proteins in each category are indicated. PA, Proteome Analyst; ER, endoplasmatic reticulum.

NAC transcription factors are putative candidates for relocalization during oxidative stress

In this survey, we analysed the subcellular location of 18 H_2O_2-responsive transcription factors and nucleic acid-binding proteins, such as WRKY, MYB, APETALA2 (AP2), NAC, HSF and basic helix-loop-helix (bHLH; Figure S4). Seven fusion proteins from this category localized exclusively to the nucleus, 10 resided both in the nucleus and cytosol, and one localized unexpectedly in chloroplasts. In total, eight members of the NAC transcription factor family were induced by photorespiratory H_2O_2 (Chapter 3), of which five were included in this study: ANAC013 (At1g32870), ANAC032 (At1g77450), ANAC053 (At3g10500), ANAC087 (At5g18270) and ANAC102 (At5g63790; Ooka *et al.*, 2003; Figure 3a-e; Figure S4a-f). Based on the presence of a putative nuclear localization signal (NLS) in their NAC domain, all were predicted by PA as nuclear. *In vivo*, only ANAC032 appeared to be exclusively nuclear (Figure 3a), while the GFP fluorescence for ANAC013, ANAC053, and ANAC087 was observed also in the cytosol, indicating they could be regulated by nucleocytoplasmic partitioning (Figure 3b-e).

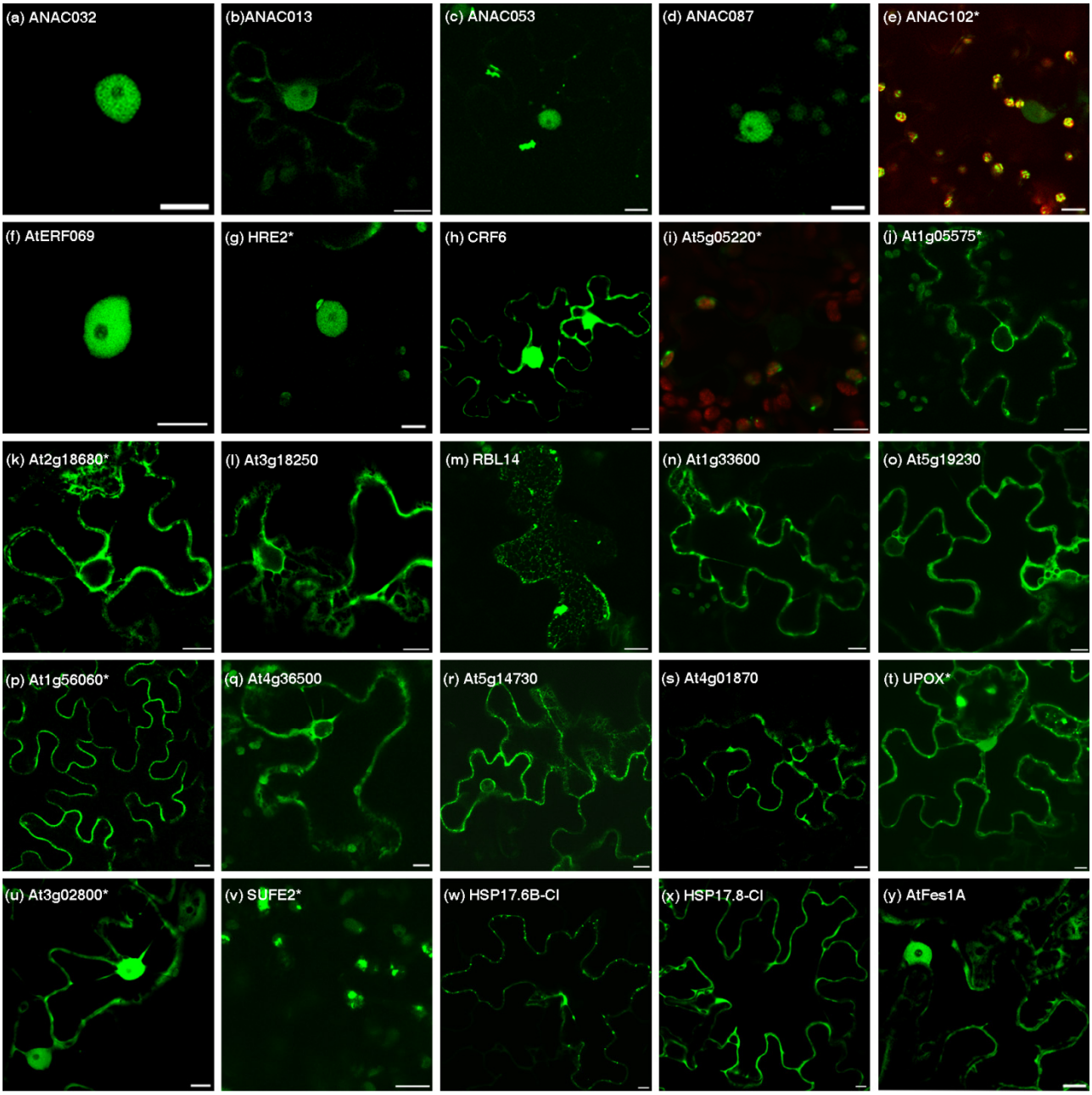

Figure 3. Experimentally determined subcellular localizations of H_2O_2-induced proteins discussed in text. Localizations determined with C-terminal GFP fusions are indicated with an asterisk. Bars, 10 μm.

Both ANAC013 and ANAC053 had previously been identified as possible membrane-associated NAC proteins and were designated as NAC with transmembrane motif 1-like (NTL; Kim *et al.*, 2007), NTL1 and NTL4, respectively. In response to incoming stimuli, membrane-anchored NTL proteins are released and hence activated by a controlled proteolytic cleavage mechanism, called RIP, which provides a rapid post-translational activation of these NAC proteins (Kim *et al.*, 2008 - Chapter 1). Both NTL1 and NTL4 displayed a nucleocytosolic localization in tobacco (Figure 3b-c), besides a vesicular pattern visible in the case of GFP-NTL4 (Figure 3c) and a putative ER localization in the case for GFP-NTL1

(Figure 3b and Figure 4a-d). Several studies have reported that overexpression of NTLs leads to premature proteolytic processing (Kim *et al.*, 2007; Kim *et al.*, 2008; Seo *et al.*, 2010a; Seo *et al.*, 2010b). The nucleocytosolic localizations of NTL1 and NTL4 may be caused by agro-infiltration which results in ROS accumulation and activation of a defense response (Pruss *et al.*, 2008). In turn, this might lead to regulated proteolysis, thereby releasing NTL1 and NTL4 in the cytosol where they are directed to the nucleus by the presence of a NLS. Indeed, NTL4 was recently shown to be proteolytically activated during drought-induced leaf senescence to bind to the promoters of genes encoding ROS biosynthetic enzymes (Lee *et al.*, 2012).

To investigate whether GFP-NTL1 is proteolytically processed, we transiently expressed GFP-NTL1 fusion constructs in *N. benthamiana* and subsequently detected GFP-tagged proteins in total leaf extracts by performing western blot analysis using a monoclonal anti-GFP antibody (Figure 4e). Two bands were detected with similar sizes as the full-size form of GFP-NTL1 (~83 kDa) and the processed form of GFP-NTL1 (GFP-NTL1 ΔC; ~65 kDa; Figure 4e). Next, we assessed whether NTL1 is processed in stable transgenic Arabidopsis *GFP-NTL1*^{OE} lines. While several kanamycin-resistant primary transformants of *GFP-NTL1* and *GFP-NTL4* fusion constructs could be obtained of which several displayed developmental defects and delayed flowering (Figure 4f-g), none of them showed GFP fluorescence. However, we could detect the full-size GFP-NTL1 and a fully processed form (GFP-NTL1 ΔC) by western blot analysis (Figure 4e). In addition, we detected a strong upper band with an estimated molecular mass of approximately 120 kDa that could represent a post-translationally modified (ubiquitinated or glycosylated) form - that has been reported for other NTLs (Seo *et al.*, 2010a) - and a band between the full-size and the fully processed GFP-NTL1, that could represent an intermediary processed form (Figure 4e). Taken together, we could demonstrate that overexpression leads to proteolytic processing of GFP-NTL1 in which the C-terminal transmembrane domain is removed, resulting in the release of GFP-NTL1 ΔC into the cytosol that, in turn, is redirected to the nucleus by the presence of an NLS in its NAC domain (Ooka *et al.*, 2003). Further experiments are necessary to determine the exact subcellular localization of NTL1 and to assess which developmental and/or environmental signal(s) trigger(s) the proteolytically activation of NTL1.

Besides being H_2O_2-responsive, ANAC102 is also induced under hypoxic conditions (Klok *et al.*, 2002; Christianson *et al.*, 2009). In the transient assay, the localization pattern of ANAC102 differed depending on the position of the GFP tag: when GFP was positioned at the N-terminus, it was mainly nucleocytosolic, although a cytoskeletal localization was apparent as well (Figure S4e), but ANAC102-GFP proteins displayed an exclusively chloroplastic localization both in tobacco and in transgenic Arabidopsis plants (Figure 3e; Figure S4f; Chapter 3). Increasing evidence is available that nuclear regulators, such as transcription factors, are present in organelles like mitochondria and plastids (Krause

and Krupinska, 2009). Because the chloroplastic localization of ANAC102 was unexpected, we investigated whether ANAC102 could be released from the chloroplast by a certain stimulus (Chapter 3).

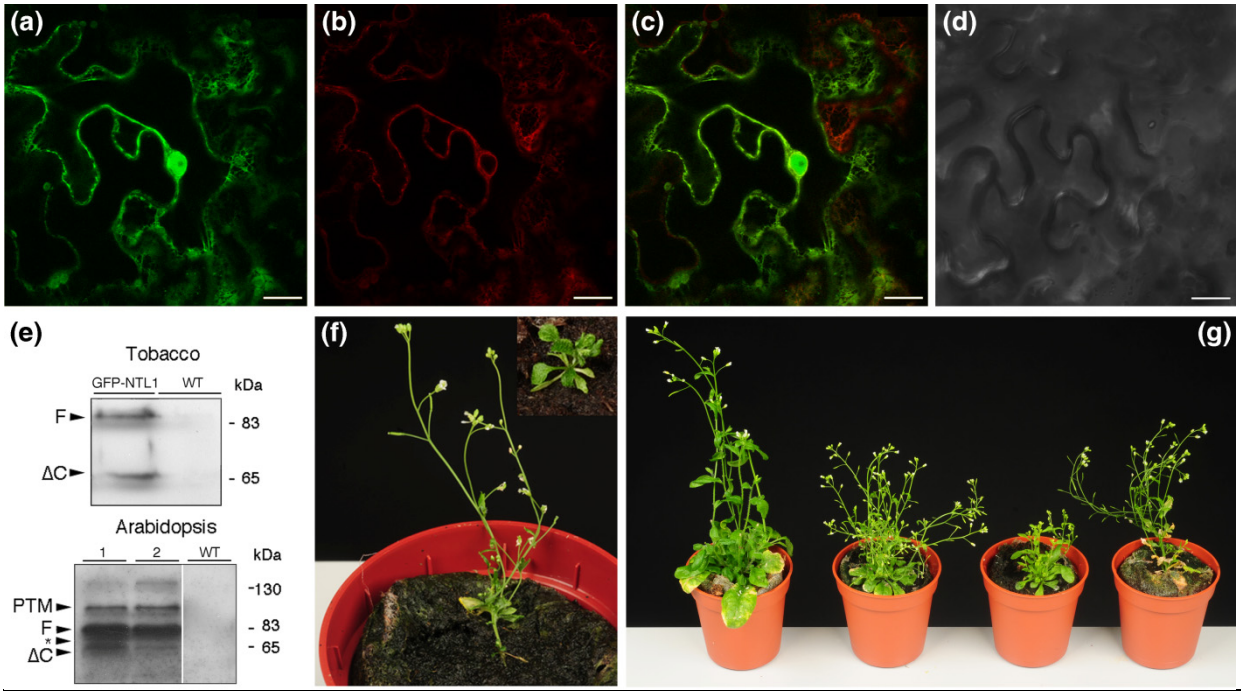

Figure 4. Overexpression of GFP-tagged NTLs results in premature processing leading to a nucleocytosolic localization and developmental defects.

(a-d) Localization of GFP-NTL1 and an mCherry-labeled ER marker (ER-rk; Nelson *et al.*, 2007) in *N. benthamiana.* Pictures depict (a) GFP fluorescence, (b) mCherry fluorescence, (c) merged images from GFP and mCherry fluorescence and (d) bright-field image. Bars, 20 μm.

(e) NTL1 processing. The *GFP-NTL1* gene fusion constructs were transiently or stably expressed in tobacco or Arabidopsis transgenic lines, respectively. Different forms of GFP-NTL1 were immunologically detected using an anti-GFP antibody. In tobacco, we could detect the full-size GFP-NTL1 (F, ~83 kDa) and the fully processed form of GFP-NTL1 (ΔC). Besides the full-size and the processed GFP-NTL1 forms, putatively post-translationally modified forms of GFP-NTL1 (PTM; ~120 kDa) and partially processed forms (indicated with an asterisk) were detected in two independent Arabidopsis transgenic lines (1 and 2). ΔC, fully processed form of GFP-NTL1; F, full-size GFP-NTL1; kDa, kilodalton; PTM, post-translationally modified GFP-NTL1; TR, transient expression; WT, wild type.

(f) 50-days-old (1-month-old, top right corner image) primary transformant of GFP-NTL1 overexpression plant with a stunted growth and severe delayed flowering.

(g) Images of wild type (left) and three independent transgenic lines overexpressing GFP-NTL4 with a bushy stature and loss of apical dominance.

AP2 transcription factors

The AP2 transcription factor family is plant-specific and comprises approximately 145 genes that are characterized by the presence of a DNA-binding AP2/ERF domain of 60–70 amino acids (Gutterson and Reuber, 2004). In our analysis, five members of the AP2 superfamily were included: AtERF069 (CRF7; At1g22985), AtERF071 (At2g47520), AtERF019 (At1g22810), DREB2A (At5g05410), and CRF6 (At3g61630; Figure S4). Both GFP fusions of AtERF069 (CRF7) localized to the nucleus and were excluded from the nucleolus (Figure 3f and Figure S4k). AtERF071, also known as HRE2, is induced under hypoxic conditions and involved in low oxygen signaling (Licausi *et al.*, 2010). Upon transient expression in tobacco, GFP-AtERF071 localizes to the nucleus and cytosol and AtERF071-GFP to the nucleus. In Arabidopsis, however, the N-terminal fusion protein displays an exclusively nuclear localization (Figure 3g). Discrepancies between localizations in tobacco and Arabidopsis might hint towards putative relocalizations during oxidative stress. To investigate the behavior of GFP-tagged AtERF071 during oxidative stress, a transient expression assay in Arabidopsis mesophyll protoplasts was used, but no nucleocytosolic partitioning occurred after the addition of 1.5 mM or 3 mM H_2O_2 (data not shown). This study also included CRF6. CRFs are a small subclass of AP2 domain-containing transcription factors and are characterized by their transcriptional regulation by cytokinins. Arabidopsis contains in total eight CRF proteins that all have a unique CRF domain (Rashotte and Goertzen, 2010). Interestingly, six members of the CRF family relocalize from the cytosol to the nucleus upon cytokinin treatment (Rashotte *et al.*, 2006). Here, CRF6 has a clear nucleocytosolic localization (Figure 3h), which is in contrast with the previous observation that CRF6 is exclusively cytosolic (Rashotte *et al.*, 2006).

Hydrogen peroxide-inducible proteins of unknown function

In total, we studied 25 proteins of unknown function and could assign them to chloroplasts (1), ER/plasma membrane (6), nucleus and cytosol (11) or to no specific compartment (7) (Table 1 and Figure S5). Despite the absence of a genuine N-terminal chloroplast transit peptide, the only protein with unknown function targeted to the chloroplasts is At5g05220 (Figure 3i), although it had been predicted as cytosolic by PA, illustrating the need to experimentally validate *in silico* predictions. Six proteins of unknown function have an ER and/or plasma membrane localization [At1g05575, At2g18680, At3g18250, At3g17611 (AtRBL14), At2g25735, and At1g26380] (Figure S5b-g). Transient expression of both At1g05575 and At2g18680 indicated an ER localization (Figure 3j-k), whereas ectopic overexpression of *At2g18680-GFP* in Arabidopsis also revealed a large granular localization. Because of the hydrophobic nature of this protein, this localization might be an artefact. Both GFP fusions of At3g18250 and AtRBL14 (At3g17611) in tobacco and Arabidopsis appeared in a perinuclear ring, which is characteristic for an ER localization (Figure 3l-m). AtRBL14 contains four helical transmembrane regions (characteristic for rhomboid-like proteins) and a Zinc Finger of the RANBP2-

type. Our observations indicate a punctuate plasma membrane localization of AtRBL14. Because, rhomboid proteins are integral membrane serine proteases known to be involved in RIP, it would be interesting to identify substrates that are potentially cleaved by AtRBL14 under oxidative stress conditions.

Furthermore, 11 H_2O_2-induced proteins with unknown function displayed a nuclear or nucleocytosolic localization (Table 1 and Figure S5h-r), whereas seven fusion proteins (At1g33600, At5g19230, At1g56060, At4g36500, At5g14730, At4g01870 and At2g21640) could not be assigned to a specific subcellular localization (Figure S5s-z). The localization of At1g33600, a leucine-rich repeat-containing protein, exhibited ER characteristics (Figure 3n). Another protein, At5g19230 is an unknown membrane glycophosphatidylinositol (GPI)-anchored protein (Borner *et al.*, 2002; Borner *et al.*, 2003) that contains an N-terminal secretory signal peptide and an hydrophobic C-terminal peptide necessary for GPI-anchoring in membranes. However, removal of this GPI-anchor by cleavage can result in a redistribution in the soluble compartment (Borner *et al.*, 2002; Borner *et al.*, 2003). Interestingly, the transient expression of *GFP-At5g19230* in tobacco revealed a perinuclear ring, a vesicular pattern, some features of the tonoplast and a plasma membrane localization (Figure 3o). Presumably, the presence of the GFP tag at the N-terminus blocks the signal peptide for targeting to the secretory pathway leading to mistargeting, whereas the hydrophobic C-terminal GPI-anchoring site still allows the association with internal membranes resulting in this particular localization. For At1g56060, the localization differed depending on the position of the GFP tag. GFP-At1g56060 had a distinct granular pattern and plasma membrane localization (Figure S5t), whereas production of the C-terminal fusion protein resulted in fluorescence in the ER in some cells, but a clear plasma membrane localization in most cells (Figure 3p). Therefore, we assume that At1g56060 is located in the plasma membrane. The localization of GFP-At4g36500 displayed ER features, such as the perinuclear ring and a reticular pattern (Figure 3q). At5g14730, one of the most highly induced HIGs of our data set, contains a domain of unknown function (DUF1645, IPR012442). The localization of the N-terminal GFP fusion again shows ER features (Figure 3r). However, it is very likely that the presence of GFP hampers efficient ER targeting. At4g01870 contains three domains: one N-terminal dipeptidyl peptidase IV (DPP IV) region domain, one WD-40 β-propeller repeat, and one TolB-related β-propeller domain. In tobacco, GFP-At4g01870 again showed the characteristic perinuclear ring and a plasma membrane localization, but in Arabidopsis, only a plasma membrane localization was apparent (Figure 3s). UPOX (At2g21640) had previously been identified as a mitochondrial oxidative stress marker protein (Sweetlove *et al.*, 2002; Gadjev *et al.*, 2006; Giraud *et al.*, 2008; Ho *et al.*, 2008; Van Aken *et al.*, 2009). In tobacco, UPOX-GFP localizes to punctate structures and to the nucleus and cytosol (Figure 3t), whereas in Arabidopsis, it has a nucleocytosolic localization. Further detailed studies are necessary to pinpoint the exact localization of these unknown

proteins.

HIGs with miscellaneous functions

Besides transcription factors and proteins of unknown function, some transcripts with miscellaneous functions were also included in our study because of their strong induction by photorespiratory H_2O_2 (Table 1 and Figure S6). At3g02800-GFP, a phosphoprotein tyrosine phosphatase, localized to the nucleus and cytosol (Figure 3u). For SufE2 (At1g67810), which is involved in iron-sulphur metabolism, we could confirm the previously reported chloroplastic localization (Figure 3v; Murthy *et al.*, 2007). Furthermore, we also determined the localization of 18 heat shock-responsive genes, including two sHSPs (HSP17.6B-CI and HSP17.8-CI), a DnaJ N-terminal domain-containing protein (AtDjC68) and AtFes1A (At3g09350). Both HSP17.6B-CI and HSP17.8-CI belong to the class I subfamily, suggesting a cytosolic localization (Miernyk, 2001). Interestingly, transient expression of *GFP-HSP17.6B-CI* in tobacco revealed, in addition to a cytosolic, also a granular localization (Figure 3w and Figure S6c). These granules resemble the well-known cytosolic heat stress granules (HSGs) formed under elevated temperatures into which sHSPs - together with other HSPs - are incorporated (Nakamoto and Vígh, 2007). In non-stressed Arabidopsis transgenic plants generated with the same GFP construct, only a cytosolic localization was found (Figure S6d), suggesting that these HSGs might also be formed under other stress conditions, such upon accumulation of ROS that results from *Agrobacterium* infiltration (Pruss *et al.*, 2008). In contrast to the suggested cytosolic localization of HSP17.8-CI (Miernyk, 2001), it was nucleocytosolic both in tobacco and Arabidopsis (Figure 3x). AtFes1A, an ortholog of the human HspBP-1 and yeast Fes1p, had recently been published as a high temperature-induced protein that interacts with HSP70 (Zhang *et al.*, 2010). Transient expression in mesophyll protoplasts of *AtFes1A-GFP* revealed a nucleocytosolic localization (Zhang *et al.*, 2010), in agreement with our observations (Figure 3y).

Localization to subnuclear structures

The use of GFP fusion proteins also enables an *in vivo* localization to subcompartments. For instance, some proteins of our study localized to subnuclear structures (Figure 5). Besides a plasma membrane localization, At2g25735 showed a punctate, nuclear speckle-like pattern that is thought to be in involved in mRNA splicing. Moreover, the nuclear localization pattern of At2g25735 showed also a ring around the nucleolus, which is the site of rDNA transcription and ribosome biogenesis (Figure 5a). Because of the lack of evidence for a functional border between the nucleus and the nucleolus, nucleolar targeting is based on direct and indirect interactions with rDNA and its transcripts (Carmo-Fonseca *et al.*, 2000). The nucleolar ring-like localization might be assigned to one of the three morphological components of the nucleolus (the fibrillar centres, the dense fibrillar component and the granular component; Pendle *et al.*,

2005). Both At1g28190 and At3g02840 displayed an increased accumulation in the nucleolus. In fact, the nucleolus is considered to play a role in multiple stress responses (Figure 5b-c; Shaw and Brown, 2004).

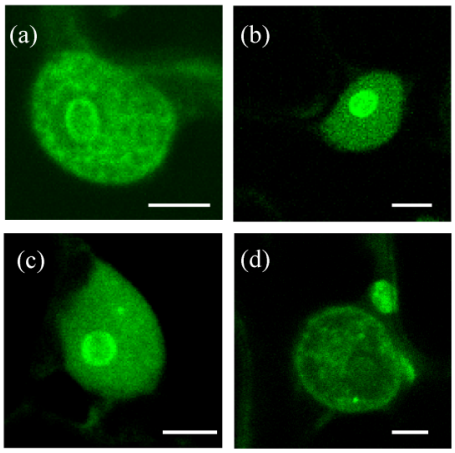

Figure 5. Targeting to subnuclear structures in tobacco.
(a) At2g25735, a protein of unknown function, showing both a plasma membrane localization and a speckle-like pattern in the nucleus. Both At1g28190 (b) and At3g02840 (c) displayed a nuclear localization with an increased accumulation in the nucleolus. (d) AtDjC68, a DnaJ heat shock N-terminal domain-containing protein (At1g71000), localized in nuclear speckles. Bars, 5 μm.

AtDjC68, a DnaJ heat shock N-terminal domain-containing protein (At1g71000) localized in nuclear speckles in tobacco (Figure 5d). Transient expression of *AtDj68* in Arabidopsis mesophyll protoplasts resulted in a nucleocytosolic localization, whereas the addition of 1.5 mM H_2O_2 resulted in an exclusively nuclear localization in almost 15% of the protoplasts (Figure 6).

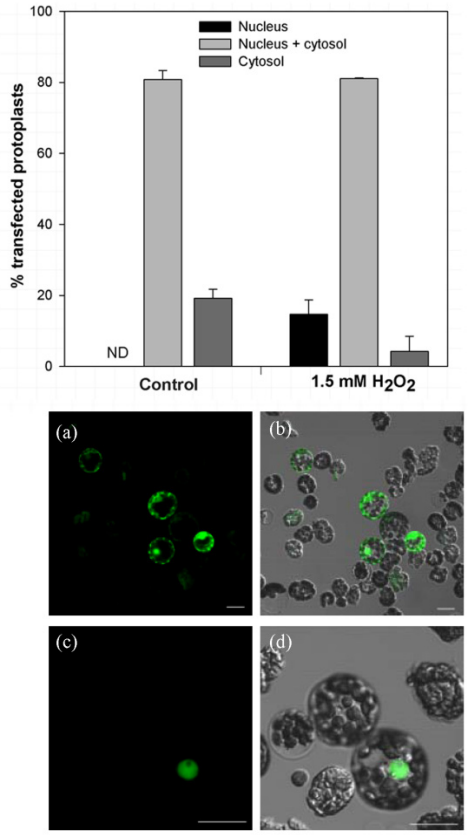

Figure 6. Oxidative stress-induced relocalization of AtDjC68.
Top, Percentage of AtDjC68 transfected Arabidopsis mesophyll protoplasts in the absence (control) or presence of 1.5 mM H_2O_2. Data are means ± SEM (n = 2). In each biological repeat experiment, the subcellular localization of 80-100 GFP-positive protoplasts was assessed.
Bottom, Subcellular localization of AtDjC68 in Arabidopsis mesophyll protoplasts. Before the addition of H_2O_2, a heterogeneous population with cytosolic or nucleocytosolic fluorescence was apparent (a,b). Ten hours after the addition of 1.5 mM H_2O_2, protoplasts with an exclusively nuclear localization were present, whereas the population of protoplasts with a cytosolic localization decreased (c,d). (a,c) GFP fluorescence; (b,d) Merged image of GFP fluorescence and bright-field image. Bars, 20 μm. GFP, green fluorescent protein.

CONCLUSION

With this analysis, we provide a framework of subcellular localizations of oxidative stress-induced genes in plants that depicts the subcellular localization of 49 and 31 H_2O_2-induced proteins, determined by transient expression in tobacco and stable expression in transgenic Arabidopsis plants, respectively. Furthermore, we identified several proteins as putative candidates for relocalization under oxidative stress conditions. Future detailed investigation of these candidates will provide new insights into the dynamic trafficking during oxidative stress and in the overall ROS signaling cascade in plants. The integration of protein interaction data of these H_2O_2-induced proteins together with the subcellular localization data can provide additional information on the biological function of these proteins and their role in the overall response towards H_2O_2.

ACKNOWLEDGEMENTS

We thank Dr. Martine De Cock for help in preparing the manuscript. This work was supported by Ghent University (Multidisciplinary Research Partnership 'Biotechnology for a Sustainable Economy' project no. 01MRB510W). A.I. and S.V. are predoctoral and postdoctoral fellows of the Research Foundation-Flanders, respectively.

MATERIALS AND METHODS

Microarray meta-analysis

For the comparative analysis on transcriptional changes induced in catalase-deficient plants after HL exposure, we compiled the data of one in-house stored and two published H_2O_2-dependent microarray experiments that were generated with different platforms (for experimental details, see Table S1). A previous cross-platform comparison of Affymetrix ATH1, Agilent and Complete Arabidopsis Transcriptome MicroArray (CATMA) arrays revealed a comparable sensitivity and a fair agreement of signal intensities (Allemeersch *et al.*, 2005). From the Affymetrix ATH1 data set, genes showing at least a threefold induction in CAT2HP1 plants after 3 h of HL exposure were selected (Vanderauwera *et al.*, 2005), whereas from the Agilent Arabidopsis V3 data set, genes showing a significant induction [two-way analysis of variance, interaction significance + genotype and treatment significance (P<0.001; Q<0.05), and threefold induction] in CAT2HP2 plants after 1 h of HL exposure were retained (Vanderauwera *et al.*,

2011) and from the CATMA (v2.3, ArrayExpress accession n° A-MEXP-120) experiment, a data set was created of genes showing a significant induction [mixed model according to Wolfinger *et al.*, 2001): interaction significance (P<0.001)] in CAT2HP1 plants after 8 h of HL irradiation (Hoeberichts *et al.,* unpublished results).

Subcellular localization predicted *in silico* with Proteome Analyst

Protein sequences were downloaded from The Arabidopsis Information Resource (TAIR7; Rhee *et al.*, 2003; http://www.arabidopsis.org), converted to FASTA format and analyzed in Proteome Analyst (PA), a web-based tool for high-throughput prediction of protein features (http://www.cs.ualberta.ca/~bioinfo/PA; Szafron *et al.*, 2004).

Hydrogen peroxide-induced genes within different abiotic stresses

Within the different tools of GENEVESTIGATOR, the Response Viewer was used to find the response profiles of individual H_2O_2-induced genes (designated HIGs) to various environmental stimuli (Zimmermann *et al.*, 2004; Zimmermann *et al.*, 2005). Out of the different conditions annotated, the AtGenExpress abiotic stress time series (Kilian *et al.*, 2007) and AtGenExpress light treatments UV-A and UV-AB (Peschke and Kretsch, 2011) were selected. Expression values were median-centered across each gene and subjected to hierarchical average linkage clustering (Euclidian distance) using the GENESIS software (Sturn *et al.*, 2002).

BiNGO analysis

Overrepresented gene ontology (GO) terms in the HIG data set were identified with the Biological Networks Gene Ontology (BiNGO) tool (Maere *et al.*, 2005) in Cytoscape 2.6.0 (Shannon *et al.*, 2003). The hypergeometric test was chosen at a significance value of 0.05 with the Benjamini and Hochberg false discovery rate correction for multiple testing (Benjamini and Yekutieli, 2001).

CORNET analysis

The online data mining tool CORrelation NETworks (CORNET; http://bioinformatics.psb.ugent.be/cornet; De Bodt *et al.*, 2010) provides insights in co-expression networks with transcriptome data and integrates proteome data, localization data (both *in silico* and experimental) and functional data of Arabidopsis. Out of the different predefined data sets available, the AtGenExpress abiotic stress time series (Kilian *et al.*, 2007) were used. With the co-expression tool, the Pearson correlation coefficient threshold was set >0.7 and pairwise correlation between HIGs was calculated. The output was visualized in Cytoscape 2.6.0 (Shannon *et al.*, 2003).

Cloning of open reading frames

Full-length open reading frames (with and without stop codon) were amplified by polymerase chain reaction (PCR) from first-strand cDNA of *Arabidopsis thaliana* (L.) Heynh. ecotype Columbia (Col-0), respectively, with gene-specific primers extended with the *attB* sites for Gateway cloning (Invitrogen Carlsbad, CA, USA) (Table S2). PCR reactions were run with high-fidelity Phusion DNA polymerase (Finnzymes OY, Espoo, Finland) and fragments were cloned into the Gateway entry vectors (Invitrogen) according to the manufacturer's instructions.

Generation of GFP-protein fusion constructs

Constitutive promoter-driven expression clones were generated in the binary destination vectors pK7FWG2 and pK7WGF2 (Karimi *et al.*, 2007), resulting in C- and N-terminal green fluorescent protein (GFP)-protein fusions, respectively, under the control of the cauliflower mosaic virus 35S (CaMV35S) promoter. All constructs were transferred into the *Agrobacterium tumefaciens* strain C58C1 harboring the virulence plasmid MP90. The 35S promoter-driven GFP-fusion constructs for protoplast transfection were made by means of the high-copy plasmids p2FGW7 and p2GWF7, resulting in N- and C-terminal fusions, respectively (Karimi *et al.*, 2007).

Transient expression and stable genetic transformation

All GFP protein fusion constructs were transiently expressed in leaf epidermal cells of 5-week-old wild-type tobacco (*Nicotiana benthamiana*) by *Agrobacterium tumefaciens*–mediated leaf infiltration (Sparkes *et al.*, 2006). Arabidopsis mesophyll protoplasts were prepared and transfected according to Yoo *et al.*, (2007). Protoplasts (1 x 10^5) were incubated in washing and incubation solution (0.5 M mannitol, 4 mM 2-(N-*morpholino*)ethanesulfonic acid, pH 5.7, and 20 mM KCl) supplemented with 1.5 mM or 3 mM H_2O_2 at 21°C (continuous light). To identify potential relocalizations, the subcellular localization of, in total three times, 100 protoplasts was assessed at different time points by laser scanning confocal microscopy.

For stable expression, the constructs were transformed into Arabidopsis Col-0 plants by *Agrobacterium*-mediated floral dip (Clough and Bent, 1998). Kanamycin-resistant plants were selected on half-strength (½) Murashige and Skoog (MS) medium (Duchefa Biochemie, Haarlem, The Netherlands), 1% (w/v) sucrose, 0.7% (w/v) agar, pH 5.7 and 35 mg L^{-1} kanamycin (Sigma-Aldrich, St. Louis, MO, USA) at 21°C and 16-h light/8-h dark photoperiod. For each construct, 10 kanamycin-resistant 3-week-old plants were analyzed for GFP fluorescence using laser scanning confocal microscopy. Homozygous lines with a single T-DNA locus were selected by segregation.

Confocal microscopy and image analysis

The adaxial leaf epidermis was scanned by fluorescence microscopy with a confocal microscope 100M and software package LSM 510 version 3.2 (Zeiss, Jena, Germany), equipped with a 63x water corrected objective (numerical aperture 1.2). GFP fluorescence was imaged in a single channel setting with 488 nm for GFP excitation.

Expression analysis

Plants were grown *in vitro* on ½ MS medium (21°C, 16-h/8-h photoperiod) till stage 1.04 (4^{th} true leaf 1 mm in size; Boyes *et al.*, 2001). For each transgenic line, 32 plants were pooled and crushed with liquid nitrogen. For the northern blot analysis, total RNA was prepared using TRI Reagent (MRC, USA) according to manufacturer's instructions. For each sample, 8 μg RNA was mixed with 15 μL 100% DMSO, 3 μL 40% glyoxal and 3 μL 1 M sodium phosphate. After electrophoresis in 1% agarose gels, RNA was transferred overnight to a Hybond N^+ membrane (https://www.roche-applied-science.com). Subsequently, the RNA was cross-linked to the membrane using a UV cross-linker. After a pre-hybridization step, the membrane was hybridized overnight with full-length cDNA probe generated by PCR from cDNA clones using the DIG probe synthesis kit (Roche). After washing at high-stringency (2 x 5' at 2 x SSC, 0.1% SDS followed by 2 x 15' at 0.2 x SSC, 0.1% SDS at 68°C), membranes were visualized with chemiluminescence using an anti-DIG antibody. As a loading control, rRNA was visualized by methylene blue staining of membranes, using standard methods.

For the western blot analysis, total protein extracts were prepared by grinding leaf material (100 mg) in 200 μL of extraction buffer (100 mM HEPES (pH 7.5), 1 mM EDTA, 10 mM β-mercaptoethanol and 1 mM phenylmethanesulfonylfluoride) and a protease inhibitor cocktail (COMPLETE; Roche). Insoluble debris was removed by centrifugation at 20800 x g for 15 min at 4°C. Protein concentrations were determined with the Bradford method (Zor and Selinger, 1996). Proteins (10 μg) were separated on a 12.5% SDS PAGE gel, transferred to a P membrane (Millipore, http://www.millipore.com/) and immunodetected with the Living Colors A.v. Monoclonal antibody (JL-8; Clontech Laboratories; http://www.clontech.com/) by means of the Western Lightning kit (GE-Healthcare; http://gehealthcare.com/).

ADDENDUM

Phenotypic and expression analyses of Arabidopsis lines overexpressing GFP-tagged hydrogen peroxide-induced genes

Stable expression of GFP-tagged HIGs not only allowed us to consolidate the subcellular localizations, but also permitted us to assess the impact on plant growth and development. In total, 60 fusion constructs (both N- and C-terminal), that were functional in the primary screen in *N. benthamiana*, were introduced into Arabidopsis wild-type plants. Per construct, at least 10 kanamycin-resistant primary transformants were analyzed for GFP fluorescence using confocal laser scanning microscopy. In total, GFP-positive transgenic lines were obtained for 34 constructs, representing 30 different proteins (Table 2).

Table 2. Overview of the transgenic Arabidopsis lines expressing HIGs.

AGI code	Protein description	*In vivo* localization	Generation	Phenotype
At2g21640	**UPOX**	**UD**	**T3**	
At5g42380	Calmodulin-like 37 (CML37)	NC	T1	
At5g13080	WRKY75	NU	T1	
At2g29500	**HSP17.6B-CI**	**CY**	**T3**	
At1g07400	HSP17.8-CI	CY	T2	
At3g02800	**Tyrosine phoshatase**	**NC**	**T3**	**bigger rosettes when grown *in vitro***
At5g36925	**Unknown protein**	**NC**	**T3**	**bushy stature, dark curled leaves**
At3g47550	**RING/FYVE/PHD zinc finger**	**NC**	**T3**	**premature death**
At5g24110	**WRKY30**	**NC**	**T3**	**curled leaves**
At1g05340	Unknown protein	NC	T1	
At1g10585	bHLH transcription factor	NC	T2	
At1g22810	AtERF019	NC	T1	smaller, died prematurely
At1g22985	**AtERF069**	**NU**	**T3**	**smaller**
At1g22985*	**AtERF069**	**NU**	**T3**	**smaller**
At1g26380	FAD-binding berberine family protein	ER	T2	
At1g26380*	FAD-binding berberine family protein	ER	T2	
At1g56060	**Unknown protein**	**UD**	**T3**	**smaller, delayed flowering**
At1g77450	**ANAC032**	**NU**	**T3**	
At2g18680	Unknown protein	ER	T2	
At2g18680*	Unknown Protein	ER	T1	
At2g38250	Homeodomain-like superfamily protein	NU	T1	
At2g41730	Unknown protein	NC	T2	
At2g47520	HRE2	NU	T2	
At3g07090	PPPDE putative thiol peptidase	NC	T2	
At3g18250	Putative membrane lipoprotein	ER	T2	
At3g61630	**CRF6**	**NC**	**T3**	**darker plants, seedless siliques**
At4g01390	**MATH domain-containing protein**	**NC**	**T3**	**severe defects at seedling stage**
At4g01870	TolB protein-related	UD	T2	
At4g39670	ACDH110	NC	T1	
At3g17611	RHOMBOID-like protein 14 (RBL14)	ER	T2	
At5g40690	Unknown protein	NC	T1	abnormal leave shape, smaller plants
At4g22530	SAM-dependent methyltransferase	NC	T2	
At4g22530*	SAM-dependent methyltransferase	NC	T2	
At5g63790	**ANAC102**	**CL**	**T3**	

For 30 HIGs, GFP-positive transgenic Arabidopsis lines were obtained. The *in vivo* localization, generation and observed phenotypes are indicated. C-terminal GFP fusion constructs are indicated with an asterisk and constructs for which homozygous transgenic lines are available are indicated in bold. HIG, H_2O_2-induced gene; NU, nucleus; CY, cytosol; NC, nucleus and cytosol; CL, chloroplasts; ER, endoplasmic reticulum; UD, undetermined.

Within these GFP fusion transgenics, eleven of them showed phenotypic abnormalities ranging from improved or decreased growth, delayed flowering, aberrant leaf morphology to severe developmental defects or even premature death (Table 2 and Figure 7). For instance, overexpression of *GFP-At5g36925*, a peptide of unknown function, led to a bushy stature with thick contorted leaves (Figure 7a – Chapter 5). Overexpression of an N-terminal fusion of *At3g47550*, encoding a RING/FYVE/PHD Zinc Finger family protein, resulted in premature death (Figure 7b and Figure 8d). Although *GFP-At3g47550* transcripts were detected with northern blot analysis (Figure 8b), GFP-At3g47750 was not detected by western blot analysis (Figure 8c), indicating that the observed phenotype could be a loss-of-function phenotype. In fact, constitutive and strong expression of GFP-tagged proteins often results in gene-silencing or protein aggregation that often leads to protein degradation (de Folter *et al.*, 2007; Miyawaki, 2011). Several independent overexpression lines of *GFP-WRKY30* had curled leaves (Figure 7b and Figure 8d) and accumulated processed forms of GFP-WRKY30 (Figure 8c). Several GFP fusion transgenic lines were visibly smaller in comparison to wild-type plants. For example, *GFP-AtERF019* overexpression lines were significantly smaller and died prematurely. In the case of GFP-At1g56060, a protein of unknown function, the phenotype was dependent on the degree of expression (Figure 7e,f). While strong overexpression lines of *GFP-At1g56060* were markedly smaller than wild type (Figure 7e and Figure 8), plants of the weak overexpression line (Figure 7f and Figure 8) seemed at first comparable to wild-type plants but were later significantly darker and developed serrated leaves (Figure 7f). As GFP-At1g56060 was localized in granules (see above) that could represent GFP aggregates (Miyawaki, 2011), this phenotype could be the result of the formation of non-functional protein complexes. In the case of CRF6, we obtained several independent stable overexpression transgenic lines of both N- and C-terminal fusions with seedless siliques (Figure 7g,h). In fact, double mutants of both *crf5* and *crf6* showed a similar phenotype (Rashotte and Goertzen, 2010). As CRFs form homo- or heterodimers (Rashotte and Goertzen, 2010), the overexpression of a GFP-tagged version of CRF6 could result in a dominant negative effect by sequestering both CRF6 and CRF5. A drastic phenotype was seen in several independent overexpression lines of *GFP-At4g01390*: seedlings had a short swollen root and hypocotyls, and thick amorphous cotyledons that often retained the seed coat.

Figure 7. Phenotypes of transgenic Arabidopsis plants overexpressing GFP fusion constructs.

(a) 50-days-old *GFP-At5g36925*^{OE} plant (T1). (b) 2-week-old homozygous transgenic line expressing a C-terminal GFP fusion construct of *At3g47550*, encoding a RING/FYVE/PHD ZF family protein, displaying premature death. (c) 1-month-old wild type (left) and three primary transformants overexpressing *GFP-WRKY30*. (d) 1-month-old wild type (left) and a *GFP-AtERF019*^{OE} line (T1). (e,f) 2-week-old independent homozygous lines with strong (e) or weak (f) expression of an N-terminal GFP fusion of At1g56060, a protein of unknown function. (g) 1-month-old wild type (left) and a primary transformant with weak *CRF6-GFP* expression. (h) From left to right: wild type, two primary transformants harboring the *GFP-CRF6* construct and one the *CRF6-GFP* construct. (i,j) 12-days-old homozygous transgenic plant overexpressing an N-terminal GFP fusion of a MATH domain containing protein (At4g01390). Images were taken with stereomicroscope (i) or a stereomicroscope equipped for epifluorescence imaging (j).

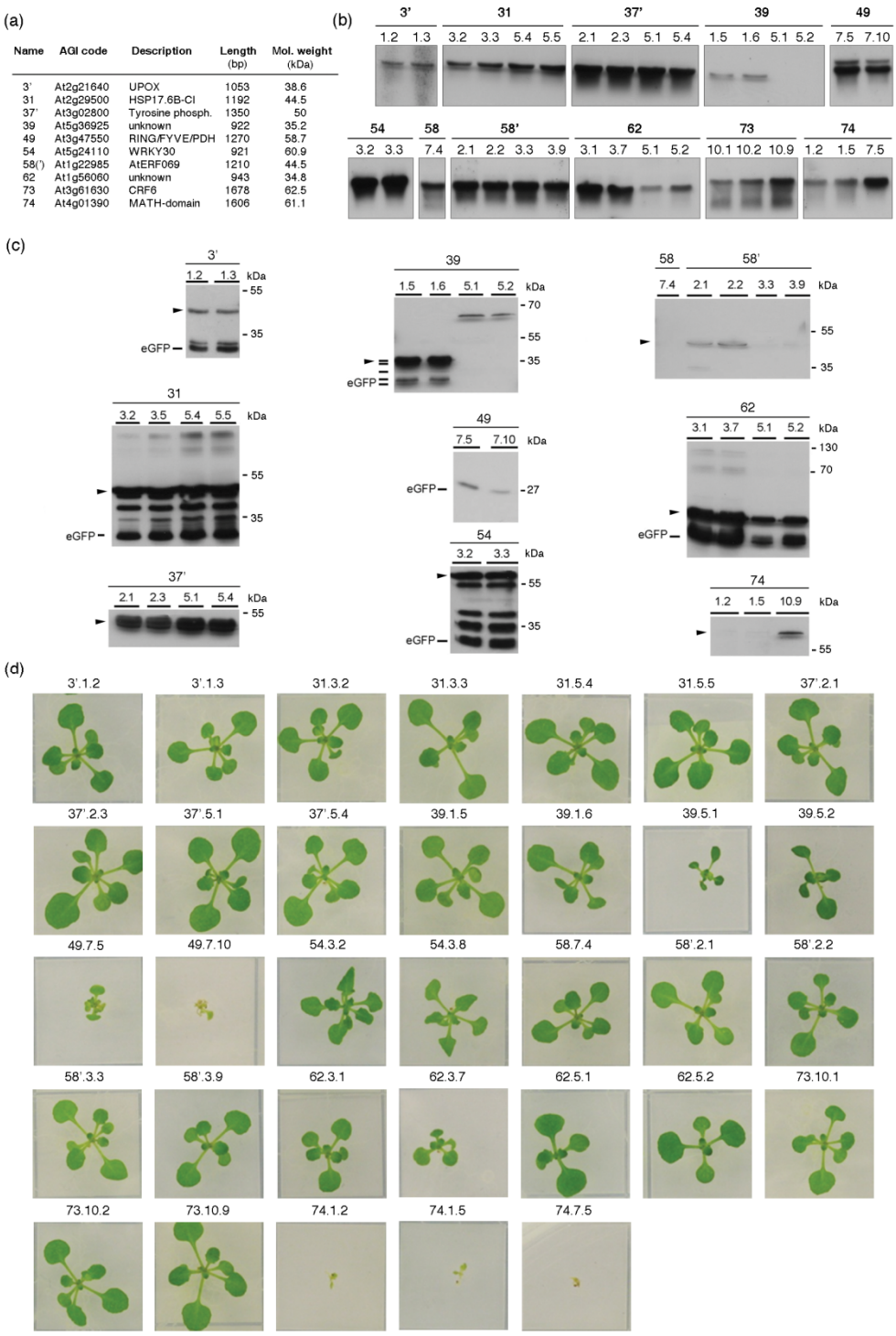

Figure 8. Expression and phenotypic analyses of homozygous Arabidopsis lines expressing GFP fusion constructs.

(a) Overview of the homozygous lines used in this expression analyses. The length of the fusion construct and the molecular weight are indicated. Bp, base bairs; kDa, kilodalton.

(b) Northern blot analysis. Total RNA was extracted from 2-week-old seedlings and mRNA was detected using gene-specific probes.

(c) Detection of GFP-tagged proteins by western blot analysis using a monoclonal anti-GFP antibody. Full-size GFP-tagged proteins are indicated by an arrowhead.

(d) Images of 2-week-old of representative homozygous plants expressing GFP fusion constructs.

SUPPORTING INFORMATION

Supplemental Figures S1-6 and Tables S1-4 are available from the online version of this article (http://onlinelibrary.wiley.com/doi/10.1111/j.1365-3040.2011.02323.x/suppinfo).

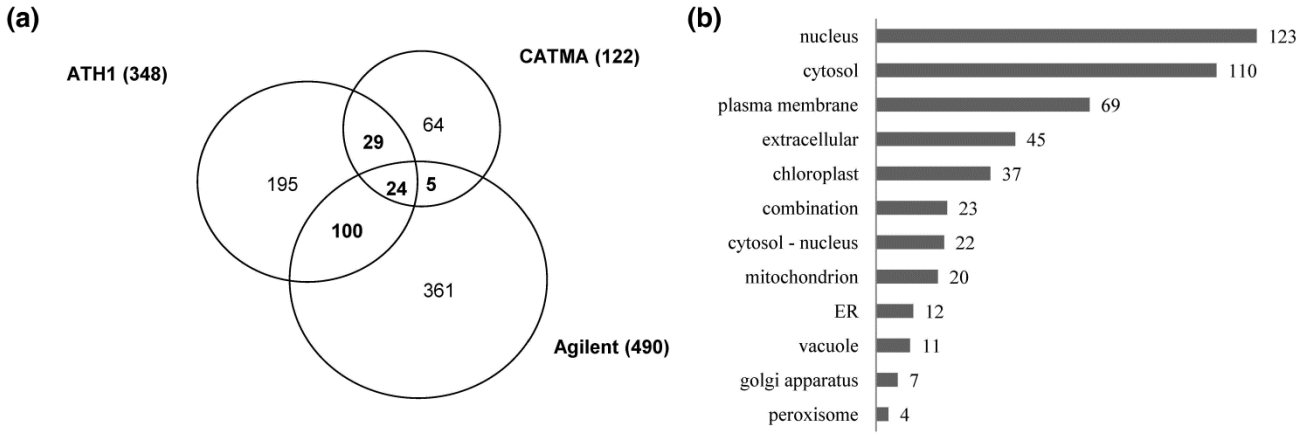

Figure S1. Microarray comparison and *in silico* prediction of the subcellular localization of 783 HIGs.

(a) Venn diagram showing the distribution of 783 HIGs within the three microarray experiments (Affymetrix, CATMA, and Agilent). Numbers of genes induced within each experiment are indicated in parentheses. In total, 24 genes (3%) were positively regulated in all experiments, whereas 158 transcripts (20%) accumulated in at least two experiments.

(b) *In silico* prediction of the subcellular localization of 783 HIGs by Proteome Analyst (PA; http://www.cs.ualberta.ca/~bioinfo/PA/; Szafron *et al.*, 2004). The different subcellular localization sites are indicated together with the number of proteins predicted to reside within that subcellular compartment. Proteins predicted to reside in two or more subcellular compartments are grouped in 'combination', with the exception of the nucleocytosolic localized proteins that are presented separately. Most proteins are predicted to reside in the nucleus, cytosol or plasma membrane. Entries without a significant *in silico* prediction were not included.

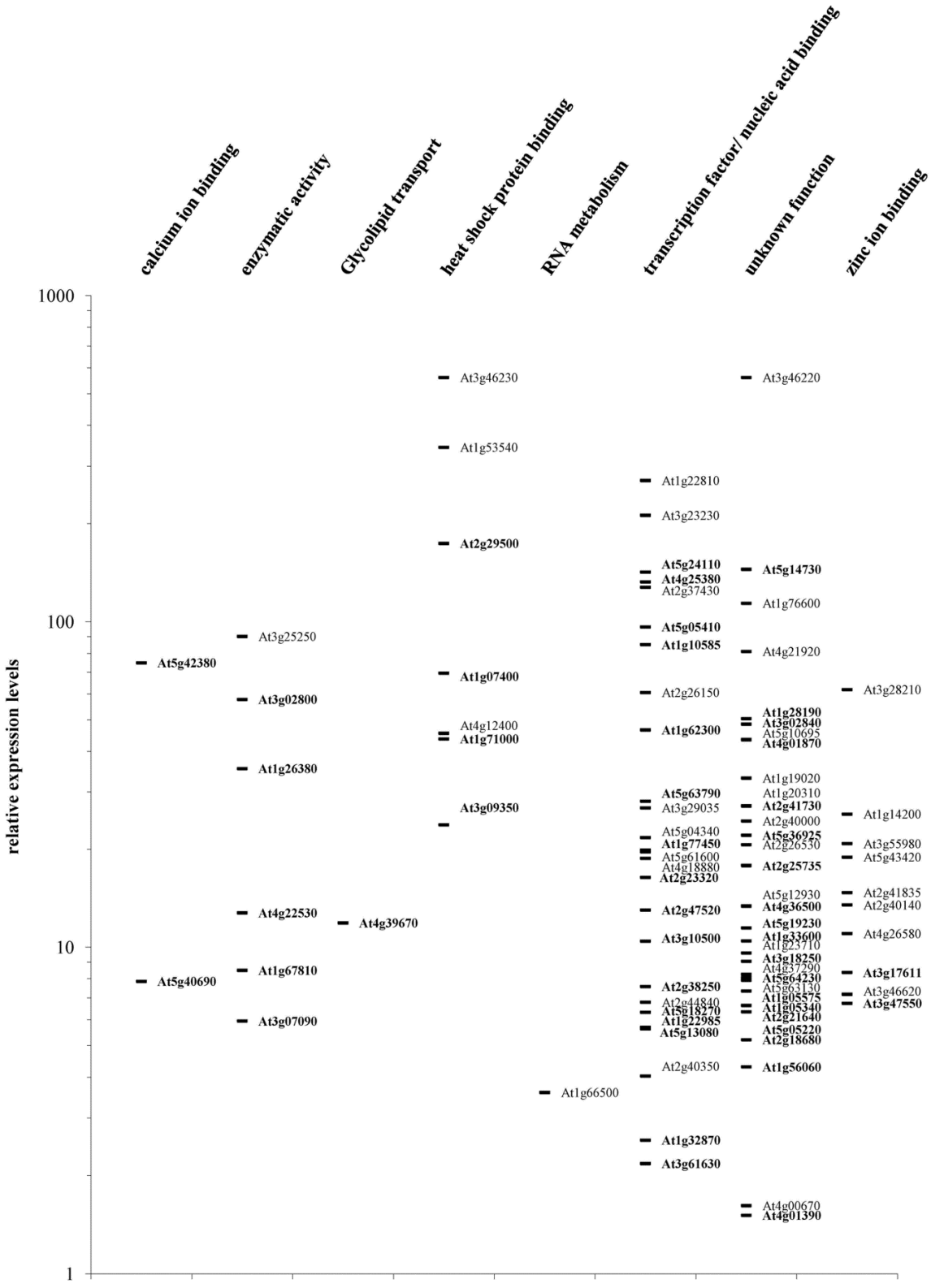

Figure S2. Distribution in transcriptional induction towards photorespiratory H_2O_2 of the 85 selected HIGs.

Genes were first categorised according to their functional annotation. For each gene, the strongest response towards photorespiratory H_2O_2 was plotted in terms of peak fold change in gene expression on the y-axis. Three genes were induced by photorespiratory H_2O_2 more than 250-fold: 342-fold, 271-fold, and 561-fold for AtHSP17.6-CI (At1g53540), AtERF019 (At1g22810), and a gene of unknown function (At3g46280), respectively. For 49 HIGs, the protein localizations were determined (indicated in bold).

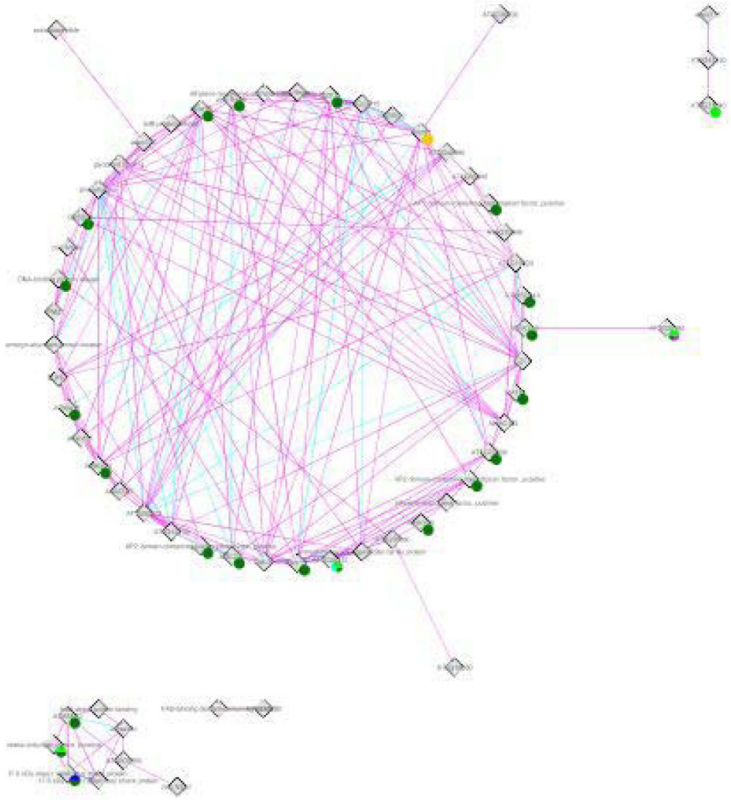

Figure S3. Co-expression analysis of 85 HIGs during abiotic stress with CORNET. The co-expression network was based on pair-wise correlation analyses with the AtGenExpress abiotic stress compendium by means of web tool CORNET. Nearly all genes were part of one or two tightly co-regulated networks.

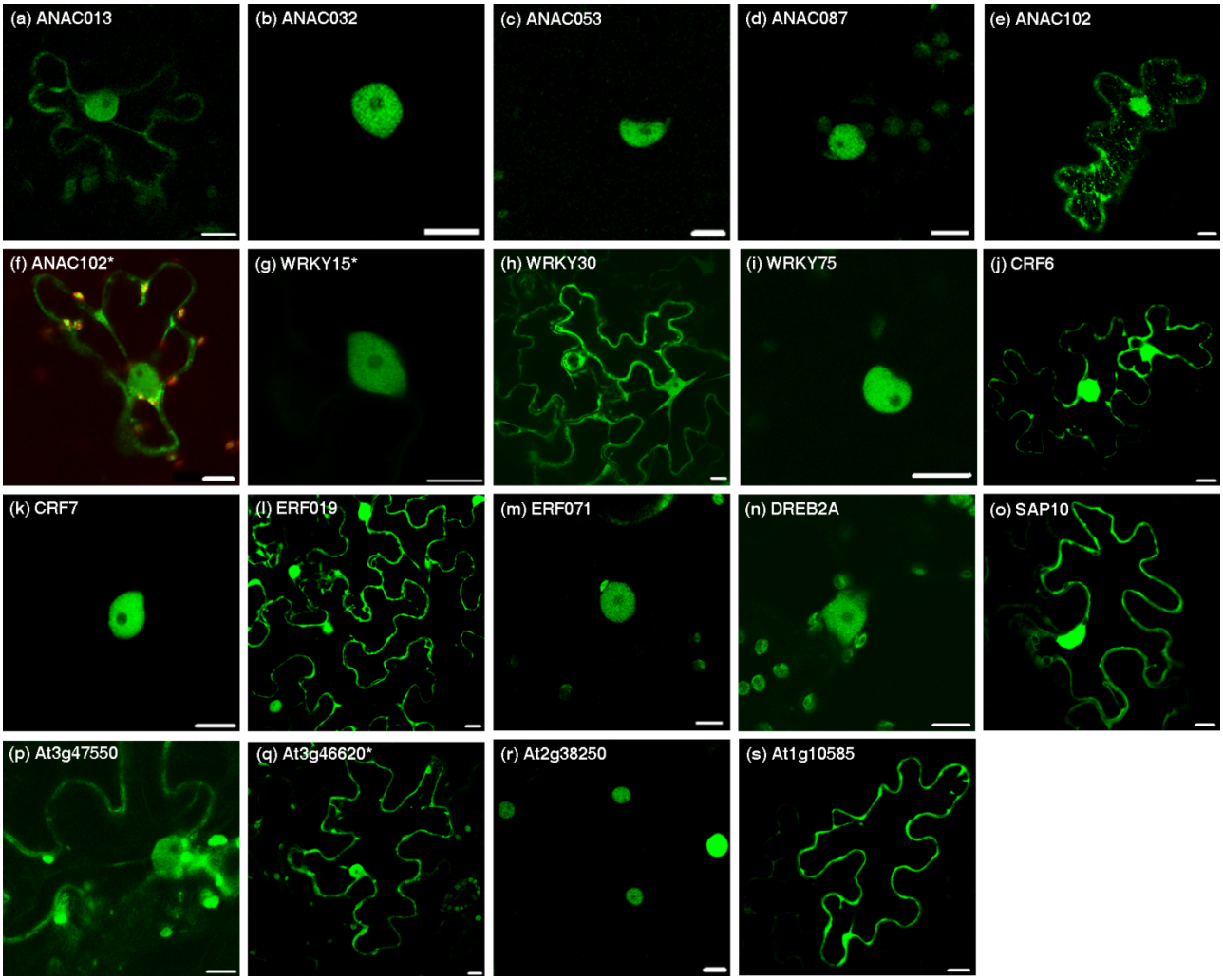

Figure S4. *In vivo* localization of transcription factors and nucleic acid-binding proteins in *N. benthamiana*.

Localizations determined with C-terminal GFP fusions are indicated with an asterisk. Bars, 10 μm.

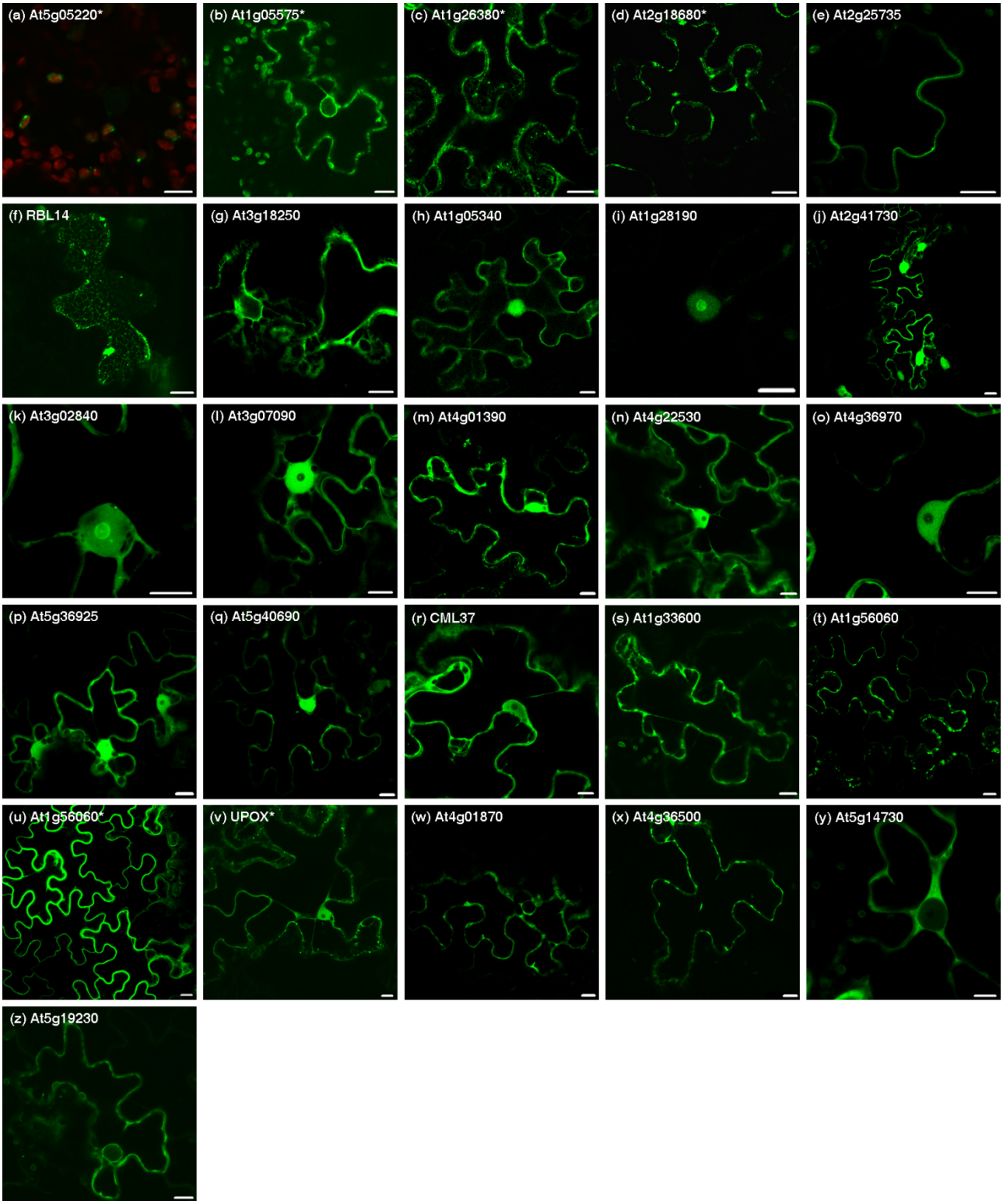

Figure S5. *In vivo* localizations of proteins of unknown function in *N. benthamiana.*

Localizations determined with C-terminal GFP fusions are indicated with an asterisk. Bars, 10 μm.

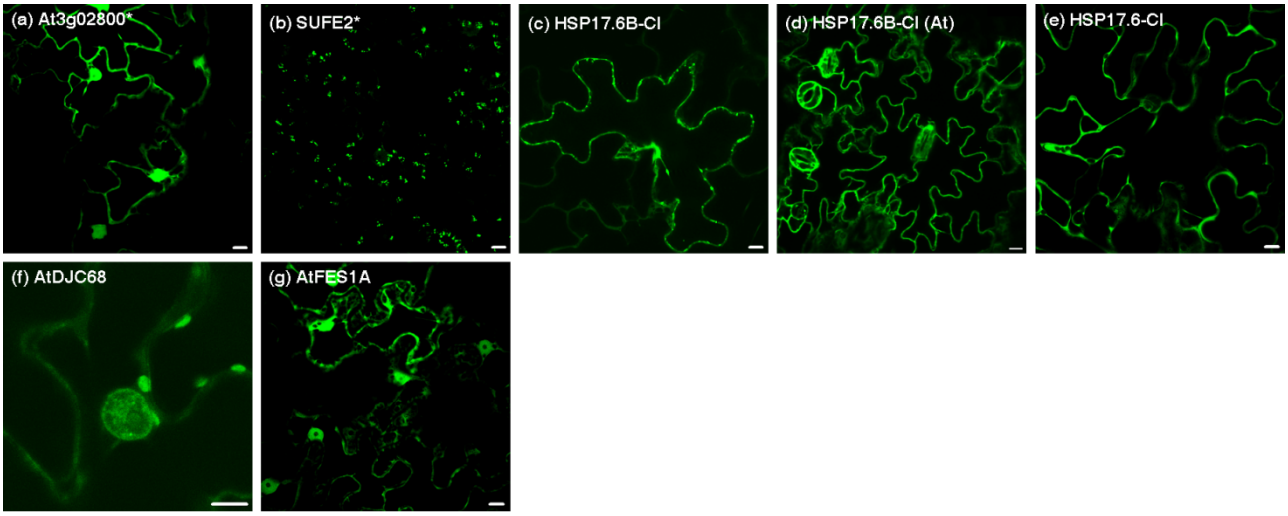

Figure S6. *In vivo* localization of proteins with miscellaneous functions in *N. benthamiana* and *A. thaliana* (At). Localizations determined with C-terminal GFP fusions are indicated with an asterisk. Bars, 10 μm.

Table S1. Overview of the three independent genome-wide microarray experiments included in the comparative analysis.

Microarray Platform	Microarray Type	# Probes	CAT-deficient line	Residual CAT activity	HL treatment $\mu mol.m^{-2}.s^{-1}$	Time points (h)	Source
Affymetrix	ATH1 GeneChip	22,763 probe sets	CAT2HP1	20%	2000	0, 3, 8	Vanderauwera *et al.,* 2005
CATMA	CATMA v2.3	22,072 GSTs	CAT2HP1	20%	2000	0, 1, 8	Hoeberichts *et al.,*
Agilent	Arabidopsis v3 Oligo array	40,000 features	CAT2HP2	7%	1000	0, 1	Vanderauwera *et al.*, 2011

For each experiment, details on the experimental parameters and microarray platform are listed. CAT, catalase; CATMA, Complete Arabidopsis Transcriptome MicroArray; GST, Gene specific tag.

Table S2. Primers for ORF amplification and subsequent cloning in pDONR221.

See online version of this article (http://onlinelibrary.wiley.com/doi/10.1111/j.1365-3040.2011.02323.x/suppinfo) and from the attached CD with Supporting Information, Chapter 2.

Table S3 Overview of the overrepresented GO terms of the HIG data set.

The BiNGO overrepresentation analysis software was used to identify enriched GO categories in the HIG data set compared to all other GO-annotated genes in the *Arabidopsis* genome. GO categories with a *P*-value ≤0.05 were considered to be enriched in the HIG data set.

(a) Top 20 of overrepresented GO terms (p<0.05) in the 783 HIGs data set.

GO-ID	Description	*p*-value	corr. *p*-value	# selected	# total	frequency
Biological Process						
50896	response to stimulus	2.47E-24	1.15E-21	125	1755	7.1
6950	response to stress	9.10E-19	2.12E-16	64	665	9.6
6951	response to heat	2.44E-16	3.78E-14	21	73	28.8
42221	response to chemical stimulus	4.78E-16	5.56E-14	65	775	8.4
9404	toxin metabolism	4.16E-13	3.22E-11	15	45	33.3
9407	toxin catabolism	4.16E-13	3.22E-11	15	45	33.3
9636	response to toxin	5.48E-13	3.64E-11	16	54	29.6
9266	response to temperature stimulus	1.15E-11	6.71E-10	26	190	13.7
9628	response to abiotic stimulus	2.32E-09	1.20E-07	40	513	7.8
19748	secondary metabolism	5.09E-08	2.37E-06	25	261	9.6
16567	protein ubiquitination	1.17E-07	4.94E-06	13	76	17.1
32446	protein modification by small protein conjugation	3.93E-07	1.52E-05	13	84	15.5
9611	response to wounding	7.61E-07	2.72E-05	12	75	16.0
6800	oxygen and reactive oxygen species metabolism	8.25E-07	2.74E-05	17	152	11.2
9605	response to external stimulus	3.49E-05	9.59E-04	14	143	9.8
6979	response to oxidative stress	3.49E-05	9.59E-04	14	143	9.8
6512	ubiquitin cycle	3.50E-05	9.59E-04	13	125	10.4
9719	response to endogenous stimulus	6.16E-05	1.59E-03	33	584	5.7
7582	physiological process	1.09E-04	2.66E-03	285	8922	3.2
6118	electron transport	2.53E-04	5.87E-03	20	304	6.6
Molecular Function						
16491	oxidoreductase activity	3.57E-11	1.25E-08	61	914	6.7
3824	catalytic activity	2.16E-09	3.79E-07	228	6139	3.7
4842	ubiquitin-protein ligase activity	4.05E-06	3.89E-04	15	138	10.9
19787	small conjugating protein ligase activity	4.43E-06	3.89E-04	15	139	10.8
16881	acid-amino acid ligase activity	6.30E-06	4.42E-04	15	143	10.5
5516	calmodulin binding	2.32E-05	1.36E-03	11	89	12.4
16879	ligase activity, forming carbon-nitrogen bonds	3.76E-05	1.89E-03	15	166	9.0
16629	12-oxophytodienoate reductase activity	1.78E-04	6.94E-03	3	5	60.0
9916	alternative oxidase activity	1.78E-04	6.94E-03	3	5	60.0
16740	transferase activity	3.55E-04	1.25E-02	84	2192	3.8
9055	electron carrier activity	4.10E-04	1.31E-02	10	103	9.7
4364	glutathione transferase activity	5.99E-04	1.75E-02	3	7	42.9
16682	oxidoreductase activity, acting on diphenols and related substances as donors, oxygen as acceptor	9.39E-04	2.54E-02	3	8	37.5
8270	zinc ion binding	1.11E-03	2.79E-02	34	729	4.7
16679	oxidoreductase activity, acting on diphenols and related substances as donors	1.38E-03	3.23E-02	4	19	21.1
8194	UDP-glycosyltransferase activity	1.53E-03	3.37E-02	10	122	8.2
15036	disulfide oxidoreductase activity	1.87E-03	3.78E-02	8	85	9.4
9973	adenylyl-sulfate reductase activity	2.07E-03	3.78E-02	2	3	66.7
3700	transcription factor activity	2.13E-03	3.78E-02	48	1178	4.1
46872	metal ion binding	2.33E-03	3.78E-02	44	1061	4.1

(b) Overrepresented GO terms (p< 0.05) in the overlap (158) of 783 HIGs data set.

GO-ID	Description	*p*-value	corr. *p*-value	# selected	# total	frequency
Biological Process						
6951	response to heat	2.47E-18	4.29E-16	14	73	19.18
9266	response to temperature stimulus	1.25E-13	7.83E-12	15	190	7.89
6950	response to stress	1.35E-13	7.83E-12	24	665	3.61
50896	response to stimulus	2.72E-11	1.19E-09	34	1755	1.94
9628	response to abiotic stimulus	1.87E-08	6.50E-07	16	513	3.12
42221	response to chemical stimulus	1.97E-07	5.71E-06	18	775	2.32
6979	response to oxidative stress	1.16E-06	2.88E-05	8	143	5.59
6800	oxygen and reactive oxygen species metabolism	1.83E-06	3.99E-05	8	152	5.26
6118	electron transport	2.61E-04	5.04E-03	8	304	2.63
Molecular Function						
9055	electron carrier activity	2.24E-04	2.46E-02	5	103	4.85
16491	oxidoreductase activity	3.52E-04	2.46E-02	14	914	1.53

(c) Overrepresented GO terms ($p < 0.05$) in the 24 common genes of the 783 data set.

GO-ID	Description	*p*-value	corr. *p*-value	# selected	# total	frequency
Biological Process						
6951	response to heat	3.69E-13	2.59E-11	7	73	9.6
6950	response to stress	1.47E-10	5.14E-09	10	665	1.5
9266	response to temperature stimulus	3.37E-10	7.87E-09	7	190	3.7
50896	response to stimulus	8.50E-09	1.49E-07	12	1755	0.7
9628	response to abiotic stimulus	3.16E-07	4.43E-06	7	513	1.4
43335	protein unfolding	9.63E-04	9.63E-03	1	1	100.0
15692	lead ion transport	9.63E-04	9.63E-03	1	1	100.0
46685	response to arsenic	1.93E-03	1.68E-02	1	2	50.0
10262	somatic embryogenesis	2.89E-03	2.25E-02	1	3	33.3
30001	metal ion transport	5.88E-03	4.12E-02	2	120	1.7
1666	response to hypoxia	7.68E-03	4.89E-02	1	8	12.5
Molecular Function						
16667	oxidoreductase activity, acting on sulfur group of donors	1.53E-04	7.04E-03	2	24	8.3
45174	glutathione dehydrogenase (ascorbate) activity	2.31E-03	2.36E-02	1	3	33.3
16672	oxidoreductase activity, acting on sulfur group of donors. quinone or similar compound as acceptor	2.31E-03	2.36E-02	1	3	33.3
9973	adenylyl-sulfate reductase activity	2.31E-03	2.36E-02	1	3	33.3
15038	glutathione disulfide oxidoreductase activity	3.08E-03	2.36E-02	1	4	25.0
15037	peptide disulfide oxidoreductase activity	3.08E-03	2.36E-02	1	4	25.0

(d) Overrepresented GO terms ($p < 0.05$) in the 85 HIGs data set.

GO-ID	Description	*p*-value	corr *p*-value	# selected	# total	frequency
Biological Process						
6951	response to heat	9.77E-08	5.18E-06	6	73	8.2
9266	response to temperature stimulus	2.62E-05	6.94E-04	6	190	3.2
10286	heat acclimation	2.59E-04	4.13E-03	2	8	25.0
45449	regulation of transcription	3.71E-04	4.13E-03	11	1064	1.0
19219	regulation of nucleobase, nucleoside, nucleotide and nucleic acid metabolism	3.89E-04	4.13E-03	11	1070	1.0
31323	regulation of cellular metabolism	4.96E-04	4.23E-03	11	1101	1.0
19222	regulation of metabolism	5.59E-04	4.23E-03	11	1117	1.0
6350	transcription	6.39E-04	4.23E-03	11	1135	1.0
6950	response to stress	9.66E-04	5.32E-03	8	665	1.2
51244	regulation of cellular physiological process	1.05E-03	5.32E-03	11	1205	0.9
50794	regulation of cellular process	1.10E-03	5.32E-03	11	1213	0.9
50791	regulation of physiological process	1.38E-03	6.09E-03	11	1247	0.9
9873	ethylene mediated signaling pathway	1.71E-03	6.99E-03	2	20	10.0
6355	regulation of transcription. DNA-dependent	2.10E-03	7.97E-03	7	585	1.2
6351	transcription. DNA-dependent	2.61E-03	8.73E-03	7	608	1.2
32774	RNA biosynthesis	2.64E-03	8.73E-03	7	609	1.1
50789	regulation of biological process	3.22E-03	1.00E-02	11	1389	0.8
160	two-component signal transduction system (phosphorelay)	4.11E-03	1.21E-02	2	31	6.5
9628	response to abiotic stimulus	4.93E-03	1.38E-02	6	513	1.2
6979	response to oxidative stress	9.81E-03	2.60E-02	3	143	2.1
6800	oxygen and reactive oxygen species metabolism	1.16E-02	2.92E-02	3	152	2.0
50896	response to stimulus	1.75E-02	4.22E-02	11	1755	0.6
Molecular Function						
3700	transcription factor activity	3.25E-12	7.79E-11	22	1178	1.9
3677	DNA binding	2.59E-11	3.11E-10	24	1600	1.5
30528	transcription regulator activity	6.18E-11	4.94E-10	22	1370	1.6
3676	nucleic acid binding	5.37E-09	3.22E-08	25	2259	1.1
5488	binding	1.01E-06	4.87E-06	34	5061	0.7
8270	zinc ion binding	3.89E-04	1.56E-03	9	729	1.2
43169	cation binding	9.35E-04	3.20E-03	10	999	1.0
46914	transition metal ion binding	1.30E-03	3.53E-03	9	864	1.0
46872	metal ion binding	1.47E-03	3.53E-03	10	1061	0.9
43167	ion binding	1.47E-03	3.53E-03	10	1061	0.9

Table S4. Overview of the 85 selected HIGs.

AGI code	Description	PA	*in vivo* localization	ATH1[a]	CATMA[b]	AGILENT[c]
Calcium ion-binding						
At5g42380	CML37		NC	**7.61**	2.24	**74.86**
At5g40690	unknown protein	NU	NC	**7.86**	2.39	2.57
Enzymatic activity						
At3g25250	AGC2-1	PM		**11.60**	4.97	**90.18**
At4g22530	embryo-abundant protein-related		NC	**12.73**	9.60	39.41
At1g26380	FAD-binding berberine family protein		ER	**26.32**	1.99	**35.44**
At1g67810	SUFE2	CY	CL	**8.49**	3.32	64.18
At3g02800	Tyrosine phosphatase	CY	NC	**6.16**	2.76	**57.79**
At3g07090	unknown protein	CY	NC	**4.66**	**5.95**	2.58
Glycolipid transport						
At4g39670	similar to ACD11		NC	**11.86**	3.13	73.65
Heat shock protein-binding						
At1g71000	AtDJC68	CY	NC	**17.29**	13.65	**43.72**
At3g09350	Fes1A		NC	**15.21**	**23.81**	**14.26**
At3g46230	HSP17.4	CY		3.26	**560.93**	34.46
At2g29500	HSP17.6B-CI	CY	CY	**3.93**	**173.87**	**60.17**
At1g53540	HSP17.6C-CI (AA 1-156)	CY		2.84		**342.92**
At1g07400	HSP17.8-CI	CY	CY	2.87	**69.55**	**13.28**
At4g12400	stress-inducible protein			**10.17**	**45.48**	**13.61**
RNA metabolism						
At1g66500	Pre-mRNA cleavage complex II	NU		**3.60**		1.05
Transcription factor and DNA-binding proteins						
At1g32870	ANAC013	NU	NU	**2.45**	**2.57**	**1.48**
At1g77450	ANAC032	NU	NU	**5.03**		**19.92**
At3g10500	ANAC053	NU	NC	2.05	2.25	**10.43**
At3g29035	ANAC059	NU	-		1.37	**26.84**
At5g18270	ANAC087	NU	NC	**4.10**	**6.33**	2.48
At5g63790	ANAC102	NU	CL	**3.25**		**28.14**
At2g44840	AtERF013	NU		-6.42	-4.35	**6.79**
At1g22810	AtERF019	NU	NC	**24.15**	4.51	**271.18**
At2g40350	AtERF047 (DREB2B)	NU		**4.04**		1.54
At2g47520	AtERF071	NU	NU	**12.99**	7.00	2.13
At3g23230	AtERF098	NU		**10.30**	-1.05	**212.09**
At5g61600	AtERF104	NU	-	-2.95	-1.30	**19.67**
At2g26150	AtHSFA2	NU		27.64	60.68	**9.97**
At4g18880	AtHSFA4A	NU		1.88	1.67	**18.79**
At1g10585	bHLH DNA-binding superfamily protein	NU	NC	**85.12**		20.22
At3g61630	CRF6	NU	NC	**1.96**	**2.18**	-1.09
At1g22985	CRF7	NU	NU	**5.64**	4.70	1.45
At5g05410	DREB2A	NU	NU	**8.01**	1.77	**96.44**
At4g25380	SAP10		NC	**132.39**	6.10	5.85
At2g38250	Trihelix transcription factor GT-3b	NU	NU	**4.98**	2.14	**7.58**
At2g23320	WRKY15	NU	NU	2.50	2.49	**16.35**
At5g24110	WRKY30	NU	NC	**14.80**	1.98	**142.00**
At1g62300	WRKY6	NU		**7.60**	3.30	46.58
At5g13080	WRKY75	NU	NU	**5.69**	4.52	5.84
At2g37430	ZAT11	NU	-		2.23	**127.52**
At5g04340	ZAT6	NU	-	1.73		**21.76**
Proteins of unknown function						
At2g26530	AR781	NU		1.03	1.38	**20.69**
At3g02840	ARM repeat superfamily protein	PM	NC	**3.43**	1.33	**48.52**
At1g33600	LRR family protein		UD	**3.97**	2.49	**10.45**
At5g63130	Octicosapeptide/Phox/Bem1p (PB1) domain-containing protein	NC	-	1.95	1.70	**8.06**
At4g00670	Remorin family protein	NU, PM		**-6.70**	**-1.20**	**1.62**
At4g01870	TolB protein-related		UD	**43.38**	26.81	69.88
At4g01390	TRAF-like family protein	NP	NC	**-3.94**		**1.51**
At5g19230	Uncharacterized GPI-anchored protein	PM	UD		1.42	**11.45**
At1g05340	Unknown protein	NU	NC	**7.34**		1.00
At1g05575	Unknown protein	PM	ER	**7.92**		5.64
At1g19020	Unknown protein		-	**9.22**	**8.21**	**33.12**
At1g23710	Unknown protein	NU		1.57	1.19	**9.60**
At1g56060	Unknown protein		UD	**4.30**		2.53
At1g76600	Unknown protein		-	**5.69**	1.70	**113.84**
At2g18680	Unknown protein	PM	ER	**5.21**		9.66
At2g21640	Unknown protein		UD	**4.86**	**6.64**	1.26
At2g25735	Unknown protein		PM	1.33	-1.13	**17.76**
At2g40000	Unknown protein			-1.24	-1.26	**24.45**
At2g41730	Unknown protein	NC	NC	**27.27**		2.78
At3g18250	Unknown protein		ER	**2.15**	**9.05**	**1.23**
At3g46220	Unknown protein	EX		-1.27	**560.93**	-1.19

Table S4. Overview of the 85 selected HIGs. (*Continued).*

AGI code	Description	PA	*in vivo* localization	ATH1[a]	CATMA[b]	AGILENT[c]
Proteins of unknown function						
At4g21920	Unknown protein	NU			1.06	**81.12**
At4g36500	Unknown protein	CY	UD	1.20	8.48	**13.34**
At4g37290	Unknown protein		-	**8.26**	4.34	15.75
At5g05220	Unknown protein	CY	CL	**6.35**	2.43	33.78
At5g10695	Unknown protein	CY	-	**6.30**		**43.53**
At5g12930	Unknown protein			**13.38**	8.56	**8.47**
At5g14730	Unknown protein	ER, EX	UD	**23.18**	2.59	**144.77**
At5g36925	Unknown protein		NC			**22.12**
At5g64230	Unknown protein			**8.07**	7.69	**3.88**
At1g20310	Unknown protein	NU	-	1.04	-1.59	**27.20**
At1g28190	Unknown protein		NU	**3.01**		**50.46**
Zinc ion-binding						
At3g17611	RHOMBOID-like protein 14 (AtRBL14)	GA	PM	**8.36**	6.60	**3.55**
At4g26580	RING/U-box superfamily protein	NU			1.45	**11.00**
At1g14200	RING/U-box superfamily protein	CY		**6.54**	3.25	**25.68**
At5g43420	RING/U-box superfamily protein				2.15	**18.94**
At3g55980	SALT-INDUCIBLE ZINC FINGER1 (AtSZF1)	CY		-1.55	1.58	**20.84**
At2g40140	SALT-INDUCIBLE ZINC FINGER2 (AtSZF2)	CY		1.13	1.46	**13.47**
At3g28210	SAP12			**57.61**	**30.36**	**61.94**
At2g41835	ZF (C_2H_2-type, AN1-like) family protein		-			**14.70**
At3g46620	ZF (C_3HC_4-type RING finger) family protein	CY	NC	1.32	1.49	**7.17**
At3g47550	ZF (C_3HC_4-type RING finger) family protein		NC	1.92	2.23	**6.74**

For 85 HIGs, the *in silico* subcellular localization was predicted by Proteome Analyst (PA; Szafron *et al.*, 2004) and the *in vivo* subcellular localization was determined for 49 HIGs. For each gene, the AGI code, gene description and the fold changes in each H_2O_2-related experiment (ATH1, CATMA and AGILENT) are indicated. FC, fold changes; HIG, H_2O_2-induced gene; HL, high light; WT, wild type. NU, nucleus; CY, cytosol; NC, nucleus and cytosol; CL, chloroplasts; NP, nucleus and peroxisomes; PM, plasma membrane; ER, endoplasmatic reticulum; EX, extracellular; GA, golgi apparatus; UD, undetermined. Hyphen, no fluorescence. Significant values are indicated in bold.

[a] relative FC in *cat2* mutant versus WT plants after 3 h of HL exposure (Vanderauwera *et al.,* 2005).

[b] relative FC in *cat2* mutant versus WT plants after 8 h of HL irradiation (Hoeberichts *et al.,* unpublished results).

[c] relative FC in *cat2* mutant versus WT plants after 1 h of HL irradiation (Vanderauwera *et al.*, 2011).

REFERENCES

Allemeersch, J., Durinck, S., Vanderhaeghen, R., Alard, P., Maes, R., Seeuws, K., Bogaert, T., Coddens, K., Deschouwer, K., Van Hummelen, P., Vuylsteke, M., Moreau, Y., Kwekkeboom, J., Wijfjes, A.H.M., May, S., Beynon, J., Hilson, P. and Kuiper, M.T.R. (2005) Benchmarking the CATMA microarray. A novel tool for *Arabidopsis* transcriptome analysis. *Plant Physiol.*, **137**, 588-601.

Altschul, S.F., Madden, T.L., Schäffer, A.A., Zhang, J., Zhang, Z., Miller, W. and Lipman, D.J. (1997) Gapped BLAST and PSI-BLAST: a new generation of protein database search programs. *Nucleic Acids Res.*, **25**, 3389-3402.

Apel, K. and Hirt, H. (2004) Reactive oxygen species: metabolism, oxidative stress, and signal transduction. *Annu. Rev. Plant Biol.*, **55**, 373-399.

Benjamini, Y. and Yekutieli, D. (2001) The control of the false discovery rate in multiple testing under dependency. *Ann. Stat.*, **29**, 1165-1188.

Borner, G.H.H., Lilley, K.S., Stevens, T.J. and Dupree, P. (2003) Identification of glycosylphosphatidylinositol-anchored proteins in *Arabidopsis*. A proteomic and genomic analysis. *Plant Physiol.*, **132**, 568-577.

Borner, G.H.H., Sherrier, D.J., Stevens, T.J., Arkin, I.T. and Dupree, P. (2002) Prediction of glycosylphosphatidylinositol-anchored proteins in *Arabidopsis*. A genomic analysis. *Plant Physiol.*, **129**, 486-499.

Boyes, D.C., Zayed, A.M., Ascenzi, R., McCaskill, A.J., Hoffman, N.E., Davis, K.R. and Gorlach, J. (2001) Growth stage-based phenotypic analysis of *Arabidopsis*: a model for high throughput functional genomics in plants. *Plant Cell*, **13**, 1499-1510.

Carmo-Fonseca, M., Mendes-Soares, L. and Campos, I. (2000) To be or not to be in the nucleolus. *Nat. Cell Biol.*, **2**, 107-112.

Christianson, J.A., Wilson, I.W., Llewellyn, D.J. and Dennis, E.S. (2009) The low-oxygen-induced NAC domain transcription factor ANAC102 affects viability of *Arabidopsis* seeds following low-oxygen treatment. *Plant Physiol.*, **149**, 1724-1738.

Clough, S.J. and Bent, A.F. (1998) Floral dip: a simplified method for *Agrobacterium*-mediated transformation of *Arabidopsis thaliana*. *Plant J.*, **16**, 735-743.

Dat, J.F., Inzé, D. and van Breusegem, F. (2001) Catalase-deficient tobacco plants: tools for *in planta* studies on the role of hydrogen peroxide. *Redox Rep.*, **6**, 37-42.

De Bodt, S., Carvajal, D., Hollunder, J., Van den Cruyce, J., Movahedi, S. and Inzé, D. (2010) CORNET: a user-friendly tool for data mining and integration. *Plant Physiol.*, **152**, 1167-1179.

de Folter, S., Urbanus, S., van Zuijlen, L., Kaufmann, K. and Angenent, G. (2007) Tagging of MADS domain proteins for chromatin immunoprecipitation. *BMC Plant Biol.*, **7**, 47.

Devaiah, B.N., Karthikeyan, A.S. and Raghothama, K.G. (2007) WRKY75 transcription factor is a modulator of phosphate acquisition and root development in *Arabidopsis*. *Plant Physiol.*, **143**, 1789-1801.

Gadjev, I., Vanderauwera, S., Gechev, T.S., Laloi, C., Minkov, I.N., Shulaev, V., Apel, K., Inzé, D., Mittler, R. and Van Breusegem, F. (2006) Transcriptomic footprints disclose specificity of reactive oxygen species signaling in *Arabidopsis*. *Plant Physiol.*, **141**, 436-445.

Gechev, T.S., Van Breusegem, F., Stone, J.M., Denev, I. and Laloi, C. (2006) Reactive oxygen species as signals that modulate plant stress responses and programmed cell death. *BioEssays*, **28**, 1-11.

Giraud, E., Ho, L.H.M., Clifton, R., Carroll, A., Estavillo, G., Tan, Y.-F., Howell, K.A., Ivanova, A., Pogson, B.J., Millar, A.H. and Whelan, J. (2008) The absence of *ALTERNATIVE OXIDASE1a* in *Arabidopsis* results in acute

sensitivity to combined light and drought stress. *Plant Physiol.*, **147**, 595-610.

Gutterson, N. and Reuber, T.L. (2004) Regulation of disease resistance pathways by AP2/ERF transcription factors. *Curr. Opin. Plant Biol.*, **7**, 465-471.

Ho, L.H.M., Giraud, E., Uggalla, V., Lister, R., Clifton, R., Glen, A., Thirkettle-Watts, D., Van Aken, O. and Whelan, J. (2008) Identification of regulatory pathways controlling gene expression of stress-responsive mitochondrial proteins in *Arabidopsis*. *Plant Physiol.*, **147**, 1858-1873.

Kaminaka, H., Nake, C., Epple, P., Dittgen, J., Schutze, K., Chaban, C., Holt, B.F., Merkle, T., Schafer, E., Harter, K. and Dangl, J.L. (2006) bZIP10-LSD1 antagonism modulates basal defense and cell death in *Arabidopsis* following infection. *EMBO J.*, **25**, 4400-4411.

Karimi, M., Bleys, A., Vanderhaeghen, R. and Hilson, P. (2007) Building blocks for plant gene assembly. *Plant Physiol.*, **145**, 1183-1191.

Katiyar-Agarwal, S., Zhu, J., Kim, K., Agarwal, M., Fu, X., Huang, A. and Zhu, J.-K. (2006) The plasma membrane Na^+/H^+ antiporter SOS1 interacts with RCD1 and functions in oxidative stress tolerance in *Arabidopsis*. *Proc. Natl. Acad. Sci. USA*, **103**, 18816-18821.

Kilian, J., Whitehead, D., Horak, J., Wanke, D., Weinl, S., Batistic, O., D'Angelo, C., Bornberg-Bauer, E., Kudla, J. and Harter, K. (2007) The AtGenExpress global stress expression data set: protocols, evaluation and model data analysis of UV-B light, drought and cold stress responses. *Plant J.*, **50**, 347-363.

Kim, S.-G., Kim, S.-Y. and Park, C.-M. (2007) A membrane-associated NAC transcription factor regulates salt-responsive flowering via *FLOWERING LOCUS* in *Arabidopsis*. *Planta*, **226**, 647-654.

Kim, S.-G., Lee, A.-K., Yoon, H.-K. and Park, C.-M. (2008) A membrane-bound NAC transcription factor NTL8 regulates gibberellic acid-mediated salt signaling in *Arabidopsis* seed germination. *Plant J.*, **55**, 77-88.

Kinkema, M., Fan, W. and Dong, X. (2000) Nuclear localization of NPR1 is required for activation of *PR* gene expression. *Plant Cell*, **12**, 2339-2350.

Klok, E.J., Wilson, I.W., Wilson, D., Chapman, S.C., Ewing, R.M., Somerville, S.C., Peacock, W.J., Dolferus, R. and Dennis, E.S. (2002) Expression profile analysis of the low-oxygen response in *Arabidopsis* root cultures. *Plant Cell*, **14**, 2481-2494.

Kmiec-Wisniewska, B., Krumpe, K., Urantowka, A., Sakamoto, W., Pratje, E. and Janska, H. (2008) Plant mitochondrial rhomboid, AtRBL12, has different substrate specificity from its yeast counterpart. *Plant Mol. Biol.*, **68**, 159-171.

Krause, K. and Krupinska, K. (2009) Nuclear regulators with a second home in organelles. *Trends Plant Sci.*, **14**, 194-199.

Lee, S., Seo, P.J., Lee, H.-J. and Park, C.-M. (2012) A NAC transcription factor NTL4 promotes reactive oxygen species production during drought-induced leaf senescence in Arabidopsis. *Plant J.*, *in press*, DOI 10.1111/j.1365-1313X.2012.04932.x.

Licausi, F., Van Dongen, J.T., Giuntoli, B., Novi, G., Santaniello, A., Geigenberger, P. and Perata, P. (2010) HRE1 and HRE2, two hypoxia-inducible ethylene response factors, affect anaerobic responses in *Arabidopsis thaliana*. *Plant J.*, **62**, 302-315.

Maere, S., Heymans, K. and Kuiper, M. (2005) BiNGO: a Cytoscape plugin to assess overrepresentation of Gene Ontology categories in Biological Networks. *Bioinformatics*, **21**, 3448-3449.

Miernyk, J.A. (2001) The J-domain proteins of *Arabidopsis thaliana*: an unexpectedly large and diverse family of chaperones. *Cell Stress Chaperones*, **6**, 209-218.

Miller, G. and Mittler, R. (2006) Could heat shock transcription factors function as hydrogen peroxide sensors in plants?

Ann. Botany, **98**, 279-288.

Mittler, R., Vanderauwera, S., Gollery, M. and Van Breusegem, F. (2004) Reactive oxygen gene network of plants. *Trends Plant Sci.*, **9**, 490-498.

Miyawaki, A. (2011) Proteins on the move: insights gained from fluorescent protein technologies. *Nat. Rev. Mol. Cell Biol.*, **12**, 656-668.

Murthy, N.M.U., Ollagnier-de-Choudens, S., Sanakis, Y., Abdel-Ghany, S.E., Rousset, C., Ye, H., Fontecave, M., Pilon-Smits, E.A.H. and Pilon, M. (2007) Characterization of *Arabidopsis thaliana* SufE2 and SufE3. *J. Biol. Chem.*, **282**, 18254-18264.

Nakamoto, H. and Vígh, L. (2007) The small heat shock proteins and their clients. *Cell. Mol. Life Sci.*, **64**, 294-306.

Nelson, B.K., Cai, X. and Nebenfuhr, A. (2007) A multicolored set of *in vivo* organelle markers for co-localization studies in *Arabidopsis* and other plants. *Plant J.*, **51**, 1126-1136.

Noctor, G., Veljovic-Jovanovic, S., Driscoll, S., Novitskaya, L. and Foyer, C.H. (2002) Drought and oxidative load in the leaves of C3 plants: a predominant role for photorespiration? *Ann. Botany*, **89**, 841-850.

Ooka, H., Satoh, K., Doi, K., Nagata, T., Otomo, Y., Murakami, K., Matsubara, K., Osato, N., Kawai, J., Carninci, P., Hayashizaki, Y., Suzuki, K., Kojima, K., Takahara, Y., Yamamoto, K. and Kikuchi, S. (2003) Comprehensive Analysis of *NAC* Family Genes in *Oryza sativa* and *Arabidopsis thaliana*. *DNA Res.*, **10**, 239-247.

Pendle, A.F., Clark, G.P., Boon, R., Lewandowska, D., Lam, Y.W., Andersen, J., Mann, M., Lamond, A.I., Brown, J.W.S. and Shaw, P.J. (2005) Proteomic analysis of the *Arabidopsis* nucleolus suggests novel nucleolar functions. *Mol. Cell. Biol.*, **16**, 260-269.

Peschke, F. and Kretsch, T. (2011) Genome-wide analysis of light-dependent transcript accumulation patterns during early stages of *Arabidopsis* seedling deetiolation. *Plant Physiol.*, **155**, 1353-1366.

Pruss, G.J., Nester, E.W. and Vance, V. (2008) Infiltration with *Agrobacterium tumefaciens* induces host defense and development-dependent responses in the infiltrated zone. *Mol. Plant Microbe Interact.*, **21**, 1528-1538.

Rashotte, A. and Goertzen, L. (2010) The CRF domain defines Cytokinin Response Factor proteins in plants. *BMC Plant Biol.*, **10**, 74.

Rashotte, A.M., Mason, M.G., Hutchison, C.E., Ferreira, F.J., Schaller, G.E. and Kieber, J.J. (2006) A subset of *Arabidopsis* AP2 transcription factors mediates cytokinin responses in concert with a two-component pathway. *Proc. Natl. Acad. Sci. USA*, **103**, 11081-11085.

Rhee, S.Y., Beavis, W., Berardini, T.Z., Chen, G., Dixon, D., Doyle, A., Garcia-Hernandez, M., Huala, E., Lander, G., Montoya, M., Miller, N., Mueller, L.A., Mundodi, S., Reiser, L., Tacklind, J., Weems, D.C., Wu, Y., Xu, I., Yoo, D., Yoon, J. and Zhang, P. (2003) The *Arabidopsis* Information Resource (TAIR): a model organism database providing a centralized, curated gateway to *Arabidopsis* biology, research materials and community. *Nucleic Acids Res.*, **31**, 224-228.

Sakuma, Y., Maruyama, K., Osakabe, Y., Qin, F., Seki, M., Shinozaki, K. and Yamaguchi-Shinozaki, K. (2006) Functional analysis of an *Arabidopsis* transcription factor, DREB2A, involved in drought-responsive gene expression. *Plant Cell*, **18**, 1292-1309.

Seo, P.J., Kim, M.J., Park, J.-Y., Kim, S.-Y., Jeon, J., Lee, Y.-H., Kim, J. and Park, C.-M. (2010a) Cold activation of a plasma membrane-tethered NAC transcription factor induces a pathogen resistance response in *Arabidopsis*. *Plant J.*, **61**, 661-671.

Seo, P.J., Kim, M.J., Song, J.-S., Kim, Y.-S., Kim, H.-J. and Park, C.-M. (2010b) Proteolytic processing of an *Arabidopsis* membrane-bound NAC transcription factor is triggered by cold-induced changes in membrane fluidity. *Biochem. J.*,

427, 359-367.

Seo, P.J., Kim, S.-G. and Park, C.-M. (2008) Membrane-bound transcription factors in plants. *Trends Plant Sci.*, **13**, 550-556.

Shannon, P., Markiel, A., Ozier, O., Baliga, N.S., Wang, J.T., Ramage, D., Amin, N., Schwikowski, B. and Ideker, T. (2003) Cytoscape: a software environment for integrated models of biomolecular interaction metworks. *Genome Res.*, **13**, 2498-2504.

Shaw, P.J. and Brown, J.W.S. (2004) Plant nuclear bodies. *Curr. Opin. Plant Biol.*, **7**, 614-620.

Sparkes, I.A., Runions, J., Kearns, A. and Hawes, C. (2006) Rapid, transient expression of fluorescent fusion proteins in tobacco plants and generation of stably transformed plants. *Nature Protoc.*, **1**, 2019-2025.

Sturn, A., Quackenbush, J. and Trajanoski, Z. (2002) Genesis: cluster analysis of microarray data. *Bioinformatics*, **18**, 207-208.

Sweetlove, L.J., Heazlewood, J.L., Herald, V., Holtzapffel, R., Day, D.A., Leaver, C.J. and Millar, A.H. (2002) The impact of oxidative stress on *Arabidopsis* mitochondria. *Plant J.*, **32**, 891-904.

Szafron, D., Lu, P., Greiner, R., Wishart, D.S., Poulin, B., Eisner, R., Lu, Z., Anvik, J., Macdonell, C., Fyshe, A. and Meeuwis, D. (2004) Proteome Analyst: custom predictions with explanations in a web-based tool for high-throughput proteome annotations. *Nucleic Acids Res.*, **32**, W365-W371.

Van Aken, O., Zhang, B., Carrie, C., Uggalla, V., Paynter, E., Giraud, E. and Whelan, J. (2009) Defining the mitochondrial stress response in *Arabidopsis thaliana*. *Mol. Plant*, **2**, 1310-1324.

Van Breusegem, F. and Dat, J.F. (2006) Reactive oxygen species in plant cell death. *Plant Physiol.*, **141**, 384-390.

Vandenabeele, S., Van Der Kelen, K., Dat, J., Gadjev, I., Boonefaes, T., Morsa, S., Rottiers, P., Slooten, L., Van Montagu, M., Zabeau, M., Inzé, D. and Van Breusegem, F. (2003) A comprehensive analysis of hydrogen peroxide-induced gene expression in tobacco. *Proc. Natl. Acad. Sci. USA*, **100**, 16113-16118.

Vandenabeele, S., Vanderauwera, S., Vuylsteke, M., Rombauts, S., Langebartels, C., Seidlitz, H.K., Zabeau, M., Van Montagu, M., Inzé, D. and Van Breusegem, F. (2004) Catalase deficiency drastically affects gene expression induced by high light in *Arabidopsis thaliana*. *Plant J.*, **39**, 45-58.

Vanderauwera, S., Suzuki, N., Miller, G., van de Cotte, B., Morsa, S., Ravanat, J.-L., Hegie, A., Triantaphylidès, C., Shulaev, V., Van Montagu, M.C.E., Van Breusegem, F. and Mittler, R. (2011) Extranuclear protection of chromosomal DNA from oxidative stress. *Proc. Natl. Acad. Sci. USA*, **108**, 1711-1716.

Vanderauwera, S., Zimmermann, P., Rombauts, S., Vandenabeele, S., Langebartels, C., Gruissem, W., Inzé, D. and Van Breusegem, F. (2005) Genome-wide analysis of hydrogen peroxide-regulated gene expression in *Arabidopsis* reveals a high light-induced transcriptional cluster involved in anthocyanin biosynthesis. *Plant Physiol.*, **139**, 806-821.

Willekens, H., Chamnongpol, S., Davey, M., Schraudner, M., Langebartels, C., Van Montagu, M., Inzé, D. and Van Camp, W. (1997) Catalase is a sink for H_2O_2 and is indispensable for stress defence in C3 plants. *EMBO J.*, **16**, 4806-4816.

Wolfinger, R.D., Gibson, G., Wolfinger, E.D., Bennett, L., Hamadeh, H., Bushel, P., Afshari, C. and Paules, R.S. (2001) Assessing gene significance from cDNA microarray expression data via mixed models. *J. Comput. Biol.*, **8**, 625-637.

Yoo, S.-D., Cho, Y.-H. and Sheen, J. (2007) *Arabidopsis* mesophyll protoplasts: a versatile cell system for transient gene expression analysis. *Nature Protoc.*, **2**, 1565-1572.

Zhang, J.-X., Wang, C., Yang, C.-Y., Wang, J.-Y., Chen, L., Bao, X.-M., Zhao, Y.-X., Zhang, H. and Liu, J. (2010) The role of arabidopsis AtFes1A in cytosolic Hsp70 stability and abiotic stress tolerance. *Plant J.*, **62**, 539-548.

Zimmermann, P., Hennig, L. and Gruissem, W. (2005) Gene-expression analysis and network discovery using

Genevestigator. *Trends Plant Sci.*, **10**, 407-409.

Zimmermann, P., Hirsch-Hoffmann, M., Hennig, L. and Gruissem, W. (2004) GENEVESTIGATOR. Arabidopsis microarray database and analysis toolbox. *Plant Physiol.*, **136**, 2621-2632.

3

Oxidative stress-induced retrograde relocalization of a chloroplastic NAC transcription factor

Annelies Inzé, Inge De Clercq, Sandy Vanderauwera, Brigitte van de Cotte,

Riet De Rycke and Frank Van Breusegem

AUTHOR CONTRIBUTIONS

A.I wrote the manuscript with help of S.V., I.D.C. and F.V.B. A.I. produced the GFP transgenic lines, designed, performed and analyzed the subcellular (re)localization and processing experiments. I.D.C designed, performed and analyzed the yeast one-hybrid experiments, qRT-PCR experiments on the ANAC102 target genes and the stress assays. S.V. produced the *ANAC102*^{OE} and *ANAC102*^{KO} lines. B.v.d.C. performed the chloroplast fractionation experiments.

ABSTRACT

Due to their sessile lifestyle, plants are continuously exposed to adverse environmental conditions that affect plant growth and development. To cope with these stress conditions, plants have developed complex signal transduction mechanisms to tightly regulate an appropriate stress response. In addition, abiotic and biotic stress conditions perturb the reactive oxygen species (ROS) homeostasis leading to a fast release of ROS that play a key role in stress signaling. Many components of the ROS signaling network have been identified including ROS-responsive transcription factors belonging to several major transcription factor families. Within these, several NAC transcription factors were identified. Here, we present the involvement of the hydrogen peroxide (H_2O_2)-induced NAC transcription factor ANAC102 in regulating several stress-responsive genes during chloroplast-derived oxidative stress conditions. During normal conditions, ANAC102 is localized in the chloroplasts. However, perturbation of the chloroplastic redox balance leads to the intercompartimental relocalization of ANAC102 from the chloroplast to the nucleus where it regulates several oxidative stress-related genes. Moreover, transgenic plants with enhanced or decreased *ANAC102* expression displayed an altered growth response when grown under oxidative stress conditions. Our results indicate that ANAC102 could play an important role during chloroplast retrograde signaling by controlling the stress response.

INTRODUCTION

Adverse environmental conditions are the major causing agents of global crop losses world-wide (http://faostat.fao.org/). Therefore, a detailed understanding of the mechanisms how plants respond and adapt to abiotic and biotic stress conditions is prerequisite to develop sustainable solutions to increase crop yield, including the development of stress-tolerant transgenic crops. Plant adaptation to adverse environmental conditions is mediated by a wide variety of mechanisms of which mutual players, including kinases and transcription factors, are involved in complex gene regulatory networks (Fujita *et al.*, 2006). Common to many stress responses is the accumulation of reactive oxygen species (ROS; Apel and Hirt, 2004). Several ROS-responsive transcription factors have been identified, including members of the AP2-EREBP, bHLH, HSF, MYB, WRKY, Zinc Finger (ZF) and NAC transcription factor families (op den Camp *et al.*, 2003; Vandenabeele *et al.*, 2003; Gechev *et al.*, 2004; Vandenabeele *et al.*, 2004; Vanderauwera *et al.*, 2005; Gadjev *et al.*, 2006; Vanderauwera *et al.*, 2011).

The NAC domain protein family is one of the largest plant-specific transcription factor families with 105 members in *Arabidopsis thaliana* (ANACs; Ooka *et al.*, 2003). NAC family proteins are characterized by the presence of an N-terminal NAC (petunia NO APICAL MERISTEM (NAM) and Arabidopsis ATAF1, ATAF2, and CUP-SHAPED COTYLEDON 2 (CUC2)) domain and a variable C-terminal transcriptional activation region (Souer *et al.*, 1996; Aida *et al.*, 1997; Lu *et al.*, 2007; Jensen *et al.*, 2010). The NAC domain is comprised of five subdomains A to E of which the highly conserved subdomains C and D are thought to be involved in DNA-binding whereas the divergent B and E subdomains may account for the functional diversity seen amongst NACs (Ooka *et al.*, 2003). Based on similarities in NAC domain structures, NAC family proteins are further classified into several subfamilies (Ooka *et al.*, 2003). NAC proteins have been shown to be involved in developmental programs (Souer *et al.*, 1996; Xie *et al.*, 2000; Mitsuda *et al.*, 2005) and the response to biotic and abiotic stresses (Collinge and Boller, 2001; Fujita *et al.*, 2004; Tran *et al.*, 2004; Delessert *et al.*, 2005; He *et al.*, 2005; Kim *et al.*, 2008; Yoon *et al.*, 2008). For instance, four Arabidopsis NAC genes (*ANAC019*, *ANAC055*, *ANAC072* (also known as *RESPONSIVE TO DESSICATION 26* (*RD26*)) and *ATAF1*) are involved in the response to drought stress and modulating their expression levels increased tolerance to drought (Fujita *et al.*, 2004; Tran *et al.*, 2004; Lu *et al.*, 2007; Tran *et al.*, 2007). NAC transcription factors are under the complex control of different regulatory mechanisms including transcriptional regulation, post-transcriptional control such as microRNA-mediated cleavage of mRNAs and phloem long-distance transport; post-translational regulation by regulated intramembrane proteolytic cleavage of membrane anchored NACs, nucleocytoplasmic partitioning and modifications with N-acetyl glucosamine (Olsen *et al.*, 2005).

ANAC102 (At5g63790) belongs to the ATAF subfamily that includes *ATAF1* (*ANAC002*), *ATAF2* (*ANAC081*) and *ANAC032* (Ooka *et al.*, 2003). *ATAF1* and *ATAF2* negatively regulate responses to drought and wounding, respectively (Delessert *et al.*, 2005; Lu *et al.*, 2007). ANAC102 was previously identified as an important regulator of seed germination during flooding stress (Christianson *et al.*, 2009). While *ANAC102* overexpression lines germinated comparable to wild-type plants during both normal and hypoxic conditions, *ANAC102* knock-out lines had an impaired germination after hypoxia treatment (Christianson *et al.*, 2009).

Here, we report the intercompartimental relocalization of a hydrogen peroxide (H_2O_2)-responsive NAC transcription factor (ANAC102) from the chloroplasts to the nucleus during chloroplast-derived oxidative stress conditions. Perturbation of intracellular ROS homeostasis leads to the release of ANAC102 from the chloroplasts into the cytoplasm where it is redirected to the nucleus to regulate several oxidative stress-related genes. Under oxidative stress conditions, overexpression of *ANAC102* leads to the partial repression of these target genes, leading to a decreased tolerance towards oxidative stress conditions.

RESULTS

Identification of NAC transcription factors induced by hydrogen peroxide

Previously, we made a comprehensive inventory of more than 700 photorespiratory H_2O_2-induced genes (HIGs) by comparing several microarray data sets that profiled the Arabidopsis transcriptome during elevated photorespiratory H_2O_2 levels (Vanderauwera *et al.*, 2005; Vanderauwera *et al.*, 2011; Inzé *et al.*, 2012; Chapter 2). The perturbation of catalase activity, that results in a decreased antioxidant capacity of the cell, together with high light (HL) stress, low CO_2 availability and day length leads to the accumulation of photorespiratory H_2O_2 (Willekens *et al.*, 1997; Noctor *et al.*, 2002; Queval *et al.*, 2007; Queval *et al.*, 2011). Within the 783 HIGs, 73 genes encode transcription factors that belong to the AP2-EREBP (13), bHLH (4), HSF (7), MYB (4), WRKY (10), ZF (12) and NAC (8) transcription factor families (Table S1). Within these eight H_2O_2-induced NACs, all members of the ATAF subfamily are present. All H_2O_2-induced NAC transcription factors were constitutively induced in plants lacking catalase (*cat2*) when grown under normal conditions (Table 1). Plants with decreased levels of cytosolic ascorbate peroxidase (*apx1*), a key regulator of H_2O_2 levels and H_2O_2 signaling in plants (Asada, 1999; Apel and Hirt, 2004; Davletova *et al.*, 2005), also accumulated higher transcript levels of these NAC transcription factors after 1 h of HL irradiance compared to wild-type plants (Vanderauwera *et al.*, 2011;

Table 1). Moreover, direct application of 10 mM H_2O_2 to wild-type seedlings led to a significant induction of these NAC transcription factors (Denecker *et al.,* unpublished results).

Table 1. Overview of H_2O_2-induced NAC transcription factors.

AGI code	Annotation	ATH1[a]	CATMA[b]	AGILENT[c]			H_2O_2 addition[d]
				cat2 vs WT (0 h)	*cat2* vs WT (1 h)	*apx1* vs WT (1 h)	
At1g01720	ATAF1/ANAC002			4.48	9.60	3.60	6.19
At5g08790	ATAF2/ANAC081			2.78	37.00	13.35	
At1g32870	ANAC013	2.45	2.57	1.68	1.48	1.60	12.84
At1g77450	ANAC032	5.03		7.52	19.92	8.52	11.46
At3g10500	ANAC053			2.01	10.43	5.83	4.36
At3g29035	ANAC059			1.72	22.84	1.49	
At5g18270	ANAC087		6.33				13.86
At5g63790	ANAC102	3.25		5.31	28.14	11.48	7.62

For each gene, the AGI code, annotation and the fold changes in the different H_2O_2-related transcript profiling studies (ATH1, CATMA, AGILENT and H_2O_2 addition experiment) are presented. FC, fold changes; WT, wild type.

[a] relative FC in *cat2* mutant versus WT plants after 3 h of HL exposure (Vanderauwera *et al.*, 2005).

[b] relative FC of *cat2* mutant versus WT plants after 8 h of HL irradiation (Hoeberichts *et al.*, unpublished results).

[c] relative FC in mutant (*cat2* or *apx1*) versus WT plants (Vanderauwera *et al.*, 2011).

[d] relative FC in H_2O_2-treated WT seedlings versus mock-treated plants after 24 h of treatment (Denecker *et al.*, unpublished results).

Transcriptional regulation of *ANAC102* during abiotic stress

We assessed the responsiveness of *ANAC102* under diverse abiotic stress conditions with the AtGenExpress abiotic stress time series (Kilian *et al.*, 2007) using the Response Viewer tool of GENEVESTIGATOR (Zimmermann *et al.*, 2004). *ANAC102* is induced by cold-, osmotic-, drought-, salt-, oxidative- and wounding stresses, but is down-regulated by heat stress (Table 2).

Stress	Time point/ tissue	Signal ratio
cold	E	1.29
	L	2.72
heat	G	0.60
	R	0.89
osmotic	E	2.92
	L	2.53
drought	E	2.68
	L	1.32
salt	E	5.63
	L	11.28
oxidative	E	0.68
	L	2.51
wounding	E	2.71
	L	2.11

Table 2. Meta-analysis of the ANAC102 expression profile towards abiotic stresses.

Expression data were obtained with GENEVESTIGATOR (Zimmermann *et al.*, 2004; Zimmermann *et al.*, 2005) using the AtGenExpress abiotic stress time series (Kilian *et al.*, 2007). Values represent signal intensity ratios between treated and untreated samples. E, early; L, late; G, green tissues; R, root tissues.

The transcriptional regulation of *ANAC102* was further investigated by searching for known regulatory elements within the 1.5 kb promoter region using the Arabidopsis Gene Regulatory Information Server (AGRIS; http://arabidopsis.med.ohio-state.edu/) and the Plant *cis*-acting regulatory DNA elements (PLACE) database, (http://www.dna.affrc.go.jp/PLACE/; Higo *et al.*, 1999). Interestingly, we found several *cis*-elements involved in abiotic stress regulation (Figure 1). Several W-box elements [TYTGACY] (Eulgem *et al.*, 2000) were found of which two are located in close proximity of the open reading frame of *ANAC102*. Several elements involved in drought-responsive gene expression were found, including two abscisic acid (ABA)-responsive elements (ABRE) [YACGTGKC] (Guiltinan *et al.*, 1990; Mundy *et al.*, 1990), two MYB2 elements [YAACKG] and six MYC [CANNTG] consensus recognition sites (Abe *et al.*, 1997). In accordance with the role of ANAC102 during hypoxia (Christianson *et al.*, 2009), we identified three anaerobic response consensus elements ANAERO1 [AAACAAA], ANAERO2 [AGCAGC], ANAERO3 [TCATCAC] that are involved in hypoxia regulation (Mohanty *et al.*, 2005). Moreover, several light-response elements were found including two closely positioned HD-ZIP2-AtATHB2 elements [TAATMATTA] (Ohgishi *et al.*, 2001), three G-boxes [CACGTG] (Giuliano *et al.*, 1988), and SORLIP1 [GCCACR] and SORLIP 2 [TGGGCC] elements (Hudson and Quail, 2003).

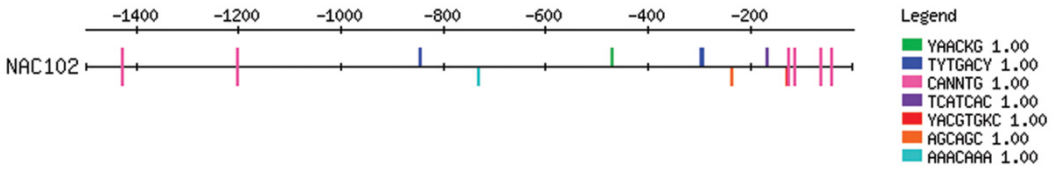

Figure 1. Abiotic stress-related *cis*-elements present in the promoter of *ANAC102*.

Abiotic stress-related *cis*-elements were found within the 1.5 kb upstream promoter region using the Arabidopsis Gene Regulatory Information Server (AGRIS; http://arabidopsis.med.ohio-state.edu/) and the Plant *cis*-acting regulatory DNA elements (PLACE) database (http://www.dna.affrc.go.jp/PLACE/; Higo *et al.*, 1999). The different motifs were visualized with the DNA pattern tool of the Regulatory Sequence Analysis Tools (RSAT; http://rsat.ulb.ac.be/rsat; van Helden, 2003).

To obtain more insight in the biological function of ANAC102, we searched for genes that are co-expressed during abiotic stress with *ANAC102* with the web tool CORNET (CORrelation NETworks; De Bodt *et al.*, 2010; https://cornet.psb.ugent.be/main/). Many of the co-expressed genes of *ANAC102* are transcription factors that play an important role in the abiotic stress response, such as *ANAC032*, *ATAF1*, *AZF2*, *CZF1*, *DREB2A*, *WRKY6*, *ZAT6* (Figure S1; Robatzek and Somssich,

2002; Sakamoto *et al.*, 2004; Vogel *et al.*, 2005; Sakuma *et al.*, 2006a; Sakuma *et al.*, 2006b; Lu *et al.,* 2007; Chen *et al.,* 2009; Kasajima *et al.*, 2010).

Taken together, *ANAC102* is transcriptionally regulated by H_2O_2 and several abiotic stress treatments and has a similar expression pattern as important transcriptional regulators of abiotic stress responses, indicating that ANAC102 could function in abiotic stress signaling.

Identification of organellar NAC transcription factors

In a previous subcellular localization study of H_2O_2-induced proteins, we demonstrated that ANAC102-GFP localizes to the chloroplasts (Inzé *et al.*, 2012 - Chapter 2). *ANAC102* encodes a 312 amino acid protein with an N-terminal conserved NAC domain (50-208 amino acids) containing a predicted bipartite nuclear localization signal (NLS; Kikuchi *et al.*, 2000; Figure 2a,b). Protein sequence alignment of ANAC102 with its closest homolog ATAF2 showed a high degree of sequence identity (> 78%), particularly in the five subelements of the NAC domain (Figure 2a). Interestingly, the N-terminal region of ANAC102 (43 amino acids) is completely absent in ATAF2 and contains a predicted chloroplast transit peptide (cTP; Emanuelsson *et al.*, 2007; Figure 2a).

Next, we constructed a homology-based three-dimensional model of ANAC102 with the Protein/Homology/analogy Recognition Engine (PHYRE2.0, intensive mode) web server that uses template-based homology modeling to construct structural predictions (Bennett-Lovsey *et al.*, 2008; Kelley and Sternberg, 2009). As expected, ANAC102 showed a high degree of structural homology with the NAC domain of ANAC (ABA-responsive NAC (ANAC019); Protein Data Bank codes 1UT4 and 1UT7; Ernst *et al.*, 2004; Figure 2c). Almost half of the residues of the predicted ANAC102 protein structure were modeled with a high confidence level (> 90%; indicated in red) and mainly comprised the NAC domain fold that is characterized by a twisted 7-stranded β-sheet (half-barrel; Figure 2c and Figure S2). The C-terminus of ANAC102 was predicted as highly disordered and was therefore also designated as NORS region (NO Regular Structure; Figure 2b,c). The C-termini of NAC transcription factors are often highly disordered and predominantly function as a flexible transcriptional activation domain (Jensen *et al.*, 2010).

Because an organellar localization of a nuclear-encoded transcription factor is unexpected, we assessed whether other members of the Arabidopsis NAC transcription factor family have predicted organellar targeting sequences by using the *in silico* prediction program TargetP (Emanuelsson *et al.*, 2007). For eleven NAC proteins, the presence of an N-terminal cTP or mitochondrial import sequence (mTP) was predicted (Table 3). In accordance, ANAC050 was previously identified in an *in silico*-based screening of Arabidopsis and rice (*Oryza sativa*) transcription factors with putative cTPs and mTPs

(Schwacke *et al.*, 2007). Moreover, a putative cTP was identified in a rice NAC transcription factor, ONAC071 (Os03g59730) that belongs to the same subfamily as ANAC102 (Schwacke *et al.*, 2007).

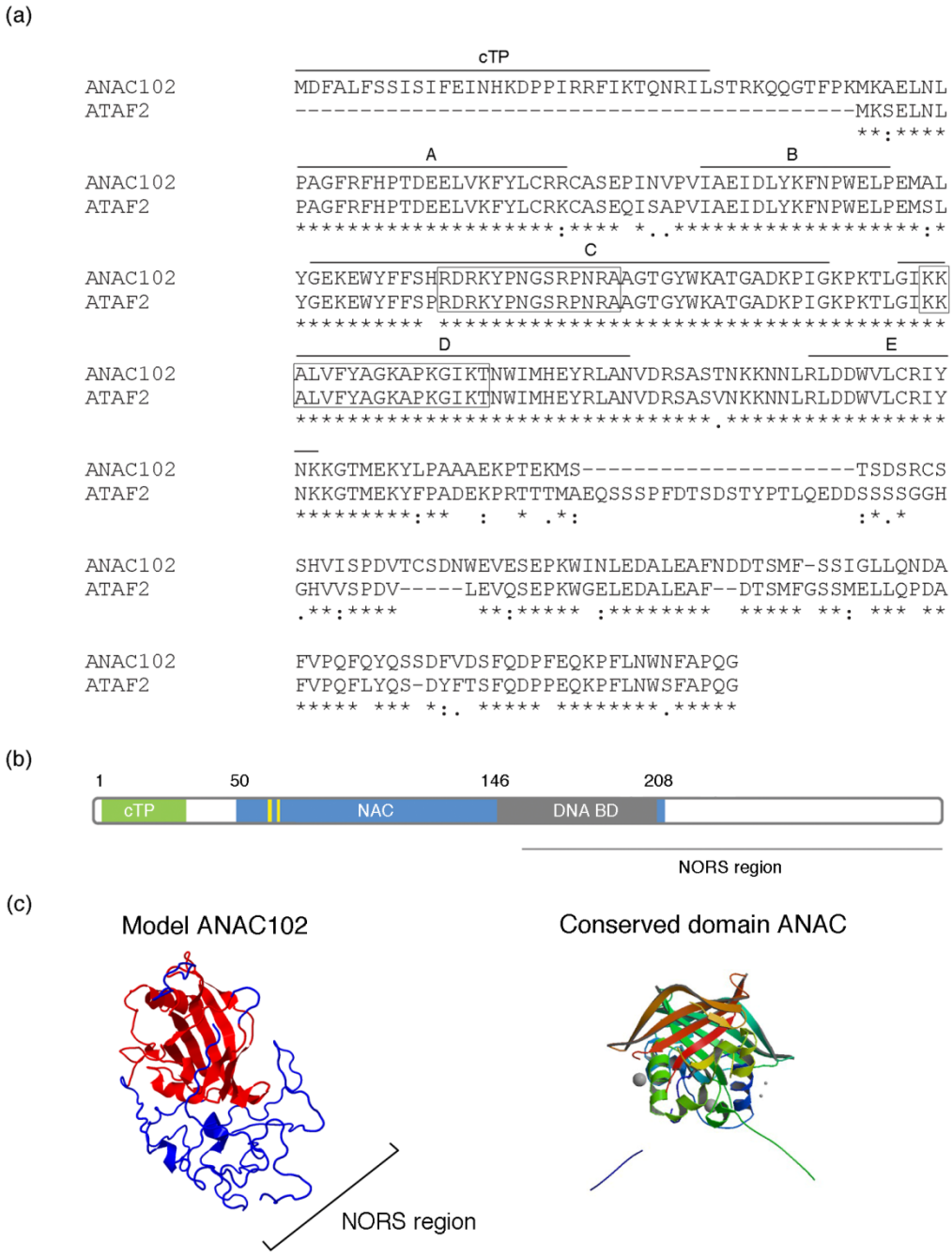

Figure 2. Structural features of ANAC102.

(a) Protein sequence alignment between ANAC102 and its closest Arabidopsis homolog ATAF2. The five subdomains (A-E) of the NAC domain are indicated with lines above the sequence and the putative bipartite NLS as described by Kikuchi *et al.*, 2000 is indicated by two boxes. '*' indicates that residues in that column are identical. ':' indicates conserved substitutions. '.' indicates semi-conserved substitutions. cTP; chloroplast transit peptide; NLS, nuclear localization signal.

Figure 2. Structural features of ANAC102. (*Continued).*

(b) Schematic representation of the different domains present in ANAC102. ANAC102 has two putative redox-sensitive cysteines (indicated in yellow) and a C-terminal NORS region. DNA BD, DNA binding domain; NAC, NAC domain; NORS, NO Regular Secondary Structure region.

(c) Tertiary structure *ab initio* model of ANAC102 predicted by PHYRE 2.0 (intensive mode; Bennett-Lovsey *et al.*, 2008; Kelley and Sternberg, 2009) and based on structural homology with the conserved NAC domain of ANAC (Protein Data Bank code 1UT7; Ernst *et al.*, 2004). The model is color-coded by confidence level (red, high; blue, low). The highly disordered NORS region is indicated.

Table 3. Overview of NAC transcription factors with predicted targeting sequences.

AGI code	Description	Length	Score				Predicted localization	Predicted cleavage site
			cTP	mTP	SP	other		
At1g25580	ANAC008	449	0.568	0.369	0.050	0.830	chloroplastic	41
At1g64100	PPR*	806	0.655	0.065	0.034	0.552	chloroplastic	53
At3g10480	ANAC050	447	0.397	0.205	0.216	0.197	chloroplastic	23
At3g56530	ANAC064	319	0.506	0.462	0.015	0.137	chloroplastic	48
At5g63790	ANAC102	312	0.628	0.038	0.060	0.529	chloroplastic	32
At1g03490	ANAC06	281	0.040	0.685	0.072	0.311	mitochondrial	30
At1g56010	ANAC021/22	257	0.046	0.712	0.013	0.533	mitochondrial	109
At2g33480	ANAC041	268	0.050	0.749	0.030	0.394	mitochondrial	75
At3g01600	ANAC044	370	0.036	0.305	0.221	0.201	mitochondrial	120
At5g14490	ANAC085	350	0.064	0.658	0.046	0.395	mitochondrial	29
At5g41090	ANAC095	212	0.035	0.833	0.054	0.291	mitochondrial	79

The final scores for the presence of a chloroplast transit peptide (cTP), mitochondrial targeting peptide (mTP), signal peptide for targeting to the secretory pathway (SP) and signals for targeting to another location (other) according to the prediction of TargetP (Emanuelsson *et al.*, 2007) are indicated. The predicted subcellular localizations, based on the final scores, are listed together with the predicted presequence length. At1g64100 (indicated with an asterisk) is a pentatricopeptide repeat (PPR)-containing protein that has a C-terminal NAC domain but was not included in the classification by Ooka *et al.* (2003).

To experimentally determine the subcellular localization of ANAC102, we fused the open reading frame (ORF) of *ANAC102* in frame with the ORF of green fluorescent protein (*GFP*) both at the N- and C-terminus and placed it under the control of the constitutive cauliflower mosaic virus 35S (CaMV35S) promoter (Figure 3a). While transient expression of the N-terminal GFP fusion of ANAC102 in the leaf epidermis of *N. benthamiana* led to both a nucleocytosolic and a putative cytoskeletal localization, ANAC102-GFP colocalized with the red fluorescence of the chloroplasts and was also present in the nucleus (Figure S3; Inzé *et al.*, 2012; Chapter 2). Next, we assessed the subcellular localization in leaf epidermis cells of at least two independent transgenic Arabidopsis plants. While no

GFP-positive primary transformants overexpressing GFP-ANAC102 could be obtained, the nuclear and chloroplastic localization of ANAC102-GFP could be confirmed in several independent *ANAC102-GFP*^{OE} plants (Figure 3b). Within the chloroplasts, GFP fluorescence was not evenly distributed but appeared in speckles. Because overexpression of a GFP-tagged protein could lead to protein mistargeting, we made transgenic plants expressing the N- and C-terminal GFP fusion construct under the transcriptional control of the native *ANAC102* promoter (prom$_{ANAC102}$:*GFP-ANAC102* and prom$_{ANAC102}$:*ANAC102-GFP*) in both a wild-type and *cat2* mutant background (Vandenabeele *et al.*, 2004; Figure 3a). Unfortunately in the wild-type background, no GFP fluorescence was observed for both constructs and this was probably due to the low expression of *ANAC102* in leaves during normal growth conditions. Because *ANAC102* transcript levels are constitutively increased in leaves of *cat2* mutants (Table 1), a strong GFP fluorescence in the prom$_{ANAC102}$:*ANAC102-GFP* (*cat2*) lines was observed (Figure 3b). While overexpression of *ANAC102-GFP* resulted in both a nuclear and a chloroplastic localization, native expression of *ANAC102-GFP* led to an exclusive chloroplastic localization in the *cat2* mutant (Figure 3b). Moreover, native expression of *GFP-ANAC102* showed no GFP fluorescence. Positioning of GFP at the N-terminus of ANAC102 presumably shields the cTP and, therefore, the observed cytoskeletal localization in *GFP-ANAC102*^{OE} plants probably resulted from blockage of the cTP, leading to mistargeting of ANAC102.

To further consolidate the chloroplastic localization and determine the suborganellar location of ANAC102, we isolated intact chloroplasts from leaves of both *ANAC102-GFP*^{OE} and prom$_{ANAC102}$:*ANAC102-GFP* lines. Subsequently, chloroplasts were lysed in a hypotonic medium and chloroplast thylakoids were separated from the stroma fraction by centrifugation. GFP-tagged proteins were detected by western blot analysis using a monoclonal anti-GFP antibody. Preliminary results indicated that ANAC102-GFP is present in intact chloroplasts, consolidating our GFP localization data (Figure 3c). Within the chloroplast, ANAC102-GFP was mainly found in the thylakoid fraction.

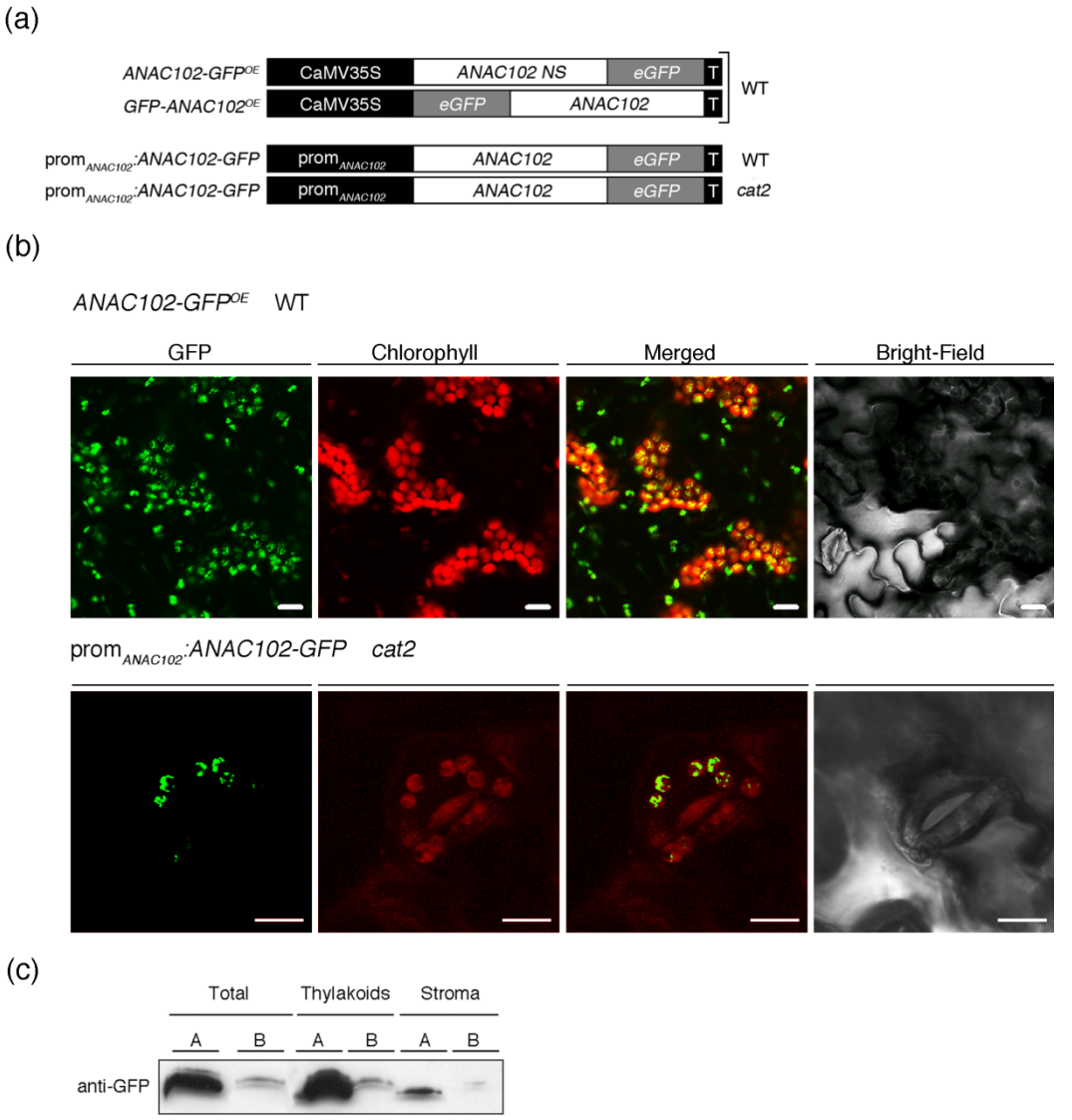

Figure 3. ANAC102 is targeted to the chloroplasts.

(a) Constructs used to determine the subcellular localization of ANAC102.

(b) ANAC102-GFP localizes to chloroplasts. Subcellular localization of ANAC102-GFP in stable transgenic Arabidopsis wild-type and *cat2* lines. Bars, 20 μm. GFP, green fluorescent protein; Merged, overlay of GFP and chlorophyll (red) fluorescence images.

(c) Suborganellar localization of ANAC102-GFP. Intact chloroplasts were isolated from leaves of *ANAC102-GFP*^{OE} (A) and prom$_{ANAC102}$:*ANAC102-GFP* (B) lines and fractionated into stromal and thylakoid fractions. Fifteen micrograms of each fraction was separated by SDS-PAGE, and protein gel blot analysis was performed using a monoclonal anti-GFP antibody.

Next, the targeting properties of the different domains of ANAC102 were assessed by making GFP-tagged truncated versions of ANAC102 (Figure 4a). First, to functionally validate the targeting properties of the predicted cTP, a construct was made in which the N-terminal domain of ANAC102 (1-43 amino acids), that includes the predicted cTP sequence, was translationally fused with GFP

(cTP$_{ANAC102}$-GFP) and placed under the constitutive promoter CaMV35S (Figure 4a; Karimi *et al.*, 2007). This construct was transiently expressed in leaf epidermis cells of *Nicotiana benthamiana* by means of agro-infiltration (Sparkes *et al.*, 2006). While transient expression of full length *ANAC102-GFP* resulted in a nuclear and chloroplastic localization, cTP$_{ANAC102}$-GFP displayed a nucleocytosolic localization (Figure 4b). On the other hand, ANAC102-GFP proteins that lack this N-terminal domain (Δ cTP ANAC102-GFP) displayed an exclusive nuclear localization (Figure 4b).

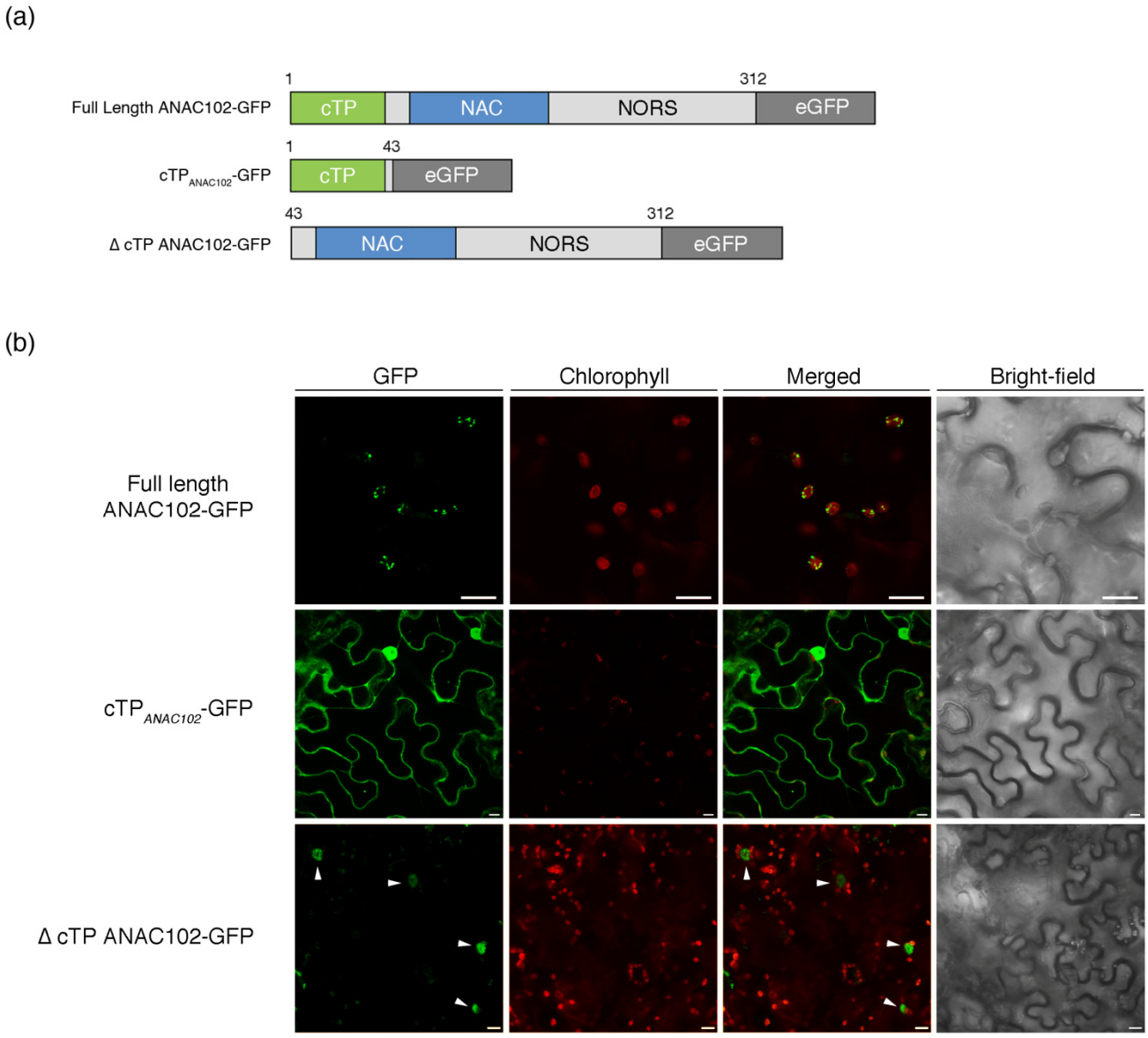

Figure 4. Deletion constructs of ANAC102-GFP.

(a) Schematic representation of the full length and deletion constructs.

(b) Transient expression of the deletion constructs in leaf epidermis cells of *N. benthamiana*. Similar results were obtained with independent experiments. cTP, chloroplast transit peptide; Merged, overlay of GFP and chlorophyll (red) fluorescence images; NORS; NO Regular Secondary Structure region. Bars, 10 μm.

Functionality of ANAC102-GFP

Previously, overexpression of a nuclear form of *ANAC102* has been shown to modulate the expression of 221 genes (113 up-regulated, 98 down-regulated; cut-off 1.5-fold, *P*-value ≤ 0.05; Christianson *et al.*, 2009). To determine whether ANAC102-GFP is functional as a transcription factor, we assessed the expression of several *ANAC102*^{OE}-modulated genes in *ANAC102-GFP*^{OE} plants. Therefore, we performed quantitative real-time (qRT)-PCR analyses on RNA extracted from 2-week-old wild-type and *ANAC102-GFP*^{OE} plants. Of the six strongest up-regulated genes in *ANAC102*^{OE} plants (Christianson *et al.*, 2009), five genes (*BGLU11, AtTDX1, ADH1, UGT74E2* and *ABCC10*), that nearly all contained the consensus NAC-binding site in their promoter regions (Christianson *et al.*, 2009), had also a higher expression (> 1.5-fold) in our *ANAC102-GFP*^{OE} plants compared to wild-type plants (Figure 5). These results indicate that that GFP-tagging of ANAC102 does not interfere with its transcriptional activity.

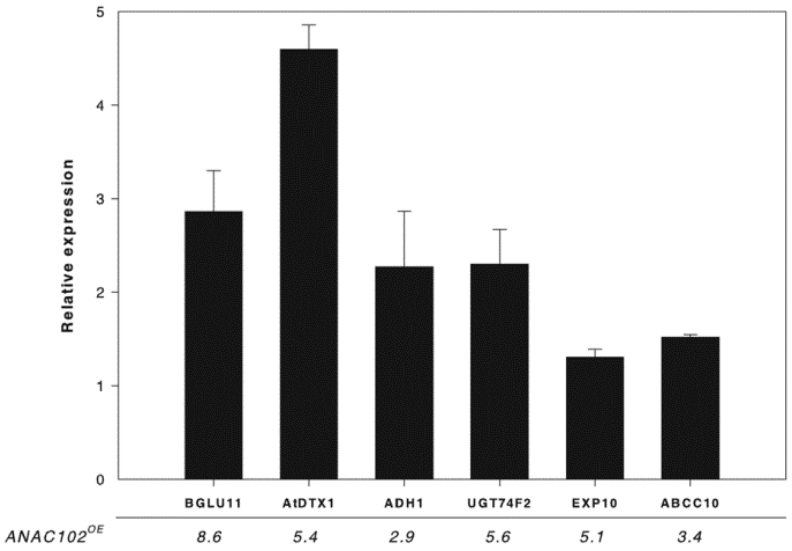

Figure 5. qRT-PCR analysis of selected *ANAC102*^{OE}-modulated genes in *ANAC102-GFP*^{OE} plants. Relative mRNA transcript levels were monitored in 2-week-old Arabidopsis wild-type and *ANAC12-GFP*^{OE} plants. Data presented are fold changes expressed relative to wild type and normalized to *ACTIN RELATED PROTEIN7* (*ARP7*). Error bars represent ± SE (n=3). The relative expression ratios of the selected genes in the *ANAC102*^{OE} plants reported in Christianson *et al.,* (2009) are indicated below the graph.

Relocalization of ANAC102 during oxidative stress conditions

The chloroplastic localization of ANAC102 is at first sight contradictory with its role to regulate nuclear gene expression. Therefore, we hypothesized that ANAC102 proteins might redistribute to the nucleus under a certain stimulus. Oxidative stress-induced subcellular relocalizations of proteins have been reported for a number of proteins (Chapter 1). Therefore, we assessed whether the subcellular localization of ANAC102 changes during oxidative stress conditions. Together with the mitochondria and peroxisomes, chloroplasts are the major ROS production sites. To increase ROS levels in the chloroplasts, we used the herbicide methyl viologen (MV, 1,1'-dimethyl-4,4'-bipyridinium dichloride),

also known as paraquat. MV is a redox-active compound that in light accelerates the generation of superoxide radicals ($O_2^{\bullet-}$) and H_2O_2 in chloroplasts (Yabuta *et al.*, 2004; Figure 6a). Prom$_{ANAC102}$:*ANAC102-GFP* lines (*cat2*) were grown *in vitro* for two weeks on half-strength (½) MS on nylon mesh and were subsequently transferred to plates containing 50 µM MV. Whereas ANAC102-GFP colocalized exclusively with chloroplasts prior to MV treatment, GFP fluorescence was also observed in nuclei after 6 h of MV treatment (Figure 6b).

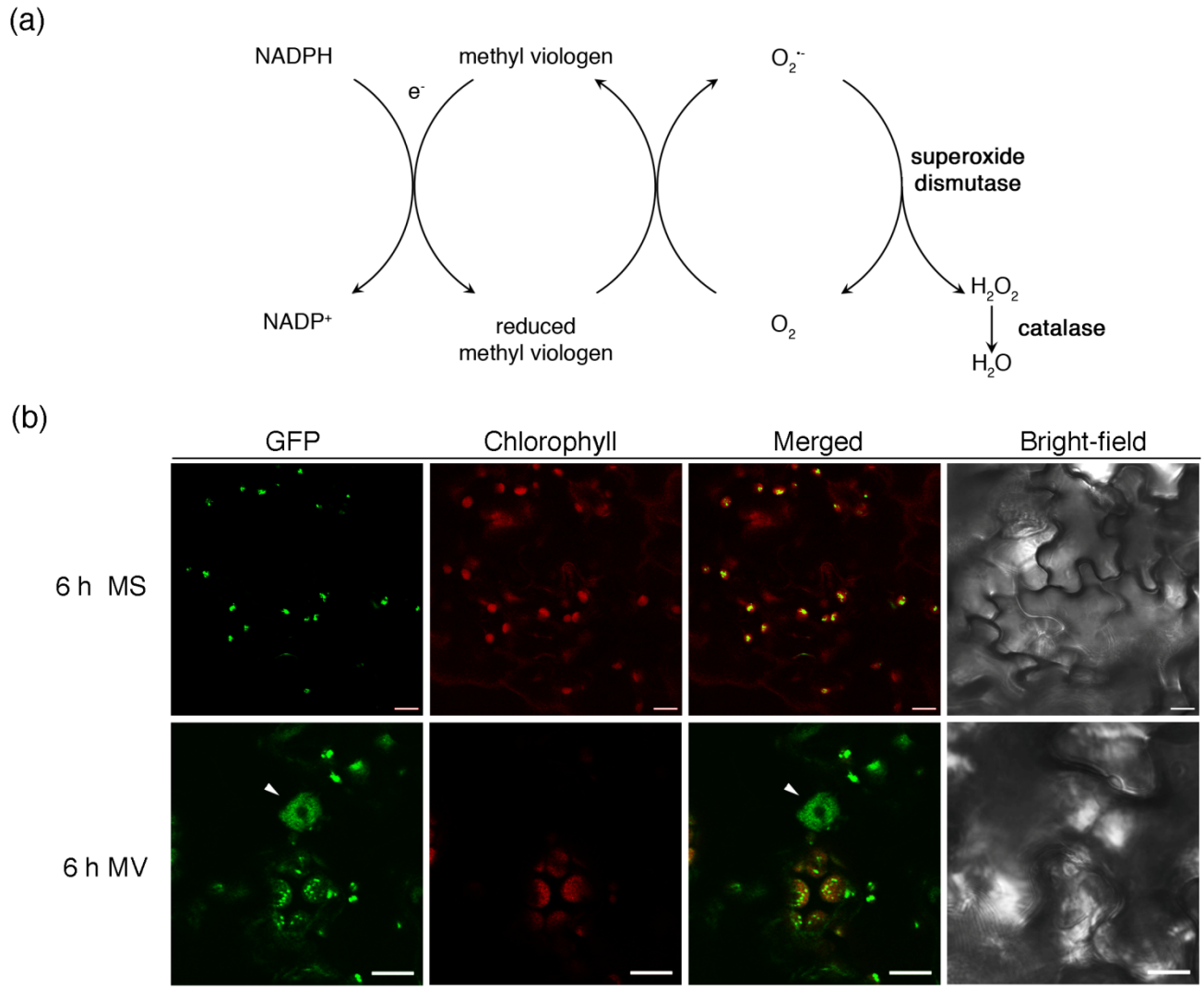

Figure 6. ANAC102 relocalization from the chloroplasts to the nucleus during MV treatment.

(a) Schematic representation of the mode of action of MV. MV disrupts the photosynthetic electron transport chain and inhibits the conversion of $NADP^+$ to NADPH leading to the accumulation of free electrons. The electron acceptance of molecular oxygen (O_2) leads to the formation of superoxide radicals ($O_2^{\bullet-}$) which are converted by superoxide dismutase into hydrogen peroxide (H_2O_2) molecules. H_2O_2 can freely diffuse between subcellular compartments and is readily scavenged by peroxisomal catalases. Enzymes are indicated in bold.

Figure 6. ANAC102 relocalization from the chloroplasts to the nucleus during MV treatment. *(Continued).*
(b) ANAC102 relocalization upon MV treatment in *cat2* mutants. In non-stressed conditions, ANAC102-GFP was exclusively localized to chloroplasts. After 6 h of MV treatment, ANAC102-GFP was localized both to chloroplasts and nuclei (indicated with an arrow). Similar results were obtained with independent experiments. Merged, merged images of GFP and chlorophyll fluorescence images.

Next, we assessed whether ANAC102 is proteolytically processed upon relocalization. Therefore, we treated *ANAC102-GFP*^{OE} and prom$_{ANAC102}$:*ANAC102-GFP* (*cat2*) plants with 50 μM MV as described above and immunodetected GFP-tagged proteins with an anti-GFP antibody. We used *GFP*^{OE} plants as a positive control for GFP signal. Both in the *ANAC102-GFP*^{OE} and the prom$_{ANAC102}$:*ANAC102-GFP* lines, the full length ANAC102-GFP (~63 kDa) and a band that corresponds in size with ANAC102-GFP without the N-terminal cTP (Δ cTP ANAC102-GFP; ~58 kDA) were detected (Figure 7). Moreover in *ANAC102-GFP*^{OE} lines, additional cleavage products of ANAC102-GFP were detected (~45 and ~30 kDa) irrespective of the MV treatment (Figure 7a). Because overexpression leads to a nuclear localization, the cleavage of a C-terminal region of approximately 18 kDa could be necessary for release from the chloroplasts. Unfortunately, we could not detect the presence of these cleavage products in the prom$_{ANAC102}$:*ANAC102-GFP* lines (Figure 7b) and, thus, could not directly link the relocalization with the MV-induced processing of ANAC102.

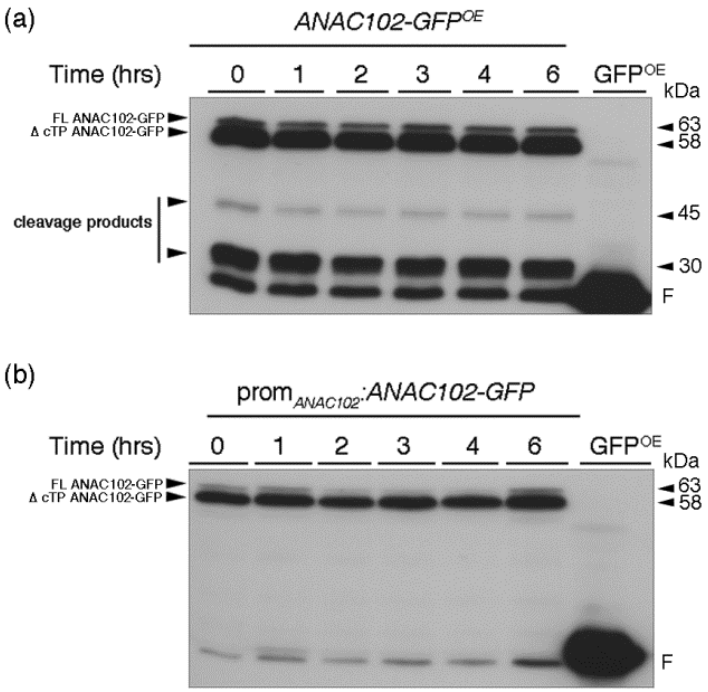

Figure 7. Processing of ANAC102.
ANAC102-GFP^{OE} (a) and prom$_{ANAC102}$:*ANAC102-GFP* (*cat2*; b) lines were grown till stage 1.04 on ½ MS agar plates and treated with 50 μM MV. Fifteen micrograms of protein were separated by SDS PAGE, and protein gel blot analyses were performed with a monoclonal anti-GFP antibody. The full length (FL) ANAC102-GFP (63 kDa), the ANAC102-GFP without cTP (Δ cTP ANAC102-GFP; 58 kDa) are indicated by an arrow. F, free GFP.

ANAC102 overexpression leads to the partial repression of oxidative-stress related genes and an increased sensitivity towards oxidative stress

By using a yeast one-hybrid approach, ANAC102 was identified to bind the promoters of several nuclear oxidative stress-regulated genes (De Clercq *et al.*, unpublished results), including two *ANAC102*^{OE}-modulated genes (Christianson *et al.*, 2009). ANAC102 binds to the promoters of *ALTERNATIVE OXIDASE1a* (*AOX1a*), *DETOXIFICATION1* (*AtTDX1*), two *UDP-GLYCOSYL TRANSFERASES* (*UGT74E2* and *UGT73C6*), *SULFOTRANSFERASE1* (*AtST1*), *ATP-BINDING CASSETTE B4* (*ATPGP4*), *SMALL HEAT SHOCK PROTEIN23.5* (*sHSP23.5*) and a gene of unknown function (At2g41730). These genes are significantly up-regulated by MV-induced oxidative stress (Zimmermann *et al.*, 2004; Table 4)

AGI code	Description	Expression ratio after MV treatment
At3g22370	AOX1a	1.96
At2g04040	AtDTX1	3.19
At1g05680	UGT74E2	12.78
At2g36790	UGT73C6	3.71
At2g03760	AtST1	5.64
At2g47000	AtPGP4	6.81
At5g51440	sHSP23.5	11.44
At2g41730	Unknown protein	8.86

Table 4. Expression ratios of the target genes of ANAC102 after MV treatment.

The MV-induced oxidative stress response of the selected genes were obtained from the AtGenExpress abiotic stress time series (Kilian *et al.*, 2007) with the GENEVESTIGATOR Meta profile analysis tool (Zimmermann *et al.*, 2004). Values present signal ratios.

Next, we assessed whether the expression of these putative target genes is modulated by *ANAC102* overexpression during normal and oxidative stress conditions. Therefore, we generated constitutive overexpression lines with the CaMV35S promoter. Two independent homozygous transgenic lines (*ANAC102*^{OE1} and *ANAC102*^{OE2}) with elevated *ANAC102* transcript levels (35-fold and 143-fold, respectively; assayed with qRT-PCR analyses) were selected. Wild-type and mutant *ANAC102* transgenic lines were germinated and grown on nylon mesh on ½ MS agar plates till developmental stage 1.04 (4th true leaf 1 mm in size). Then, the plants were transferred to ½ MS agar plates supplemented with 50 μM MV. We followed the expression of five target genes of *ANAC102* (*AOX1a*, *AtDTX1*, *AtST1*, *UGT73C6* and *UGT74E2*) in time by performing qRT-PCR analyses on RNA extracted from control and MV-treated wild-type and *ANAC102*^{OE} plants. These putative ANAC102 target genes were significantly induced by MV treatment in wild-type plants (Figure 8a). In contrast, the induction of these genes by MV was significantly reduced in the *ANAC102*^{OE} lines compared to wild-type plants, indicating that ANAC102 could function as a transcriptional repressor of these genes under oxidative stress conditions (Figure 8a).

As *ANAC102* overexpression resulted in the partial repression of *AOX1a*, *AtDTX1*, *AtST1*, *UGT73C6* and *UGT74E2* under oxidative stress, we assayed the performance of the *ANAC102*^{OE} and a *ANAC102*^{KO} line under these conditions. A transgenic line with decreased *ANAC102* transcript levels was obtained by selecting a T-DNA insertion mutant from the SALK collection with a T-DNA in the coding region of *ANAC102* (Alonso *et al.,* 2003). Homozygous plants from the Arabidopsis T-DNA insertion mutant SALK_030702C, in which the T-DNA was inserted into the second exon of the *ANAC102* gene, showed 6.5% residual *ANAC102* transcript levels. First, we tested the performance of the overexpression lines during MV treatment. Therefore, plants were germinated and grown on nylon mesh on ½ MS agar plates under normal growth conditions. After two weeks, plants were transferred to ½ MS agar plates supplemented with 2 μM MV and the rosette leaves were compared throughout the treatment. After one week of MV treatment, *ANAC102*^{OE} plants were larger and seemed to have lower anthocyanin pigmentation (Figure 8b). However when the MV treatment was prolonged to five weeks, *ANAC102*^{OE} plants had completely died, while the wild-type plants remained green with visible higher anthocyanin pigmentation (Figure 8b).

Next, we determined the performance of the *ANAC102*^{OE} and *ANAC102*^{KO} lines under photorespiration-promoting conditions with a bioassay in which the production of photorespiratory H_2O_2 is increased by restricting gas exchange within the plates (Mühlenbock *et al.,* unpublished results; see Experimental Procedures). While the strongest *ANAC102* overexpression line (*ANAC102*^{OE2}) was more susceptible to oxidative stress, the *ANAC102*^{KO} plants showed an increased performance (Figure 8c). In addition, we monitored the photochemical performance, an early indicator of stress, of the *ANAC102*^{OE} and *ANAC102*^{KO} plants under these conditions by measuring the maximum quantum efficiency of photosystem II (PSII) under light adapted conditions (F_v'/F_m'; Badger *et al.*, 2009). Accordingly, the photochemical performance of the *ANAC102*^{KO} plants was increased, while a reduction was seen in the *ANAC102*^{OE} lines (Figure S4).

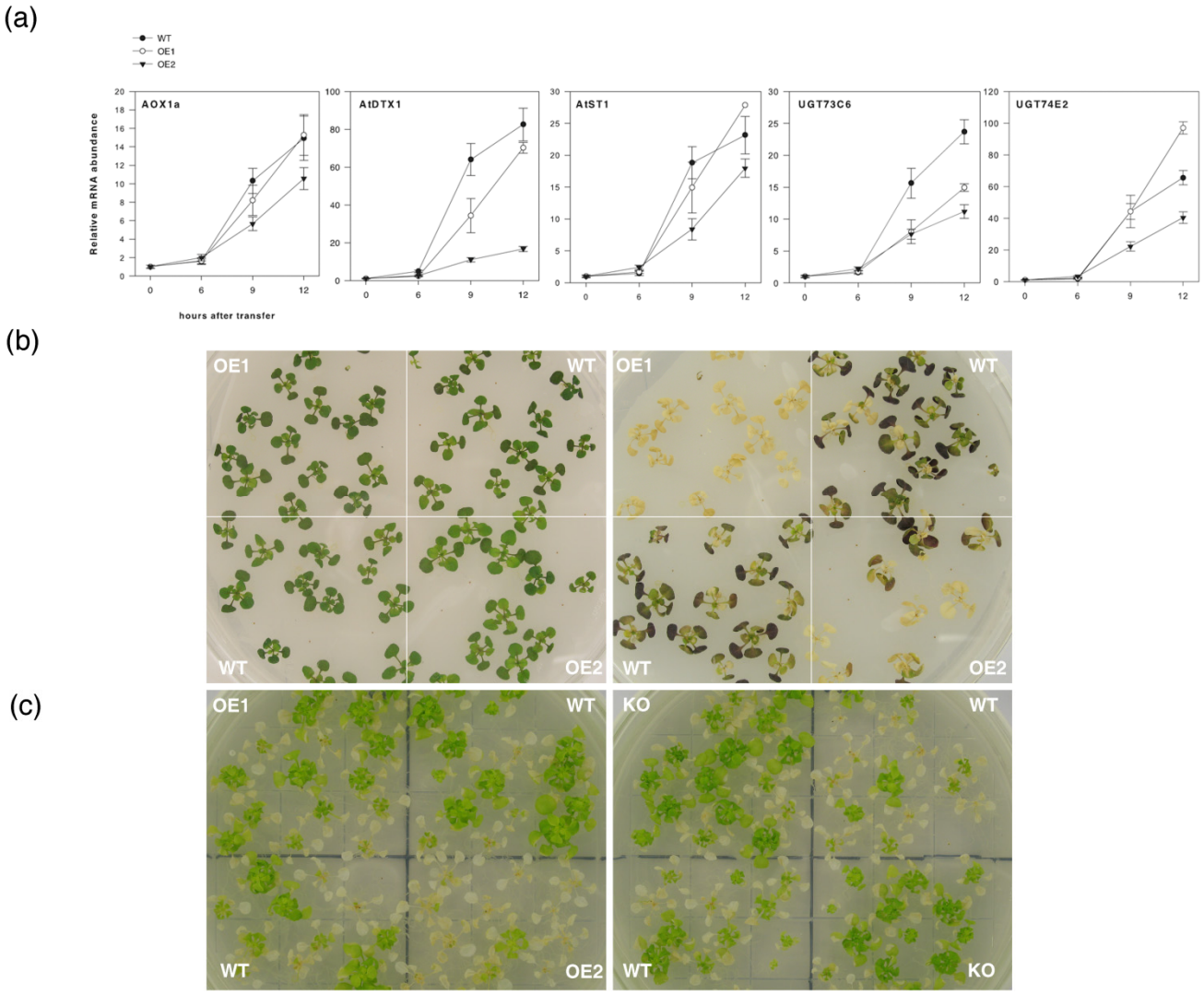

Figure 8. Phenotype of *ANAC102*^{OE} and *ANAC102*^{KO} plants under oxidative stress conditions.

(a) Expression profile of the *ANAC102* target genes during MV treatment in wild-type plants and two independent *ANAC102*^{OE} lines. Values are expressed relative to mock-treated wild type and are normalized against *ARP7*. Data represent average ± SE (n = 3). Similar results were obtained with an independent experiment.

(b) Phenotype of the *ANAC102*^{OE} lines during MV treatment. 2-week-old wild-type and transgenic *ANAC102*^{OE} plants grown under control conditions were transferred to plates containing 2 µM MV. Left: one week after transfer. Right: five weeks after transfer.

(c) Phenotype of 6-week-old *ANAC102*^{OE} (left) and *ANAC102*^{KO} (right) lines under three weeks of photorespiration-promoting conditions. WT, wild type.

DISCUSSION

NAC transcription factors belong to one of the largest plant-specific transcription factor families, with 75 and 105 members in rice and Arabidopsis, respectively (Ooka *et al.*, 2003) and have been shown to play a role in both embryonic, floral and vegetative developmental processes as well as in stress signaling in both model plants and agronomical important crops (Olsen *et al.*, 2005). Previous transcriptome analyses allowed us to identify eight NAC transcription factors, including all members of the ATAF subfamily, whose expression is tightly regulated by H_2O_2 (Vanderauwera *et al.*, 2005; Vanderauwera *et al.*, 2011; Inzé *et al.*, 2012; Denecker *et al.*, unpublished results; Hoeberichts *et al.,* unpublished results).

ANAC102 is transcriptionally regulated by abiotic stresses

ATAF subfamily NACs are transcriptionally regulated by a variety of biotic and abiotic stress conditions and have been shown to play a role in multiple stress responses (Christianson *et al.*, 2010). Besides the induction by cold, drought and salinity stress, *ANAC102* transcript levels were increased by oxidative and wounding stress and decreased by heat stress (Zimmermann *et al.*, 2004). Most NAC genes that are induced by cold stress are repressed by heat stress and vice versa (Jensen *et al.*, 2010). The regulation of *ANAC102* expression by abiotic stresses might be linked with the prevalence of several abiotic stress-related *cis*-elements in its promoter region such as W-box elements, the drought-responsive elements ABRE (Guiltinan *et al.*, 1990; Mundy *et al.*, 1990), MYB2 and MYC motifs (Abe *et al.*, 1997), anaerobic response consensus sequences (Mohanty *et al.*, 2005) and several light-responsive elements (Giuliano *et al.*, 1988; Ohgishi *et al.*, 2001; Hudson and Quail, 2003). Previously, *ANAC102* was also identified as being significantly up-regulated by a combination of cold and light treatment (Soitamo *et al.*, 2008). The combination of cold and light is thought to modulate the photosynthetic machinery and the chloroplast redox status (Soitamo *et al.*, 2008). Transcription factors induced by this treatment are likely to regulate cold-/light-responsive genes. In total, 237 genes showed a differential gene expression in response to the cold and light treatment of which approximately one third are targeted to the chloroplasts (Soitamo *et al.*, 2008). These data indicate that ANAC102 might play a role in the transcriptional control of stress-responsive genes during abiotic stresses.

ANAC102 is a regulator of nuclear gene expression and is located in the chloroplasts

In our subcellular localization study of H_2O_2-induced proteins we demonstrated that ANAC102 localizes to the chloroplasts (Inzé *et al.*, 2012 - Chapter 2). Increasing evidence arises of regulators of nuclear gene expression that are present in organelles such as mitochondria and chloroplasts (Wagner and Pfannschmidt, 2006; Schwacke *et al.*, 2007; Krause and Krupinska, 2009). In Arabidopsis, we found five

NAC domain-containing proteins with a predicted chloroplastic localization and six putative mitochondrial NACs. The chloroplastic localization of ANAC102 was confirmed by expression of GFP fusion constructs in stable transgenic Arabidopsis plants. Strong overexpression resulted in a dual targeting of ANAC102 to the chloroplasts and the nucleus, demonstrating that both the cTP and the NLS are functional. Interestingly, expression of *ANAC102-GFP* constructs under the control of the endogenous *ANAC102* promoter resulted in an exclusive chloroplastic localization, demonstrating hierarchical dominance of the cTP over the NLS. Furthermore, preliminary fractionation experiments of the different subcompartments of the chloroplasts showed that ANAC102 is predominantly associated with the thylakoids. Further experiments are necessary to confirm these results. Unfortunately, immune-electron microscopy experiments to determine the precise localization of ANAC102 within the chloroplast failed. Although we could not demonstrate the targeting properties and exact nature of the predicted cTP directly, deletion of the N-terminal sequence of ANAC102 containing the cTP resulted in an exclusive nuclear localization. These results indirectly demonstrate that the N-terminal region harbors information for chloroplast import although other regions of ANAC102 might also be important. In fact, efficient translocation of a native protein with a chloroplast import sequence does not necessarily mean that only the transit peptide is required as signals often shorter than 60 amino acids are not sufficient for the transport of a protein into the chloroplasts (Bionda *et al.*, 2010).

Nuclear regulators with an organellar localization must at one point, either by a developmental stimulus or during a stress response, be released from the organelle into the cytoplasm where they are redirected to the nucleus to control nuclear gene expression. In yeast and mammalian cells, several reports of development- and environment-induced protein relocalizations from organelles to the nucleus have been described (Susin *et al.*, 1999; Cregan *et al.*, 2002; Ruchalski *et al.*, 2006). In *cat2* mutant lines expressing native levels of *ANAC102-GFP*, we could trigger the relocalization of ANAC102-GFP from the chloroplasts to the nucleus by using MV, a redox-active compound that leads to the formation of chloroplast-localized ROS, including H_2O_2. Because of its relative stability, H_2O_2 can easily migrate from the chloroplasts to adjacent compartments (Henzler and Steudle, 2000; Bienert *et al.*, 2006). The lack of the H_2O_2-scavenging enzyme catalase, that plays a crucial role in maintaining low levels of photorespiratory H_2O_2 in the peroxisomes (Mhamdi *et al.*, 2010) but also acts as a sink for intracellular H_2O_2 (Willekens *et al.*, 1997), might further perturb ROS homeostasis and enhance ROS-induced changes in the cellular redox state. Several cleavage products of ANAC102-GFP were observed by western blot analysis in *ANAC102-GFP*^{OE} lines that contain ANAC102 both in the chloroplasts and the nucleus. This could indicate that processing might play a role in the release of ANAC102 from the chloroplasts. Although the exact nature of the cleavage products is not known, it is tempting to speculate from the band size that the C-terminal disordered region (18 kDa), that includes the transactivation

domain, is removed. Unfortunately, we could not detect these cleavage products in the native GFP expression lines and can therefore not rule out the possibility that the observed cleavage products are the result of *ANAC102-GFP* overexpression. Additional experiments are necessary to address and clarify this issue. In this aspect, the development of an ANAC102-specific antibody is crucial. Antibodies raised against full length ANAC102 were produced, but lacked specificity presumably by the presence of the conserved NAC domain. Therefore, the more divergent C-terminal domain could be used to produce more specific antibodies. In addition, determining the exact nature of the cleavage products observed in the overexpression lines by amino acid sequencing could provide more insight in the proteolytic processing of ANAC102 and could give a first indication which potential proteases could be involved.

During abiotic stress, a defense response is initiated through the complex regulation of transcription, including both transcriptional activation and repression. By using a yeast one-hybrid approach, ANAC102 was identified to bind several promoter regions of nuclear oxidative stress-regulated genes (De Clercq *et al.*, unpublished results), including several *ANAC102*^{OE}-induced genes (Christianson *et al.*, 2009). Furthermore, the induction of several of these target genes by MV is dampened by *ANAC102* overexpression. These results indicate that ANAC102 might function as a transcriptional repressor during oxidative stress conditions (De Clercq *et al.,* unpublished results). Moreover, the light-harvesting chlorophyll a/b binding proteins 1.1a and 2.4 are down-regulated in *ANAC102*^{OE} plants (Christianson *et al.*, 2009; Vanderauwera, personal communication). The expression of *Lhcb* genes, coding for light-harvesting proteins of PSII, are frequently down-regulated in photo-oxidized plants (Fey *et al.*, 2005). Most NAC transcription factors operate as transcriptional activators such as NAC1, AtNAM and ANAC019 (Xie *et al.*, 2000; Duval *et al.*, 2002; Fujita *et al.*, 2004; Tran *et al.*, 2004). However, increasing evidence emerges that NAC transcription factors can also function as transcriptional repressors. For instance, a calmodulin (CaM)-binding NAC protein (CBNAC) was identified that functions as a CaM-regulated repressor (Kim *et al.*, 2007). Moreover, VASCULAR-RELATED NAC-DOMAIN (VND)-INTERACTING 2 (VNI2), that regulates xylem cell specification, can act both as an active or passive repressor (Yamaguchi *et al.*, 2010). It would be interesting to determine whether the C-terminal transactivational domain of ANAC102 is cleaved off during oxidative stress. In this case, ANAC102 would still be able to bind its nuclear target genes but cannot activate them anymore.

Transgenic *ANAC102*^{OE} lines showed enhanced sensitivity under oxidative stress conditions, whereas *ANAC102*^{KO} lines were more resistant. At first, *ANAC102*^{OE} plants seemed to have an improved growth response with lower anthocyanin pigmentation. During biotic and abiotic stress conditions, anthocyanins and other flavonoids accumulate and are thought to function as antioxidants that scavenge stress-derived ROS (Vanderauwera *et al.*, 2005; Hernández *et al.*, 2009). As *ANAC102*^{OE}

plants initially keep growing and seem to accumulate less anthocyanins during oxidative stress conditions, they could have a repressed or reduced stress response. Prolongation of severe stress conditions further leads to severe intracellular damage and eventually leads to cell death in the *ANAC102* overexpression lines while the wild type still seems to cope with the stress (De Clercq *et al.,* unpublished results). Because constitutive activation of the stress response is energetically expensive and often related with a growth reduction, plants have evolved several mechanisms, including transcriptional repressors, to tightly control the expression of stress-responsive genes. For instance, RAP2.1 tightly controls the expression of stress-related genes during cold and drought (Dong and Liu, 2010).

Future prospects: ANAC102, a novel plastidial signal involved in chloroplast retrograde signaling?

The presence of nuclear regulators in organelles could be an important strategy for interorganellar communication. During plant cell evolution, the plastid genome size was strongly reduced, either by loss of organellar genes or by gene transfer to the nucleus (Martin and Herrmann, 1998). Therefore, plastids are semi-autonomous and are strongly dependent on nuclear gene expression (Stern *et al.*, 1997; Barkan and Goldschmidt-Clermont, 2000), requiring a strong communication from the nucleus to the chloroplasts, also called anterograde signaling, and a flow of information backwards (chloroplasts-to-nucleus), known as retrograde signaling. During adverse environmental conditions, such as fluctuating illumination and limiting CO_2 fixation by low temperature, salinity, low nutrient, and water availability, the homeostasis of photosynthetic processes is disturbed (Fey *et al.*, 2005). Therefore, chloroplasts are often seen as sensors of adverse environmental conditions that communicate back to the nucleus to initiate an appropriate response. Although chloroplast retrograde signaling has been studied for decades, the process is still poorly understood. Recent studies have indicated that the production of ROS and the redox status of the components of the electron transport chain play an important role in chloroplast retrograde signaling (Pfannschmidt, 2010).

Here, we provide the first evidence for the retrograde relocalization of a chloroplastic NAC transcription factor that negatively regulates the expression of oxidative stress-related genes during chloroplast-derived oxidative stress conditions. Although the mechanism of relocalization is not resolved yet, different scenarios are plausible (Figure 9). The perturbed chloroplastic redox state could modify ANAC102 directly or indirectly by changing an unidentified NAC-binding protein that, in turn, binds or alters ANAC102. ANAC102 has two closely positioned cysteines that could indicate for redox-sensitive regulation. The oxidation of redox-sensitive transcription factors could lead to a conformational change that can affect the subcellular localization (Sun and Oberley, 1996 – Chapter 1). The interaction of NAC transcription factors with other proteins is often governed by their C-terminal transcription regulatory

domain that frequently has a high degree of flexibility and lacks the ability to form an ordered three-dimensional structure (Jensen *et al.*, 2010). Once modified, ANAC102 has to cross the chloroplast membrane(s). Several translocation mechanisms are plausible, such as transport by vesicles, trafficking by envelope transporters, stromule tip shedding and close intercompartimental contacts (Krause and Krupinska, 2009). In addition, severe oxidative stress could disrupt the chloroplast structure. However, preliminary electron microscopy experiments showed that the chloroplast ultrastructure was not affected at the same time and conditions of relocalization (data not shown). After the stress-induced release of ANAC102 into the cytoplasm, ANAC102 is imported into the nucleus where it represses stress-responsive gene expression. Interestingly, ANAC102 negatively regulates the expression of *AOX1a*, a well-known reporter gene used in mitochondrial retrograde signaling studies (Zarkovic *et al.*, 2005). Moreover, ABI4 – a known plastidial retrograde signal – is also involved in the regulation of *AOX1a* suggesting that retrograde signaling from both organelles might converge at some point (Giraud *et al.*, 2009).

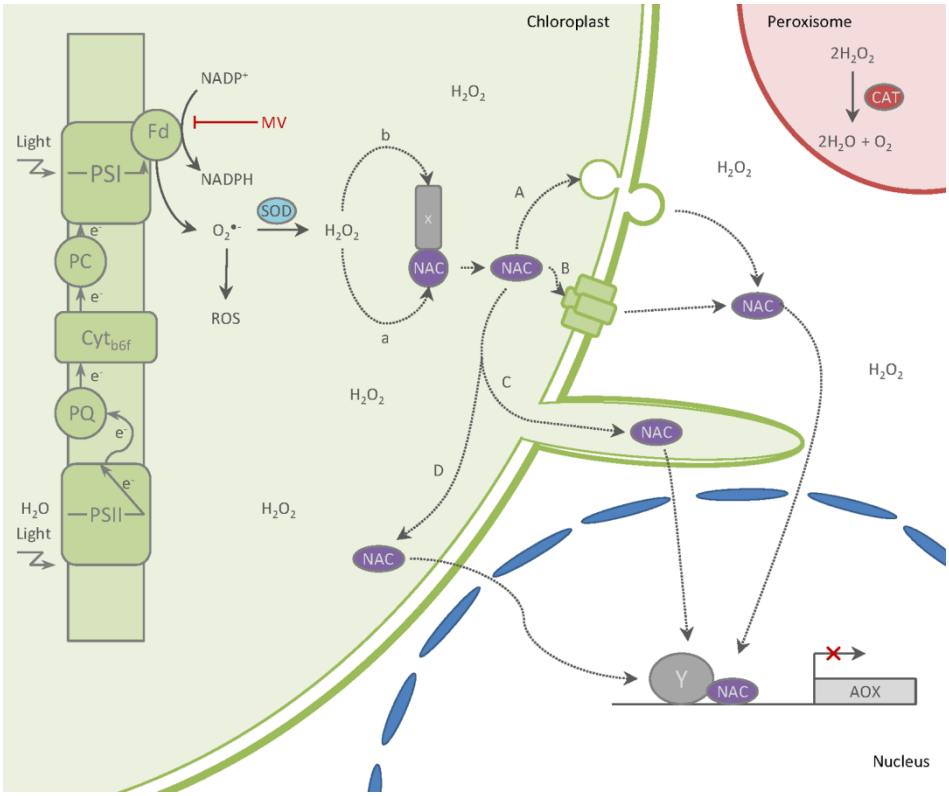

Figure 9. Possible mechanisms of ANAC102 relocalization.

During MV treatment, the conversion of $NADP^+$ to NADPH is inhibited, leading to the accumulation of $O_2^{\bullet-}$ that subsequently gives rise to other ROS. In our experiments, the cellular oxidative strain is further enhanced by the lack of the peroxisomal H_2O_2-scavenging enzyme catalase that acts as sink of intracellular H_2O_2. The accumulation of ROS can directly (a) or indirectly (b) modify ANAC102 either by oxidation or by modifying an interacting protein, respectively.

Figure 9. Possible mechanisms of ANAC102 relocalization. *(Continued).*

Once altered, the release of ANAC102 into the cytoplasm can occur through different mechanisms: (A) vesicle–mediated release, (B) transporters, (C) stromule tip shedding and (D) close intercompartimental contacts (Krause and Krupinska, 2009). After the release into the cytoplasm, ANAC102 is redirected to the nucleus where it regulates the expression of stress response genes.

EXPERIMENTAL PROCEDURES

Plant growth conditions and treatments

For *in vitro* experiments, *A. thaliana* (L.) Heynh ecotype Columbia (Col-0) plants (wild type) were grown until stage 1.04 (unless stated otherwise; 4th true leaf 1 mm in size; Boyes *et al.*, 2001) on half-strength (½) Murashige and Skoog (MS) medium (Duchefa Biochemie; http://www.duchefa.com/), 1% (w/v) sucrose, 0.7% (w/v) agar, pH 5.7 at 21°C and under a 16-h light/8-h dark photoperiod, 150 μmol $m^{-2}s^{-1}$ light intensity and 50% relative humidity. For the ANAC102 relocalization and processing experiments, wild-type and mutant seeds were sown and germinated on nylon mesh on ½ MS plates. At stage 1.04, plants were transferred to ½ MS plates containing 50 μM MV. For the ANAC102 processing experiments, a pool of 32 plants was harvested at each time point. Two independent experiments were carried out (independent sets of plants sown and treated on different dates). For the qRT-PCR analyses of the ANAC102 targets, wild type, *ANAC102* overexpression and knock-out lines were treated with the same conditions as the relocalization experiment. At each time point, three biological repeats of six plants were harvested. For the MV stress assay, 2-week-old mesh-grown plants were transferred to ½ MS plates supplemented with 2 μM MV. The stress assays were performed with two biological repeats. For the photorespiration-promoting conditions, plants were grown under control conditions for two weeks. Then, the petri plates were sealed with parafilm to restrict gas exchange. Photosynthetic efficiency of PSII was determined by measuring the light-adapted maximum quantum yield of PSII (F_v'/F_m') with the IMAGING-PAM M-Series Chlorophyll Fluorescence System (WALZ; Effeltrich, Germany; http://www.walz.com/).

Transcriptional regulation of *ANAC102*

Within the different tools of GENEVESTIGATOR, the Response Viewer was used to find the response profile of *ANAC102* to abiotic environmental stimuli (Zimmermann *et al.*, 2004; Zimmermann *et al.*, 2005). Out of the different conditions annotated, the AtGenExpress abiotic stress time series (Kilian *et al.*, 2007) was selected.

CORNET analysis

The online data mining tool CORrelation NETworks (CORNET; http://bioinformatics.psb.ugent.be/cornet/; De Bodt *et al.*, 2010) provides insights in co-expression networks with transcriptome data and integrates proteome data, localization data (both *in silico* and experimental), and functional data of Arabidopsis. Out of the different predefined data sets available, the abiotic stress compendium was used. With the co-expression tool, the Pearson correlation coefficient threshold was set > 0.7 and co-expressed genes were identified. The output was visualized in Cytoscape 2.6.0 (Shannon *et al.*, 2003).

***In silico* prediction of putative targeting sequences in the NAC transcription factor family**

Protein sequences of the Arabidopsis NAC transcription factor family were retrieved from the Plant Transcription Factor DataBase (PlnTFDB 3.0; http://plntfdb.bio.uni-potsdam.de/v3.0/; Pérez-Rodríguez *et al.*, 2010). For the prediction of the targeting signals, sequences were submitted in the TargetP 1.1 prediction server (Emanuelsson *et al.*, 2007).

Cloning of open reading frames and promoters

The full length open reading frame (with and without stop codon), the sequence encoding the putative chloroplast targeting peptide (cTP), the ORF without the cTP, the ORF without the C-terminal region and the promoter of *ANAC102* were amplified by polymerase chain reaction (PCR) from first-strand cDNA and genomic DNA of *A. thaliana* (L.) Heynh. ecotype Columbia (Col-0), respectively, with gene/promoter-specific primers extended with the *attB* sites for Gateway cloning (Invitrogen Carlsbad, CA, USA; Table S2). PCR reactions were run with high-fidelity Phusion DNA polymerase (Finnzymes OY, Espoo, Finland) and fragments were cloned into the Gateway entry vectors (Invitrogen) according to the manufacturer's instructions.

Generation of transgenic Arabidopsis plants

GFP fusion overexpression plants - Constitutive promoter-driven expression clones were generated with the binary destination vectors pK7FWG2 and pK7WGF2 (Karimi *et al.*, 2007), resulting in C- and N-terminal GFP protein fusions, respectively, under the control of the cauliflower mosaic virus 35S (CaMV35S) promoter.

*Endogenous promoter-driven translational fusion*s were created with the MultiSite Gateway technology (Invitrogen) that combined the *ANAC102* ORF and GFP fragments downstream of the endogenous promoter in the pK7m34GW destination vector (Karimi *et al.*, 2007).

Overexpression plants – A constitutive promoter-driven expression construct was generated in the binary destination vector pK7WG2D (Karimi *et al.*, 2007).

All constructs were transferred into the *Agrobacterium tumefaciens* strain C58C1 harboring the virulence plasmid MP90.

Loss-of-function plants – Homozygous plants were selected from the SALK_030702C T-DNA insertion line by genomic PCR with gene-specific and T-DNA-specific primers. The expression level of *ANAC102* was determined by qRT-PCR.

Transient expression and stable genetic transformation

All GFP-protein fusion constructs were transiently expressed in leaf epidermal cells of 5-week-old wild-type tobacco (*Nicotiana benthamiana*) by *A. tumefaciens*–mediated leaf infiltration (Sparkes *et al.*, 2006). For stable expression, the constructs were transformed into wild-type or catalase-deficient plants (CAT2HP2 (*cat2*); 7% residual catalase activity; Vandenabeele *et al.*, 2004) by *Agrobacterium*-mediated floral dip (Clough and Bent, 1998). Kanamycin-resistant plants were selected on ½ MS medium (Duchefa Biochemie, Haarlem, The Netherlands), 1% (w/v) sucrose, 0.7% (w/v) agar, pH 5.7 and 35 $mg.L^{-1}$ kanamycin (Sigma-Aldrich, St. Louis, MO, USA) at 21°C and 16-h light/8-h dark photoperiod. Homozygous lines with a single T-DNA locus were selected by segregation.

Chloroplast fractionation experiments

Chloroplasts were isolated and fractionated into stroma and thylakoids from 3.4 g leaves of 4-week-old *A. thaliana* (wild type, *ANAC102-GFP*^{OE} and prom$_{ANAC102}$:*ANAC102-GFP*) plants according to the method described by Lamkemeyer *et al.*, 2006.

qRT-PCR experiments

RNA isolation, cDNA synthesis and qRT-PCR analyses were carried out as described by Vanderauwera *et al.* (2007) with specific primers. Primers were designed with the Universal ProbeLibrary Assay Design center ProbeFinder software (Roche; https://www.roche-applied-science.com/; Table S2).

Protein extraction and western blot analysis

Total protein extracts were prepared by grinding leaf material (100 mg) in 200 µL extraction buffer (100 mM HEPES (pH 7.5), 1 mM EDTA, 10 mM β-mercaptoethanol and 1 mM phenylmethanesulfonylfluoride) and a protease inhibitor cocktail (COMPLETE; Roche). Insoluble debris was removed by centrifugation at 20800 x g for 15 min at 4°C. Protein concentrations were determined with the Bradford method (Zor and Selinger, 1996). Proteins (15 µg) were separated on a

12.5% SDS PAGE gel, transferred to a P membrane (Millipore; http://www.millipore.com/) and immunodetected with the Living Colors A.v. Monoclonal antibody (JL-8; Clontech Laboratories; http://www.clontech.com/) for the detection of GFP-tagged proteins by means of the Western Lightning kit (GE-Healthcare; http://www.gehealthcare.com/).

Fluorescence microscopy

For fluorescence microscopy, a confocal microscope 100M with software package LSM 510 version 3.2 was used (Zeiss; http://www.zeiss.com/), equipped with a 63x water-corrected objective (numerical aperture 1.2) to scan the leaf epidermis and underlying cell layers. GFP fluorescence was imaged in a single channel setting with 488 nm for GFP excitation.

Accession numbers

Sequence information of the genes mentioned in this article can be found at The Arabidopsis Information Resource (TAIR; http://www.arabidopsis.org) under the following accession numbers: *ANAC102* (At5g63790), *ATAF2* (*ANAC081*; At5g08790), *ANAC* (*ANAC019*; At1g52890), *BGLU11* (At1g02850), *AtTDX1* (At2g04040), *UGT74F2* (At2g43820), *EXP10* (At1g26770), *ABCC10* (At3g59140), *AOX1a* (At3g22370), *UGT74E2* (At1g05680), *UGT73C6* (At2g36790), *AtST1* (At2g03760) and ARP7 (At3g60830).

ACKNOWLEDGEMENTS

This work was supported by Ghent University (Multidisciplinary Research Partnership 'Ghent Bio-Economy' project no. 01MRB510Z) and the Research Foundation Flanders (G.0414.09N). S.V. and A.I are respectively a postdoctroral and predoctoral fellow of the Research Foundation-Flanders. I.D.C is a predoctoral fellow of the Institute for the Promotion of Innovation by Science and Technology in Flanders. We thank Brigitte van de Cotte and Riet De Rycke for excellent technical assistance.

SUPPORTING INFORMATION

Figure S1. Co-expression analysis of *ANAC102* during abiotic stresses using CORNET.

The co-expression network was based on correlation analysis of *ANAC102* with 30 other genes with a high correlation coefficient > 0.7 with the AtGenExpress abiotic stress compendium by means of the web tool CORNET (De Bodt *et al.*, 2010; https://cornet.psb.ugent.be/main/). Node colors indicate predicted subcellular localization: dark green, nucleus; light green, mitochondria; pink, plastids; blue, chloroplasts; yellow, golgi; red, extracellular.

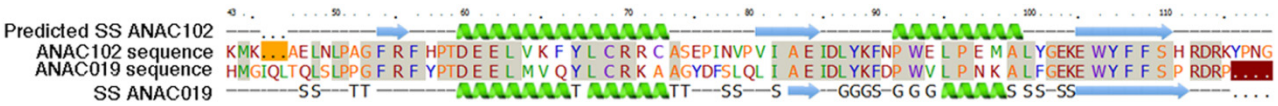

Figure S2. Homology-based secondary structure prediction of ANAC102.

The ANAC019 homology-based secondary structure prediction of ANAC102 by PHYRE (Protein Homology/analogY Recognition Engine; Bennett-Lovsey *et al.*, 2008; Kelley and Sternberg, 2009) is depicted.

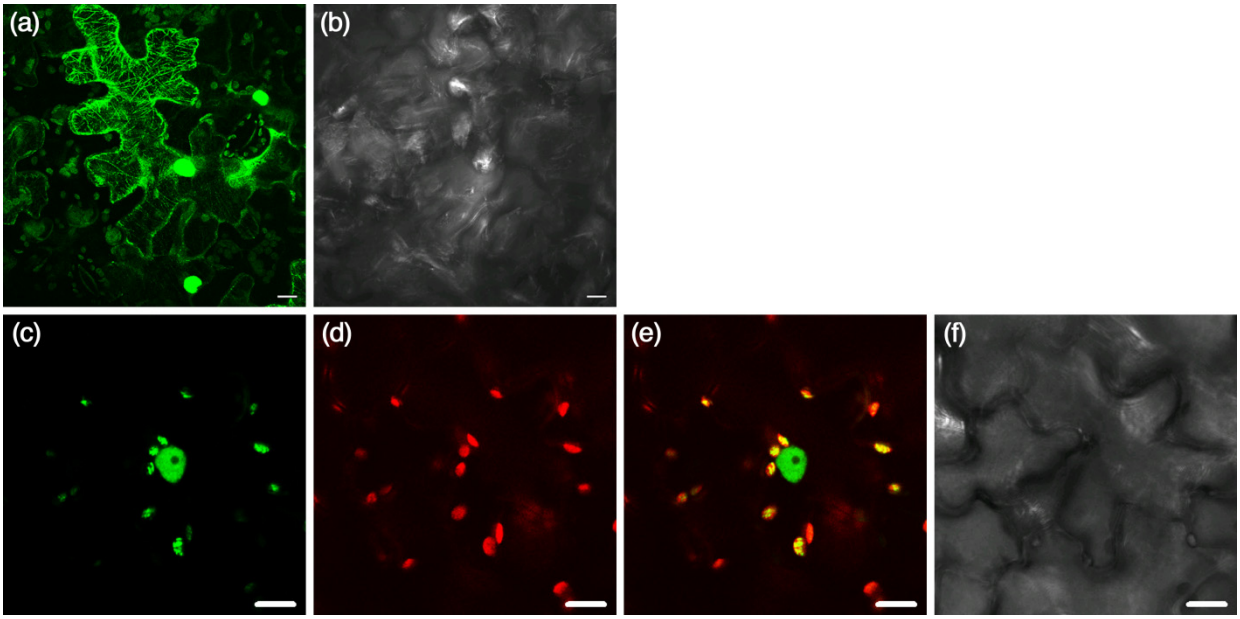

Figure S3. Transient expression of GFP-tagged fusions of ANAC102 in leaf epidermis cells of *N. benthamiana*.

(a-b) Transient overexpression of *GFP-ANAC102* results in a cytoskeletal localization.

(c-f) Overexpression of *ANAC102-GFP* in *N. benthamiana* leaf epidermis cells leads to a nuclear and chloroplastic localization. (a,c) GFP fluorescence; (d) chlorophyll fluorescence; (e) merged GFP and chlorophyll fluorescence; (b,f) bright-field images. Scale bars, 10 μm.

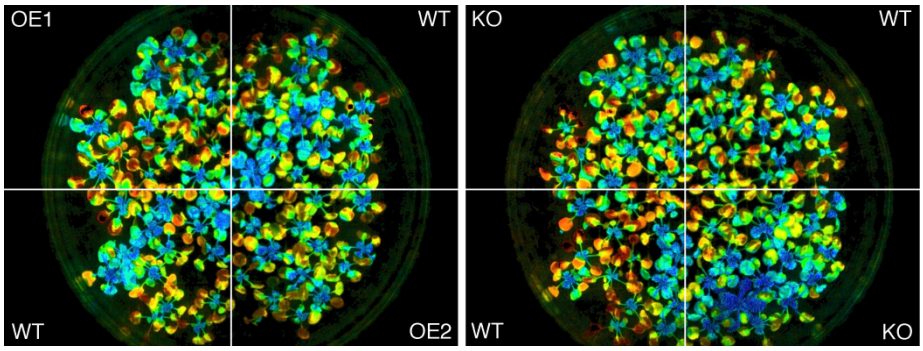

Figure S4. Photochemical performance of *ANAC102*^{OE} and *ANAC*^{KO} lines under photorespiratory promoting-conditions.

Maximum quantum efficiency of PSII under light adapted conditions (F'_v/F'_m) in leaves of 3-week-old (left) *ANAC02*^{OE} lines and (right) *ANAC102*^{KO} plants after 8 d of photorespiration promoting conditions.

Table S1. Transcription factors induced by photorespiratory H_2O_2.

AGI code	Description	ATH1[a]	CATMA[b]	AGILENT[c]
APETALA2 (AP2) and Ethylene-Responsive Element Binding protein (EREBP) family				
At1g22810	AtERF019	24.15		271.18
At1g22985	CYTOKININ RESPONSE FACTOR7 (CRF7)	5.64		
At1g71520	AtERF020			8.00
At2g40350	AtERF047 (DREB2B)	4.04		
At2g44840	AtERF013			6.79
At2g47520	AtERF071	12.99		
At3g23230	AtERF098	10.30		212.09
At3g61630	CRF6	1.96	2.18	-1.09
At5g05410	DREB2A	8.01		96.44
At5g47230	AtERF05			11.50
At5g51190	AtERF105			6.91
At5g61590	AtERF107			3.78
At5g61600	AtERF104			19.67
basic helix-loop-helix (bHLH) family				
At1g10585	bHLH DNA-binding superfamily protein	85.12		
At2g46970	PHYTOCHROME INTERACTING FACTOR 3-LIKE1 (PIL1)		1.15	
At3g47640	POPEYE (PYE)			3.02
At5g46830	NACL-INDUCILE GENE1 (AtNIG1)		2.06	
Basic region/leucine zipper motif (bZIP) family				
At1g06850	AtbZIP52		1.80	
At3g62420	AtbZIP53			6.29
At5g28770	AtbZIP63			5.36
At5g49450	AtbZIP1			3.95
Zinc Finger (ZF) transcription factors				
At2g47890	ZF protein CONSTANS-LIKE13 (COL13)			4.88
At5g39660	CYCLING DOF FACTOR2 (CDF2)			6.28
At1g27730	ZAT10			12.82
At2g37430	ZAT11			127.52
At2g41835	ZF (C_2H_2-type, AN1-like) domain-containing stress associated protein 11			14.70
At3g45260	ZF protein (C_2H_2-like)			4.52
At5g04340	ZAT6			21.76
At5g43170	ZF PROTEIN3 (ZF3)			15.55
At5g59820	ZAT12	3.27		28.47
At2g25900	TANDEM ZF PROTEIN1 (AtTZF1)			6.03
At2g40140	SALT-INDUCIBLE ZF2 (AtSZF2)			13.47
At3g55980	SALT-INDUCIBLE ZF1 (AtSZF1)			20.84
Heat shock transcription factor(HSF) family				
At1g67970	AtHSFA8			3.78
At2g26150	AtHSFA2	27.64	60.68	9.97
At3g51910	AtHSFA7a	28.77		
At4g11660	AtHSFB2b	4.38		
At4g18880	AtHSFA4a			18.79
At4g36990	AtHSFB1			5.70
At5g62020	AtHSFB2a		3.08	5.56
MYB and MYB-related proteins				
At2g46410	CAPRICE (CPC)			3.18
At3g50060	AtMYB77			7.07
At5g17300	REVEILLE1 (RVE1)			4.62
At5g37260	CIRCADIAN1 (CIR1)			4.36
NAC				
At1g01720	ATAF1			9.60
At1g32870	ANAC013	2.45	2.57	1.48
At1g77450	ANAC032	5.03		19.92
At3g10500	ANAC053			10.43
At3g29035	ANAC059			26.84
At5g08790	ATAF2			36.99
At5g18270	ANAC087	4.10	6.33	
At5g63790	ANAC102	3.25		28.14
WRKY				
At1g62300	WRKY6	7.68		46.59
At2g23320	WRKY15			16.35
At2g46400	WRKY46			6.36
At3g04670	WRKY39	3.02		4.62
At4g01250	WRKY22			5.49
At4g31550	WRKY11			10.77
At5g13080	WRKY75	5.70		
At5g24110	WRKY30	14.85		142.61
At5g28650	WRKY74			4.14
At5g49520	WRKY48	6.13		

Table S1. Transcription factors induced by photorespiratory H_2O_2. *(Continued).*

AGI code	Description	ATH1[a]	CATMA[b]	AGILENT[c]
Others				
At1g07520	SCARECROW-LIKE PROTEIN 31 (AtSCL31)			4.12
At2g29060	AtSCL33			3.75
At2g32250	FAR1-RELATED SEQUENCE2 (FRS2)	3.69		
At3g24500	MULTIPROTEIN BRIDGING FACTOR1C (AtMBF1C)	6.98	8.70	
At2g38250	Trihelix transcription factor GT-3b	4.98		7.58
At4g17900	PLATZ transcription factor family protein	3.08		14.61
At4g19660	NON-EXPRESSOR OF PATHOGENES RELATED GENES4 (NPR4)			5.10
At4g37610	BTB/POZ AND TAZ DOMAIN PROTEIN5 (BT5)			21.64
At5g46910	Jumonji (Jmj) family protein			6.33
At5g47370	Homeobox-leucine zipper protein (HAT2)		3.70	
At5g59990	CCT motif family protein			6.15

For each gene, the AGI code, gene description and the fold changes in the different H_2O_2-related transcript profiling studies (ATH1, CATMA and AGILENT) are presented. FC, fold changes; WT, wild type.

[a] relative FC in *cat2* mutant versus WT plants after 3 h of HL exposure (Vanderauwera *et al.*, 2005).

[b] relative FC of *cat2* mutant versus WT plants after 8 h of HL irradiation (Hoeberichts *et al.*, unpublished results).

[c] relative FC in *cat2* mutant versus WT plants after 1 h of HL exposure (Vanderauwera *et al.*, 2011).

Table S2. Primers used.

Primers	Sequence
attB4F-Pat5g63790	GGGGACAACTTTGTATAGAAAAGTTGGAGATTCTACAACTGAATTACCAAAATGCCCC
attB1rR-Pat5g63790	GGGGACTGCTTTTTTGTACAAACTTGTGGAGCTTTTATAAACGAAGGGGAGG
attB2rF-At5g63790	GGGGACAGCTTTCTTGTACAAAGTGGGAATGGACTTTGCTCTCTTCTCCTCG
attB3R-At5g63790	GGGGACAACTTTGTATAATAAAGTTGTTTACCCTTGAGGAGCAAAATTCCAATTC
attB4F-Pat5g63790	GGGGACAACTTTGTATAGAAAAGTTGGAAAGACTTGGACCCAACACAGC
attB1rR-Pat5g63790	GGGGACTGCTTTTTTGTACAAACTTGTGGAGCTTTTATAAACGAAGGG
At1g02850_PL_FW	TCTTTGGCTCTGGCACATC
At1g02850_PL_RV	GTTCTCCCATCTTCGTCAGC
At1g77120_PL_FW	GGGAAGCTAAGGGACAAACA
At1g77120_PL_RV	CACATGATCTCCTGGCTGAA
At2g43820_PL_FW	CTTCCTGTGGGTGGTCAGAT
At2g43820_PL_RV	TGTCTCAAGAAACCCTGATGG
At1g26770_PL_FW	AACGCTCACGCCACTTTT
At1g26770_PL_RV	TTACCATATCCACAAGCACCAC
At3g59140_PL_FW	GTTGTTGGTTACACATCAAGTGG
At3g59140_PL_RV	GATTTCTCCATCTGACATCAACA

REFERENCES

Abe, H., Yamaguchi-Shinozaki, K., Urao, T., Iwasaki, T., Hosokawa, D. and Shinozaki, K. (1997) Role of *Arabidopsis* MYC and MYB homologs in drought- and abscisic acid-regulated gene expression. *Plant Cell*, **9**, 1859-1868.

Aida, M., Ishida, T., Fukaki, H., Fujisawa, H. and Tasaka, M. (1997) Genes involved in organ separation in *Arabidopsis*: an analysis of the *cup-shaped cotyledon* mutant. *Plant Cell*, **9**, 841-857.

Alonso, J.M., Stepanova, A.N., Leisse, T.J., Kim, C.J., Chen, H., Shinn, P., Stevenson, D.K., Zimmerman, J., Barajas, P., Cheuk, R., Gadrinab, C., Heller, C., Jeske, A., Koesema, E., Meyers, C.C., Parker, H., Prednis, L., Ansari, Y., Choy, N., Deen, H., Geralt, M., Hazari, N., Hom, E., Karnes, M., Mulholland, C., Ndubaku, R., Schmidt, I., Guzman, P., Aguilar-Henonin, L., Schmid, M., Weigel, D., Carter, D.E., Marchand, T., Risseeuw, E., Brogden, D., Zeko, A., Crosby, W.L., Berry, C.C. and Ecker, J.R. (2003) Genome-wide insertional mutagenesis of *Arabidopsis thaliana*. *Science*, **301**, 653-657.

Apel, K. and Hirt, H. (2004) Reactive oxygen species: metabolism, oxidative stress, and signal transduction. *Annu. Rev. Plant Biol.*, **55**, 373-399.

Asada, K. (1999) The water-water cycle in chloroplasts: scavenging of active oxygens and dissipation of excess photons. *Annu. Rev. Plant Physiol. Plant Mol. Biol.*, **50**, 601-639.

Badger, M.R., Fallahi, H., Kaines, S. and Takahashi, S. (2009) Chlorophyll fluorescence screening of *Arabidopsis thaliana* for CO_2 sensitive photorespiration and photoinhibition mutants. *Funct. Plant Biol.*, **36**, 867-873.

Barkan, A. and Goldschmidt-Clermont, M. (2000) Participation of nuclear genes in chloroplast gene expression. *Biochimie*, **82**, 559-572.

Bennett-Lovsey, R.M., Herbert, A.D., Sternberg, M.J.E. and Kelley, L.A. (2008) Exploring the extremes of sequence/structure space with ensemble fold recognition in the program Phyre. *Proteins*, **70**, 611-625.

Bienert, G.P., Schjoerring, J.K. and Jahn, T.P. (2006) Membrane transport of hydrogen peroxide. *Biochim. Biophys. Acta*, **1758**, 994-1003.

Bionda, T., Tillmann, B., Simm, S., Beilstein, K., Ruprecht, M. and Schleiff, E. (2010) Chloroplast import signals: the length requirement for translocation *in vitro* and *in vivo*. *J. Mol. Biol.*, **402**, 510-523.

Boyes, D.C., Zayed, A.M., Ascenzi, R., McCaskill, A.J., Hoffman, N.E., Davis, K.R. and Gorlach, J. (2001) Growth stage-based phenotypic analysis of *Arabidopsis*: a model for high throughput functional genomics in plants. *Plant Cell*, **13**, 1499-1510.

Chen, Y.-F., Li, L.-Q., Xu, Q., Kong, Y.-H., Wang, H. and Wu, W.-H. (2009) The WRKY6 transcription factor modulates *PHOSPHATE1* expression in response to low P_i stress in *Arabidopsis*. *Plant Cell*, **21**, 3554-3566.

Christianson, J.A., Dennis, E.S., Llewellyn, D.J. and Wilson, I.W. (2010) ATAF NAC transcription factors: regulators of plant stress signaling. *Plant Signal. Behav.*, **5**, 428-432.

Christianson, J.A., Wilson, I.W., Llewellyn, D.J. and Dennis, E.S. (2009) The low-oxygen-induced NAC domain transcription factor ANAC102 affects viability of *Arabidopsis* seeds following low-oxygen treatment. *Plant Physiol.*, **149**, 1724-1738.

Clough, S.J. and Bent, A.F. (1998) Floral dip: a simplified method for *Agrobacterium*-mediated transformation of *Arabidopsis thaliana*. *Plant J.*, **16**, 735-743.

Collinge, M. and Boller, T. (2001) Differential induction of two potato genes, *Stprx2* and *StNAC*, in response to infection by *Phytophthora infestans* and to wounding. *Plant Mol. Biol.*, **46**, 521-529.

Cregan, S.P., Fortin, A., MacLaurin, J.G., Callaghan, S.M., Cecconi, F., Yu, S.-W., Dawson, T.M., Dawson, V.L., Park, D.S., Kroemer, G. and Slack, R.S. (2002) Apoptosis-inducing factor is involved in the regulation of caspase-independent neuronal cell death. *The Journal of Cell Biology*, **158**, 507-517.

Davletova, S., Schlauch, K., Coutu, J. and Mittler, R. (2005) The Zinc-Finger protein Zat12 plays a central role in reactive oxygen and abiotic stress signaling in *Arabidopsis*. *Plant Physiol.*, **139**, 847-856.

De Bodt, S., Carvajal, D., Hollunder, J., Van den Cruyce, J., Movahedi, S. and Inzé, D. (2010) CORNET: a user-friendly tool for data mining and integration. *Plant Physiol.*, **152**, 1167-1179.

Delessert, C., Kazan, K., Wilson, I.W., Van Der Straeten, D., Manners, J., Dennis, E.S. and Dolferus, R. (2005) The transcription factor ATAF2 represses the expression of pathogenesis-related genes in *Arabidopsis*. *Plant J.*, **43**, 745-757.

Dong, C.-J. and Liu, J.-Y. (2010) The *Arabidopsis* EAR-motif-containing protein RAP2.1 functions as an active transcriptional repressor to keep stress responses under tight control. *BMC Plant Biol.*, **10**, 47.

Duval, M., Hsieh, T.-F., Kim, S.Y. and Thomas, T.L. (2002) Molecular characterization of *AtNAM*: a member of the *Arabidopsis* NAC domain superfamily. *Plant Mol. Biol.*, **50**, 237-248.

Emanuelsson, O., Brunak, S., von Heijne, G. and Nielsen, H. (2007) Locating proteins in the cell using TargetP, SignalP and related tools. *Nature Protoc.*, **2**, 953-971.

Ernst, H.A., Nina Olsen, A., Skriver, K., Larsen, S. and Lo Leggio, L. (2004) Structure of the conserved domain of ANAC, a member of the NAC family of transcription factors. *EMBO Rep.*, **5**, 297-303.

Eulgem, T., Rushton, P.J., Robatzek, S. and Somssich, I.E. (2000) The WRKY superfamily of plant transcription factors. *Trends Plant Sci.*, **5**, 199-206.

Fey, V., Wagner, R., Bräutigam, K. and Pfannschmidt, T. (2005) Photosynthetic redox control of nuclear gene expression. *J. Exp. Bot.*, **56**, 1491-1498.

Fujita, M., Fujita, Y., Maruyama, K., Seki, M., Hiratsu, K., Ohme-Takagi, M., Tran, L.-S.P., Yamaguchi-Shinozaki, K. and Shinozaki, K. (2004) A dehydration-induced NAC protein, RD26, is involved in a novel ABA-dependent stress-signaling pathway. *Plant J.*, **39**, 863-876.

Fujita, M., Fujita, Y., Noutoshi, Y., Takahashi, F., Narusaka, Y., Yamaguchi-Shinozaki, K. and Shinozaki, K. (2006) Crosstalk between abiotic and biotic stress responses: a current view from the points of convergence in the stress signaling networks. *Curr. Opin. Plant Biol.*, **9**, 436-442.

Gadjev, I., Vanderauwera, S., Gechev, T.S., Laloi, C., Minkov, I.N., Shulaev, V., Apel, K., Inzé, D., Mittler, R. and Van Breusegem, F. (2006) Transcriptomic footprints disclose specificity of reactive oxygen species signaling in *Arabidopsis*. *Plant Physiol.*, **141**, 436-445.

Gechev, T.S., Gadjev, I.Z. and Hille, J. (2004) An extensive microarray analysis of AAL-toxin-induced cell death in *Arabidopsis thaliana* brings new insights into the complexity of programmed cell death in plants. *Cell. Mol. Life Sci.*, **61**, 1185-1197.

Giraud, E., Van Aken, O., Ho, L.H.M. and Whelan, J. (2009) The transcription factor ABI4 is a regulator of mitochondrial retrograde expression of *ALTERNATIVE OXIDASE1a*. *Plant Physiol.*, **150**, 1286-1296.

Giuliano, G., Pichersky, E., Malik, V.S., Timko, M.P., Scolnik, P.A. and Cashmore, A.R. (1988) An evolutionarily conserved protein binding sequence upstream of a plant light-regulated gene. *Proc. Natl. Acad. Sci. USA*, **85**, 7089-7093.

Guiltinan, M., Marcotte, W. and Quatrano, R. (1990) A plant leucine zipper protein that recognizes an abscisic acid response element. *Science*, **250**, 267-271.

He, X.-J., Mu, R.-L., Cao, W.-H., Zhang, Z.-G., Zhang, J.-S. and Chen, S.-Y. (2005) AtNAC2, a transcription factor downstream of ethylene and auxin signaling pathways, is involved in salt stress response and lateral root development. *Plant J.*, **44**, 903-916.

Henzler, T. and Steudle, E. (2000) Transport and metabolic degradation of hydrogen peroxide in *Chara corallina*: model calculations and measurements with the pressure probe suggest transport of H_2O_2 across water channels. *J. Exp. Bot.*, **51**, 2053-2066.

Hernández, I., Alegre, L., Van Breusegem, F. and Munné-Bosch, S. (2009) How relevant are flavonoids as antioxidants in plants? *Trends Plant Sci.*, **14**, 125-132.

Higo, K., Ugawa, Y., Iwamoto, M. and Korenaga, T. (1999) Plant *cis*-acting regulatory DNA elements (PLACE) database: 1999. *Nucleic Acids Res.*, **27**, 297-300.

Hudson, M.E. and Quail, P.H. (2003) Identification of promoter motifs involved in the network of phytochrome A-regulated gene expression by combined analysis of genomic sequence and microarray data. *Plant Physiol.*, **133**, 1605-1616.

Inzé, A., Vanderauwera, S., Hoeberichts, F.A., Vandorpe, M., Van Gaever, T. and Van Breusegem, F. (2012) A subcellular localization compendium of hydrogen peroxide-induced proteins. *Plant Cell Environ.*, **35**, 308-320.

Jensen, M.K., Kjaersgaard, T., Nielsen, M.M., Galberg, P., Petersen, K., O'Shea, C. and Skriver, K. (2010) The *Arabidopsis thaliana* NAC transcription factor family: structure–function relationships and determinants of ANAC019 stress signalling *Biochem. J.*, **426**, 183-196.

Karimi, M., Bleys, A., Vanderhaeghen, R. and Hilson, P. (2007) Building blocks for plant gene assembly. *Plant Physiol.*, **145**, 1183-1191.

Kasajima, I., Ide, Y., Yokota Hirai, M. and Fujiwara, T. (2010) WRKY6 is involved in the response to boron deficiency in *Arabidopsis thaliana*. *Physiol. Plant*, **139**, 80-92.

Kelley, L.A. and Sternberg, M.J.E. (2009) Protein structure prediction on the web: a case study using the Phyre server. *Nature Protoc.*, **4**, 363-371.

Kikuchi, K., Ueguchi-Tanaka, M., Yoshida, K.T., Nagato, Y., Matsusoka, M. and Hirano, H.Y. (2000) Molecular analysis of the *NAC* gene family in rice. *Mol. Gen. Genet.*, **262**, 1047-1051.

Kilian, J., Whitehead, D., Horak, J., Wanke, D., Weinl, S., Batistic, O., D'Angelo, C., Bornberg-Bauer, E., Kudla, J. and Harter, K. (2007) The AtGenExpress global stress expression data set: protocols, evaluation and model data analysis of UV-B light, drought and cold stress responses. *Plant J.*, **50**, 347-363.

Kim, H.S., Park, B.O., Yoo, J.H., Jung, M.S., Lee, S.M., Han, H.J., Kim, K.E., Kim, S.H., Lim, C.O., Yun, D.-J., Lee, S.Y. and Chung, W.S. (2007) Identification of a calmodulin-binding NAC protein as a transcriptional repressor in *Arabidopsis*. *J. Biol. Chem.*, **282**, 36292-36302.

Kim, S.-G., Lee, A.-K., Yoon, H.-K. and Park, C.-M. (2008) A membrane-bound NAC transcription factor NTL8 regulates gibberellic acid-mediated salt signaling in *Arabidopsis* seed germination. *Plant J.*, **55**, 77-88.

Krause, K. and Krupinska, K. (2009) Nuclear regulators with a second home in organelles. *Trends Plant Sci.*, **14**, 194-199.

Lamkemeyer, P., Laxa, M., Collin, V., Li, W., Finkemeier, I., Schöttler, M.A., Holtkamp, V., Tognetti, V.B., Issakidis-Bourguet, E., Kandlbinder, A., Weis, E., Miginiac-Maslow, M. and Dietz, K.-J. (2006) Peroxiredoxin Q of *Arabidopsis thaliana* is attached to the thylakoids and functions in context of photosynthesis. *Plant J.*, **45**, 968-981.

Lu, P.-L., Chen, N.-Z., An, R., Su, Z., Qi, B.-S., Ren, F., Chen, J. and Wang, X.-C. (2007) A novel drought-inducible gene *ATAF1* encodes a NAC family protein that negatively regulates the expression of stress-responsive genes in *Arabidopsis*. *Plant Mol. Biol.*, **63**, 289-305.

Martin, W. and Herrmann, R.G. (1998) Gene transfer from organelles to the nucleus: how much, what happens, and why? *Plant Physiol.*, **118**, 9-17.

Mhamdi, A., Queval, G., Chaouch, S., Vanderauwera, S., Van Breusegem, F. and Noctor, G. (2010) Catalase function in plants: a focus on *Arabidopsis* mutants as stress-mimic models. *J. Exp. Bot.*, **61**, 4197-4220.

Mitsuda, N., Seki, M., Shinozaki, K. and Ohme-Takagi, M. (2005) The NAC transcription factors NST1 and NST2 of *Arabidopsis* regulate secondary wall thickenings and are required for anther dehiscence. *Plant Cell*, **17**, 2993-3006.

Mohanty, B., Krishnan, S.P.T., Swarup, S. and Bajic, V.B. (2005) Detection and preliminary analysis of motifs in promoters of anaerobically induced genes of different plant species. *Ann. Botany*, **96**, 669-681.

Mundy, J., Yamaguchi-Shinozaki, K. and Chua, N.H. (1990) Nuclear proteins bind conserved elements in the abscisic acid-responsive promoter of a rice *rab* gene. *Proc. Natl. Acad. Sci. USA*, **87**, 1406-1410.

Noctor, G., Veljovic-Jovanovic, S., Driscoll, S., Novitskaya, L. and Foyer, C.H. (2002) Drought and oxidative load in the leaves of C3 plants: a predominant role for photorespiration? *Ann. Botany*, **89**, 841-850.

Ohgishi, M., Oka, A., Morelli, G., Ruberti, I. and Aoyama, T. (2001) Negative autoregulation of the *Arabidopsis* homeobox gene *ATHB-2*. *Plant J.*, **25**, 389-398.

Olsen, A.N., Ernst, H.A., Leggio, L.L. and Skriver, K. (2005) NAC transcription factors: structurally distinct, functionally diverse. *Trends Plant Sci.*, **10**, 79-87.

Ooka, H., Satoh, K., Doi, K., Nagata, T., Otomo, Y., Murakami, K., Matsubara, K., Osato, N., Kawai, J., Carninci, P., Hayashizaki, Y., Suzuki, K., Kojima, K., Takahara, Y., Yamamoto, K. and Kikuchi, S. (2003) Comprehensive analysis of NAC family genes in *Oryza sativa* and *Arabidopsis thaliana*. *DNA Res.*, **10**, 239-247.

op den Camp, R.G.L., Przybyla, D., Ochsenbein, C., Laloi, C., Kim, C., Danon, A., Wagner, D., Hideg, É., Göbel, C., Feussner, I., Nater, M. and Apel, K. (2003) Rapid induction of distinct stress responses after the release of singlet oxygen in *Arabidopsis*. *Plant Cell*, **15**, 2320-2332.

Pérez-Rodríguez, P., Riaño-Pachón, D.M., Corrêa, L.G.G., Rensing, S.A., Kersten, B. and Mueller-Roeber, B. (2010) PlnTFDB: updated content and new features of the plant transcription factor database. *Nucleic Acids Res.*, **38**, 822-827.

Pfannschmidt, T. (2010) Plastidial retrograde signalling - a true 'plastid factor' or just metabolite signatures? *Trends Plant Sci.*, **15**, 427-435.

Queval, G., Issakidis-Bourguet, E., Hoeberichts, F.A., Vandorpe, M., Gakiere, B., Vanacker, H., Miginiac-Maslow, M., Van Breusegem, F. and Noctor, G. (2007) Conditional oxidative stress responses in the *Arabidopsis* photorespiratory mutant *cat2* demonstrate that redox state is a key modulator of daylength-dependent gene expression, and define photoperiod as a crucial factor in the regulation of H_2O_2-induced cell death. *Plant J.*, **52**, 640-657.

Queval, G., Neukermans, J., Vanderauwera, S., Van Breusegem, F. and Noctor, G. (2011) Day length is a key regulator of transcriptomic responses to both CO_2 and H_2O_2 in *Arabidopsis*. *Plant Cell Environ.*, **in press**.

Robatzek, S. and Somssich, I.E. (2002) Targets of AtWRKY6 regulation during plant senescence and pathogen defense. *Genes Dev.*, **16**, 1139-1149.

Ruchalski, K., Mao, H., Li, Z., Wang, Z., Gillers, S., Wang, Y., Mosser, D.D., Gabai, V., Schwartz, J.H. and Borkan, S.C. (2006) Distinct hsp70 domains mediate apoptosis-inducing factor release and nuclear accumulation. *J. Biol. Chem.*, **281**, 7873-7880.

Sakamoto, H., Maruyama, K., Sakuma, Y., Meshi, T., Iwabuchi, M., Shinozaki, K. and Yamaguchi-Shinozaki, K. (2004) *Arabidopsis* Cys_2/His_2-type Zinc-Finger proteins function as transcription repressors under drought, cold, and high-salinity stress conditions. *Plant Physiol.*, **136**, 2734-2746.

Sakuma, Y., Maruyama, K., Osakabe, Y., Qin, F., Seki, M., Shinozaki, K. and Yamaguchi-Shinozaki, K. (2006a) Functional analysis of an *Arabidopsis* transcription factor, DREB2A, involved in drought-responsive gene expression. *Plant Cell*, **18**, 1292-1309.

Sakuma, Y., Maruyama, K., Qin, F., Osakabe, Y., Shinozaki, K. and Yamaguchi-Shinozaki, K. (2006b) Dual function of an *Arabidopsis* transcription factor DREB2A in water-stress-responsive and heat-stress-responsive gene expression. *Proc. Natl. Acad. Sci. USA*, **103**, 18822-18827.

Schwacke, R., Fischer, K., Ketelsen, B., Krupinska, K. and Krause, K. (2007) Comparative survey of plastid and mitochondrial targeting properties of transcription factors in *Arabidopsis* and rice. *Mol. Gen. Genom.*, **277**, 631-646.

Shannon, P., Markiel, A., Ozier, O., Baliga, N.S., Wang, J.T., Ramage, D., Amin, N., Schwikowski, B. and Ideker, T. (2003) Cytoscape: a software environment for integrated models of biomolecular interaction metworks. *Genome Res.*, **13**, 2498-2504.

Soitamo, A., Piippo, M., Allahverdiyeva, Y., Battchikova, N. and Aro, E.-M. (2008) Light has a specific role in modulating *Arabidopsis* gene expression at low temperature. *BMC Plant Biol.*, **8**, 13.

Souer, E., van Houwelingen, A., Kloos, D., Mol, J. and Koes, R. (1996) The *No Apical Meristem* gene of petunia is required for pattern formation in embryos and flowers and is expressed at meristem and primordia boundaries. *Cell*, **85**, 159-170.

Sparkes, I.A., Runions, J., Kearns, A. and Hawes, C. (2006) Rapid, transient expression of fluorescent fusion proteins in tobacco plants and generation of stably transformed plants. *Nature Protoc.*, **1**, 2019-2025.

Stern, D.S., Higgs, D.C. and Yang, J. (1997) Transcription and translation in chloroplasts. *Trends Plant Sci.*, **2**, 308-315.

Sun, Y. and Oberley, L.W. (1996) Redox regulation of transcriptional activators. *Free Radical Biology and Medicine*, **21**, 335-348.

Susin, S.A., Lorenzo, H.K., Zamzami, N., Marzo, I., Snow, B.E., Brothers, G.M., Mangion, J., Jacotot, E., Costantini, P., Loeffler, M., Larochette, N., Goodlett, D.R., Aebersold, R., Siderovski, D.P., Penninger, J.M. and Kroemer, G. (1999) Molecular characterization of mitochondrial apoptosis-inducing factor. *Nature*, **397**, 441-446.

Tran, L.-S.P., Nakashima, K., Sakuma, Y., Osakabe, Y., Qin, F., Simpson, S.D., Maruyama, K., Fujita, Y., Shinozaki, K. and Yamaguchi-Shinozaki, K. (2007) Co-expression of the stress-inducible zinc finger homeodomain ZFHD1 and NAC transcription factors enhances expression of the *ERD1* gene in *Arabidopsis*. *Plant J.*, **49**, 46-63.

Tran, L.-S.P., Nakashima, K., Sakuma, Y., Simpson, S.D., Fujita, Y., Maruyama, K., Fujita, M., Seki, M., Shinozaki, K. and Yamaguchi-Shinozaki, K. (2004) Isolation and functional analysis of *Arabidopsis* stress-inducible NAC transcription factors that bind to a drought-responsive *cis*-element in the *early responsive to dehydration stress 1* promoter. *Plant Cell*, **16**, 2481-2498.

van Helden, J. (2003) Regulatory sequence analysis tools. *Nucleic Acids Res.*, **31**, 3593-3596.

Vandenabeele, S., Van Der Kelen, K., Dat, J., Gadjev, I., Boonefaes, T., Morsa, S., Rottiers, P., Slooten, L., Van Montagu, M., Zabeau, M., Inzé, D. and Van Breusegem, F. (2003) A comprehensive analysis of hydrogen peroxide-induced gene expression in tobacco. *Proc. Natl. Acad. Sci. USA*, **100**, 16113-16118.

Vandenabeele, S., Vanderauwera, S., Vuylsteke, M., Rombauts, S., Langebartels, C., Seidlitz, H.K., Zabeau, M., Van Montagu, M., Inzé, D. and Van Breusegem, F. (2004) Catalase deficiency drastically affects gene expression induced by high light in *Arabidopsis thaliana*. *Plant J.*, **39**, 45-58.

Vanderauwera, S., Suzuki, N., Miller, G., van de Cotte, B., Morsa, S., Ravanat, J.-L., Hegie, A., Triantaphylidès, C., Shulaev, V., Van Montagu, M.C.E., Van Breusegem, F. and Mittler, R. (2011) Extranuclear protection of chromosomal DNA from oxidative stress. *Proc. Natl. Acad. Sci. USA*, **108**, 1711-1716.

Vanderauwera, S., Zimmermann, P., Rombauts, S., Vandenabeele, S., Langebartels, C., Gruissem, W., Inzé, D. and Van Breusegem, F. (2005) Genome-wide analysis of hydrogen peroxide-regulated gene expression in *Arabidopsis* reveals a high light-induced transcriptional cluster involved in anthocyanin biosynthesis. *Plant Physiol.*, **139**, 806-821.

Vogel, J.T., Zarka, D.G., Van Buskirk, H.A., Fowler, S.G. and Thomashow, M.F. (2005) Roles of the CBF2 and ZAT12 transcription factors in configuring the low temperature transcriptome of *Arabidopsis*. *Plant J.*, **41**, 195-211.

Wagner, R. and Pfannschmidt, T. (2006) Eukaryotic transcription factors in plastids — Bioinformatic assessment and implications for the evolution of gene expression machineries in plants. *Gene*, **381**, 62-70.

Willekens, H., Chamnongpol, S., Davey, M., Schraudner, M., Langebartels, C., Van Montagu, M., Inzé, D. and Van Camp, W. (1997) Catalase is a sink for H_2O_2 and is indispensable for stress defence in C3 plants. *EMBO J.*, **16**, 4806-4816.

Xie, Q., Frugis, G., Colgan, D. and Chua, N.-H. (2000) Arabidopsis NAC1 transduces auxin signal downstream of TIR1 to promote lateral root development. *Genes Dev.*, **14**, 3024-3036.

Yabuta, Y., Maruta, T., Yoshimura, K., Ishikawa, T. and Shigeoka, S. (2004) Two distinct redox signaling pathways for cytosolic *APX* induction under photooxidative stress. *Plant Cell Physiol.*, **45**, 1586-1594.

Yamaguchi, M., Ohtani, M., Mitsuda, N., Kubo, M., Ohme-Takagi, M., Fukuda, H. and Demura, T. (2010) VND-INTERACTING2, a NAC Domain transcription factor, negatively regulates xylem vessel formation in *Arabidopsis*. *Plant Cell*, **22**, 1249-1263.

Yoon, H.-K., Kim, S.-G., Kim, S. and Park, C.-M. (2008) Regulation of senescence by NTL9-mediated osmotic stress signaling in *Arabidopsis*. *Mol. Cells*, **25**, 438-445.

Zarkovic, J., Anderson, S.L. and Rhoads, D.M. (2005) A reporter gene system used to study developmental expression of *alternative oxidase* and isolate mitochondrial retrograde regulation mutants in *Arabidopsis*. *Plant Mol. Biol.*, **57**, 871-888.

Zimmermann, P., Hennig, L. and Gruissem, W. (2005) Gene-expression analysis and network discovery using Genevestigator. *Trends Plant Sci.*, **10**, 407-409.

Zimmermann, P., Hirsch-Hoffmann, M., Hennig, L. and Gruissem, W. (2004) GENEVESTIGATOR. Arabidopsis microarray database and analysis toolbox. *Plant Physiol.*, **136**, 2621-2632.

Zor, T. and Selinger, Z. (1996) Linearization of the Bradford protein assay increases its sensitivity: theoretical and experimental studies. *Anal. Biochem.*, **236**, 302-308.

Part II

Identification of two novel hydrogen peroxide-induced peptides involved in plant innate immunity

4

Plant antimicrobial peptides as a defense strategy against biotic and abiotic stress

Annelies Inzé and Frank Van Breusegem

AUTHOR CONTRIBUTIONS

A.I. wrote the chapter.

ABSTRACT

As plants are continuously exposed by phytopathogenic microorganisms, they evolved both preformed and inducible defense barriers to resist microbial infection. An important evolutionary component of the innate immune system of plants is the production of antimicrobial peptides (AMPs). These small, hydrophobic and predominantly cationic peptides are hallmarked for their broad-spectrum antimicrobial activity. In plants, AMPs are classified into several families, such as plant defensins, lipid-transfer proteins, hevein- and knottin-type peptides, cyclotides, snakins, maize (*Zea mays*) basic peptide 1, and polyprotein precursor AMPs from both *Macadamia integrifolia* and *Impatiens balsamina*. Besides their antimicrobial action, other biological roles have been reported such as protein inhibition, redox regulation, ion channel inhibition, zinc tolerance mediation and developmental roles. Moreover, increasing evidence has shown that they could play a role in abiotic stress tolerance. First, this review gives a general overview of AMPs and their mode of action. Then, we focus on the classification of plant AMPs and their biological roles and discuss how they could be implemented in novel strategies to combat plant diseases.

GENERAL INTRODUCTION

Mechanisms of attack and defense against microbial pathogens in plants

Plants are continuously exposed to a wide range of phytopathogenic microorganisms that use diverse strategies to attack their host. Therefore, to resist pathogen invasion, plant immunity is comprised of complex and efficient preformed and inducible defense mechanisms (Jones and Dangl, 2006). Pathogens must avoid or overcome multiple morphological barriers, secondary metabolites and antimicrobial proteins to successfully invade plant tissues. First, they have to protrude preformed structural barriers such as the epidermis cuticle layer and the rigid cell wall and circumvent chemical barriers (VanEtten *et al.*, 1994; Osbourn, 1996). Once contact has been made, both pathogen-derived elicitors (called pathogen-associated molecular patterns or PAMPs) and endogenous plant molecules liberated during pathogen invasion (called danger-associated molecules or DAMPs) accumulate that, in turn, trigger a second line of defenses including the production of reactive oxygen species (ROS; Jabs *et al.*, 1997; Alvarez *et al.*, 1998; Kawano, 2003), the reinforcement and lignification of the cell wall (Brisson *et al.*, 1994; Caño-Delgado *et al.*, 2003), the activation of several protein kinase pathways (Scheel, 1998; Zhang and Klessig, 2001) and the production of a range of signaling intermediates (Kunkel and Brooks, 2002). Subsequently, these events are followed by the onset of a hypersensitive response in which cells undergo programmed cell death (Lam *et al.*, 2001; Greenberg and Yao, 2004), or by the release of antimicrobial compounds such as phytoalexins (Darvill and Albersheim, 1984) and pathogenesis-related (PR) proteins (> 100 amino acids) and small peptides (< 100 amino acids; Van Loon *et al.*, 2006). In addition, plants may be further protected systemically against unrelated pathogens via systemic acquired resistance (SAR; Ross, 1961; Durrant and Dong, 2004).

Overview on antimicrobial peptides

Antimicrobial peptides (AMPs) are an evolutionary conserved component of innate immune systems found throughout all kingdoms ranging from bacteria, invertebrates, plants and vertebrates and are hallmarked for their broad-spectrum antimicrobial activity (Broekaert *et al.*, 1997; Ganz and Lehrer, 1998; García-Olmedo *et al.*, 1998; Otvos, 2000; Zasloff, 2002). Accordingly, the production of AMPs has been an effective defense strategy throughout evolution. Due to the pressure imposed upon them by competition amongst pathogens, AMPs are rapidly evolving molecules and, thus, highly diverse in sequence. Consequently, the classification of AMPs is difficult and predominantly based on secondary structure, comprising four major groups: β-sheet, α-helical, loop and extended peptides (Figure 1; Brogden, 2005). The number of AMPs is continuously increasing and is compiled in the Antimicrobial Peptide Database (Wang and Wang, 2004; http://aps.unmc.edu/AP/main.php/).

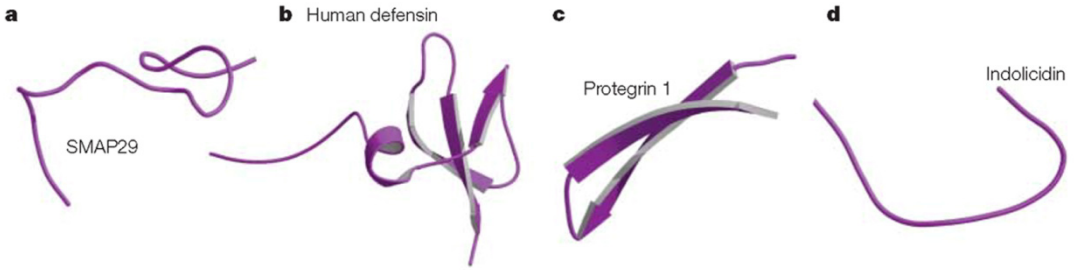

Figure 1. Structural classes of AMPs.

(a) Linear α-helical peptides (e.g. SMAP29 [PDB code 1fry]), (b,c) peptides containing cysteine residues that form disulfide bonds (e.g. (b) Human β-defensin 3 [PDB code 1k6] and (c) Protegrin 1 [PDB code 1pg1]), (d) extended peptides enriched with specific amino acids (e.g. Indolicidin [PDB code 1qxq]; From Brogden, 2005).

AMPs are small (< 50 amino acids), cationic (positive net charge at physiological pH) and hydrophobic peptides usually enriched in one or two amino acids, often proline, glycine, histidine, arginine, tryptophan, or cysteine (Cys; Boman, 2003; Bulet *et al.*, 2004). The majority of AMPs have multiple Cys residues that enable disulfide bond formation, making the peptide structure compact and remarkably stable against adverse biochemical conditions and protease degradation. Whereas the positions of these Cys residues are highly conserved, the intervening amino acid sequences vary extremely. In general, AMPs are often expressed as preproprotein precursors in which the predomain is the signal peptide and is positioned at the N-terminus, the prodomain is often anionic necessary for neutralizing the highly cationic mature domain and ensuring that the AMP is inactive when it is still intracellular. These precursor domains are released by proteolytic processing after insertion into the lumen of the endoplasmatic reticulum (ER; predomain) and after secretion into the extracellular space (prodomain).

Mode of action

The antimicrobial activity of AMPs is predominantly based on the ability to disrupt the pathogen's membrane via both specific and non-specific electrostatic and hydrophobic interactions (Shai, 2002; Thevissen *et al.*, 2003). However, increasing evidence has demonstrated that the activity of AMPs can also be based on more targeted mechanisms through interactions with microbe-specific lipid receptors (Wilmes *et al.*, 2011). Besides their action on membranes, AMPs can operate through binding intracellular targets resulting in the inhibition of multiple processes, such as nucleic acid and/or protein synthesis, chaperone-assisted protein folding, enzymatic activity, cytoplasmic membrane septum formation and cell wall synthesis (Nicolas, 2009; Figure 2).

Prerequisite for the antimicrobial action of AMPs is the peptide's amphipathic structure that is defined by clusters of hydrophobic and basic amino acids spatially organized in discrete sectors of the peptide. This facilitates the interaction and insertion of the peptide into the anionic cell walls and phospholipid membranes of microorganisms. Some peptides adopt only an amphipathic structure upon reaching the target's membrane, e.g. the linear peptides cecropin and magainin, others have already a preformed rigid amphipathic structure that is stabilized by Cys residues (e.g. defensins). All AMPs interact with membranes and can be divided into two mechanistic classes: (I) membrane disruptive (barrel-stave, toroidal, carpet, micellar aggregate and Shai-Matsuzaki-Huang models) and (II) non-membrane disruptive (intracellular targets; see below).

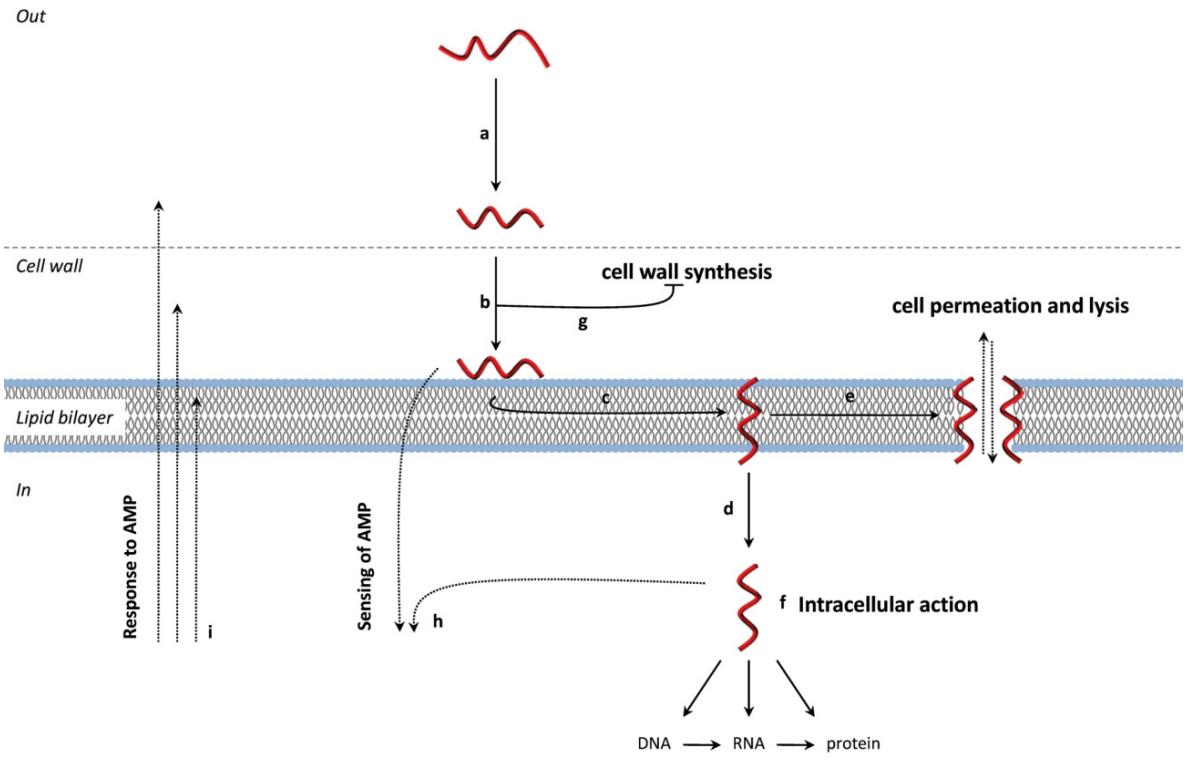

Figure 2. General overview of the antimicrobial action of AMPs.

First, (a) AMPs (red) interact with the outer cell envelope by electrostatic interactions. After binding to the membrane surface (b), the AMP is inserted into the lipid bilayer of the microbial membrane (c). Depending on the properties of the AMP, the AMP can translocate into the bilayer thereby entering the microbial cytosol (non-disruptive AMP) or permeabilize the membrane (e) (disruptive AMP; see further). Internalized AMPs can bind to DNA, RNA, and/or proteins, and disrupt DNA replication, RNA synthesis, or enzyme activity, depending on the peptide (f). Other modes of AMP action are disruption of cell wall synthesis, cell architecture, or cell morphology (g). Microorganisms can detect the presence of AMPs (h) leading to altered gene expression and protein activities (i). Adapted from Marcos *et al.*, 2008.

Throughout evolution, AMPs took advantage of the main differences between the composition of microbial membranes and multicellular organisms. For instance in bacteria, the composition of the outer membrane of Gram-negative and Gram-positive bacteria greatly differs. Whereas in Gram-negative bacteria the outer membrane consists of anionic molecules such as phospholipids and lipopolysaccharides, the membrane of Gram-positive bacteria is mainly characterized by the asymmetric distribution of acidic polysaccharides (teichoic acids). As a result, the membranes of both Gram-negative and Gram-positive bacteria have a net negative charge. On the contrary, mammalian membranes are predominantly enriched with zwitterionic phospholipids (Giuliani *et al.*, 2007). In addition, the presence of cholesterol – a major constituent of mammalian membranes – reduces the fluidity necessary for efficiently disrupting the membrane by AMPs.

I. Membrane disruptive AMPs

The molecular mechanisms behind membrane permeabilization and disruption depend on multiple factors such as the nature of the peptide (e.g. α-helical peptides versus defensins), the membrane lipid composition, the peptide concentration and the environmental condition (Bechinger and Lohner, 2006). Although several membrane permeabilization models have been proposed, no consensus has been made in the field.

Barrel-stave model. Although this model has been proposed several decades ago, convincing evidence has only been shown for a few peptides (Ehrenstein and Lecar, 1977; Christensen *et al.*, 1988; Duclohier *et al.*, 1989; Westerhoff *et al.*, 1989; Matsuzaki *et al.*, 1991). This model is based on the perpendicular insertion and aggregation of individual peptides or peptide complexes, also called 'staves', in a 'barrel-like' ring inside the hydrophobic area of the membrane, leading to the formation of a transmembrane pore or channel with a cylindrical structure. In this barrel, the hydrophobic surfaces of α-helical or β-sheet peptides are faced outward - toward the hydrophobic core of the membrane - and the hydrophilic stretches of the peptides line the inner surface of the pore. Only a few transmembrane pores are required to permeabilize the target membrane (Shai, 2002).

Toroidal pore model. This model is also based on the formation of transmembrane helical bundles in a barrel-stave organization. However, these transmembrane pores are lined by both overlapping peptides and membrane phospholipid head groups. These negatively charged membrane phospholipid head groups reduce the repulsive forces of the cationic portions of the peptides thereby stabilizing the transmembrane pore structure. In contrast, this displaces the polar head groups of the target membrane thereby straining the membrane curvature (Yeamn and Yount, 2003).

Carpet model. In this model, positively charged peptides (in monomeric or oligomeric form) bind to acidic phospholipid-rich regions of lipid bilayers mainly via electrostatic interactions. This leads to the formation of high density clusters covering the bilayer and eventually to a 'peptide carpet' on the membrane. Subsequently, the peptides reorient themselves by facing their hydrophobic portions towards the membrane lipid core and the hydrophilic sides towards the phospholipid head groups. As a result, these high density clusters significantly strain the membrane bilayer curvature. Once a critical peptide density has been reached, the membrane eventually disrupts leading to cell death.

Micellar aggregate or 'detergent-like' model. This model is based on the intercalation of peptides into the membrane bilayer. Subsequently, these inserted peptides cluster together forming unstructured aggregates and this, in turn, allows the formation of transient intramembrane spanning pores (Bechinger and Lohner, 2006).

Shai-Matsuzaki-Huang model. A general model was proposed that explains the activity of most AMPs (Zasloff, 2002). The Shai-Matsuzaki-Huang (SMH) model is a compilation of the mechanisms described above (Matsuzaki, 1999; Shai, 1999; Yang *et al.*, 2000) and proposes the interaction of AMPs with the target membrane, followed by the displacement of membrane phospholipids and, thus, altering the membrane structure and, in some cases, leading to the uptake of the peptide in the interior of the cell (Figure 3).

II. Non-membrane disruptive AMPs: intracellular targets

Increasing evidence indicates that the antimicrobial action of some AMPs can also be based on the interaction with intracellular targets by crossing membranes in a non-destructive manner (Joliot and Prochiantz, 2004; Henriques *et al.*, 2006). Once entered the microbial cytoplasm, the AMP may interact with nucleic acids and/or cellular proteins and inhibit synthesis of these molecules (Brogden, 2005; Gifford *et al.*, 2005; see further).

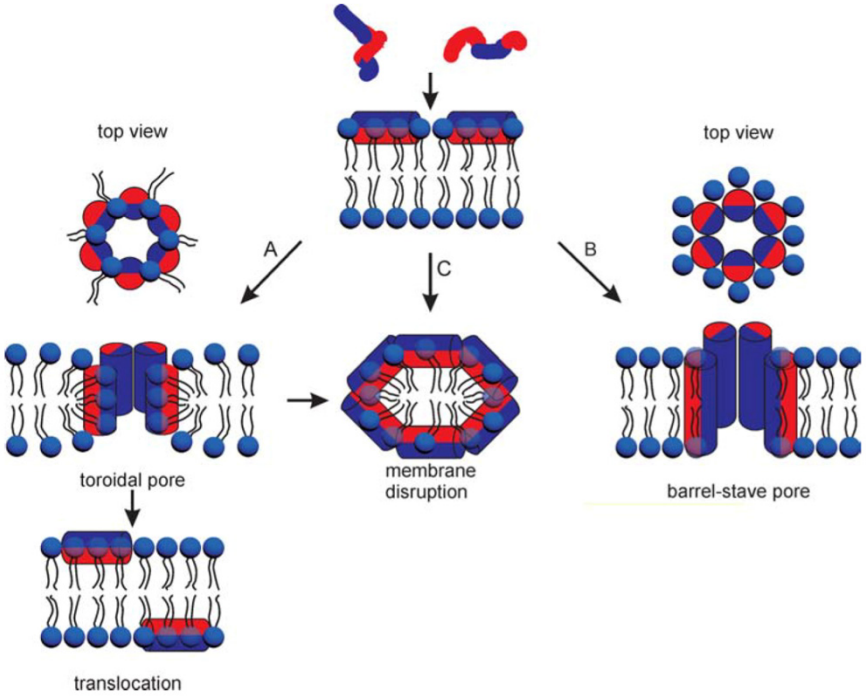

Figure 3. SMH model of membrane permeabilization.
Upon interaction with membrane phospholipids (blue, hydrophilic head group; black, hydrophobic acyl sidechains), the unstructured AMP adopts an amphipathic, α-helical conformation (blue part, hydrophilic side; red part, hydrophobic part). Depending on the peptide's nature, peptide concentration and membrane lipid composition, a toroidal pore (A) or a barrel-stave pore (B) can be formed. Alternatively, the plasma membrane can be irreversibly disrupted (C). Pore formation can be followed by translocation of the peptide from the outer leaflet to the inner leaflet of the membrane. SMH, Shai-Matsuzaki-Huang. From Theis and Stahl, 2004.

ANTIMICROBIAL PEPTIDES IN PLANTS

Introduction

AMPs are widespread throughout the plant kingdom and are classified into thionins (Fernandez De Caleya *et al.*, 1972; Bohlmann and Broekaert, 1994; Epple *et al.*, 1997), plant defensins (Terras *et al.*, 1992; Broekaert *et al.*, 1995; Broekaert *et al.*, 1997; Lay *et al.*, 2003; Lay and Anderson, 2005), lipid-transfer proteins (Molina *et al.*, 1993; Cammue *et al.*, 1995; Kader, 1996), cyclotides (Craik and Conibear, 2011), snakins, hevein- and knottin-like peptides (Broekaert *et al.*, 1992; Cammue *et al.*, 1992; Shao *et al.*, 1999; Van Damme *et al.*, 1999) and polyprotein precursor AMPs from both *Macadamia integrifolia* (Marcus *et al.*, 1997; McManus *et al.*, 1999) and *Impatiens balsamina* (Tailor *et al.*, 1997; Patel *et al.*, 1998; Figure 4).

In addition, several AMPs do not belong to these classes (Guo *et al.*, 2009; Lin and Ng, 2009). The PhytAMP database contains general information about the physicochemical and biological properties of plant AMPs showing antibacterial (33%), antifungal (51%), antiviral (10%), anti-yeast (2%), insecticidal (3%) and ion channel-blocking activities (1%) (Hammami *et al.*, 2009). Currently, 271 plant AMPs are present in this database and includes cyclotides (76), defensins (55), hevein-like (14), impatiens (4), knottins (4), lipid-transfer proteins (45), shepherins (2), snakins (20), thionins (43), vicilin-like (6), MBP-1 (18) and β-barellin (19) isolated from a wide variety of species including members of the Amaranthaceae, Andropogoneae, Brassicaceae, Oryzeae, Santalaceae, Spermacoceae, Triticaceae, Vicieae and Violaceae families (Figure 4). As expected, the majority has a net charge varying from 0 to +10 and the average net charge of all plant AMPs is +4.6 (Hammami *et al.*, 2009). The majority of plant AMP families are plant-specific, such as thionin, lipid-transfer protein, cyclotide and snakin families. Most plant AMPs have an even number (typically 4, 6 or 8) and linear arrangement of Cys residues necessary for intramolecular disulfide bridges formation in class-specific three-dimensional folds (Broekaert *et al.*, 1997).

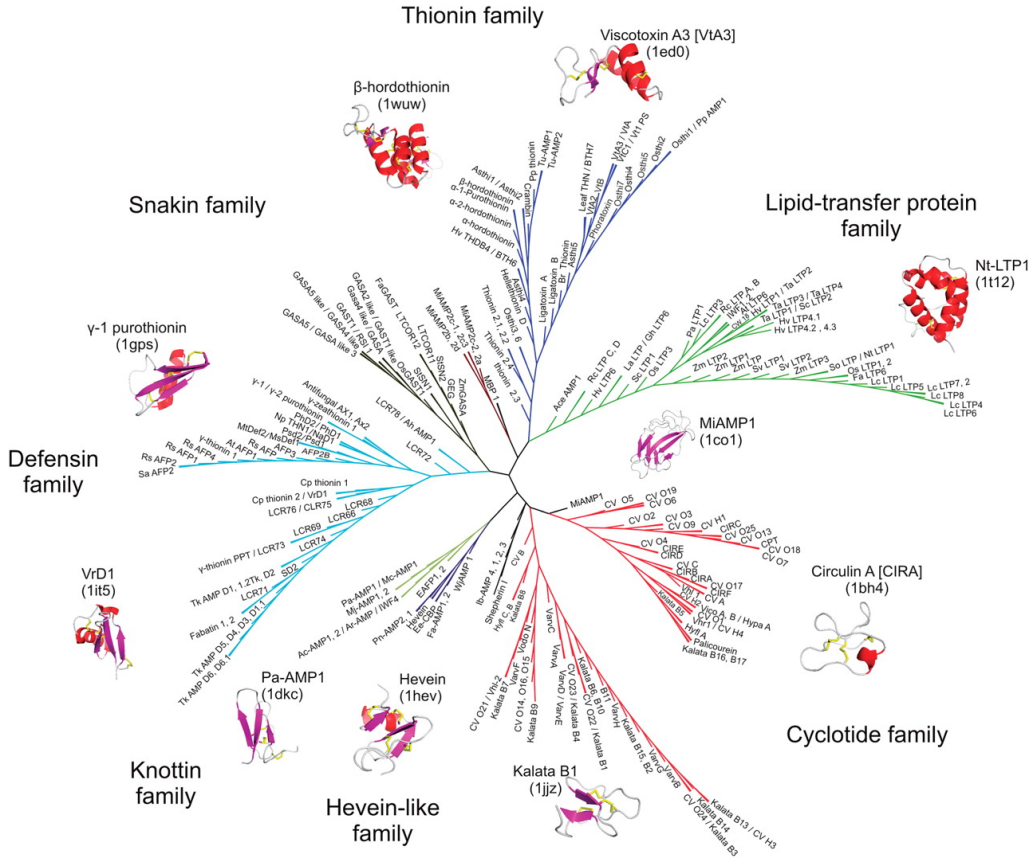

Figure 4. Unrooted phylogenetic tree of plant AMPs compiled in the PhytAMP database (http://phytamp.pfba-lab.org; Hammami *et al.*, 2009). α-helices and β-sheets are shown in red and purple, respectively. From Hammami *et al.*, 2009.

Plant AMPs are predominantly expressed in peripheral tissues as a front-line in defense and are often specifically regulated by both biotic and abiotic stresses (Broekaert *et al.*, 1997). Most members have antimicrobial activities *in vitro* and several examples are reported of transgenic plants expressing AMPs that have an increased tolerance against a broad-spectrum of bacterial and fungal pathogens (see further; Broekaert *et al.*, 1997).

Classification

Thionins

Thionins are small (~5 kDa), basic peptides that were first isolated from cereals (Bohlmann *et al.*, 1988). They have a characteristic three-dimensional folding pattern that is stabilized by six to eight disulfide bridges and contains two antiparallel α-helices and an antiparallel double-stranded β-sheet. So far, around 100 individual thionin sequences have been identified in more than 15 different plant species, including both monocots and dicots (Stec, 2006) and have been subdivided into five different classes (Bohlmann and Apel, 1991). In *Arabidopsis thaliana*, six thionins were found (Sels *et al.*, 2008). Hitherto, only one study showed an active role for plant thionins in plant defense (Epple *et al.*, 1997).

Thionins are toxic to different biological systems such as bacteria, fungi, cultured mammalian cells, whole animals, and insect larva (Stec, 2006). Thionins are predominantly present in the vacuolar compartment (Broekaert *et al.*, 1997), though targeting to the cell wall was also reported (Iwai *et al.*, 2002). Thionins are synthesized as non-toxic preproproteins (Ponz *et al.*, 1983) that are activated upon pathogen attack by proteolytic processing thereby releasing the mature toxic thionin domain (Stevens *et al.*, 1996; Thevissen *et al.*, 1996; Romero *et al.*, 1997). Interestingly, the acidic prodomain of thionins is often better conserved than the mature domain itself, indicating that it might play an important role. First, the net charge of the prodomain is correlated with the charge of the mature domain. For instance, a highly basic mature peptide is neutralized by the presence of an acidic prodomain, whereas a neutral and hydrophobic domain is linked to a neutral prodomain (Schrader-Fischer and Apel, 1994). Therefore, it is postulated that both domains interact with each other. This prodomain may act as a transient intramolecular chaperone by assisting the folding of the mature domain.

Plant defensins (γ-thionins)

Plant defensins are small (5-7 kDa), basic (pI~9) AMPs with eight strictly conserved disulfide-linked Cys residues and are found ubiquitously throughout the plant kingdom. The first plant defensins were isolated from wheat (*Triticum aestivum*) and barley (*Hordeum vulgare*) grains and were initially thought to be a novel type belonging to the thionin family because of their similar size and number of cysteines. Accordingly, they were called 'γ-thionins' (Carrasco *et al.*, 1981; Colilla *et al.*, 1990; Mendez *et al.*, 1990). However, it was later found that thionins and γ-thionins are structurally unrelated to each other (Bruix *et al.*, 1993). As a matter of fact, γ-thionins showed structural and functional similarities with insect defensins and mammalian β-defensins and were consequently named 'plant defensins' (PDFs; Terras *et al.*, 1995). PDFs can have different effects on fungal growth and are therefore categorized into two groups: the morphogenic and non-morphogenic defensins. Whereas morphogenic defensins inhibit fungal growth and morphologically alter the fungal hyphae, such as branching, swelling and shortening, non-morphogenic defensins reduce hyphal elongation without causing any morphological perturbations (Broekaert *et al.*, 1995; Thomma *et al.*, 2002). In *Arabidopsis*, 15 putative PDFs were identified and classified into three subfamilies, called AtPDF1- (7), AtPDF2- (2), AtPDF3-family (6) (Thomma *et al.*, 2002). Three AtPDF genes were purified so far, namely AtPDF1.1, AtPDF1.2 and AtPDF1.3 and showed *in vitro* antifungal activities (Terras *et al.*, 1993; Penninckx *et al.*, 1996; Sels *et al.*, 2008).

PDFs are characterized by their small and globular three-dimensional structure that consists of a structural motif composed of disulfide bonds, called the Cys-stabilized α-helix β-sheet motif (CSαβ; e.g. RS-AFP1; Bruix *et al.*, 1993; Bloch *et al.*, 1998; Fant *et al.*, 1998; Fant *et al.*, 1999; Almeida *et al.*, 2002). Some defensin genes are strictly developmentally regulated (Epple *et al.*, 1997), whereas others are regulated by biotic and abiotic environmental stimuli (Kragh *et al.*, 1995; Broekaert *et al.*, 1997). In contrast to thionins, the majority of PDFs have an N-terminal signal peptide for targeting to the extracellular space (predomain) and lack the prodomain. However, some PDFs isolated from tobacco (*Nicotiana tabacum*; Gu *et al.*, 1992) and tomato (*Lycopersicon esculentum*; Milligan and Gasser, 1995) are produced as preproproteins with the propeptide located at the C-terminus (Lay and Anderson, 2005). Interestingly, the majority of the N-terminal signal peptides of PDFs are quite acidic. Therefore, the signal peptide could be bifunctional: trafficking to the secretory pathway and neutralizing the basic mature peptide. Although numerous biological activities of PDFs were demonstrated *in vitro*, including inhibition of α-amylases (Bloch and Richardson, 1991; Zhang *et al.*, 1997), protein translation (Colilla *et al.*, 1990; Mendez *et al.*, 1990) and proteases (Wijaya *et al.*, 2000; Melo *et al.*, 2002), ion channel-blocking, antibacterial and antifungal activities (Carvalho and Gomes, 2009), the precise *in vivo* mode of action of PDFs remains unclear.

Hevein- and knottin-type AMPs

Hevein is the most predominant peptide (43 amino acids) in the latex of rubber trees (*Hevea* sp.) and shows homology to the Cys-rich chitin-binding domain present in different types of chitin-binding proteins (Archer *et al.*, 1969; Walujono *et al.*, 1975). Although hevein has rather weak antifungal properties (Van Parijs *et al.*, 1991), much more potent homologs have been found in the seeds of *Amaranthus caudatus* (Broekaert *et al.*, 1992), *Amaranthus retroflexus* (Lipkin *et al.*, 2005) and *Pharbitis nil* (Koo *et al.*, 1998), the leaves of *Beta vulgaris* (Nielsen *et al.*, 1997) and *Sambucus nigra* fruits (Van Damme *et al.*, 1999) and are called 'hevein-type AMPs'. Hevein and hevein-type peptides have an N-terminal signal peptide and a C-terminal propeptide that shows homology to PR-4 from tobacco and has eight disulfide-linked cysteines that form four disulfide bridges. On the other hand, the amaranth hevein-like peptides originate from a similar precursor but their prodomains are shorter and thus they have only six Cys residues. Both hevein and hevein-like peptides are secreted into the apoplast.

Knottins or cystine-knot miniproteins are a large family found in many species with a variety of biological functions such as inhibitory, antimicrobial, insecticidal, cytotoxic, anti-HIV or hormone-like activities (Chiche *et al.*, 2004). An overview is given in the KNOTTIN database (http://knottin.cds.cnrs.fr/; Gracy *et al.*, 2008). Knottins consist of approximately 30 amino acids and share a highly stable and compact knotted tertiary scaffold that is formed and stabilized by a characteristic pattern of disulfide bonds, called the 'knottin fold'.

Both hevein- and knottin-type peptides have a similar antimicrobial spectrum and inhibit a broad range of phytopathogenic fungi and Gram-positive bacteria (Broekaert *et al.*, 1992; Cammue *et al.*, 1995).

Cyclotides

Cyclotides are Cys-rich circular peptides ranging from 28 to 37 amino acids and are exclusively found in plants, specifically in the Rubiaceae, Violaceae, Cucurbitaceae and Fabaceae families (Camarero, 2011; http://www.cyclotide.com/). Various biological functions have been reported such as antimicrobial, insecticidal, antihelmintic, cytotoxic, antitumor, antiviral, protease inhibition and uterotonic effects (Gran *et al.*, 2000; Avrutina *et al.*, 2005; Daly *et al.*, 2009). Cyclotides have a unique three-dimensional fold typified by a head-to-tail cyclized peptide backbone with a cyclic Cys-knot topology. Due to this cyclic and rigid framework, cyclotides are extremely resistant to thermal and chemical denaturation and enzymatic degradation (Colgrave and Craik, 2004). In fact, these properties make cyclotides promising candidates for pharmaceutical and agricultural applications (Garcia and Camarero, 2010; Jagadish and Camarero, 2010). Unfortunately, several attempts to express cyclotides in transgenic Arabidopsis and tobacco plants failed (Saska *et al.*, 2007; Gillon *et al.*, 2008). Recently, cyclotides have been isolated from

Clitoria ternatea, a member of the Fabaceae family of which many species (e.g. peas and beans) are of great economic importance. This could open new possibilities to express cyclotides in a genetically modified legume crop (Poth *et al.*, 2011).

Lipid-transfer proteins

Lipid-transfer proteins (LTPs) are basic (~pI 9), small proteins (9-10 kDa) that were originally identified for their ability to facilitate lipid shuttling between membranes *in vitro*. However, it was later shown that LTPs are secreted (Sterk *et al.*, 1991) and, thus, located in the extracellular space, thereby ruling out the putative role in lipid transfer (Segura *et al.*, 1993; Pyee and Kolattukudy, 1995). Hitherto, numerous LTPs were identified in both mono- and dicotyledonous species including barley, grapevine (*Vitis vinifera*), wheat, *A. thaliana*, spinach (*Spinacia oleracea*) and onion (*Allium cepa*; Sels *et al.*, 2008). The Arabidopsis LTP family consists of 15 members that are all regulated by developmental and environmental cues (Arondel *et al.*, 2000; Sels *et al.*, 2008).

Plant LTPs are synthesized as precursors with an N-terminal signal peptide and a mature LTP domain containing eight conserved Cys residues forming four disulfide bridges at the C-terminus. The tertiary structure of plant LTPs is comprised of four α-helices and is classified as an all-α-type structure. These four α-helices are connected by flexible loops that form a hydrophobic cavity that can accommodate lipids (Shin *et al.*, 1995). Many biological functions have been attributed to plant LTPs such as a role in cutin synthesis (Pyee *et al.*, 1994), β-oxidation (Tsuboi *et al.*, 1992), defense signaling (Buhot *et al.*, 2001; Maldonado *et al.*, 2002) and response (Molina *et al.*, 1993; Kristensen *et al.*, 2000; Girault *et al.*, 2008). As plant LTP expression is induced upon pathogen infection, they were classified as PR peptides (Sels *et al.*, 2008). Several plant LTPs have been reported to exert both antifungal and antibacterial activities (Molina *et al.*, 1993; Cammue *et al.*, 1995). Their antimicrobial action could be linked to the ability of plant LTPs to bind biological membranes together with their high isoelectric point by acting as membrane-permeabilizing agents (Kader, 1996).

Four-Cys AMPs

Four-Cys AMPs are a group of small basic peptides in which the number and distribution of Cys residues show no structural homology with other plant AMPs. Members of this group are MPB-1, Ib-AMPs and EcAMP1.

MPB-1 was first isolated from maize seeds as a 33 residue AMP (3.7 kDa) with four disulfide-linked cysteines (Duvick *et al.*, 1992) that are organized in two CXXXC segments. MBP-1 showed inhibitory activities against both gram-positive (*Clavibacter michiganense*) and gram-negative (*Escherichia coli*) bacteria and several fungi (Duvick *et al.*, 1992).

Recently, an antifungal peptide EcAMP1 of 37 amino acids was isolated from the kernels of barnyard grass (*Echinochloa crus-galli)* with an unusual four-Cys motif (Nolde *et al.*, 2011) that is also present in MBP-1, MiAMP2 from *Macadamia integrifolia,* and the trypsin inhibitors BWI-2b from buckwheat and VhTI from *Veronica hederefolia*. Moreover, EcAMP1 showed a 67% sequence identity with MPB-1. EcAMP1 adopts a disulfide-stabilized α-helical hairpin structure that is unprecedented among naturally occurring AMPs. EcAMP1 exhibits high antifungal activities against *Fusarium* sp. by inhibiting hyphal elongation without disrupting the fungal membrane (Nolde *et al.*, 2011).

The Ib-AMP family consists out of four small basic peptides (20 amino acids) isolated from the seeds of *Impatiens balsamina* that contain four Cys residues that are linked by two disulfide bridges (Tailor *et al.*, 1997). These peptides are closely related to each other but lack homology with other AMPs. Interestingly, all four Ib-AMP peptides are produced from one 333 amino acid translation product encoded by one gene. This multipeptide precursor has an N-terminal signal peptide for targeting to the secretory pathway. Within this translation product, all Ib-AMPs are each time flanked by moderately conserved anionic prodomains that likely function in neutralizing the highly basic mature Ib-AMP peptides. Both antibacterial and antifungal activities against a number of species have been demonstrated *in vitro* for all four Ib-AMPs (Tailor *et al.*, 1997).

Snakins

Snakins include small AMPs (< 11 kDa) that are characterized by the presence of twelve Cys residues and are expressed as preproproteins. The first purified snakins, StN1 and StN2, were isolated from the tubers of potato (*Solanum tuberosum*) and showed antimicrobial activity against a number of important pathogens *in vitro* (Segura *et al.*, 1999; Berrocal-Lobo *et al.*, 2002). StSN1 and StSN2 are similar with members of the GAST and GASA family from tomato and Arabidopsis, respectively. Consequently, they were classified into a novel snakin/GASA family (Berrocal-Lobo *et al.*, 2002). This further led to the identification of additional homologs in a wide range of species including mono- and dicotyledonous plants (Shi *et al.*, 1992; Ben-Nissan and Weiss, 1996; Kotilainen *et al.*, 1999; Furukawa *et al.*, 2006). Snakins have been shown to play a role in cell division, cell elongation, cell growth, transitioning to flower, signaling pathways and defense (Aubert *et al.*, 1998; Kotilainen *et al.*, 1999; Segura *et al.*, 1999; Berrocal-Lobo *et al.*, 2002; Ben-Nissan *et al.*, 2004; de la Fuente *et al.*, 2006; Furukawa *et al.*, 2006; Roxrud *et al.*, 2007).

Other biological roles of AMPs in plants

Protein inhibitors

Besides their antimicrobial activity, many AMPs have been shown to exert protein-inhibitory activities (Broekaert *et al.*, 1997; Lay and Anderson, 2005). For instance, several plant AMPs have been shown to inhibit animal α-amylase activity, including members of the PDF (Bloch and Richardson, 1991), LTP (Campos and Richardson, 1984) and the knottin-type families (Chagolla-Lopez *et al.*, 1994). As α-amylases are the major digestive enzymes in the gut of herbivores, plant AMPs could be involved in the defense against herbivores (Shade *et al.*, 1994). Interestingly, PDFs that exhibit α-amylase activity seemed to have no antifungal or antibacterial activities and vice versa (Osborn *et al.*, 1995). Other plant AMPs were shown to inhibit serine proteases (Wijaya *et al.*, 2000; Melo *et al.*, 2002; Chiche *et al.*, 2004) and protein translation (Colilla *et al.*, 1990; Mendez *et al.*, 1990). Purothionins are able to inhibit the enzymatic activity of ribonucleotide reductase, interfere with DNA synthesis and irreversibly inactivate β-glucuronidase (Johnson *et al.*, 1987; Diaz *et al.*, 1992).

Redox regulation

SPD1, a defensin isolated from sweet potato (*Ipomoea batatas*), was shown to regenerate both monodehydroascorbate and dehydroascorbate to ascorbic acid in the presence of glutathione. Accordingly, it was proposed that SPD1 regulates the redox status of ascorbic acid (Huang *et al.*, 2008). Purothionins have been shown to influence the redox potential of thioredoxins and are also known to activate chloroplast fructose-1,6-bisphosphatase by promoting disulfide bond formation (Wada and Buchanan, 1981; Johnson *et al.*, 1987). This has led to the development of the commercial product Corystein™ (TaKaRa Co) that is used as an oxidizing/reducing agent catalyzing the formation of correct disulfide bonds in proteins.

Ion channel inhibitors

Two γ-zeathionins (defensin family) isolated from maize were shown to block the conductance of voltage-gated sodium channels in animal cells (Kushmerick *et al.*, 1998). Interestingly, these peptides showed structural similarities with μ-conotoxins, a class of neurotoxic Cys-rich peptide amides that block muscle-type sodium channels (Ohizumi *et al.*, 1986). Moreover, a plant defensin, called *Medicago sativa* Defensin1 (MsDef1), was shown to selectively block the mammalian L-type Ca^{2+} channel in a similar way as KP4, a viral encoded killer toxin from the corn smut fungus *Ustilago maydis* (Spelbrink *et al.*, 2004).

Metal physiology

In a screen to determine novel components involved in the zinc (Zn) tolerance of the hyper-accumulating plant *Arabidopsis halleri*, several cDNAs encoding PDFs were identified (AhPDFs; Mirouze *et al.*, 2006). These defensins are constitutively present in the shoots of *A. halleri* and accumulate in response to Zn stress. Overexpression of one of these AhPDFs in transgenic *A. thaliana* plants resulted in an increased Zn tolerance compared to wild-type plants. Because these PDF genes have a much higher basal expression level in *A. halleri* as in *A. thaliana* and a strong response to Zn treatment, these defensins could play a role in the Zn tolerance of *A. halleri*. Two main hypotheses for the mechanisms behind this Zn tolerance were proposed: AhPDFs could act as Zn-chelating agents or as ion channel-blocking agents (Mirouze *et al.*, 2006).

Development

Several studies have shown the involvement of defensins in plant development. For instance in *Brassica*, interaction between a defensin-like peptide secreted from pollen with the cognate S-locus receptor kinase on the stigma activates a self-incompatibility response that prevents self-fertilization (Takayama *et al.*, 2001). Silencing of DEF2, a defensin highly expressed in immature flower buds of tomato, leads to the retardation of meiosis resulting in pollen viability defects. During later stages of flower development, inactivation of DEF2 is required for survival and development of pollen grains (Stotz *et al.*, 2009).

Abiotic stress tolerance

Increasing evidence indicates that plant AMPs play a role in abiotic stress responses. First, the expression of many PR genes, including plant AMPs, is modulated by abiotic stress, such as drought stress, low and high temperature stress, high light stress and high salinity stress (Hon *et al.*, 1995; Broekaert *et al.*, 2000; Zeier *et al.*, 2004; Van Loon *et al.*, 2006; Seo *et al.*, 2008). For instance, PDFs are responsive towards abiotic stresses, including cold (Koike *et al.*, 2002), drought (Do *et al.*, 2004), metal stress (Mirouze *et al.*, 2006; see above) and nutrient starvation (Armengaud *et al.*, 2004). Moreover, several reports have shown that the overexpression of antimicrobial genes conferred not only tolerance to pathogenic microorganisms, but also to environmental stresses. For instance, the antimicrobial protein gene *CaAMP1*, isolated from *Capsicum annuum*, is induced by abscisic acid (ABA), high salinity, drought and low temperature stress (Lee and Hwang, 2009). Constitutive expression of *CaAMP1* in transgenic Arabidopsis plants leads to an enhanced tolerance towards ABA, high salinity and drought stress, and is linked to an earlier induction of the *AtRD29A* gene that is involved in drought, low temperature, high salinity and ABA responses (Shinozaki and Yamaguchi-Shinozaki, 1997; Ishitani *et al.*, 1998; Piao *et al.*, 2001; Narusaka *et al.*, 2003; Lee and Hwang, 2009). Several reports have shown that

LTP and LTP-like proteins are involved in the acclimation to several environmental conditions, such as cold, salt stress and drought stress (Kader, 1996). In addition, overexpression of an antimicrobial gene can lead an enhanced tolerance towards oxidative stress. For instance, rice plants that overexpress *cecropin A*, a plant codon-optimized synthetic gene from the Cecropia moth (*Hyalophora cecropia*; Table 1), showed an increased tolerance towards hydrogen peroxide that is correlated with an increased expression of ROS-scavenging enzymes (Campo *et al.*, 2008).

AMPs are promising candidates for novel applications in plant disease control

Plant diseases caused by phytopathogenic microorganisms are responsible for major reductions in food quality and safety (http://faostat.fao.org/). This leads to enormous losses of both cultivated and stored crops and is thus a major hurdle in effective food distribution world-wide. Several agricultural practices were developed to protect crops, such as irrigation, crop rotation, fertilizers, chemical pesticides and resistant cultivars obtained by conventional breeding. Nevertheless, in an era of massive monocultures, decreasing arable land area and an exponentially growing world population, these practices will be insufficient to maintain the global food and feed demand (http://faostat.fao.org/). The extensive usage of agrochemicals, that often have a narrow mode of action, has led to the strong development of resistant phytopathogens. In addition, agrochemicals can have long-term repercussions on the environment. Crossbreeding of resistant cultivars is difficult because suitable genetical sources containing specific disease resistance genes are limited or in some cases not known yet. Hence, more efficient and durable strategies need to be developed to control plant diseases. In this respect, genetic engineering provides an opportunity to introduce genes conferring resistance to phytopathogenic organisms of agronomical important crop cultivars. In general, candidate genes must confer a durable resistance to a broad-spectrum of pathogens while being safe for all other organisms, including the crop itself, and the animals and humans that consume them (van der Biezen, 2001).

Antimicrobial genes of both plant and non-plant origin have been used to generate disease-resistant plants (Brogue *et al.*, 1991; Lorito *et al.*, 1998). However, introducing a single antimicrobial gene (e.g. chitinase, β-1-3-glucanase) often leads to a limited level of disease resistance and a narrow spectrum of protection. In contrast, AMPs have been proposed as promising candidates for use in agriculture because of their small size, broad-spectrum activity with a high affinity for microbial membranes, high resistance against proteolysis, rapid antibacterial and antifungal action, limited immunogenicity and a mode of action that is difficult to develop resistance against (Table 1; Jaynes *et al.*, 1987; Casteels *et al.*, 1989; Rao, 1995; van der Biezen, 2001; Bulet *et al.*, 2004; Montesinos, 2007; Marcos *et al.*, 2008).

AMPs can be applied in crop protection through different ways. First, plant diseases can be controlled through the administration of synthetic peptides. Because the activity of AMPs greatly

depends on the microenvironment where the interaction between the peptide, the pathogen and the plant tissue takes place, extensive studies have to be carried out to ensure the peptide remains active *in situ* (Marcos *et al.*, 2008). When using peptides at a large-scale, the production needs to be cost-effective and is therefore often based on recombinant expression systems with micro-organisms and even transgenic plants (molecular farming; Zhang *et al.*, 1998; Lee *et al.*, 2002; Nandi *et al.*, 2005). The application of synthetic peptides could be used in the combat against postharvest diseases as an additional postharvest additive (López-García *et al.*, 2000; Liu *et al.*, 2007a; Liu *et al.*, 2007b). Next, AMPs could be combined with microorganisms in a process called biological control, an alternative disease-control method using natural enemies of phytopathogens. Yeast strains that occur naturally on the surfaces of fruits or vegetables have been proposed as biocontrol agents of postharvest diseases (Chalutz and Wilson, 1990; Jeffries and Jeger, 1990; Droby *et al.*, 1991; Janisiewicz, 1991; Smilanick *et al.*, 1993; Jones and Prusky, 2002). For instance, the expression of an antifungal peptide in *Saccharomyces cerevisiae* led to the efficient growth inhibition of the tomato fruit fungal pathogen *Colletotrichum coccodes*, a major causing agent of postharvest diseases (Jones and Prusky, 2002).

Another strategy is the overexpression of transgenes encoding natural or synthetic AMPs and has been successful in the protection of plants against diseases caused by a variety of bacterial and fungal phytopathogens (Table 1; Carmona *et al.*, 1993; Molina and García-Olmedo, 1997; Zhang *et al.*, 1998; Gao *et al.*, 2000; Oldach *et al.*, 2001; Takase *et al.*, 2005). To efficiently improve crop disease resistance by AMP overexpression, a detailed understanding of the target, host and AMP is prerequisite and can limit potential drawbacks, such as species specificity of the peptides, partial resistance, biotoxicity, reduced fitness, peptide instability and poor bioavailability. One strategy to improve disease resistance is to combine multiple AMPs with complementary modes of action and host spectra. For instance, AMPs acting at different infection stages of a phytopathogen can be combined to increase resistance against resilient disease-causing microbes. This can be established by co-expression (Xing *et al.*, 2006), chimeric hybridization (Osusky *et al.*, 2000) or the expression of polyprotein precursor constructs of multiple AMPs (François *et al.*, 2002; François *et al.*, 2004). An efficient strategy to minimize the potential instability (e.g. by post-translational degradation) and, thus, to increase the bioavailability of the peptide, is targeting the peptide to another subcellular compartment, preferentially where protease activity is presumed to be lower (Sharma *et al.*, 2000; Li *et al.*, 2001; Coca *et al.*, 2006). Constitutive overexpression can also decrease the stability of the AMP. For instance, overexpression of Cys-rich peptides (i.e. thionins) can lead to aspecific binding to other cellular components, possibly through disulfide linkage, thereby limiting the *in vivo* peptide availability and activity (Piñeiro *et al.*, 1995; Banzet *et al.*, 2002). In turn, these aspecific interactions can have pleotropic effects often leading to morphological perturbations (Banzet *et al.*, 2002). In respect of this, the expression of AMPs via the chloroplast genome

offers several advantages in terms of protein stability and toxicity. Compartmentalization of AMPs in the chloroplasts, that has predominantly neutral membrane lipids, allows the storage of a high amounts of AMPs because of to the high copy number associated with chloroplast expression and prevents pollen-mediated escape of transgenes (DeGray *et al.*, 2001). Another disadvantage of the constitutive overexpression of a disease resistance protein is the promotion of co-evolution of resistant phytopathogens. Therefore, the generation of plants expressing AMPs on-demand by using synthetic or native inducible promoters activated upon pathogen attack is preferred.

The detailed knowledge of the biophysical and structural properties of these natural peptides could serve as a basis for the rational design of less toxic non-natural bioactive AMPs. Recent advances in the synthesis of peptides, peptide collections and libraries, allows to asses if rationally designed peptide modifications, additions or deletions have an impact on the specificity, the toxicity against plant and animal cells, the stability and the action spectrum. Different strategies are employed to design novel AMPs such as the modification of the sequence of natural AMPs, fusion of fragments of natural AMPs and peptide cyclization of synthetic peptides (Marcos *et al.*, 2008).

Although the benefits of using AMPs in plant protection have been repeatedly demonstrated, several remarks about biosafety have to be kept in mind. The expression of a transgene could affect the host gene expression. Therefore, extensive studies have to be carried to address if the expression of an antimicrobial gene affects the natural inducible plant defense responses. Several studies have demonstrated that overexpression of an antimicrobial gene perturbed nuclear gene expression and implied an altered immune status (Campo *et al.*, 2008; Distefano *et al.*, 2008; Rahnamaeian *et al.*, 2009; Rahnamaeian and Vilcinskas, 2011). For instance, overexpression of *cecropin A* in rice altered the expression of genes involved in the protection against oxidative stress, processes of synthesis, folding and stabilization of proteins that enter the secretory pathway, translational machinery and genes encoding components of the vesicle-associated transport machinery (Campo *et al.*, 2008). Another important remark regarding biosafety of using AMPs in crop protection is the effect on the mutualistic interaction between plants and beneficial symbionts. These plant-microbe interactions often lead to an increased fitness by supporting water and mineral uptake as well increasing disease resistance (Bonfante and Genre, 2008). Therefore, a detailed understanding of the mode of action and specificity of the AMP is essential for the application in transgenic crops.

Table 1. Overview of AMP expression in transgenic plants (Adapted from Rahnamaeian and Vilcinskas, 2011).

Origin	Source	AMP	Host	Pathogens	Efficacy	Reference
Insects	*Heliothis verescens*	Heliomicin	Tobacco	*Cercospora nicotianae*	Significant decrease in disease symptoms	Banzet *et al.*, 2002
	Drosophila melanogaster	Drosomycin				
		Sarcotoxin IA	Tobacco	*Pseudomonas syringae* pv. *tabaci*	Significant decrease in disease symptoms	Ohshima *et al.*, 1999
				Erwinia carotovora ssp. *carotovora*		
		Mtk	Barley	*Blumeria graminis*	60% decreased colony formation	Rahnamaeian and Vilcinskas, 2011
				Fusarium graminearum	80% decrease in fungal biomass	Rahnamaeian *et al.*, 2009
	Podisus maculiventris	Thanatin	Rice	*Magnaporthe oryzae*	50% decrease in disease index[a]	Imamura *et al.*, 2010
	Hyalophora cecropia	Attacin	Apple	*Erwinia amylovora*	50% reduction in lesion length	Ko *et al.*, 2000
		Cecropin A	Rice	*Magnaporthe grisea*	Significant reduction in lesion size	Coca *et al.*, 2006
				Xanthomonas oryzae		
		Cecropin B	Rice	*Magnaporthe grisea*	~85% reduction in lesion diameter; ~55% increase plant survival	Sharma *et al.*, 2000
				Xanthomonas oryzae	Significant decreased lesion growth	
			Arabidopsis	*Pseudomonas syringae* pv. *tomato*	100-fold reduction in *in planta* proliferation	Oard and Karki, 2006
				Fusarium oxysporum	Qualitatively significant decrease in disease symptoms	
	Galleria mellonella	Gallerimycin	Tobacco	*Erysiphe cichoracearum*	45-66% inhibition of spore germination	Langen *et al.*, 2006
				Sclerotinia minor	Visible reduction in lesion size	
Arthropods	*Tachypleus tridentatus*	Tachyplesin I	Potato	*Erwinia carotovora*	Slight reduced rot in tubers	Allefs *et al.*, 1996
	Mytilus edulis chilensis	mussel defensin	Tobacco	*Pseudomonas syringae* pv. *syringae*	Visible reduction disease symptoms	Arenas *et al.*, 2006
Amphibians	*Xenopus leavis*	Magainin-2	Tobacco	*Pseudomonas syringae* pv. *tabaci*	Leaf extracts inhibited 96% growth	DeGray *et al.*, 2001
				Aspergillus flavus, Fusarium monoliforme, Verticilium dahliae	Leaf extracts inhibited > 95% growth	
				Colletotrichum destructivum	Significant visual resistance	
			Grapevine	*Uncinula necator*	Significant reduction in disease symptoms	Vidal *et al.*, 2006
				Agrobacterium vitis		
	Rana esculenta	Esculentin-1	Tobacco	*Pseudomonas aeruginosa*	Significant reduction in lesion size	Ponti *et al.*, 2003
				Pseudomonas syringae pv. *tabaci*		
Mammals	*Homo sapiens*	hBD-2	Arabidopsis	*Botrytis cinerea*	Significant reduction in percentage decayed leaves	Aerts *et al.*, 2007
Plants	*Raphanus sativus*	RsAFP2	Tobacco Tomato	*Alternaria longipes*	8-fold (~85%) reduction in lesion diameter	Terras *et al.*, 1995
	Medicago sativa	alfAFP	Potato	*Verticillium dahliae*	6-fold (~80%) reduction in *in planta* pathogen proliferation	Gao *et al.*, 2000

Table 1. Overview of AMP expression in transgenic plants (Adapted from Rahnamaeian and Vilcinskas, 2011). *(Continued).*

Origin	Source	AMP	Host	Pathogens	Efficacy	Reference
Plants	*Picea abies*	Spi1	Tobacco	*Erwinia carotovora*	Limited bacterial growth	Elfstrand *et al.*, 2001
	Pisum sativum	DRR206	Canola Tobacco	*Leptosphaeria maculans*	Significant reduction in symptom development	Wang *et al.*, 1999
	Brassica campestris	BSD1	Tobacco	*Phytophthora parasitica* var. *nicotianae*	Qualitatively enhanced disease resistance	Park *et al.*, 2002
	Wasabi japonica	WT1	Rice	*Magnaporthe grisea*	50% reduction in lesion size	Kanzaki *et al.*, 2002
	Dahlia merckii	Dm-AMP1	Eggplant	*Botrytis cinerea*	36-100% reduction in necrotic lesion size	Turrini *et al.*, 2004
	Mirabilis jalapa	Mj-AMP1	Papaya	*Verticillium albo-atrum*	60% reduction in mycelial growth	Zhu *et al.*, 2007
				Phytophtora palmivora	60% reduction in *in planta* pathogen proliferation; ~55% reduction in lesion diameter	
			Tomato	*Alternaria solani*	Qualitatively significant reduction in disease symptoms	Schaefer *et al.*, 2005
	Pharbitis nil	PnAMP-h2	Tobacco	*Phytophthora parasitica*	80% reduced wilting	Koo *et al.*, 2002
	Allium cepa	AcAMP1	Rice	*Magnaporthe grisea*	86% decrease in disease leaf area	Patkar and Chattoo, 2006
				Rhizoctonia solani	67% decreased infection	
				Xanthomonas oryzae	82% reduction in average length of diseased leaf area	
	Brassica juncea	BjD	Tobacco Peanut	*Fusarium monoliforme*	Qualitatively significant reduction in disease symptoms	Swathi Anuradha *et al.*, 2008
				Phytophthora parasitica var. *nicotianae*		
				Phaeosariopsis personata	~90% reduction in lesion frequency	
				Cercospora arachidicola		
	Solanum chacoense	Snakin1 (Sn1)	Potato	*Rhizoctonia solani*	30-60% increased survival rates	Almasia *et al.*, 2008
				Erwinia carotovora	46-88% lesion reduction	
	Hordeum vulgare	α-thionin	Tobacco	*Pseudomonas syringae* pv. *tabaci*	Significant reduction in necrotic lesion percentage	Carmona *et al.*, 1993
				Pseudomonas syringae pv. *syringae*		
	Stellaria media	SmAMP1 SmAMP2	Arabidopsis	*Bipolaris sorokiniana*	Increased seedling survival rate	Shukurov *et al.*, 2011
			Tobacco	*Thieviopsis basicola*		
Viruses	*UMV4 virus*	KP4	Maize	*Ustilago maydis*	Qualitatively significant reduction in disease symptoms	Allen *et al.*, 2011

Table 1. Overview of AMP expression in transgenic plants (Adapted from Rahnamaeian and Vilcinskas, 2011). *(Continued).*

Origin	Source	AMP	Host	Pathogens	Efficacy	Reference
Fungi	*Apergillus giganteus*	AFP	Rice	*Magnaporthe grisea*	Qualitatively significant reduction in disease symptoms	Moreno *et al.*, 2005
						Coca *et al.*, 2004
		Ag-scFv	Wheat	*Fusarium asiaticum*	Significant increase in grain weights	Li *et al.*, 2008
Synthetic	*Xenopus leavis' magainin 2*	Shiva-1	Tobacco	*Pseudomonas solanacearum*	Qualitatively significant reduction in disease symptoms	Jaynes *et al.*, 1993
			Potato	*Erwinia carotovora*		Yi *et al.*, 2004
			Pauwlonia tomentosa	*PWB Phytoplasma*		Du *et al.*, 2005
			Anthurium	*Xanthomonas axonopodis* pv. *dieffenbachiae*	Significant reduction in disease severity	Kuehnle *et al.*, 2004
		Myp30	Tobacco	*Peronospora tabacina*	16% reduction in lesion diameter	Li *et al.*, 2001
				Erwinia carotovora	40% increased survival rate	
	Magainin-like	ESF12	Poplar	*Septoria musiva*	77% reduction of necrotic area	Liang *et al.*, 2002
	Hyalophora cecropia's cecropin SB3	MB-39	Tobacco	*Pseudomonas syringae* pv. *tabaci*	Qualitatively significant; 10-fold reduction in *in planta* pathogen proliferation	Huang *et al.*, 1997
			Apple	*Erwinia amylovara*	3-fold increased resistance	Liu *et al.*, 2001
	Cecropin analogue	SB-37	Potato	*Erwinia carotovora*	Reduced severity of disease symptoms	Arce *et al.*, 1999
	Hyalophora cecropia's cecropin A - Xenopus leavis' melittin hybrids	MrsA1	Potato	*Fusarium solani*	Qualitatively significant increased resistance	Osusky *et al.*, 2000
				Phytophthora cactorum		
				Erwinia carotovora		
		D4E1	Tobacco	*Colletotrichum destructivum*	~35% reduction in anthracnose severity	Cary *et al.*, 2000
			Poplar	*Agrobacterium tumefaciens*	Reduced severity of disease symptoms	Mentag *et al.*, 2003
				Xanthomonas populi pv. *populi*		
			Cotton	*Fusarium verticillioides*	40% reduction in growth of pre-germinated conidia	Rajasekaran *et al.*, 2005
				Verticillium dahliae	40-75% reduction in growth of pre-germinated conidia	
				Thielaviopsis basicola	25% reduction in disease symptoms	
				Aspergillus flavus	50-75% growth reduction	
		MSI-99	Tobacco	*Sclerotinia sclerotiorum*	40-70% reduction in lesion diameter	Chakrabarti *et al.*, 2003
				Alternaria alternata	80% reduction in lesion diameter	
				Botrytis cinerea	40-70% reduction in lesion diameter	
				Colletotrichum destructivum	Qualitative reduction in disease symptoms	DeGray *et al.*, 2001
				Pseudomonsas syringae pv. *tabaci*		

Table 1. Overview of AMP expression in transgenic plants (Adapted from Rahnamaeian and Vilcinskas, 2011). *(Continued).*

Origin	Source	AMP	Host	Pathogens	Efficacy	Reference
Synthetic	*Hyalophora cecropia's cecropin A - Xenopus leavis' melittin hybrids*	MSI-99	Grapevine	*Uncinula necator*	~40% reduction in disease symptoms	Vidal *et al.*, 2006
				Agrobacterium vitis	Significant reduction in grown gall size	
			Banana	*Fusarium oxysporum* f. sp. *cubense*	Qualitatively significant reduction in disease symptoms	Chakrabarti *et al.*, 2003
				Mycospaerella musicola	40% reduction in lesion area	
			Tomato	*Pseudomonas syringae* pv. *tomato*	Significant reduction in disease severity	Alan *et al.*, 2004
		CEMA	Tobacco	*Fusarium solani*	Qualitatively significant reduction in disease symptoms	Yevtushenko *et al.*, 2005
	Phyllomedusa bicolor's dermaspetin B1	MsrA2	Potato	*Phytophthora erythroseptica*	91-94% reduction in infection area	Osusky *et al.*, 2005
				Phytophthora infestans	Qualitatively significant reduction in disease symptoms	
				Fusarium solani		
				Pythium paroecandrum		
				Pythium splendens		
				Rhizoctonia solani		
				Erwinia carotovora	50-86% reduction in bacterial growth	
			Tobacco	*bacteria, fungi, oomycetes*	Qualitatively significant reduction in disease symptoms	Yevtushenko and Misra, 2007
	Synthetic neurodisruptive peptides	ACHE-I-7,1	Potato	*Globodera pallida*	61% reduction in nematodes per root system	Liu *et al.*, 2005
	Bovine neutrophils' indolicidine	Rev4	Tobacco	*Peronospora tabacina*	Up to 34% increase in biomass yield[b]	Xing *et al.*, 2006
				Erwinia carotovora ssp. *carotovora*		
			Arabidopsis	*Pseudomonas syringae* pv. *maculicola*	Significant reduction in disease index	
	Bovine indolicidine/ Xenopus leavis' magainin 2	Rev4 and Myp-30 coexpression	Arabidopsis	*Pseudomonas syringae* pv. *maculicola*	Significant reduction in disease index	
				Peronospora parasitica		
	Variants of indolicidin	10R, 11R	Tobacco	*Erwinia carotovora* ssp. *carotovora*	Qualitatively significant reduction in disease symptoms	Bhargava *et al.*, 2007b
				Botrytis cinerea		
				Verticilium sp.		
				TMV		
	Variant of polyphemusin from Limulus polyphemus	PV5	Tobacco	*Erwinia carotovora*	Qualitatively significant reduction in disease symptoms	Bhargava *et al.*, 2007a
				Botrytis cinerea		
				Verticilium sp.		
				Fusarium oxysporum		
				TMV		

[a] The disease index represents the mean disease severity (1= light to 5=severe).

[b] Field trials

CONCLUDING REMARKS AND PERSPECTIVES

AMPs are an important evolutionary conserved part of innate immunity found throughout all kingdoms, including plants. These highly diverse peptides are characterized by their small size and amphipathic structure by clustered cationic and hydrophobic amino acid residues, that is prerequisite for their antimicrobial activity.

Plant diseases lead to major annual crop losses around the world. To meet the world's future needs in food and feed production, the development of novel and more sustainable agricultural practices for crop protection are necessary. The application of AMPs is a promising strategy for plant disease control. A thorough knowledge of the biochemical and structural properties of natural AMPs together with the mode of action is prerequisite for their application and determines the durability and efficacy. Several aspects need to be examined in detail, such as the activity under physiological conditions, selectivity and synergistic effects. Most membrane permeabilization studies were carried out with artificial phospholipid membranes and may not represent the actual situation. Therefore, the development of novel assays using membranes of different pathogens is crucial. In addition, AMPs acting on intracellular targets are promising candidates for future research. High-throughput identification of novel synthetic AMPs is currently accomplished by using synthetic combinatorial peptide libraries and allows – together with the knowledge-based design of peptide analogs – the development of improved peptides with enhanced stability, selectivity and activity and together with reduced nonspecific toxicity. Currently, the research on mammalian AMPs greatly extends plant AMP research. Hence, future research using a systems biology approach will further identify novel AMPs that, in turn, will give more insights in the mode of actions and the roles of AMPs in disease resistance. Furthermore, other biological roles of AMPs are still poorly understood, including their role in abiotic stress tolerance.

REFERENCES

Aerts, A., Thevissen, K., Bresseleers, S., Sels, J., Wouters, P., Cammue, B.P.A. and François, I. (2007) *Arabidopsis thaliana* plants expressing human β-defensin-2 are more resistant to fungal attack: functional homology between plant and human defensins. *Plant Cell Rep.*, **26**, 1391-1398.

Alan, A.R., Blowers, A. and Earle, E.D. (2004) Expression of a magainin-type antimicrobial peptide gene (MSI-99) in tomato enhances resistance to bacterial speck disease. *Plant Cell Rep.*, **22**, 388.

Allefs, S., Dejong, E.R., Florack, D.E.A., Hoogendoorn, C. and Stiekema, W.J. (1996) *Erwinia* soft rot resistance of potato cultivars expressing antimicrobial peptide tachyplesin I. *Mol. Breed.*, **2**, 97-105.

Allen, A., Islamovic, E., Kaur, J., Gold, S., Shah, D. and Smith, T.J. (2011) Transgenic maize plants expressing the Totivirus antifungal protein, KP4, are highly resistant to corn smut. *Plant Biotech. J.*, **8**, 857-864.

Almasia, N.I., Bazzini, A.A., Hopp, H.E. and Vazquez-Rovere, C. (2008) Overexpression of *snakin-1* gene enhances resistance to *Rhizoctonia solani* and *Erwinia carotovora* in transgenic potato plants. *Mol. Plant Pathol.*, **9**, 329-338.

Almeida, M.S., Cabral, K.M.S., Kurtenbach, E., Almeida, F.C.L. and Valente, A.P. (2002) Solution structure of *Pisum sativum* defensin 1 by high resolution NMR: plant defensins, identical backbone with different mechanisms of action. *J. Mol. Biol.*, **315**, 749-757.

Alvarez, M.E., Pennell, R.I., Meijer, P.-J., Ishikawa, A., Dixon, R.A. and Lamb, C. (1998) Reactive oxygen intermediates mediate a systemic signal network in the establishment of plant immunity. *Cell*, **92**, 773-784.

Arce, P., Moreno, M., Gutierrez, M., Gebauer, M. and Dell'Orto, P. (1999) Enhanced resistance to bacterial infection by *Erwinia carotovora* subsp *atroseptica* in transgenic potato plants expressing the *attacin* or the *cecropin SB-37* genes. *Am. J. Potato Res.*, **76**, 169-177.

Archer, B., Audley, B.G., Sweeney, G.P. and Tan, C.H. (1969) Studies in composition of latex serum and 'bottom fraction' particles. *J. Rubber Res. Inst. Malays*, **21**, 560-569.

Arenas, A., Marshall, S., Espinoza, E., Ramírez, I. and Peña-Cortés, H. (2006) Protective effect of an antimicrobial peptide from *Mytilus edulis chilensis* expressed in *Nicotiana tabacum* L. *Electron. J. Biotechnol.*, **9**, DOI: 10.2225/vol2229-issue2222-fulltext-2222.

Armengaud, P., Breitling, R. and Amtmann, A. (2004) The potassium-dependent transcriptome of *Arabidopsis* reveals a prominent role of jasmonic acid in nutrient signaling. *Plant Physiol.*, **136**, 2556-2576.

Arondel, V., Vergnolle, C., Cantrel, C. and Kader, J.C. (2000) Lipid transfer proteins are encoded by a small multigene family in *Arabidopsis thaliana*. *Plant Sci.*, **157**, 1-12.

Aubert, D., Chevillard, M., Dorne, A.-M., Arlaud, G. and Herzog, M. (1998) Expression patterns of *GASA* genes in *Arabidopsis thaliana*: the *GASA4* gene is up-regulated by gibberellins in meristematic regions. *Plant Mol. Biol.*, **36**, 871-883.

Avrutina, O., Schmoldt, H.-U., Gabrijelcic-Geiger, D., Le Nguyen, D., Sommerhoff, C.P., Diederichsen, U. and Kolmar, H. (2005) Trypsin inhibition by macrocyclic and open-chain variants of the squash inhibitor MCoTI-II. *Biol. Chem.*, **386**, 1301-1306.

Banzet, N., Latorse, M.-P., Bulet, P., François, E., Derpierre, C. and Dubald, M. (2002) Expression of insect cystein-rich antifungal peptides in transgenic tobacco enhances resistance to a fungal disease. *Plant Sci.*, **162**, 995-1006.

Bechinger, B. and Lohner, K. (2006) Detergent-like actions of linear amphipathic cationic antimicrobial peptides. *Biochim. Biophys. Acta*, **1758**, 1529-1539.

Ben-Nissan, G., Lee, J.-Y., Borohov, A. and Weiss, D. (2004) GIP, a petunia hybrida GA-induced cysteine-rich protein: a possible role in shoot elongation and transition to flowering. *Plant J.*, **37**, 229-238.

Ben-Nissan, G. and Weiss, D. (1996) The petunia homologue of tomato *gast1*: transcript accumulation coincides with gibberellin-induced corolla cell elongation. *Plant Mol. Biol.*, **32**, 1067-1074.

Berrocal-Lobo, M., Segura, A., Moreno, M., López, G., García-Olmedo, F. and Molina, A. (2002) Snakin-2, an antimicrobial peptide from potato whose gene is locally induced by wounding and responds to pathogen infection. *Plant Physiol.*, **128**, 951-961.

Bhargava, A., Osusky, M., Forward, B.S., Hancock, R.E.W., Kay, W.W. and Misra, S. (2007a) Expression of a polyphemusin variant in transgenic tobacco confers resistance against plant pathogenic bacteria, fungi and a virus. *Plant Cell Tiss. Organ Cult.*, **88**, 301-312.

Bhargava, A., Osusky, M., Hancock, R.E.W., Forward, B.S., Kay, W.W. and Misra, S. (2007b) Antiviral indolicidin variant peptides: evaluation for broad-spectrum disease resistance in transgenic *Nicotiana tabacum*. *Plant Sci.*, **172**, 515-523.

Bloch, C.J., Patel, S.U., Baud, F., Zvelebil, M.J.J.M., Carr, M.D., Sadler, P.J. and Thornton, J.M. (1998) ^{1}H NMR structure of an antifungal γ-thionin protein SIα1: similarity to scorpion toxins. *Proteins: Structure, Function, and Bioinformatics*, **32**, 334-349.

Bloch, C.J. and Richardson, M. (1991) A new family of small (5 kDa) protein inhibitors of insect α-amylases from seeds of sorghum (*Sorghum bicolar* (L) Moench) have sequence homologies with wheat γ-purothionins. *FEBS Lett.*, **279**, 101-104.

Bohlmann, H. and Apel, K. (1991) Thionins. *Annu. Rev. Plant Physiol. Plant Mol. Biol.*, **42**, 227-240.

Bohlmann, H. and Broekaert, W. (1994) The role of thionins in plant protection. *Crit. Rev. Plant Sci.*, **13**, 1-16.

Bohlmann, H., Clausen, S., Behnke, S., Giese, H., Hiller, C., Reimann-Philipp, U., Schrader, G., Barkholt, V. and Apel, K. (1988) Leaf-specific thionins of barley - a novel class of cell wall proteins toxic to plant-pathogenic fungi and possibly involved in the defence mechanism of plants. *EMBO J.*, **7**, 1559-1565.

Boman, H.G. (2003) Antibacterial peptides: basic facts and emerging concepts. *J. Intern. Med.*, **254**, 197-215.

Bonfante, P. and Genre, A. (2008) Plants and arbuscular mycorrhizal fungi: an evolutionary-developmental perspective. *Trends Plant Sci.*, **13**, 492-498.

Brisson, L.F., Tenhaken, R. and Lamb, C. (1994) Function of oxidative cross-linking of cell wall structural proteins in plant disease resistance. *Plant Cell*, **6**, 1703-1712.

Broekaert, W., Mariën, W., Terras, F., De Bolle, M., Proost, P., Van Damme, J., Dillen, L., Claeys, M., Rees, S. and Vanderleyden, J. (1992) Antimicrobial peptides from *Amaranthus caudatus* seeds with sequence homology to the cysteine/glycine-rich domain of chitin-binding proteins. *Biochemistry*, **31**, 4308-4314.

Broekaert, W.F., Cammue, B.P.A., De Bolle, M.F., Thevissen, K., De Samblanx, G.W. and Osborn, R.W. (1997) Antimicrobial peptides from plants. *Crit. Rev. Plant Sci.*, **16**, 297-323.

Broekaert, W.F., Terras, F.R. and Cammue, B.P. (2000) Induced and preformed antimicrobial proteins. *Slusarenko A, Fraser RSS, van Loon LC eds - Mechanisms of resistance to plant diseases - Kluwer Academic Dortecht*, 371-477.

Broekaert, W.F., Terras, F.R.G., Cammue, B.P.A. and Osborn, R.W. (1995) Plant defensins: novel antimicrobial peptides as components of the host defense system. *Plant Physiol.*, **108**, 1353-1358.

Brogden, K.A. (2005) Antimicrobial peptides: pore formers or metabolic inhibitors in bacteria? *Nat. Rev. Microbiol.*, **3**, 238-250.

Brogue, K., Chet, I., Holliday, M., Cressman, R., Biddle, P., Knowlton, S., Mauvais, C.J. and Broglie, R. (1991) Transgenic plants with enhanced resistance to the fungal pathogen *Rhizoctonia solani*. *Science*, **254**, 1194-1197.

Bruix, M., Jiménez, M., Santoro, J., González, C., Colilla, F., Méndez, E. and Rico, M. (1993) Solution structure of γ ^{1}H and γ ^{1}P thionins from barley and wheat endosperm determined by ^{1}H-NMR: a structural motif common to toxic arthropod proteins. *Biochemistry*, **32**, 715-724.

Buhot, N., Douliez, J.P., Jacquemard, A., Marion, D., Tran, V., Maume, B.F., Milat, M.L., Ponchet, M., Mikès, V., Kader, J.C. and Blein, J.P. (2001) A lipid transfer protein binds to a receptor involved in the control of plant defence responses. *FEBS Lett.*, **509**, 27-30.

Bulet, P., Stöcklin, R. and Menin, L. (2004) Anti-microbial peptides: from invertebrates to vertebrates. *Immunol. Rev.*, **198**, 169-184.

Camarero, J.A. (2011) Legume cyclotides shed light on the genetic origin of knotted circular proteins. *Proc. Natl. Acad. Sci. USA*, **108**, 10025-10026.

Cammue, B.P.A., De Bolle, M.F., Terras, F.R., Proost, P., Van Damme, J., Rees, S.B., Vanderleyden, J. and Broekaert, W.F. (1992) Isolation and characterization of a novel class of plant antimicrobial peptides form *Mirabilis jalapa* L. seeds. *J. Biol. Chem.*, **267**, 2228-2233.

Cammue, B.P.A., Thevissen, K., Hendriks, M., Eggermont, K., Goderis, I.J., Proost, P., Van Damme, J., Osborn, R.W., Guerbette, F., Kader, J.C. and Broekaert, W.F. (1995) A potent antimicrobial protein from onion seeds showing sequence homology to plant lipid transfer proteins. *Plant Physiol.*, **109**, 445-455.

Campo, S., Manrique, S., García-Martínez, J. and San Segundo, B. (2008) Production of cecropin A in transgenic rice plants has an impact on host gene expression. *Plant Biotech. J.*, **6**, 585-608.

Campos, F.A.P. and Richardson, M. (1984) The complete amino cid sequence of the bifunctional α-amylase/trypsin inhibitor from seeds of ragi (Indian finger millet; *Eleusine coracana* Goertn.). *FEBS Lett.*, **152**, 300-304.

Caño-Delgado, A., Penfield, S., Smith, C., Catley, M. and Bevan, M. (2003) Reduced cellulose synthesis invokes lignification and defense responses in *Arabidopsis thaliana*. *Plant J.*, **34**, 351-362.

Carmona, M.J., Hernández-Lucas, C., San Martin, C., González, P. and García-Olmedo, F. (1993) Subcellular localization of type I thionins in the endosperms of wheat and barley. *Protoplasma*, **173**, 1-7.

Carrasco, L., Vázquez, D., Hernández-Lucas, C., Carbonero, P. and García-Olmedo, F. (1981) Thionins: plant peptides that modify membrane permeability in cultured mammalian cells. *Eur. J. Biochem.*, **116**, 185-189.

Carvalho, A.d.O. and Gomes, V.M. (2009) Plant defensins - Prospects for the biological functions and biotechnological properties. *Peptides*, **30**, 1007-1020.

Cary, J.W., Rajasekaran, K., Jaynes, J.M. and Cleveland, T.E. (2000) Transgenic expression of a gene encoding a synthetic antimicrobial peptide results in inhibition of fungal growth *in vitro* and *in planta*. *Plant Sci.*, **154**, 171-181.

Casteels, P., Ampe, C., Jacobs, F., Vaeck, M. and Tempst, P. (1989) Apidaecins - antibacterial peptides from honeybees. *EMBO J.*, **8**, 2387.

Chagolla-Lopez, A., Blanco-Labra, A., Patthy, A., Sánchez, R. and Pongor, S. (1994) A novel α-amylase inhibitor from amaranth (*Amaranthus hypocondriacus*) seeds. *J. Biol. Chem.*, **269**, 23675-23680.

Chakrabarti, A., Ganapathi, T.R., Mukherjee, P.K. and Bapat, V.A. (2003) MSI-99, a magainin analogue, imparts enhanced disease resistance in transgenic tobacco and banana. *Planta*, **216**, 587-596.

Chalutz, E. and Wilson, C.L. (1990) Postharvest biocontrol of green and blue mold and sour rot of citrus fruit by *Debaryomyces hansenii*. *Plant Dis.*, **74**, 134-137.

Chiche, L., Heitz, A., Gelly, J.C., Gracy, J., Chau, P.T., Ha, P.T., Hernandez, J.F. and Le-Nguyen, D. (2004) Squash inhibitors: from structural motifs to macrocyclic knottins. *Curr. Protein Pept. Sci.*, **5**, 341-349.

Christensen, B., Fink, J., Merrifield, R.B. and Mauzerall, D. (1988) Channel-forming properties of cecropins and related model compounds incorporated into planar lipid membranes. *Proc. Natl. Acad. Sci. USA*, **85**, 5072-5076.

Coca, M., Bortolotti, C., Rufat, M., Peñas, G., Eritja, R., Tharreau, D., del Pozo, A., Messeguer, J. and San Segundo, B. (2004) Transgenic rice plants expressing the antifungal AFP protein from *Aspergillus giganteus* show enhanced resistance to the rice blast fungus *Magnaporthe grisea*. *Plant Mol. Biol.*, **54**, 245-259.

Coca, M., Peñas, G., Gómez, J., Campo, S. and Bortolotti, C. (2006) Enhanced resistance to the rice blast fungus *Magnaporthe grisea* conferred by expression of a cecropin A gene in transgenic rice. *Planta*, **223**, 392-406.

Colgrave, M.L. and Craik, D.J. (2004) Thermal, chemical, and enzymatic stability of the cyclotide Kalata B1: the importance of the cyclic cystine knot. *Biochemistry*, **43**, 5965-5975.

Colilla, F.J., Rocher, A. and Mendez, E. (1990) γ-purothionins: amino acid sequence of two polypeptides of a new family of thionins from wheat endosperm. *FEBS Lett.*, **270**, 191-194.

Craik, D.J. and Conibear, A.C. (2011) The chemistry of cyclotides. *J. Organic Chem.*, **76**, 4805-4817.

Daly, N.L., Rosengren, K.J. and Craik, D.J. (2009) Discovery, structure and biological activities of cyclotides. *Adv. Drug Delivery. Rev.*, **61**, 918-930.

Darvill, A.G. and Albersheim, P. (1984) Phytoalexins and their elicitors - A defense against microbial infection in plants. *Annu. Rev. Plant. Physiol.*, **35**, 243-275.

de la Fuente, J.I., Amaya, I., Castillejo, C., Sánchez-Sevilla, J.F., Quesada, M.A., Botella, M.A. and Valpuesta, V. (2006) The strawberry gene *FaGAST* affects plant growth through inhibition of cell elongation. *J. Exp. Bot.*, **57**, 2401-2411.

DeGray, G., Rajasekaran, K., Smith, F., Sanford, J. and Daniell, H. (2001) Expression of an antimicrobial peptide via the chloroplast genome to control phytopathogenic bacteria and fungi. *Plant Physiol.*, **127**, 852-862.

Diaz, I., Carmona, M.J. and García-Olmedo, F. (1992) Effects of thionins on β-glucuronidase *in vitro* and in plant protoplasts. *FEBS Lett.*, **296**, 279-282.

Distefano, G., La Malfa, S., Vitale, A., Lorito, M., Deng, Z. and Gentile, A. (2008) Defence-related gene expression in transgenic lemon plants producing an antimicrobial *Trichoderma harzianum* endochitinase during fungal infection. *Transgenic Res.*, **17**, 873-879.

Do, H.M., Lee, S.C., Jung, H.W., Sohn, K.H. and Hwang, B.K. (2004) Differential expression and *in situ* localization of a pepper defensin (*CaDEF1*) gene in response to pathogen infection, abiotic elicitors and environmental stresses in *Capsicum annuum*. *Plant Sci.*, **166**, 1297-1305.

Droby, S., Chalutz, E. and Wilson, C.L. (1991) Antagonistic microorganisms as biological control agents of postharvest diseases of fruits and vegetables. *Postharvest News Inf.*, **2**, 169-173.

Du, T., Wang, Y., Hu, Q.X., Chen, J. and Liu, S. (2005) Transgenic *Paulownia* expressing *shiva-1* gene has increased resistance to Paulownia witches' broom disease. *J. Integr. Plant Biol.*, **47**, 1500-1506.

Duclohier, H., Molle, G. and Spach, G. (1989) Antimicrobial peptide magainin I from *Xenopus* skin forms anion-permeable channels in planar lipid bilayers. *Biophys. J.*, **56**, 1017-1021.

Durrant, W.E. and Dong, X. (2004) Systemic acquired resistance. *Annu. Rev. Phytopathol.*, **42**, 185-209.

Duvick, J.P., Rood, T., Rao, A.G. and Marshak, D.R. (1992) Purification and characterization of a novel antimicrobial peptide from maize (*Zea mays* L.) kernels. *J. Biol. Chem.*, **267**, 18814-18820.

Ehrenstein, G. and Lecar, H. (1977) Electrically gated ionic channels in lipid bilayers. *Q. Rev. Biophys.*, **10**, 1-34.

Elfstrand, M., Fossdal, C.G., Swedjemark, G., Clapham, D., Olsson, O., Sitbon, F., Sharma, P., Lönneborg, A. and von Arnold, S. (2001) Identification of candidate genes for use in molecular breeding - A case study with the Norway spruce defensin-like gene, *spi1*. *Silvae Genet.*, **50**, 75-81.

Epple, P., Apel, K. and Bohlmann, H. (1997) Overexpression of an endogenous thionin enhances resistance of *Arabidopsis* against *Fusarium oxysporum*. *Plant Cell*, **9**, 509-520.

Fant, F., Vranken, W., Broekaert, W. and Borremans, F. (1998) Determination of the three-dimensional solution structure of *Raphanus sativus* Antifungal Protein 1 by ^{1}H NMR. *J. Mol. Biol.*, **279**, 257-270.

Fant, F., Vranken, W.F. and Borremans, F.A.M. (1999) The three-dimensional solution structure of *Aesculus hippocastanum* antimicrobial protein 1 determined by ^{1}H nuclear magnetic resonance. *Proteins: Structure, Function, and Bioinformatics*, **37**, 388-403.

Fernandez De Caleya, R., Gonzalez-Pascual, B., García-Olmedo, F. and Carbonero, P. (1972) Susceptibility of phytopathogenic bacteria to wheat purothionins *in vitro*. *Appl. Microbiol.*, **23**, 998-1000.

François, I.E.J.A., De Bolle, M.F.C., Dwyer, G., Goderis, I.J.W.M., Woutors, P.F.J., Verhaert, P.D., Proost, P., Schaaper, W.M.M., Cammue, B.P.A. and Broekaert, W.F. (2002) Transgenic expression in *Arabidopsis* of a polyprotein construct leading to production of two different antimicrobial proteins. *Plant Physiol.*, **128**, 1346-1358.

François, I.E.J.A., Van Hemelrijck, W., Aerts, A.M., Wouters, P.F.J., Proost, P., Broekaert, W.F. and Cammue, B.P.A. (2004) Processing in *Arabidopsis thaliana* of a heterologous polyprotein resulting in differential targeting of the individual plant defensins. *Plant Sci.*, **166**, 113-121.

Furukawa, T., Sakaguchi, N. and Shimada, H. (2006) Two *OsGASR* genes, rice *GAST* homologue genes that are abundant in proliferating tissues, show different expression patterns in developing panicles. *Genes Genet. Syst.*, **81**, 171-180.

Ganz, T. and Lehrer, R.I. (1998) Antimicrobial peptides of vertebrates. *Curr. Opin. Immunol.*, **10**, 41-44.

Gao, A.G., Hakimi, S.M., Mittanck, C.A., Wu, Y. and Woerner, B.M. (2000) Fungal pathogen protection in potato by expression of a plant defensin peptide. *Nat. Biotechnol.*, **18**, 1307-1310.

García-Olmedo, F., Molina, A., Alamillo, J.M. and Rodríguez-Palenzuela, P. (1998) Plant defense peptides. *Biopolymers*, **47**, 479-491.

Garcia, A.E. and Camarero, J.A. (2010) Biological activities of natural and engineered cyclotides, a novel molecular scaffold for peptide-based therapeutics. *Curr. Mol. Pharmacol.*, **3**, 153-163.

Gifford, J., Hunter, H. and Vogel, H. (2005) Lactoferricin. *Cell. Mol. Life Sci.*, **62**, 2588-2598.

Gillon, A.D., Saska, I., Jennings, C.V., Guarino, R.F., Craik, D.J. and Anderson, M.A. (2008) Biosynthesis of circular proteins in plants. *Plant J.*, **53**, 505-515.

Girault, T., François, J., Rogniaux, H., Pascal, S., Delrot, S., Coutos-Thévenot, P. and Gomès, E. (2008) Exogenous application of a lipid transfer protein-jasmonic acid complex induces protection of grapevine towards infection by *Botrytis cinerea*. *Plant Physiol. Biochem.*, **46**, 140-149.

Giuliani, A., Pirri, G. and Nicoletto, S. (2007) Antimicrobial peptides: an overview of a promising class of therapeutics. *Cent. Eur. J. Biol.*, **2**, 1-33.

Gracy, J., Le-Nguyen, D., Gelly, J.-C., Kaas, Q., Heitz, A. and Chiche, L. (2008) KNOTTIN: the knottin or inhibitor cystine knot scaffold in 2007. *Nucleic Acids Res.*, **36**, 314-319.

Gran, L., Sandberg, F. and Sletten, K. (2000) *Oldenlandia affinis* (R&S) DC: a plant containing uteroactive peptides used in African traditional medicine. *J. Ethnopharmacol.*, **70**, 197-203.

Greenberg, J.T. and Yao, N. (2004) The role and regulation of programmed cell death in plant–pathogen interactions. *Cell. Microbiol.*, **6**, 201-211.

Gu, Q., Kawata, E., Morse, M., Wu, H. and Cheung, A. (1992) A flower-specific cDNA encoding a novel thionin in tobacco. *Mol. Gen. Genet.*, **234**, 89-96.

Guo, G., Wang, H.X. and Ng, T.B. (2009) Pomegranin, an antifungal peptide from pomegranate peels *Protein Pept. Lett.*, **16**, 82-85.

Hammami, R., Ben Hamida, J., Vergoten, G. and Fliss, I. (2009) PhytAMP: a database dedicated to antimicrobial plant peptides. *Nucleic Acids Res.*, **37**, 963-968.

Henriques, S.T., Melo, M.N. and Castanho, M.A.R.B. (2006) Cell-penetrating peptides and antimicrobial peptides: how different are they? *Biochem. J.*, **399**, 1-7.

Hon, W.C., Griffith, M., Mlynarz, A., Kwok, Y.C. and Yang, D.S.C. (1995) Antifreeze proteins in winter rye are similar to pathogenesis-related proteins. *Plant Physiol.*, **109**, 879-889.

Huang, G.-J., Lai, H.-C., Chang, Y.-S., Sheu, M.-J., Lu, T.-L., Huang, S.-S. and Lin, Y.-H. (2008) Antimicrobial, dehydroascorbate reductase, and monodehydroascorbate reductase activities of defensin from sweet potato [*Ipomoea batatas* (L.) Lam. 'Tainong 57'] storage roots. *J. Agric. Food Chem.*, **56**, 2989-2995.

Huang, Y., Nordeen, R.O., Di, M., Owens, L.D. and McBeath, J.H. (1997) Expression of an engineered cecropin gene cassette in transgenic tobacco plants confers resistance to *Pseudomonas syringae* pv. *tabaci*. *Phytopathology*, **87**, 494.

Imamura, T., Yasuda, M., Kusano, H., Nakashita, H., Ohno, Y., Kamakura, T., Taguchi, S. and Shimada, H. (2010) Acquired resistance to the rice blast in transgenic rice accumulating the antimicrobial peptide thanatin. *Transgenic Res.*, **19**, 415-424.

Ishitani, M., Xiong, L., Lee, H., Stevenson, B. and Zhu, J.-K. (1998) *HOS1*, a genetic locus involved in cold-responsive gene expression in *Arabidopsis*. *Plant Cell*, **10**, 1151-1162.

Iwai, T., Kaku, H., Honkura, R., Nakamura, S., Ochiai, H., Sasaki, T. and Ohashi, Y. (2002) Enhanced resistance to seed-transmitted bacterial diseases in transgenic rice plants overproducing an oat cell-wall-bound thionin. *Mol. Plant-Microbe Interact.*, **15**, 515-521.

Jabs, T., Tschöpe, M., Colling, C., Hahlbrock, K. and Scheel, D. (1997) Elicitor-stimulated ion fluxes and O_2 from the oxidative burst are essential components in triggering defense gene activation and phytoalexin synthesis in parsley. *Proc. Natl. Acad. Sci. USA*, **94**, 4800-4805.

Jagadish, K. and Camarero, J.A. (2010) Cyclotides, a promising molecular scaffold for peptide-based therapeutics. *Biopolymers*, **94**, 611-616.

Janisiewicz, W.J. (1991) Control of storage decay of apples with *Sporobolomyces roseus*. *Plant Dis.*, **78**, 446-470.

Jaynes, J.M., Nagpala, P., Destefanobeltran, L., Huang, J.H. and Kim, J.H. (1993) Expression of a cecropin-B lytic peptide analog in transgenic tobacco confers enhanced resistance to bacterial wilt caused by *Pseudomonas solanacearum*. *Plant Sci.*, **89**, 43-53.

Jaynes, J.M., Xanthopoulos, K.G., Destefanobeltran, L. and Dodds, J.H. (1987) Increasing bacterial disease resistance in plants utilizing antibacterial genes from insects. *BioEssays*, **6**, 263-270.

Jeffries, P. and Jeger, M.J. (1990) The biological control of postharvest diseases of fruit. *Postharvest News Inf.*, **77**, 404.

Johnson, T.C., Wada, K., Buchanan, B.B. and Holmgren, A. (1987) Reduction of purothionin by the wheat seed thioredoxin system. *Plant Physiol.*, **85**, 446-451.

Joliot, A. and Prochiantz, A. (2004) Transduction peptides: from technology to physiology. *Nat. Cell Biol.*, **6**, 189-196.

Jones, J.D.G. and Dangl, J.L. (2006) The plant immune system. *Nature*, **444**, 323-329.

Jones, R.W. and Prusky, D. (2002) Expression of an antifungal peptide in *Saccharomyces*: a new approach for biological control of the postharvest disease caused by *Colletotrichum coccodes*. *Phytopathology*, **92**, 33-37.

Kader, J.-C. (1996) Lipid-transfer proteins in plants. *Annu. Rev. Plant Physiol. Plant Mol. Biol.*, **47**, 627-654.

Kanzaki, H.K., Nirasawa, S.N., Saitoh, H.S., Ito, M.I., Nishihara, M.N., Terauchi, R.T. and Nakamura, I.N. (2002) Overexpression of the wasabi defensin gene confers enhanced resistance to blast fungus *Magnaporthe grisea* in transgenic rice. *Theor. Appl. Genet.*, **105**, 809-814.

Kawano, T. (2003) Roles of the reactive oxygen species-generating peroxidase reactions in plant defense and growth induction. *Plant Cell Rep.*, **21**, 829-837.

Ko, K., Norelli, J.L., Reynoird, J.-P., Boresjza-Wysocka, E., Brown, S.K. and Aldwinckle, H.S. (2000) Effect of untranslated leader sequence of AMV RNA 4 and signal peptide of pathogenesis-related protein 1b on attacin gene expression, and resistance to fire blight in transgenic apple. *Biotechnol. Lett.*, **22**, 373-381.

Koike, M., Okamoto, T., Tsuda, S. and Imai, R. (2002) A novel plant defensin-like gene of winter wheat is specifically induced during cold acclimation. *Biochem. Biophys. Res. Commun.*, **298**.

Koo, J., Lee, S., Chun, H., Cheong, Y., Choi, J., Kawabata, S., Miyagi, M., Tsunasawa, S., Ha, K., Bae, D., Han, C., Lee, B. and Cho, M. (1998) Two hevein homologs isolated from the seed of *Pharbitis nil* L. exhibit potent antifungal activity. *Biochim. Biophys. Acta*, **1382**, 80-90.

Koo, J.C., Chun, H.J., Park, H.C., Kim, M.C., Koo, Y.D., Koo, S.C., Ok, H.M., Park, S.J., Lee, S.-H., Yun, D.-J., Lim, C.O., Bahk, J.D., Lee, S.Y. and Cho, M.J. (2002) Over-expression of a seed specific hevein-like antimicrobial peptide from *Pharbitis nil* enhances resistance to a fungal pathogen in transgenic tobacco plants. *Plant Mol. Biol.*, **50**, 441-452.

Kotilainen, M., Helariutta, Y., Mehto, M., Pöllänen, E., Albert, V.A., Elomaa, P. and Teeri, T.H. (1999) GEG participates in the regulation of cell and organ shape during corolla and carpel development in *Gerbera hybrida*. *Plant Cell*, **11**, 1093-1104.

Kragh, K., Nielsen, J., Nielsen, K., Dreboldt, S. and Mikkelsen, J. (1995) Characterization and localization of new antifungal cysteine-rich proteins from *Beta vulgaris*. *Mol. Plant Microbe Interact.*, **8**, 424-434.

Kristensen, A.K., Brunstedt, J., Nielsen, K.K., Roepstorff, P. and Mikkelsen, J.D. (2000) Characterization of a new antifungal non-specific lipid transfer protein (nsLTP) from sugar beet leaves. *Plant Sci.*, **155**, 31-40.

Kuehnle, A.R., Fujii, R., Chen, F.C., Alvarez, A., Sugii, N., Fukui, R. and Aragon, S.L. (2004) Peptide biocides for engineering bacterial blight tolerance and susceptibility in cut flower anthurium. *Hortscience*, **39**, 1327-1331.

Kunkel, B.N. and Brooks, D.M. (2002) Cross talk between signaling pathways in pathogen defense. *Curr. Opin. Plant Biol.*, **5**, 325-331.

Kushmerick, C., de Souza Castro, M., Santos Cruz, J., Bloch, C. and Beirão, P.S.L. (1998) Functional and structural features of γ-zeathionins, a new class of sodium channel blockers. *FEBS Lett.*, **440**, 302-306.

Lam, E., Kato, N. and Lawton, M. (2001) Programmed cell death, mitochondria and the plant hypersensitive response. *Nature*, **411**, 848-853.

Langen, G., Imani, J., Altincicek, B., Kieseritzky, G., Kogel, K.-H. and Vilcinskas, A. (2006) Transgenic expression of gallerimycin, a novel antifungal insect defensin from the greater wax moth *Galleria mellonella*, confers resistance to pathogenic fungi in tobacco. *Biol. Chem.*, **387**, 549-557.

Lay, F.T. and Anderson, M.A. (2005) Defensins - Components of the innate immune system in plants *Curr. Protein Pept. Sci.*, **17**, 85-101.

Lay, F.T., Brugliera, F. and Anderson, M.A. (2003) Isolation and properties of floral defensins from ornamental tobacco and petunia. *Plant Physiol.*, **131**, 1283-1293.

Lee, S. and Hwang, B. (2009) Functional roles of the pepper antimicrobial protein gene, *CaAMP1* in abscisic acid signaling, and salt and drought tolerance in *Arabidopsis*. *Planta*, **229**, 383-391.

Lee, T.J., Coyne, D.P., Clemente, T.E. and Mitra, A. (2002) Partial resistance to bacterial wilt in transgenic tomato plants expressing antibacterial lactoferrin gene. *J. Am. Soc. Hortic. Sci.*, **127**, 158.

Li, H.-P., Zhang, J.-B., Shi, R.-P., Huang, T., Fischer, R. and Liao, Y.-C. (2008) Engineering *Fusarium* head blight resistance in wheat by expression of a fusion protein containing a *Fusarium*-specific antibody and an antifungal peptide. *Mol. Plant Microbe Interact.*, **21**, 1242-1248.

Li, Q., Lawrence, C.B., Xing, H.-Y., Babbitt, R.A., Bass, W.T., Maiti, I.B. and Everett, N.P. (2001) Enhanced disease resistance conferred by expression of an antimicrobial magainin analog in transgenic tobacco. *Planta*, **212**, 635-639.

Liang, H.Y., Catranis, C.M., Maynard, C.A. and Powell, W.A. (2002) Enhanced resistance to the poplar fungal pathogen, *Septoria musiva*, in hybrid poplar clones transformed with genes encoding antimicrobial peptides. *Biotechnol. Lett.*, **24**, 383-389.

Lin, P. and Ng, T.B. (2009) Brassiparin, an antifungal peptide from *Brassica parachinensis* seeds. *J. Appl. Microbiol.*, **106**, 554-563.

Lipkin, A., Anisimova, V., Nikonorova, A., Babakov, A., Krause, E., Bienert, M., Grishin, E. and Egorov, T. (2005) An antimicrobial peptide Ar-AMP from amaranth (*Amaranthus retroflexus* L.) seeds. *Phytochemistry*, **66**, 2426-2431.

Liu, B., Hibbard, J.K., Urwin, P.E. and Atkinson, H.J. (2005) The production of synthetic chemo-disruptive peptides *in planta* disrupts the establishment of cyst nematodes. *Plant Biotech. J.*, **3**, 487-496.

Liu, Q., Ingersoll, J., Owens, L., Salih, S., Meng, R. and Hammerschlag, F. (2001) Response of transgenic Royal Gala apple (*Malus* x *domestica* Borkh.) shoots carrying a modified cecropin *MB39* gene, to *Erwinia amylovora*. *Plant Cell Rep.*, **20**, 306-312.

Liu, X., Wang, J., Gou, P., Mao, C., Zhu, Z.R. and Li, H. (2007a) *In vitro* inhibition of postharvest pathogens of fruit and control of gray mold of strawberry and green mold of citrus by aureobasidin A. *Int. J. Food Microbiol.*, **119**, 223-229.

Liu, Z., Zeng, M., Dong, S., Xu, J., Song, H. and Zhao, Y. (2007b) Effect of an antifungal peptide from oyster enzymatic hydrolysates for control of gray mold (*Botrytis cinerea*) on harvested strawberries. *Postharvest Biol. Technol.*, **46**, 95.

López-García, B., González-Candelas, L., Pérez-Payá, E. and Marcos, J.F. (2000) Identification and characterization of a hexapeptide with activity against phytopathogenic fungi that cause postharvest decay in fruits. *Mol. Plant Microbe Interact.*, **13**, 837-846.

Lorito, M., Woo, S.L., Fernandez, I.G., Colucci, G., Harman, G.E., Pintor-Toro, J.A., Filippone, E., Muccifora, S., Lawrence, C.B., Zoina, A., Tuzun, S. and Scala, F. (1998) Genes from mycoparasitic fungi as a source for improving plant resistance to fungal pathogens. *Proc. Natl. Acad. Sci. USA*, **95**, 7860-7865.

Maldonado, A.M., Doerner, P., Dixon, R.A., Lamb, C.J. and Cameron, R.K. (2002) A putative lipid transfer protein involved in systemic resistance signalling in *Arabidopsis*. *Nature*, **419**, 399-403.

Marcos, J.F., Muñoz, A., Pérez-Payá, E., Misra, S. and López-García, B. (2008) Identification and rational design of novel antimicrobial peptides for plant protection. *Annu. Rev. Phytopathol.*, **46**, 273-301.

Marcus, J.P., Goulter, K.C., Green, J.L., Harrison, S.J. and Manners, J.M. (1997) Purification, characterisation and cDNA cloning of an antimicrobial peptide from *Macadamia integrifolia*. *Eur. J. Biochem.*, **244**, 743-749.

Matsuzaki, K. (1999) Why and how are peptide-lipid interactions utilized for self-defense? Magainins and tachyplesins as archetypes. *Biochim. Biophys. Acta*, **1462**, 1-10.

Matsuzaki, K., Harada, M., Funakoshi, S., Fujii, N. and Miyajima, K. (1991) Physicochemical determinants for the interactions of magainins 1 and 2 with acidic lipid bilayers. *Biochim. Biophys. Acta*, **1063**, 162-170.

McManus, A.M., Nielsen, K.J., Marcus, J.P., Harrison, S.J., Green, J.L., Manners, J.M. and Craik, D.J. (1999) MiAMP1, a novel protein from *Macadamia integrifolia* adopts a greek key β-barrel fold unique amongst plant antimicrobial proteins. *J. Mol. Biol.*, **293**, 629-638.

Melo, F.R., Rigden, D.J., Franco, O.L., Mello, L.V., Ary, M.B., Grossi de Sá, M.F. and Bloch, C. (2002) Inhibition of trypsin by cowpea thionin: characterization, molecular modeling, and docking. *Proteins: Structure, Function, and Bioinformatics*, **48**, 311-319.

Mendez, E., Moreno, A., Colilla, F., Pelaez, F., Limas, G.G., Mendez, R., Soriano, F., Salinas, M. and de Haro, C. (1990) Primary structure and inhibition of protein synthesis in eukaryotic cell-free system of a novel thionin, γ-hordothionin, from barley endosperm. *Eur. J. Biochem.*, **194**, 533-539.

Mentag, R., Luckevich, M., Morency, M.J. and Seguin, A. (2003) Bacterial disease resistance of transgenic hybrid poplar expressing the synthetic antimicrobial peptide D4E1. *Tree Physiol.*, **23**, 405-411.

Milligan, S. and Gasser, C. (1995) Nature and regulation of pistil-expressed genes in tomato. *Plant Mol. Biol.*, **85**, 691-711.

Mirouze, M., Sels, J., Richard, O., Czernic, P., Loubet, S., Jacquier, A., François, I.E.J.A., Cammue, B.P.A., Lebrun, M., Berthomieu, P. and Marquès, L. (2006) A putative novel role for plant defensins: a defensin from the zinc hyper-accumulating plant, *Arabidopsis halleri*, confers zinc tolerance. *Plant J.*, **47**, 329-342.

Molina, A. and García-Olmedo, F. (1997) Enhanced tolerance to bacterial pathogens caused by the transgenic expression of barley lipid transfer protein LTP2. *Plant J.*, **12**, 669-675.

Molina, A., Segura, A. and García-Olmedo, F. (1993) Lipid transfer proteins (nsLTPs) from barley and maize leaves are potent inhibitors of bacterial and fungal plant pathogens. *FEBS Lett.*, **316**, 119-122.

Montesinos, E. (2007) Antimicrobial peptides and plant disease control. *FEMS Microbiol. Lett.*, **270**, 1-11.

Moreno, A.B., Peñas, G., Rufat, M., Bravo, J.M., Estopà, M., Messeguer, J. and San Segundo, B. (2005) Pathogen-induced production of the antifungal AFP protein from *Aspergillus giganteus* confers resistance to the blast fungus *Magnaporthe grisea* in transgenic rice. *Mol. Plant Microbe Interact.*, **18**, 960-972.

Nandi, S., Yalda, D., Lu, S., Nikolov, Z. and Misaki, R. (2005) Process development and economic evaluation of recombinant human lactoferrin expressed in rice grain. *Transgenic Res.*, **14**, 237-249.

Narusaka, Y., Nakashima, K., Shinwari, Z.K., Sakuma, Y., Furihata, T., Abe, H., Narusaka, M., Shinozaki, K. and Yamaguchi-Shinozaki, K. (2003) Interaction between two *cis*-acting elements, ABRE and DRE, in ABA-dependent expression of *Arabidopsis rd29A* gene in response to dehydration and high-salinity stresses. *Plant J.*, **34**, 137-148.

Nicolas, P. (2009) Multifunctional host defense peptides: intracellular-targeting antimicrobial peptides. *FEBS J.*, **276**, 6483-6496.

Nielsen, K.K., Nielsen, J.E., Madrid, S.M. and Mikkelsen, J.D. (1997) Characterization of an new antifungal chitin-binding peptide from sugar beet leaves. *Plant Physiol.*, **113**, 83-91.

Nolde, S.B., Vassilevski, A.A., Rogozhin, E.A., Barinov, N.A., Balashova, T.A., Samsonova, O.V., Baranov, Y.V., Feofanov, A.V., Egorov, T.A., Arseniev, A.S. and Grishin, E.V. (2011) Disulfide-stabilized helical hairpin structure of a novel antifungal peptide EcAMP1 from seeds of barnyard grass (*Echinochloa crus-galli*). *J. Biol. Chem.*

Oard, S. and Karki, B. (2006) Mechanism of β-purothionin antimicrobial peptide inhibition by metal ions: molecular dynamics simulation study. *Biophys. Chem.*, **121**, 30-43.

Ohizumi, Y., Nakamura, H., Kobayashi, J. and Catterall, W.A. (1986) Specific inhibition of ^{3}H saxitoxin binding to skeletal muscle sodium channels by geographutoxin II, a polypeptide channel blocker. *J. Biol. Chem.*, **261**, 6149-6152.

Ohshima, M., Mitsuhara, I., Okamoto, M., Sawano, S., Nishiyama, K., Kaku, H., Natori, S. and Ohashi, Y. (1999) Enhanced resistance to bacterial disease of transgenic tobacco plants overexpressing sarcotoxin IA, a bactericidal peptide of insect. *J. Biochem.*, **125**, 431-435.

Oldach, K.H., Becker, D. and Lorz, H. (2001) Heterologous expression of genes mediating enhanced fungal resistance in transgenic wheat. *Mol. Plant Microbe Interact.*, **14**, 832-838.

Osborn, R.W., De Samblanx, G.W., Thevissen, K., Goderis, I., Torrekens, S., Van Leuven, F., Attenborough, S., Rees, S.B. and Broekaert, W.F. (1995) Isolation and characterisation of plant defensins from seeds of Asteraceae, Fabaceae, Hippocastanaceae and Saxifragaceae. *FEBS Lett.*, **368**, 257-262.

Osbourn, A.E. (1996) Preformed antimicrobial compounds and plant defense against fungal attack. *Plant Cell*, **8**, 1821-1831.

Osusky, M., Osuska, L., Hancock, R.E.W., Kay, W.W. and Misra, S. (2004) Transgenic potatoes expressing a novel cationic peptide are resistant to late blight and pink rot. *Transgenic Res.*, **13**, 181-190.

Osusky, M., Osuska, L., Kay, W. and Misra, S. (2005) Genetic modification of potato against microbial diseases: *in vitro* and *in planta* activity of a dermaseptin B1 derivative, MsrA2. *Theor. Appl. Genet.*, **111**, 711-722.

Osusky, M., Zhou, G., Osuska, L., Hancock, R.E., Kay, W.W. and Misra, S. (2000) Transgenic plants expressing cationic peptide chimeras exhibit broad-spectrum resistance to phytopathogens. *Nat. Biotechnol.*, **18**, 1162-1166.

Otvos, J.L. (2000) Antibacterial peptides isolated from insects. *J. Pept. Sci.*, **6**, 497-511.

Park, H.C., Hwan Kang, Y., Jin Chun, H., Choon Koo, J., Hwa Cheong, Y., Young Kim, C., Chul Kim, M., Sik Chung, W., Cheol Kim, J., Hyuk Yoo, J., Duck Koo, Y., Chul Koo, S., Oh Lim, C., Yeol Lee, S. and Je Cho, M. (2002) Characterization of a stamen-specific cDNA encoding a novel plant defensin in Chinese cabbage. *Plant Mol. Biol.*, **50**, 57-68.

Patel, S.U., Osborn, R., Rees, S. and Thornton, J.M. (1998) Structural studies of *Impatiens balsamina* antimicrobial protein (Ib-AMP1). *Biochemistry*, **37**, 983-990.

Patkar, R. and Chattoo, B. (2006) Transgenic *indica* rice expressing ns-LTP-like protein shows enhanced resistance to both fungal and bacterial pathogens. *Mol. Breed.*, **17**, 159-171.

Penninckx, I., Eggermont, K., Terras, F.R.G., Thomma, B.P.H.J., Samblanx, G.W.D., Buchala, A., Metraux, J.P., Manners, J.M. and Broekaert, W.F. (1996) Pathogen-induced systemic activation of a plant defensin gene in *Arabidopsis* follows a salicylic acid-independent pathway. *Plant Cell*, **8**, 2309-2323.

Piao, H.L., Lim, J.H., Kim, S.J., Cheong, G.-W. and Hwang, I. (2001) Constitutive over-expression of *AtGSK1* induces NaCl stress responses in the absence of NaCl stress and results in enhanced NaCl tolerance in *Arabidopsis*. *Plant J.*, **27**, 305-314.

Piñeiro, M., Diaz, I., Rodriguez-Palenzuela, P., Titarenko, E. and Garcia-Olmedo, F. (1995) Selective disulphide linkage of plant thionins with other proteins. *FEBS Lett.*, **369**, 239-242.

Ponti, D., Mangoni, M.L., Mignogna, G., Simmaco, M. and Barra, D. (2003) An amphibian antimicrobial peptide variant expressed in *Nicotiana tabacum* confers resistance to phytopathogens. *Biochem. J.*, **370**, 121-127.

Ponz, F., Paz-Ares, J., Hernández-Lucas, C., Carbonero, P. and García-Olmedo, F. (1983) Synthesis and processing of thionin precursors in developing endosperm from barley (*Hordeum vulgare* L.). *EMBO J.*, **2**, 1035-1040.

Poth, A.G., Colgrave, M.L., Lyons, R.E., Daly, N.L. and Craik, D.J. (2011) Discovery of an unusual biosynthetic origin for circular proteins in legumes. *Proc. Natl. Acad. Sci. USA*, **108**, 10127-10132.

Pyee, J. and Kolattukudy, P.E. (1995) The gene for the major cuticular wax-associated protein and three homologous genes from broccoli (*Brassica oleracea*) and their expression patterns. *Plant J.*, **7**, 49-59.

Pyee, J., Yu, H.S. and Kolattukudy, P.E. (1994) Identification of a lipid transfer protein as the major protein in the surface wax of broccoli (*Brassica oleracea*) leaves. *Arch. Biochem. Biophys.*, **311**, 460-468.

Rahnamaeian, M., Langen, G., Imani, J., Khalifa, W., Altincicek, B., von Wettstein, D., Kogel, K.-H. and Vilcinskas, A. (2009) Insect peptide metchnikowin confers on barley a selective capacity for resistance to fungal ascomycetes pathogens. *J. Exp. Bot.*, **60**, 4105-4114.

Rahnamaeian, M. and Vilcinskas, A. (2011) Defense gene expression is potentiated in transgenic barley expressing antifungal peptide metchnikowin throughout powdery mildew challenge. *J. Plant Res.*, 1-10.

Rajasekaran, K., Cary, J.W., Jaynes, J.M. and Cleveland, T.E. (2005) Disease resistance conferred by the expression of a gene encoding a synthetic peptide in transgenic cotton (*Gossypium hirsutum* L.) plants. *Plant Biotech. J.*, **3**, 545-554.

Rao, A.G. (1995) Antimicrobial peptides. *Mol. Plant Microbe Interact.*, **8**, 6-13.

Romero, A., Alamillo, J.M. and García-Olmedo, F. (1997) Processing of thionin precursors in barley leaves by a vacuolar proteinase. *Eur. J. Biochem.*, **243**, 202-208.

Ross, A. (1961) Systemic acquired resistance induced by localized vrius infections in plants. *Virology*, **14**, 340-358.

Roxrud, I., Lid, S.E., Fletcher, J.C., Schmidt, E.D.L. and Opsahl-Sorteberg, H.-G. (2007) GASA4, one of the 14-member *Arabidopsis* GASA family of small polypeptides, regulates flowering and seed development. *Plant Cell Physiol.*, **48**, 471-483.

Saska, I., Gillon, A.D., Hatsugai, N., Dietzgen, R.G., Hara-Nishimura, I., Anderson, M.A. and Craik, D.J. (2007) An asparaginyl endopeptidase mediates *in vivo* protein backbone cyclization. *J. Biol. Chem.*, **282**, 29721-29728.

Schaefer, S., Gasic, K., Cammue, B.P.A., Broekaert, W.F., van Damme, E., Peumans, W. and Korban, S. (2005) Enhanced resistance to early blight in transgenic tomato lines expressing heterologous plant defense genes. *Planta*, **222**, 858-866.

Scheel, D. (1998) Resistance response physiology and signal transduction. *Curr. Opin. Plant Biol.*, **1**, 305-310.

Schrader-Fischer, G. and Apel, K. (1994) Organ-specific expression of highly divergent thionin variants that are distinct from the seed-specific crambin in the crucifer *Crambe abyssinica*. *Mol. Gen. Genet.*, **245**, 380-389.

Segura, A., Moreno, M. and García-Olmedo, F. (1993) Purification and antipathogenic activity of lipid transfer proteins (LTPs) from the leaves of *Arabidopsis* and spinach. *FEBS Lett.*, **332**, 243-246.

Segura, A., Moreno, M., Madueño, F., Molina, A. and García-Olmedo, F. (1999) Snakin-1, a peptide from potato that is active against plant pathogens. *Mol. Plant Microbe Interact.*, **12**, 16-23.

Sels, J., Mathys, J., De Coninck, B.M.A., Cammue, B.P.A. and De Bolle, M.F.C. (2008) Plant pathogenesis-related (PR) proteins: a focus on PR peptides. *Plant Physiol. Biochem.*, **46**, 941-950.

Seo, P.J., Lee, A.-K., Xiang, F. and Park, C.-M. (2008) Molecular and functional profiling of *Arabidopsis* pathogenesis-related genes: insights into their roles in salt response of seed germination. *Plant Cell Physiol.*, **49**, 334-344.

Shade, R.E., Schroeder, H.E., Pueyo, J.J., Tabe, L.M., Murdock, L.L., Higgins, T.J.V. and Chrispeels, M.J. (1994) Transgenic pea seeds expressing the α-amylase inhibitor of the common bean are resistant to bruchid beetles. *Nat. Biotechnol.*, **12**, 793-796.

Shai, Y. (1999) Mechanism of the binding, insertion and destabilization of phospholipid bilayer membranes by α-helical antimicrobial and cell non-selective membrane-lytic peptides. *Biochim. Biophys. Acta*, **1462**, 55-70.

Shai, Y. (2002) Mode of action of membrane active antimicrobial peptides. *Biopolymers*, **66**, 236-248.

Shao, F., Hu, Z., Xiong, Y., Huang, Q., Wang, C., Zhu, R. and Wang, D. (1999) A new antifungal peptide from the seeds of *Phytolacca americana*: characterization, amino acid sequence and cDNA cloning. *Biochim. Biophys. Acta*, **1430**, 162-168.

Sharma, A., Sharma, R., Imamura, M., Yamakawa, M. and Machii, H. (2000) Transgenic expression of cecropin B, an antibacterial peptide from *Bombyx mori*, confers enhanced resistance to bacterial leaf blight in rice. *FEBS Lett.*, **484**, 7-11.

Shi, L., Gast, R.T., Gopalraj, M. and Olszewski, N.E. (1992) Characterization of a shoot-specific, GA_3- and ABA-regulated gene from tomato. *Plant J.*, **2**, 153-159.

Shin, D., Lee, J., Hwang, K., Kim, K. and Suh, S. (1995) High-resolution crystal structure of the non-specific lipid-transfer protein from maize seedlings. *Structure*, **3**, 189-199.

Shinozaki, K. and Yamaguchi-Shinozaki, K. (1997) Gene expression and signal transduction in water-stress response. *Plant Physiol.*, **115**, 327-334.

Shukurov, R.R., Voblikova, V.D., Nikonorova, A., Komakhin, R., Komakhina, V.V., Egorov, T.A., Grishin, E. and Babakov, A.V. (2011) Transformation of tobacco and *Arabidopsis* plants with *Stellaria media* genes encoding novel hevein-like peptides increases their resistance to fungal pathogens. *Transgenic Res.*, 1-13.

Smilanick, J.L., Denis-Arrue, R., Bosch, J.R., Gonzales, A.R., Henson, D.J. and Janisiewicz, W.J. (1993) Biocontrol of postharvest brown rot of nectarines and peaches by *Pseudomonas* species. *Crop Prot.*, **2**, 513-520.

Spelbrink, R.G., Dilmac, N., Allen, A., Smith, T.J., Shah, D.M. and Hockerman, G.H. (2004) Differential antifungal and calcium channel-blocking activity among structurally related plant defensins. *Plant Physiol.*, **135**, 2055-2067.

Stec, B. (2006) Plant thionins – The structural perspective. *Cell. Mol. Life Sci.*, **63**, 1370-1385.

Sterk, P., Booij, H., Schellekens, G.A., Van Kammen, A. and De Vries, S.C. (1991) Cell-specific expression of the carrot *EP2* lipid transfer protein gene. *Plant Cell*, **3**, 907-921.

Stevens, C., Titarenko, E., Hargreaves, J. and Gurr, S. (1996) Defence-related gene activation during an incompatible interaction between *Stagonospora* (*Septoria*) *nodorum* and barley (*Hordeum vulgare* L.) coleoptile cells. *Plant Mol. Biol.*, **31**, 741-749.

Stotz, H., Spence, B. and Wang, Y. (2009) A defensin from tomato with dual function in defense and development. *Plant Mol. Biol.*, **71**, 131-143.

Swathi Anuradha, T., Divya, K., Jami, S. and Kirti, P. (2008) Transgenic tobacco and peanut plants expressing a mustard defensin show resistance to fungal pathogens. *Plant Cell Rep.*, **27**, 1777-1786.

Tailor, R.H., Acland, D.P., Attenborough, S., Cammue, B.P.A., Evans, I.J., Osborn, R.W., Ray, J.A., Rees, S.B. and Broekaert, W.F. (1997) A novel family of small cysteine-rich antimicrobial peptides from seed of *Impatiens balsamina* is derived from a single precursor protein. *J. Biol. Chem.*, **272**, 24480-24487.

Takase, K., Hagiwara, K., Onodera, H., Nishizawa, Y. and Ugaki, M. (2005) Constitutive expression of human lactoferrin and its N-lobe in rice plants to confer disease resistance. *Biochem. Cell Biol.*, **83**, 239.

Takayama, S., Shimosato, H., Shiba, H., Funato, M., Che, F.-S., Watanabe, M., Iwano, M. and Isogai, A. (2001) Direct ligand-receptor complex interaction controls *Brassica* self-incompatibility. *Nature*, **413**, 534-538.

Terras, F.R.G., Eggermont, K., Kovaleva, V., Raikhel, N.V., Osborn, R.W., Kester, A., Rees, S.B., Torrekens, S., Leuven, F.V., Vanderleyden, J., Cammue, B.P.A. and Broekaert, W.F. (1995) Small cysteine-rich antifungal proteins from radish: their role in host defense. *Plant Cell*, **7**, 573-588.

Terras, F.R.G., Goderis, I.J., Van Leuven, F., Vanderleyden, J., Cammue, B.P.A. and Broekaert, W.F. (1992) *In vitro* antifungal activity of a radish (*Raphanus sativus* L.) seed protein homologous to nonspecific lipid transfer proteins. *Plant Physiol.*, **100**, 1055-1058.

Terras, F.R.G., Torrekens, S., Van Leuven, F., Osborn, R.W., Vanderleyden, J., Cammue, B.P.A. and Broekaert, W.F. (1993) A new family of basic cysteine-rich plant antifungal proteins from Brassicaceae species. *FEBS Lett.*, **316**, 233-240.

Theis, T. and Stahl, U. (2004) Antifungal proteins: targets, mechanisms and prospective applications. *Cell. Mol. Life Sci.*, **61**, 437-455.

Thevissen, K., Ferket, K.K.A., François, I.E. and Cammue, B.P.A. (2003) Interactions of antifungal plant defensins with fungal membrane components. *Peptides*, **24**, 1705.

Thevissen, K., Ghazi, A., De Samblanx, G.W., Brownlee, C., Osborn, R.W. and Broekaert, W.F. (1996) Fungal membrane responses induced by plant defensins and thionins. *J. Biol. Chem.*, **271**, 15018-15025.

Thomma, B.P.H.J., Cammue, B.P.A. and Thevissen, K. (2002) Plant defensins. *Planta*, **216**, 193-202.

Tsuboi, S., Osafune, T., Tsugeki, R., Nishimura, M. and Yamada, M. (1992) Nonspecific lipid transfer protein in castor bean cotyledon cells: subcellular localization and a possible role in lipid metabolism. *J. Biochem.*, **111**, 500-508.

Turrini, A., Sbrana, C., Pitto, L., Ruffini Castiglione, M., Giorgetti, L., Briganti, R., Bracci, T., Evangelista, M., Nuti, M.P. and Giovannetti, M. (2004) The antifungal Dm-AMP1 protein from *Dahlia merckii* expressed in *Solanum melongena* is released in root exudates and differentially affects pathogenic fungi and mycorrhizal symbiosis. *New Phytol.*, **163**, 393-403.

Van Damme, E.J.M., Charels, D., Roy, S., Tierens, K., Barre, A., Martins, J.C., Rougé, P., Van Leuven, F., Does, M. and Peumans, W.J. (1999) A gene encoding a hevein-like protein from elderberry fruits is homologous to *PR-4* and class V chitinase genes. *Plant Physiol.*, **119**, 1547-1556.

van der Biezen, E.A. (2001) Quest for antimicrobial genes to engineer disease-resistant crops. *Trends Plant Sci.*, **6**, 89.

Van Loon, L.C., Rep, M. and Pieterse, C.M.J. (2006) Significance of inducible defense-related proteins in infected plants. *Annu. Rev. Phytopathol.*, **44**, 135-162.

Van Parijs, J., Broekaert, W.F., Goldstein, I.J. and Peumans, W.J. (1991) Hevein: an antifungal protein from rubber-tree (*Hevea brasiliensis*) latex. *Planta*, **183**, 258-264.

VanEtten, H.D., Mansfield, J.W., Bailey, J.A. and Farmer, E.E. (1994) Two classes of plant antibiotics: phytoalexins versus 'phytoanticipins'. *Plant Cell*, **6**, 1191-1192.

Vidal, J.R., Kikkert, J.R., Malnoy, M.A., Wallace, P.G., Barnard, J. and Reisch, B.I. (2006) Evaluation of transgenic 'Chardonnay' (*Vitis vinifera*) containing magainin genes for resistance to crown gall and powdery mildew. *Transgenic Res.*, **15**, 69.

Wada, K. and Buchanan, B.B. (1981) Purothionin: a seed protein with thioredoxin activity. *FEBS Lett.*, **124**, 237-240.

Walujono, K., Scholma, R.A., Beintema, J.J., Mariono, A. and Hahn, A.M. (1975) Amino acid sequence of hevein. *Proc. Int. Rubber Conference, Kuala Lumpur*, **II**, 518-531.

Wang, Y., Nowak, G., Culley, D., Hadwiger, L.A. and Fristensky, B. (1999) Constitutive expression of pea defense gene DRR206 confers resistance to blackleg (*Leptosphaeria maculans*) disease in transgenic canola (*Brassica napus*). *Mol. Plant Microbe Interact.*, **12**, 410-418.

Wang, Z. and Wang, G. (2004) APD: the Antimicrobial Peptide Database. *Nucleic Acids Res.*, **32**, D590-D592.

Westerhoff, H.V., Juretić, D., Hendler, R.W. and Zasloff, M. (1989) Magainins and the disruption of membrane-linked free-energy transduction. *Proc. Natl. Acad. Sci. USA*, **86**, 6597-6601.

Wijaya, R., Neumann, G.M., Condron, R., Hughes, A.B. and Polya, G.M. (2000) Defense proteins from seed of *Cassia fistula* include a lipid transfer protein homologue and a protease inhibitory plant defensin. *Plant Sci.*, **159**, 243-255.

Wilmes, M., Cammue, B.P.A., Sahl, H.-G. and Thevissen, K. (2011) Antibiotic activities of host defense peptides: more to it than lipid bilayer perturbation. *Nat. Prod. Rep.*, **28**, 1350-1358.

Xing, H.Y., Lawrence, C.B., Chambers, O., Davies, H.M., Everett, N.P. and Li, Q.Q. (2006) Increased pathogen resistance and yield in transgenic plants expressing combinations of the modified antimicrobial peptides based on indolicidin and magainin. *Planta*, **223**, 1024.

Yang, L., Weiss, T.M., Lehrer, R.I. and Huang, H.W. (2000) Crystallization of antimicrobial pores in membranes: magainin and protegrin. *Biophys. J.*, **79**, 2002-2009.

Yeamn, M.R. and Yount, N.Y. (2003) Mechanisms of antimicrobial peptide action and resistance. *Pharmacol. Rev.*, **66**, 27-55.

Yevtushenko, D.P. and Misra, S. (2007) Comparison of pathogen-induced expression and efficacy of two amphibian antimicrobial peptides, MsrA2 and temporin A, for engineering wide-spectrum disease resistance in tobacco. *Plant Biotech. J.*, **5**, 720-734.

Yevtushenko, D.P., Romero, R., Forward, B.S., Hancock, R.E.W., Kay, W.W. and Misra, S. (2005) Pathogen-induced expression of a cecropin A-melittin antimicrobial peptide gene confers antifungal resistance in transgenic tobacco. *J. Exp. Bot.*, **56**, 1685-1695.

Yi, J.Y., Seo, H.W., Yang, M.S., Robb, E.J., Nazar, R.N. and Lee, S.W. (2004) Plant defense gene promoter enhances the reliability of *shiva-1* gene-induced resistance to soft rot disease in potato. *Planta*, **220**, 165-171.

Zasloff, M. (2002) Antimicrobial peptides of multicellular organisms. *Nature*, **415**, 389-395.

Zeier, J., Pink, B., Mueller, M.J. and Berger, S. (2004) Light conditions influence specific defence responses in incompatible plant–pathogen interactions: uncoupling systemic resistance from salicylic acid and PR-1 accumulation. *Planta*, **219**, 673-683.

Zhang, N., Jones, B. and Tao, P. (1997) Purification and characterisation of a new class of insect α-amylase inhibitors from barley. *Cereal Chem.*, **74**, 119-122.

Zhang, S. and Klessig, D.F. (2001) MAPK cascades in plant defense signaling. *Trends Plant Sci.*, **6**, 520-527.

Zhang, Z.Y., Coyne, D.P., Vidaver, A.K. and Mitra, A. (1998) Expression of human lactoferrin cDNA confers resistance to *Ralstonia solanacearum* in transgenic tobacco plants. *Phytopathology*, **88**, 730-734.

Zhu, Y., Agbayani, R. and Moore, P. (2007) Ectopic expression of *Dahlia merckii* defensin *DmAMP1* improves papaya resistance to *Phytophthora palmivora* by reducing pathogen vigor. *Planta*, **226**, 87-97.

5

ARACIN1 and *ARACIN2*, two novel Brassicaceae-specific peptides exhibiting antifungal activities against necrotrophic pathogens in *Arabidopsis thaliana*

Annelies Inzé, Janick Mathys, Brigitte van de Cotte, Bruno P.A. Cammue and Frank Van Breusegem

AUTHOR CONTRIBUTIONS

A.I. wrote the manuscript with help of F.V.B. A.I. designed, performed and analyzed the majority of the experiments. J.M. performed and analyzed the *in soil* disease assays and *in vitro* antifungal activity assays.

ABSTRACT

Plants have developed a variety of mechanisms to cope with abiotic and biotic stresses. In a previous localization study of hydrogen peroxide-induced proteins, two peptides with an unknown function (designated ARACIN1 and ARACIN2) have been identified. Although these peptides are highly similar, they are differentially regulated by several abiotic stresses, during *Botrytis cinerea* infection or after treatment with benzothiadiazole and methyl jasmonate. In the genome of *Arabidopsis thaliana*, these paralogous genes are positioned in tandem within a gene cluster of pathogen defense-related genes. *ARACINS* encode small, cationic and hydrophobic peptides and share several features with antimicrobial peptides. Their genes are expressed in peripheral cell layers prone to pathogen entry and are lineage-specific to the Brassicaceae family. Transgenic *Arabidopsis* plants that ectopically expressed *ARACIN1* were significantly better protected against infections with two agronomically and economically important necrotrophic fungi, *Botrytis cinerea* and *Alternaria brassicicola*. In addition, *in vitro* bioassays demonstrated that both ARACIN peptides had a direct antifungal effect against these pathogens.

A modified version of this chapter has been filed as an **international patent application (filing number US 61/518,833)** under the title **"Means and methods for generating microbial disease resistant plants"** by **Inzé, A., Mathys, J., Cammue, B. and Van Breusegem, F.**

A modified version of this chapter will be submitted to **Plant Physiology** by **Inzé, A., Mathys, J., van de Cotte, B., Cammue, B. and Van Breusegem, F.** under the title **"ARACIN1 and ARACIN2, two novel Brassicaceae-specific peptides exhibiting antifungal activities against necrotrophic fungal pathogens in *Arabidopsis thaliana*"**

INTRODUCTION

During biotic and abiotic stresses, the cellular metabolic status is perturbed producing a variety of reactive oxygen species (ROS) as a consequence (Van Breusegem *et al.*, 2008; Mittler *et al.*, 2011). Besides being toxic byproducts of aerobic metabolism, ROS and, more particularly, hydrogen peroxide (H_2O_2), are considered as signaling molecules that trigger signal transduction pathways involved in defense responses and cell death (Apel and Hirt, 2004; Gadjev *et al.*, 2006; Van Breusegem and Dat, 2006). Transcriptome analyses revealed an important enrichment of ROS-responsive genes during biotic and abiotic stresses, including many pathogen defense-related genes such as the pathogenesis-related (PR) genes (Broekaert *et al.*, 2000; Apel and Hirt, 2004; Torres and Dangl, 2005; Torres *et al.*, 2006; van Loon *et al.*, 2006). Amongst them, antimicrobial peptides (AMPs) are considered to play a key role in plant defense, acting both as permanent and inducible defense barriers (García-Olmedo *et al.*, 1998).

Plant AMPs are small (12 to 50 amino acids), cationic, hydrophobic and secreted peptides that are widespread throughout the plant kingdom and include plant defensins, lipid-transfer proteins, hevein- and knottin-type peptides, cyclotides, snakins, maize (*Zea mays*) basic peptide 1, and polyprotein precursor AMPs from both *Macadamia integrifolia* and *Impatiens balsamina* (Broekaert *et al.*, 1995; García-Olmedo *et al.*, 1998; Theis and Stahl, 2004; Sels *et al.*, 2008 – Chapter 4). Due to their amphipathic nature, AMPs are able to permeabilize the pathogen's membrane by both specific and non-specific electrostatic and hydrophobic interactions with cell surface groups (Shai, 2002; Thevissen *et al.*, 2003; Aerts *et al.*, 2008). However, increasing evidence shows that the antimicrobial action of some AMPs can be based on more targeted mechanisms, including the interaction with microbe-specific lipid receptors (Wilmes *et al.*, 2011). In addition, other biological roles of AMPs have been identified, such as protein inhibition (Broekaert *et al.*, 1997; Lay and Anderson, 2005), redox regulation (Huang *et al.*, 2008), ion channel inhibition (Kushmerick *et al.*, 1998; Spelbrink *et al.*, 2004) and development (Takayama *et al.*, 2001; Stotz *et al.*, 2009 – Chapter 4).

Overproduction of AMPs has been proposed as a promising strategy to increase disease resistance in transgenic plants thanks to their small size, broad-spectrum activity by targeting the pathogen's membrane, and a mode of action that is difficult to develop resistance against (Bulet *et al.*, 2004; Marcos *et al.*, 2008 – Chapter 4). Overexpression of the radish *(Raphanus sativus)* antifungal peptide *RSAFP2* in transgenic tobacco *(Nicotiana tabacum)* plants increased resistance against the fungus *Alternaria longipes* (Terras *et al.*, 1995). Overexpression of an alfalfa *(Medicago sativa)* defensin (*alfAFP*) in transgenic potato *(Solanum tuberosum)* provided high levels of field resistance against *Verticillium dahliae*, the casual agent of the agronomically important 'early dying disease' (Gao *et al.*, 2000). A more advanced and durable approach is to engineer transgenic plants that synthesize chimeras of two or more AMPs

with different modes of action to develop a broad-spectrum resistance. For example, overproduction of a chimeric cleavable polyprotein precursor containing the mature domains of the plant defensins DmAMP1 (*Dahlia merckii* AMP1) and RsAFP2 resulted in the efficient release of both bioactive antifungal peptides (François *et al.*, 2002; François *et al.*, 2004).

AMP overexpression can also confer enhanced tolerance to abiotic stresses (Mirouze *et al.*, 2006; Lee and Hwang, 2009). For instance, overexpression of the *CaAMP1* (*Capsicum annuum AMP1*) gene in *Arabidopsis thaliana* increased not only resistance against both bacterial and fungal pathogens, but also tolerance to high salt and drought stresses (Lee *et al.*, 2008; Lee and Hwang, 2009). Another example demonstrating the involvement of AMPs in abiotic stress is the zinc stress tolerance in transgenic *A. thaliana* lines obtained by overexpression of *PDF* genes of *Arabidopsis halleri* (Mirouze *et al.*, 2006).

Here, we characterized two Arabidopsis peptides, designated ARACIN1 and ARACIN2, that are transcriptionally regulated by both biotic and abiotic stresses and share many characteristics with AMPs. We demonstrate their antifungal activities *in vitro* against the broad host necrotrophic plant fungus *Botrytis cinerea,* the causing agent of gray mold disease, and *Alternaria brassicicola*, which causes black spot disease on members of the Brassicaceae family (Neergaard and Andersen, 1945; Braverman, 1971; Lawrence *et al.*, 2008). Furthermore, overexpression of *ARACIN1 in planta* significantly improved resistance against both pathogens.

RESULTS

Stress and hormone responsiveness of *ARACIN1* and *ARACIN2*

Previously, we compiled a comprehensive list of H_2O_2-responsive genes by using catalase-deficient Arabidopsis plants exposed to high light (HL) irradiation. Reduced catalase levels together with HL exposure leads to the accumulation of photorespiratory H_2O_2 that, in turn, affected the expression of more than 700 genes (Vanderauwera *et al.*, 2005; Vanderauwera *et al.*, 2011; Inzé *et al.*, 2012 – Chapter 2). ARACIN1 (At5g36925), a peptide of unknown function, was previously identified as nucleocytosolic in a subcellular localization study of H_2O_2-induced proteins (Inzé *et al.*, 2012 – Chapter 2). The expression of *ARACIN1* and the highly similar paralog *ARACIN2* (At5g36920; see below) was induced by increased levels of photorespiratory H_2O_2 (22-fold and 1.35-fold, respectively).

Due to the absence of representative probe sets on the Affymetrix ATH1 microarray platform, the array-derived expression data on both genes were rather scarce and limited to publicly available data sets that had been obtained from Agilent Arabidopsis V3 arrays and diverse tiling array platforms. From

these data sets, we could deduce a down-regulation of *ARACIN1* by abscisic acid and heat stress (Zeller *et al.*, 2009) and an up-regulation in response to *Agrobacterium tumefaciens* infection (Ditt *et al.*, 2006). To complement these array-based abiotic stress-related data, we performed a detailed expression analysis with quantitative PCR on RNA from salt-, cold- and heat-stressed plants (see Materials and Methods). Transcripts of *ARACIN1* were transiently up-regulated by both salt (3.32-fold; see Materials and Methods) and cold stress (5.92-fold after 13 h; Figure 1a), whereas *ARACIN2* expression remained unaffected. During heat stress, transcripts of *ARACIN1* were substantially down-regulated after 6 and 12 h at 37°C, whereas *ARACIN2* was up-regulated (Figure 1b).

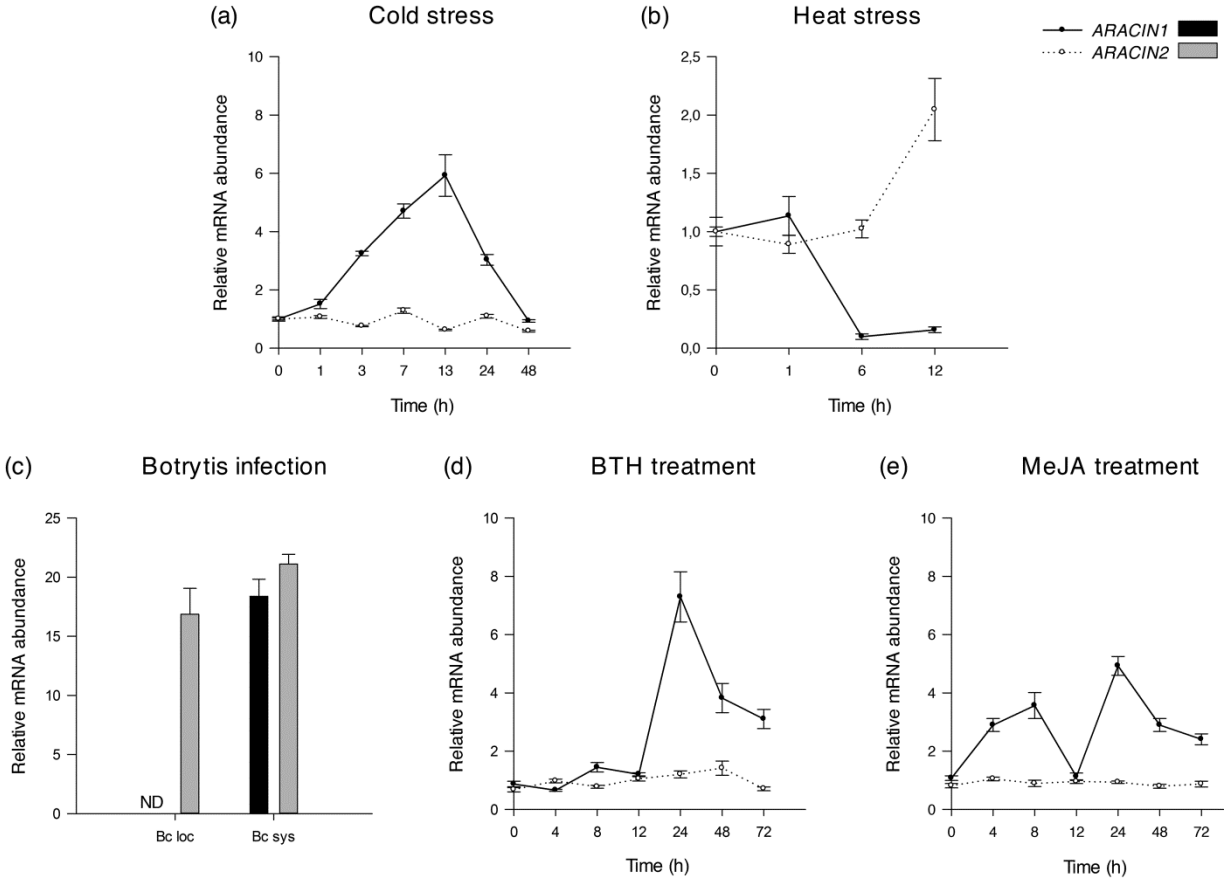

Figure 1. Transcriptional regulation of *ARACIN1* and *ARACIN2*.

Relative abundance of *ARACIN1* and *ARACIN2* transcripts after cold stress (a), heat stress (b), *Botrytis* infection (c), BTH treatment (d) and MeJA treatment (e) represented as fold change relative to wild-type/unstressed or mock-treated values and normalized against *ARP7* or *EF1-a* (see Materials and Methods). Data are the means ± SE (n=2-3). *ARACIN1* and *ARACIN2* transcript levels are respectively represented by black bars/lines and grey bars/dotted lines. Bc loc and Bc sys, local and systemic *B. cinerea* infection, respectively; ND, not detected.

To investigate the transcriptional regulation of *ARACIN1* and *ARACIN2* during biotic stress, we assessed their transcript levels after infection with the necrotrophic fungus *B. cinerea*. Therefore, 4-week-old Arabidopsis plants were inoculated with *B. cinerea* B05-10 and systemic and local leaves were collected 48 h post-inoculation. Only *ARACIN2* was strongly induced (16.8-fold) in locally infected leaves and both genes were induced in systemic leaves (Figure 1c). Further, we assessed their responsiveness towards the defense hormones salicylic acid (SA) and methyl jasmonate (MeJA). Plants were treated with benzothiadiazole (BTH), that has an analogous effect to SA and activates the plant's natural defense mechanisms (Lawton *et al.*, 1996), and with MeJA. After 24 h, the expression of *ARACIN1* was 7-fold higher in BTH-treated plants than in mock-treated plants and decreased to 3-fold after 72 h (Figure 1d). In contrast, the expression of *ARACIN2* was not affected by BTH (Figure 1d). The MeJA-response of *ARACIN1* was biphasic: after 4 h, the expression of *ARACIN1* increased almost 3-fold and reached its first maximum after 8 h, returned to basal levels after 12 h and reached a second maximum after 24 h (Figure 1e). Again, the expression of *ARACIN2* remained unaffected.

Distinct spatial expression of *ARACIN1* and *ARACIN2* promoters

Expression characteristics were further explored by *GUS* histochemical staining of transgenic plants containing promoter-*GUS* fusions in which the *ARACIN1*/*ARACIN2* promoters (intergenic regions; 1343 bp and 841 bp, respectively) were transcriptionally fused to *GUS* (Karimi *et al.,* 2007; see Materials and Methods). Similar results were obtained with two independent transgenic lines. The expression patterns of *ARACIN1* and *ARACIN2* were spatially distinct. The expression of prom$_{ARACIN1}$:*GUS* was mainly detected in young developing leaves (Figure 2a), hydathodes (Figure 2b), immature flowers (Figure 2c) and elongating pollen tubes (Figure 2d), whereas abundant expression levels of prom$_{ARACIN2}$:*GUS* occurred in young and mature trichomes, stomatal guard cells, hydathodes, the shoot apical meristem, leaf primordia and the hypocotyl (Figure 2e), and emerging lateral roots (Figure 2f). In flowers, prom$_{ARACIN2}$:*GUS* expression was found in the anther-filament junction region, female gametophytes (Figure 2g,h) and the stigma (Figure 2g).

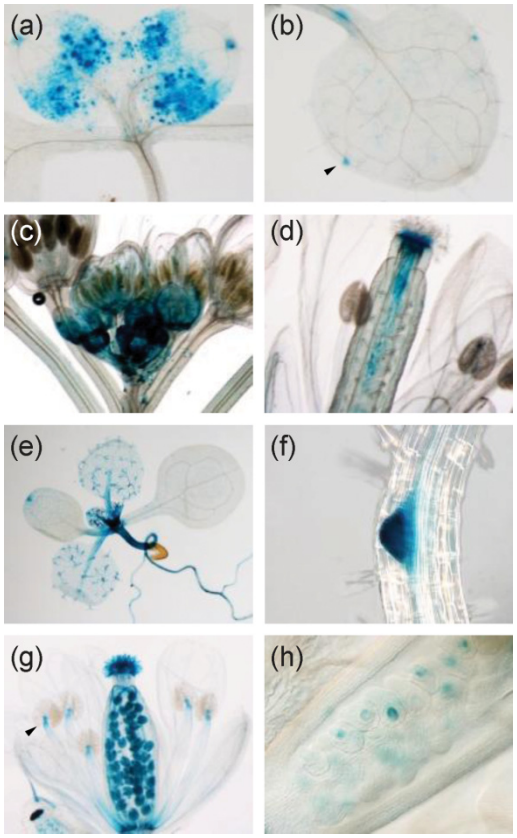

Figure 2. Tissue- and cell-specific expression of *ARACIN1* and *ARACIN2* visualized by histochemical GUS staining.
(a-d) prom$_{ARACIN1}$:*GUS* expression was mainly found in young developing leaves (a), hydathodes (b, indicated by an arrow), young developing flowers (c) and in the pollen tube (d).
(e-h) prom$_{ARACIN2}$:*GUS* displayed a strong expression in leaf trichomes, stomata, hydathodes, the shoot apical meristem, leaf primordia, the hypocotyl (e) and emerging lateral roots (f). In flowers, prom$_{ARACIN2}$:*GUS* expression was found in the junction region between anther and filament (g, indicated by an arrow), female gametophytes (g, h) and the stigma (g).

ARACINS are Brassicaceae-specific paralogs

ARACIN1 and *ARACIN2* are positioned in tandem on the complement strand of chromosome 5 and are organized in two exons separated by one intron (The Arabidopsis Information resource (TAIR); http://www.arabidopsis.org/; Figure 3a). The open reading frames (ORFs) of *ARACIN1* and *ARACIN2* are short (192 and 249 nucleotides, respectively), share 80% coding sequence (CDS) identity (Figure 3b) and encode peptides of 76 (8.2 kDa) and 82 amino acids (8.9 kDa), respectively (Figure 3c).

The current genome annotation (TAIR10) indicated a 57-nucleotide difference in the length of the CDS between *ARACIN1* and *ARACIN2*, with *ARACIN1* being shorter at the 5' side (Figure 3b). Within the upstream region adjacent to the start codon of *ARACIN1*, a sequence was found that was highly similar to the first 54 nucleotides of the CDS of *ARACIN2*. Because of this high level of identity and the presence of a start codon preceded by an adequate Kozak consensus sequence, we assumed a misannotation (Figure 3b). To determine the exact mRNA length of *ARACIN1*, a 5' rapid amplification of cDNA ends (RACE) with gene-specific primers was done. As expected, RACE fragments were obtained that contained this similar region, strengthening our assumption that this upstream sequence probably is part of the CDS (Figure S1).

Next, we assessed the presence of *ARACIN1* and *ARACIN2* in other plant genomes by using the PLAZA comparative genomics tool (Proost *et al.*, 2009; http://bioinformatics.psb.ugent.be/plaza/)

and by blasting the *Brassica rapa* (turnip) genome using the Brassica Database (BRAD; http://brassicadb.org/brad/index.php/). PLAZA 2.5 integrates structural and functional annotations of 25 species: 13 dicots, 5 monocots, 2 (club-)mosses and 5 algae. Comparative analysis revealed orthologs of *ARACIN1* and *ARACIN2* in *Arabidopsis lyrata* (Al7g33690 and Al7g33670, respectively; Figure S2a) and *B. rapa* (Figure S2b). Interestingly, multiple protein sequence alignments clearly showed that the *ARACIN1* ortholog Al7g33690 contained this additional sequence, again supporting our hypothesis that the annotation of Arabidopsis *ARACIN1* was incorrect (Figure S2a).

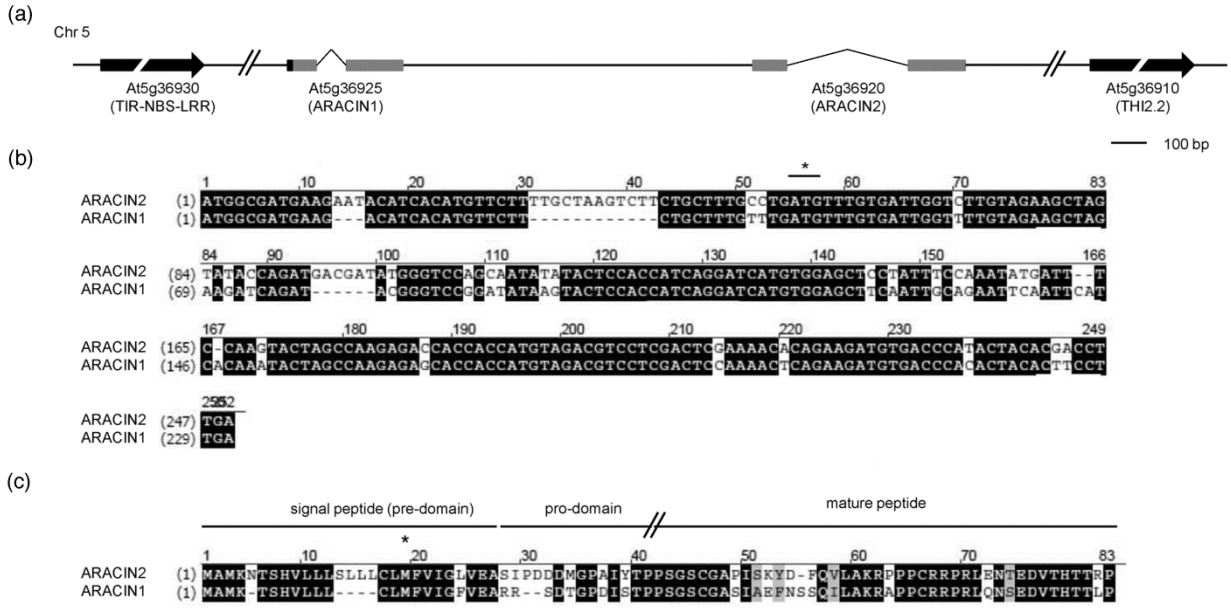

Figure 3. Sequence characteristics of *ARACIN1* and *ARACIN2*.

(a) Genomic position and gene organization of *ARACIN1* and *ARACIN2*. The 5' region upstream region of *ARACIN1* that has a high sequence identity with the 5' CDS of *ARACIN2*, is depicted by a black box.

(b) Sequence analysis revealing a 54-nucleotide sequence upstream of the annotated start codon (asterisk) of *ARACIN1* that is highly similar to the 5' CDS of *ARACIN2*.

(c) Sequence alignment of the translated full length ARACIN1 with the protein sequence of ARACIN2. The predicted signal peptide (SignalP 3.0; Emanuelsson *et al.*, 2007), the first methionine according to the TAIR annotation (asterisk), the prodomain and the highly converved C-terminal domain (see further) are indicated. Identical and similar residues are shaded black and grey, respectively. Sequence data were retrieved from The Arabidopsis Information Resource (TAIR10; http://www.arabidopsis.org/). CDS, coding sequence.

ARACIN1 and ARACIN2 are targeted to the ER

Previously, we demonstrated that the N-terminal green fluorescent protein (GFP) fusion of ARACIN1 without the similar upstream sequence (designated Δ *ARACIN1*) localizes to the nucleus and cytosol (Inzé *et al.*, 2012 – Chapter 2). Constitutive overexpression of this GFP-tagged nucleosolic version of ARACIN1 led to a drastic phenotype characterized by a severe loss in apical dominance resulting in a small bushy stature, thick and contorted leaves and a delayed flowering time (Figure S3a-d).

In silico prediction with SignalP3.0 (Emanuelsson *et al.*, 2007) deduced the presence of a signal peptide in ARACIN2 for targeting to the endoplasmic reticulum (ER; Figure 3c), whereas Δ *ARACIN1* was predicted as cytosolic. However, addition of the 5' similar sequence (see above) to the CDS of *ARACIN1* led to the formation of an intact N-terminal signal peptide (Figure 3c).

To determine the subcellular localization of full length ARACIN1 and ARACIN2, their ORFs were fused in frame with *GFP* at the C-terminus and placed under control of the constitutive cauliflower mosaic virus 35S (CaMV35S) promoter (Figure 4a). The subcellular localization was assessed in at least two independent and stable transgenic Arabidopsis plants. As expected, the addition of the 5' similar sequence altered the subcellular localization of ARACIN1 (Figure 4b): Both localization patterns of ARACIN1-GFP (Figure 4b, panels 1-2) and ARACIN2-GFP (Figure 4b, panels 3-4) showed characteristic features of the ER such as a reticular pattern and the perinuclear ring, indicating that both ARACIN1 and ARACIN2 are presumably targeted to the ER. Both peptides contained no ER retention signals, suggesting they are probably secreted into the extracellular matrix. Interestingly, while the expression of the nucleocytosolic-targeted *GFP-* Δ *ARACIN1* drastically perturbed normal growth and development (Figure S3a-d), constitutive ER-localized *ARACIN1-GFP* overexpression plants looked phenotypically similar to the wild type (data not shown). Mistargeting of ARACIN1 could perturb the cellular homeostasis which, in turn, could lead to pleiotropic defects in normal growth and development. In the case of *ARACIN2-GFP* overexpression, only one GFP-positive transgenic Arabidopsis line could be obtained. Strikingly, this line showed a similar phenotype as the *GFP-*Δ *ARACIN1*^{OE} (Figure S3e-f) and *ARACIN2*^{OE} lines (see further).

ARACINS share several characteristics with AMPs

Both ARACINS share some key structural characteristics with AMPs. First, ARACIN1 and ARACIN2 are small (8.2 and 8.9 kDa), hydrophobic (39% and 40% total hydrophobic ratios) and cationic (+4 and +2 total net charge) peptides. These features are prerequisite for the antimicrobial activity of AMPs that is mainly based on their ability to disturb the pathogen's membrane via electrostatic and hydrophobic interactions (Shai, 2002; Thevissen *et al.*, 2003). Like nearly all AMPs, *ARACIN1* and *ARACIN2* have a defined exon/intron structure, with the first exon encoding the signal peptide for targeting to the

secretory pathway and the second exon coding for the mature peptide (Silverstein *et al.*, 2005; Figures 3a and 4b).

AMPs are often produced as prepropeptides in which the predomain functions as a signal peptide that is removed during secretion. The prodomain is often acidic and thought to neutralize and, thus, inactivate the basic mature peptide when it is still intracellular. Once secreted, this propeptide is proteolytically removed, thereby activating the mature peptide (García-Olmedo *et al.*, 1998 – Chapter 4). As the C-terminal regions of both ARACIN peptides were highly conserved (Figure 3c), they could represent the mature domains necessary for antimicrobial activities. The putative prodomains of ARACIN1 and ARACIN2, that are flanked by their predomain (signal peptide) and mature domain, are acidic (pI 5.96 and 3.42, respectively) and, thus, these regions could function in the neutralization of the cationic mature domain (pI 8.96 and 9.38, respectively). The biochemical properties of these putatively different forms are given in Table 1.

Table 1. Peptide characteristics of the putatively different forms of ARACIN1 and ARACIN2.

Name	Sequence	Length (AA)	Molecular weight (kDa)	Hydrophobic ratio	Net charge	pI
preproARACIN1	MAMKTSHVLLLCLMFVIGFVEARRSDTGPDIS TPPS**GSCGASIAEFNSSQILAKRAPPCRRPRL QNSEDVTHTTLP**	76	8.2	39%	+4	8.66
proARACIN1	RRSDTGPDISTPPS**GSCGASIAEFNSSQILAKR APPCRRPRLQNSEDVTHTTLP**	54	5.7	25%	+3	8.95
mARACIN1	**GSCGASIAEFNSSQILAKRAPPCRRPRLQNSE DVTHTTLP**	40	4.2	32%	+3	8.96
preproARACIN2	MAMKNTSHVLLLSLLLCLMFVIGLVEASIPDD DMGPAIYTPPS**GSCGAPISKYDFQVLAKRPPP CRRPRLENTEDVTHTTRP**	82	8.9	40%	+2	6.70
proARACIN2	SIPDDDMGPAIYTPPS**GSCGAPISKYDFQVLA KRPPPCRRPRLENTEDVTHTTRP**	55	5.9	25%	+1	6.49
mARACIN2	**GSCGAPISKYDFQVLAKRPPPCRRPRLENTE DVTHTTRP**	39	4.3	25%	+4	9.38

The total hydrophobic ratio, total net charge and isoelectric point (pI) of the putative different forms of ARACIN1 and ARACIN2 were calculated with the peptide predictor tool of the Antimicrobial Peptide Database (ADP; http://aps.unmc.edu/AP/main.php/; Wang and Wang, 2004). The sequence length and molecular weight are indicated in number of amino acids (AA) and in kDa, respectively. The predicted signal peptide (SignalP 3.0; Emanuelsson *et al.*, 2007) is underlined and the sequence of the putative mature peptide is indicated in bold. kDa, kilodalton.

To assess whether ARACINs are processed *in vivo*, we immunodetected GFP-tagged peptides in two independent transgenic Arabidopsis *ARACIN1-GFP*^{OE} and *ARACIN2-GFP*^{OE} plants (Figure 4c). In the case of ARACIN1-GFP, the anti-GFP antibody recognized four protein bands that correspond in size with the putative preproARACIN1-GFP (~35 kDa), the proARACIN1-GFP (~30 kDa), the mature ARACIN1-GFP (~31 kDa) and free GFP (~27 kDa). This was also the case for ARACIN2-GFP. The mature ARACIN1 and ARACIN2 domains had an estimated size of approximately 4 kDa, of which the size is similar to that of the conserved C-terminal region (Figure 4c and Table 1).

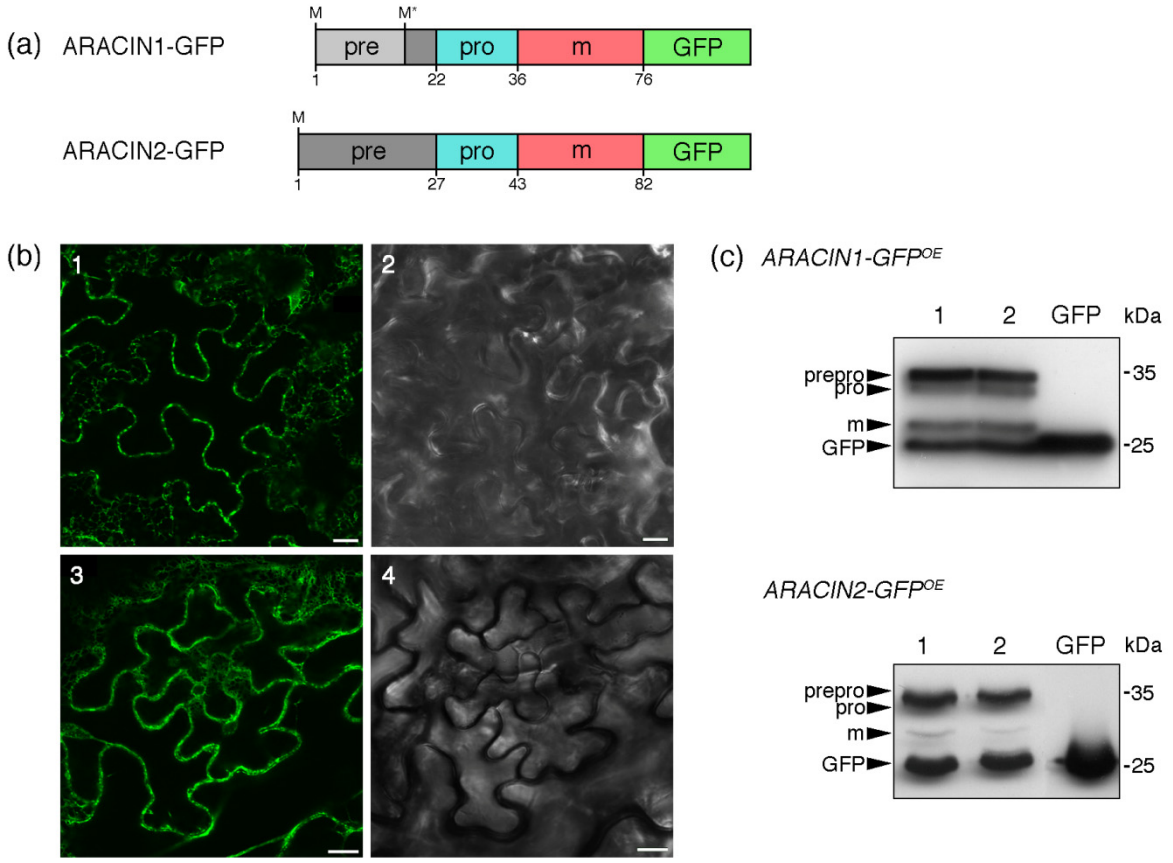

Figure 4. Subcellular targeting and processing of ARACIN1 and ARACIN2.

(a) Schematic representations of the expressed GFP-tagged peptides with their putative prepropeptide structure used to determine the subcellular localization and processing of ARACIN1 and ARACIN2 in transgenic Arabidopsis lines. The 5' upstream similar sequence of ARACIN1, that is part of the N-terminal signal peptide (pre-domain), is indicated in grey. The first methionine (M) of ARACIN1 according to the TAIR10 annotation (The Arabidopsis Information Resource; http://www.arabidopsis.org/) is indicated with an asterisk.

(b) Subcellular localizations of the GFP-tagged ARACIN peptides in 2-week-old Arabidopsis transgenic *ARACIN1-GFP*^{OE} (panels 1-2) and *ARACIN2-GFP*^{OE} (panels 3-4) lines. GFP fluorescence (1,3) and bright-field images (2,4) are depicted. Scale bars, 10 μm.

Figure 4. Subcellular targeting and processing of ARACIN1 and ARACIN2. *(Continued).*
(c) Western blot analysis of leaf extracts of 2-week-old independent (1,2) and stable transgenic *ARACIN1-GFP*^{OE} (above), *ARACIN2-GFP*^{OE} (below) and *GFP*^{OE} lines using an anti-GFP antibody. The different forms (prepro, pro and mature (m)) are indicated. GFP, green fluorescent protein; kDa, kilodalton.

Secondary structure prediction with the Protein/Homology/analogY Recognition Engine (PHYRE) web server (Bennett-Lovsey *et al.*, 2008; Kelley and Sternberg, 2009), that uses template-based homology modeling to construct structural predictions, revealed the presence of two α-helices at the C-terminus of ARACIN1 (Figure S4a) and α and β contents in ARACIN2 (Figure S4c). Moreover, homology-based three-dimensional models of ARACIN1 and ARACIN2 were constructed with PHYRE2.0 (intensive mode; Figure S4d,e). Although no structural matches with a high confidence level could be detected, most predictions had a fold occurring in proteins with a putative defense role. ARACIN1 showed an approximately 42% similarity (best hit; confidence level of 11%) with the 48 amino acid residue neurotoxin-I of sea anemone (*Stichodactyla heliantus*; Structural Classification of Proteins (SCOP) code d2sh1a; Protein Data Bank (PDB) code 2SH1; Fogh *et al.*, 1990; Wilcox *et al.*, 1993) that belongs to the defensin superfamily (Figure S4b,d). Surprisingly, matches with ARACIN2 were predominantly protease inhibitors (data not shown).

Overexpression of *ARACIN1* and *ARACIN2* perturbs the expression of defense-related genes

To assess the effect of *ARACIN* overexpression on plant development, we made constitutive overexpression lines with the CaMV35S promoter. Northern blot analysis revealed that several independent transgenic lines contained elevated levels of the *ARACIN1*/*ARACIN2* transcripts (Figure 5a). Whereas all *ARACIN1*^{OE} lines were phenotypically similar to untransformed wild-type plants, overexpression of *ARACIN2* drastically affected growth and development (Figure 5b). After normal seed germination and cotyledon expansion, *ARACIN2*^{OE} plants showed a severely retarded growth, curled dark leaves and delayed flowering (Figure 5b), resembling the observed phenotype of the *ARACIN2-GFP*^{OE} line (Figure S3e-f). As constitutive expression of a defense gene often perturbs the expression of other defense-related genes (Eckardt, 2007), we assessed the expression of the SA-responsive marker genes*, PR-1* and *PR-5* and the MeJA-responsive marker genes *PDF1.2a*, *THI2.1* and *THI2.2* in the *ARACIN1*^{OE} and *ARACIN2*^{OE} lines. Quantitative reverse-transcription (qRT)-PCR analyses showed that *ARACIN* overexpression led to a distinct response of these marker genes. In almost all overexpression lines, *PDF1.2a*, *PR-1* and *PR-5* were up-regulated, whereas *THI2.1* and *THI2.2* were down-regulated (Figure 5c, panels 1-4).

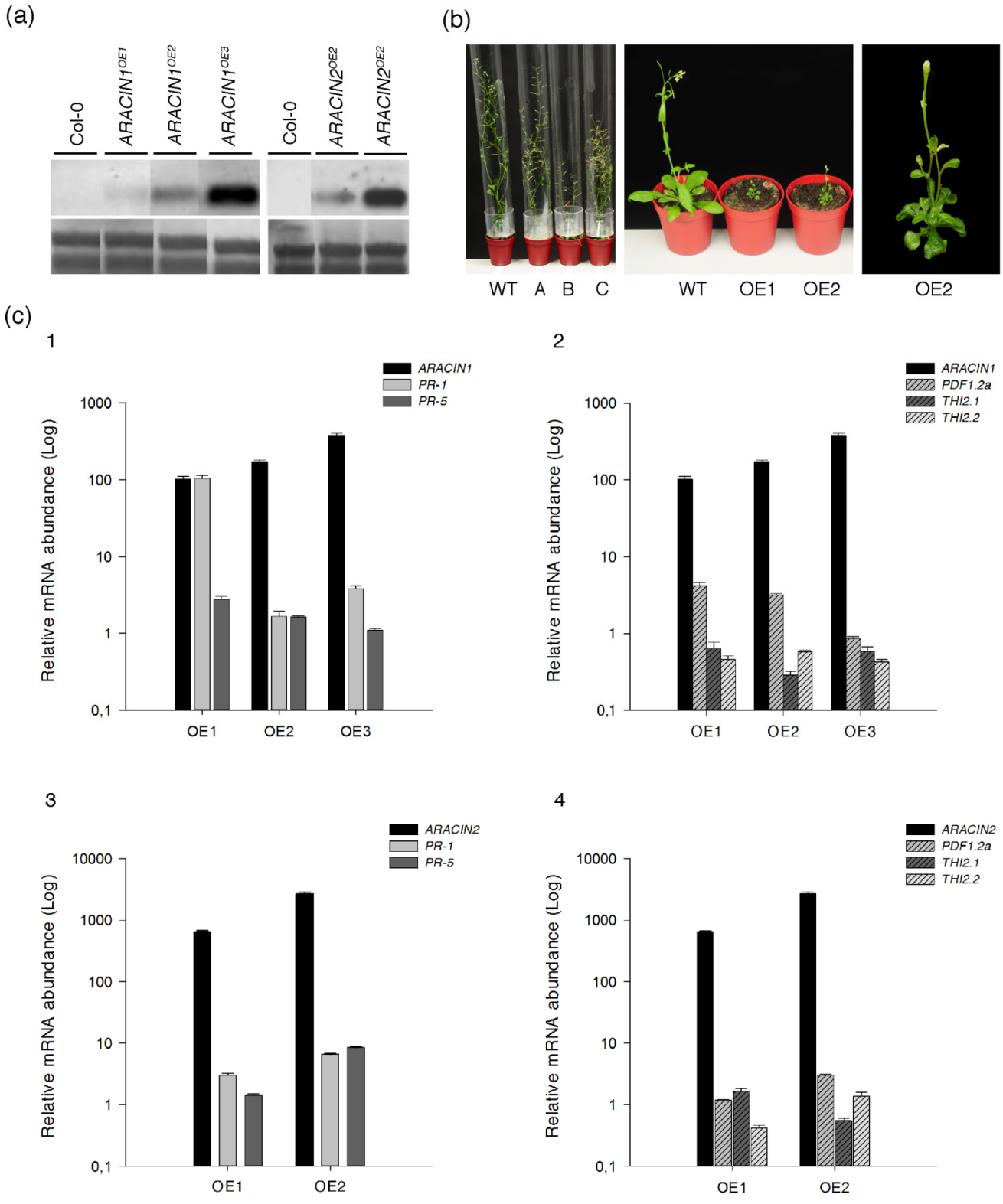

Figure 5. Expression analysis and phenotypes of the *ARACIN*^{OE} lines.

(a) Northern blot analysis of the *ARACIN1*^{OE} and *ARACIN2*^{OE} lines.

(b) Representative images of the *ARACIN1*^{OE} and *ARACIN2*^{OE} lines. (left) 1-month-old wild-type, one *ARACIN1*^{OE} (A) and two *ARACIN2*^{OE} (B,C) lines. (middle) 4-week-old wild-type and two independent *ARACIN2*^{OE} lines. (right) Enlarged image of a 4-week-old *ARACIN2*^{OE2} plant.

Figure 5. Expression analysis and phenotypes of the *ARACIN*^{OE} lines. *(Continued).*

(c) Relative abundance of *ARACIN1, ARACIN2, PR-1, PR-5, PDF1.2a, THI2.1* and *THI2.2* transcripts in two independent homozygous *ARACIN1*^{OE} (panels 1-2) and *ARACIN2*^{OE} (panels 3-4) lines. *ARP7* was used as an internal control and transcript abundance was normalized to the wild type. Values represent means ± SE (n=3).

ARACIN1 overexpression leads to a decreased sensitivity upon *A. brassicicola* and *B. cinerea* infections

To assess the effect of increased *ARACIN* levels on symptom development during fungal infection, we performed disease assays with the two necrotrophic pathogens *A. brassicicola* and *B. cinerea*. Because of the drastic phenotype of the *ARACIN2*^{OE} lines, no accurate scoring of disease symptoms was possible. Therefore, homozygous *ARACIN1*^{OE} plants from three independent transgenic events (Figure 5a) were assayed with *A. brassicicola* and *B. cinerea* B05-10 by drop inoculation ($5x10^5$ spores mL^{-1}) of 4-week-old Arabidopsis plants. Compared to the wild type, *ARACIN1*^{OE} lines had an increased resistance phenotype after inoculation with *A. brassicicola*. A drastic reduction of disease symptoms was visible four days after infection: the mean lesion size on leaves of the *ARACIN1*^{OE} overexpression lines was 50% smaller than that on wild-type leaves (Figure 6). Moreover, a statistically significant reduction in *Botrytis* lesion size was observed in the *ARACIN1*^{OE} lines (Figure 6).

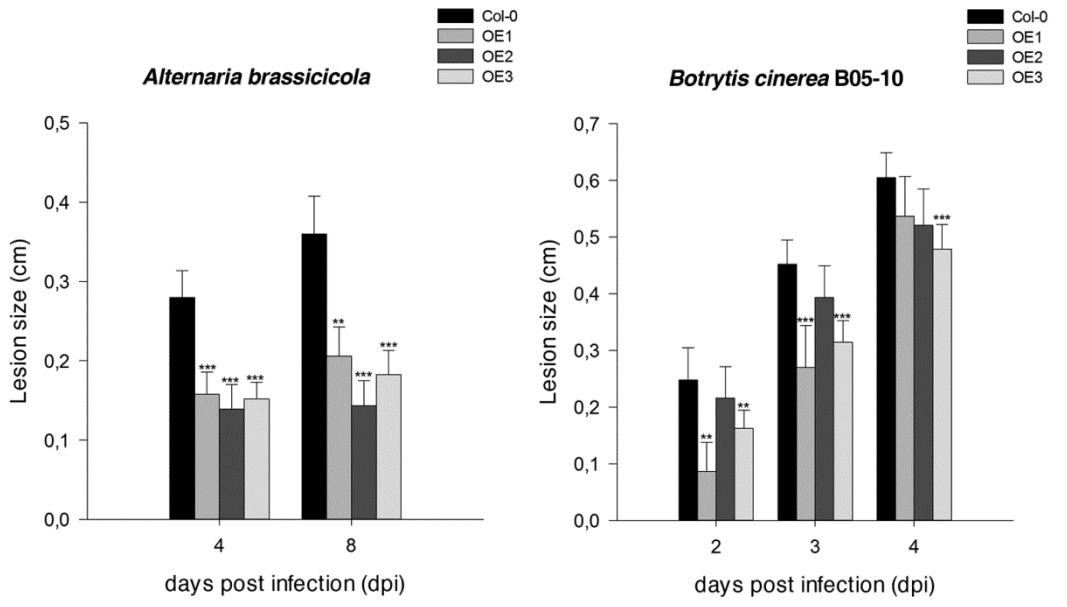

Figure 6. Decreased sensitivity upon *A. brassicicola* and *B. cinerea* infection by overexpression of *ARACIN1*.

Figure 6. Decreased sensitivity upon *A. brassicicola* and *B. cinerea* infection by overexpression of *ARACIN1*. *(Continued).*

Lesion sizes on leaves of wild-type plants and three independent *ARACIN1*^{OE} lines measured several days after inoculation with *A. brassicicola* and *B. cinerea* B05-10. Data presented are the means of at least 50 lesions. Error bars represent 95% confidence intervals (n=~50). For each assay, the average lesion diameter of wild-type and mutant plants were compared with a Student's t-test (*, $p < 0.05$; **, $p < 0.01$; ***, $p < 0.001$). The disease assays were done in duplicate, with similar results.

In vitro antifungal activity against *A. brassicicola* and *B. cinerea*

Next, we assessed the potential antifungal activity of ARACIN1 and ARACIN2 by an *in vitro* antifungal bioassay. Both propeptide and mature forms of ARACIN1 and ARACIN2 (Table 1) were produced by chemical synthesis (see Materials and Methods) and tested against *A. brassicicola*, *B. cinerea* B05-10 and *B. cinerea* Korea by means of a microtiter broth dilution assay (Figure 7 and Figure S5). Whereas proARACIN1 displayed no statistically significant inhibitory activities (data not shown), the mature form of ARACIN1 (mARACIN1) efficiently inhibited the growth of *A. brassicicola* starting at a concentration of 1 μg mL^{-1}, with a 50% growth inhibitory concentration (IC_{50}) value of 5.46 ± 0.57 μg mL^{-1}. Moreover, the growth of the strains B05-10 and Korea of *B. cinerea* was almost completely inhibited at a concentration of 10 μg mL^{-1} mARACIN1 (95.7% and 94%, respectively) with IC_{50} values of 3.05 ± 0.25 μg mL^{-1} and 2.03 ± 0.44 μg mL^{-1}, respectively. In the case of ARACIN2, proARACIN2 showed a statistically significant antifungal effect starting from 5 μg mL^{-1} (36.7% growth inhibition) against *A. brassicicola* (IC_{50} value 11.32 ± 1.28 μg mL^{-1}), and against the *B. cinerea* B05-10 and Korea strains at a higher concentration of 20 μg mL^{-1} (62% and 64.8% growth inhibition, respectively). As expected, the antifungal activity of ARACIN2 was dramatically increased when the acidic prodomain was not present: the IC_{50} value of mARACIN2 against *A. brassicicola* was significantly lower (1.55 ± 0.11 μg mL^{-1}; 86% reduction). Likewise, the antifungal activity of mARACIN2 against *B. cinerea* B05-10 and Korea was remarkably increased in comparison with proARACIN2 (Figure 7).

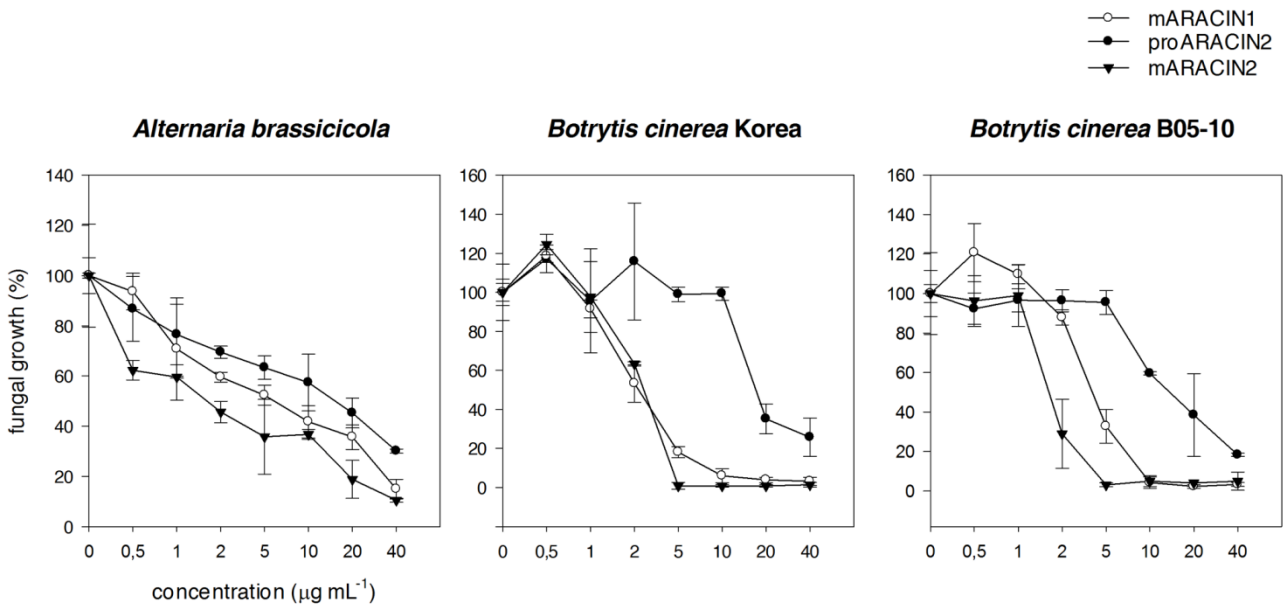

Figure 7. Inhibitory effects of mARACIN1, proARACIN2 and mARACIN2 on the growth of *A. brassicicola, B. cinerea* Korea and *B. cinerea* B05-10.

The data is represented as a mean ± SE (*n*=2). The antifungal assays were done in duplicate, with similar results.

DISCUSSION

Here, we have identified two novel cationic and hydrophobic peptides that share many characteristics with AMPs. Detailed expression analyses showed that the *ARACIN* genes are differentially regulated by abiotic and biotic stress conditions. It is well known that abiotic stresses, such as HL, high salinity, drought, low and high temperature, or wounding, can also modulate the expression of biotic defense-related genes, including plant AMPs (Hon *et al.*, 1995; Broekaert *et al.*, 2000; Zeier *et al.*, 2004; van Loon *et al.*, 2006; Seo *et al.*, 2008 – Chapter 4). *ARACIN1* and *ARACIN2* are induced by photorespiratory H_2O_2, a signaling molecule produced during abiotic and biotic stresses (Fujita *et al.*, 2006). Interestingly, *ARACIN1* is significantly induced by cold stress. The induction of plant AMPs during cold acclimation has been reported previously in winter cereals that can confer disease resistance in addition to freezing tolerance (Nakajima and Abe, 1996; Gaudet *et al.*, 1999). *ARACIN1* and *ARACIN2* have an opposite response during heat stress: while *ARACIN2* is slightly up-regulated, *ARACIN1* is significantly down-regulated. *ARACIN1* and *ARACIN2* are both induced in systemic leaves upon infection with the necrotrophic pathogen *B. cinerea*. Interestingly, the expression of *ARACIN2* - which remained unaffected during abiotic stresses - is highly induced in local infected leaves. We further demonstrated that BTH and MeJA play a role in the activation of *ARACIN1* expression, whereas *ARACIN2* transcript levels were not altered by these chemicals. In addition, the cell- and tissue-specific expression patterns of both genes are quite distinct. The differential transcriptional regulation of the *ARACIN*

genes could be attributed to their divergent promoters that have a low incidence and small overlap of *cis*-regulatory elements and, thus, these genes are probably under the control of different transcriptional regulators. Duplicated genes (i.e. paralogs) are only retained in the genome when they have acquired different or complementary functions (Tiffin and Moeller, 2006). Therefore, paralogs have often different expression patterns due to changes in the regulatory elements of their promoter region (Force *et al.*, 1999; Altschmied *et al.*, 2002; Prince and Pickett, 2002). Analysis of the 5' sequence upstream of the *ARACIN1* CDS for *cis*-acting regulatory elements revealed one putative MYC2-binding site (a CACATG sequence located at 849 nucleotides upstream of the *ARACIN1* start codon) that is absent in the *ARACIN2* promoter. MYC2 differentially regulates JA-responsive pathogen defense (including *PDF1.2a*) and wound response genes (Lorenzo *et al.*, 2004). Whereas the promoter of *ARACIN1* contains four clustered W-box elements (-255, -227, -208, and -149), the promoter of *ARACIN2* has only two dispersed W-box elements (-718 and -246). These W-box elements are bound with high affinity by WRKY transcription factors known to be involved in SA signaling and plant immunity (Pandey and Somssich, 2009). The presence of multiple MYC2 and W-box elements in the promoter of *ARACIN1* could explain its upregulation by MeJA and BTH.

Recently, 1789 Brassicaceae-specific genes (including the *ARACIN* genes) have been identified by a step-wise BLAST filtering approach and are characterized by their short peptide length (77 amino acids), few introns, low GC content, unknown function, few paralogs, enrichment for secretory peptides and increased evolutionary rates. Remarkably, these Brassicaceae-specific genes are enriched for defensin-like genes and other cysteine-rich peptides, such as defensins and thionins. These defensin-like genes show higher frequencies of tandem duplications, the major mechanism for the generation of lineage-specific genes. Furthermore, these genes are often responsive to biotic and abiotic stimuli (Donoghue *et al.*, 2011).

Both ARACINs share similarities in molecular properties, genome organization, precursor organization, spatial expression and function with plant AMPs. First, *ARACIN1* and *ARACIN2* encode small, cationic and hydrophobic peptides and are expressed in peripheral cell layers, such as stomata, hydathodes and roots tissues, representing the primary entry points for pathogens. In addition, both genes are expressed in reproductive tissues that are known to be enriched in AMPs (Jones-Rhoades *et al.*, 2007; Punwani *et al.*, 2007). As pollen are often coated with bacterial and fungal spores, AMPs are suggested to protect the female gametophyte during the fertilization phase (Cordts *et al.*, 2001). In addition, an alternative role for plant AMPs has been demonstrated in *Torenia fournieri*, in which secreted defensin-like cysteine-rich polypeptides act as pollen tube attractants (Okuda *et al.*, 2009). In this respect, it is interesting to note that *ARACIN1* and *ARACIN2* are expressed in the pollen tube and in the female gametophyte, respectively.

Within the Arabidopsis genome, both genes are positioned in tandem and are flanked by pathogen defense-related genes. The gene encoding a disease resistance protein belonging to the Toll/Interleukin1 receptor-nucleotide-binding site-leucine-rich repeat (TIR-NBS-LRR) class is positioned upstream of *ARACIN1* and a thionin gene (*THI2.2*) is positioned downstream of *ARACIN2*. NBS-LRR resistance genes are part of a large multigene family that might be involved in the first line detection of pathogens (McHale *et al.*, 2006). Defense-related genes are often positioned in gene clusters allowing a coordinated expression when plant defense is activated (Eckardt, 2007). Moreover, genes that are up-regulated during biotic stress, including cysteine-rich AMPs, expanded largely by tandem duplications (Silverstein *et al.*, 2005; Hanada *et al.*, 2008). *ARACIN1* and *ARACIN2* share the same exon/intron structure as AMPs in which the first exon encodes the signal peptide and the second a charged mature peptide (Silverstein *et al.*, 2005). Both ARACIN1 and ARACIN2 contain functional signal peptides and are targeted to the ER. Since both peptides lack ER retention signals, they are presumably targeted to the extracellular space, concomitant with their antifungal activity during fungal infection. As the fluorescent properties of GFP are lost in the apoplast due to an acidic pH, we could not directly imply that the ARACIN-GFP peptides are secreted into the extracellular matrix. Therefore, additional experiments are necessary to determine their exact localization. To circumvent the problems associated with the detection of GFP-tagged proteins in the apoplastic space, fusions with the yellow fluorescent protein (YFP) Venus, a pH-insensitive variant of GFP, will enable the detection of both ARACIN-GFP peptides in the extracellular environment. In addition, immunodetection of GFP-tagged ARACIN peptides in extracellular protein extracts isolated from GFP-tagged *ARACIN* overexpression plants could be decisive whether the ARACIN peptides are secreted into the apoplastic space. We could further demonstrate that ARACIN1 and ARACIN2 are produced as prepropeptides, which is often the case for AMPs (García-Olmedo *et al.*, 1998 – Chapter 4). The basic mature domain is frequently preceded by an anionic prodomain that might function in the neutralization and, thus, inactivation of the mature peptide when it is still intracellular. Once secreted, this prodomain is proteolytically removed from the mature domain. Although the exact cleavage sites and hence the lengths of the mature domains of the ARACIN peptides have not been determined yet, we demonstrated that both ARACIN peptides are cleaved into a smaller peptide of approximately 4 kDa, possibly corresponding to the highly conserved basic C-terminal region that represents the mature peptide. The sequence between the signal peptide and the mature domain is acidic and could function as a neutralizing prodomain. The exact nature of the different domains of both ARACINS needs to be determined by amino acid sequencing of the bands observed in the *ARACIN1-GFP* and *ARACIN2-GFP* overexpression lines.

Homology-based structure modeling (PHYRE; Bennett-Lovsey *et al.*, 2008; Kelley and Sternberg, 2009) predicted the secondary and tertiary structure of both ARACIN peptides. Although the

confidence level of the structural matches was low, many of them have a putative role in defense. AMPs are rapidly evolving molecules due to pressure imposed by competition among phytopathogens (Silverstein *et al.*, 2005). In other words, the sequence conservation between AMPs is rather limited and, therefore, may explain why only structural matches were retrieved with a low confidence level. Nevertheless, ARACIN1 matched best with neurotoxin-I of sea anemone that belongs to the defensin superfamily and acts on neuronal voltage-gated sodium channels of Crustaceae (Fogh *et al.*, 1990; Wilcox *et al.*, 1993). In contrast with ARACIN1, ARACIN2 retrieved predominantly matches with protease inhibitors. Several examples are known of AMPs with a protease-inhibitory activity (Kim *et al.*, 2009 – Chapter 4). In response to pathogen attack, plants secrete inhibitory peptides that inactivate the proteinases produced by phytopathogenic microorganisms (Ryan, 1990). Several structural categories are recognized within AMPs: (i) linear peptides that form α-helices in contact with membranes; (ii) disulfide bridge-stabilized peptides with mainly β-structural elements; and (iii) linear non-helical forming peptides usually with a high occurrence of certain amino acids, often proline, glycine, histidine, arginine, tryptophan or cysteine (Zasloff, 2002; Boman, 2003). As both ARACIN1 and ARACIN2 lack the characteristic multiple cysteine residues necessary for the stabilization of the typical three-dimensional fold of many AMPs, they are probably linear. In other eukaryotes, various examples are known of AMPs without or with few cysteine residues (Boman, 2003).

We further assessed the potential of both ARACIN peptides to protect plants against necrotrophic pathogens. Transgenic Arabidopsis plants with constitutive *ARACIN1* overexpression displayed an enhanced resistance against the necrotrophs *A. brassicicola* and *B. cinerea*. Although *A. brassicicola* is considered an incompatible fungal pathogen of Arabidopsis, the molecular basis behind the restriction of the *A. brassicicola* infection is of great interest. An incompatible Arabidopsis - *A. brassicicola* interaction triggers a strong systemic response inducing the up-regulation of the defense genes *PR-1* and *PDF1.2a* (Penninckx *et al.*, 1996). The current knowledge about the molecular mechanisms underlying the interaction between *A. brassicicola* and members of the Brassicaceae family remains rather limited. Several studies have identified important players of the incompatible interaction of the Arabidopsis - *Alternaria* pathosystem, including antimicrobial compounds (Thomma *et al.*, 1999; Schenk *et al.*, 2003; Oh *et al.*, 2005; Schuhegger *et al.*, 2006; Nafisi *et al.*, 2007). In addition, *in vitro* antifungal bioassays with chemically synthesized mARACIN1, proARACIN2 and mARACIN2 revealed their antifungal activities against *A. brassicicola*, *B. cinerea* B05-10 and *B. cinerea* Korea. Moreover, we demonstrated that the removal of the prodomains of ARACIN1 and ARACIN2 significantly improved their antifungal activity against these pathogens and, thus, we might have identified the minimal domains necessary for their antimicrobial activity.

Particularly prominent were the drastic phenotypes of the *ARACIN2*^{OE} lines. It is well known that constitutive expression of defense-related genes can be autotoxic and/or energetically costly, often leading to a decrease in fitness-relevant processes such as growth and reproduction (Bolton, 2009). Indeed in both *ARACIN1*^{OE} and *ARACIN2*^{OE} plants, the SA-dependent expression of *PR-1*, *PR-5* and the MeJA marker gene *PDF1.2a* was up-regulated, and the expression of *THI2.1* and *THI2.2* was down-regulated. Because antimicrobial activities of PR-1 and PR-5 against many pathogens have been shown previously (Fritig *et al.*, 1998; Coca *et al.*, 2000; Shatters *et al.*, 2006), the enhanced resistance of the *ARACIN1*^{OE} line could also be due to a signaling effect (Ryan *et al.*, 2007), although a clear direct antifungal activity of mARACIN1 has been shown *in vitro*.

Several examples are known where AMP overexpression conferred enhanced tolerance to abiotic stresses (Mirouze *et al.*, 2006; Lee and Hwang, 2009). As *ARACIN1* is transcriptionally regulated by abiotic stresses, we assessed whether the *ARACIN1*^{OE} lines displayed an improved tolerance against salt stress (50 and 100 mM NaCl) and oxidative stress (2 μM methyl viologen). However, no statistical significant differences (scored by measuring root growth and leaf area) were found (data not shown).

In conclusion, we characterized two novel Brassicaceae-specific peptides displaying antifungal activities against necrotrophic pathogens. *In planta* modulation of *ARACIN1* expression levels enhances the resistance against these pathogens. Both ARACIN1 and ARACIN2 share many characteristics with AMPs, but are structurally unrelated to known plant AMPs. As plant diseases caused by *A. brassicicola* and *B. cinerea* infections result in major crop losses, the usage of ARACIN peptides in transgenic Brassicaceae species could be an alternative strategy to improve disease resistance.

MATERIALS AND METHODS

Plant growth conditions and treatments

For *in vitro* experiments, *Arabidopsis thaliana* (L.) Heynh ecotype Columbia (Col-0) plants (wild type) were, unless stated otherwise, grown until stage 1.04 (4^{th} leaf 1 mm in size; Boyes *et al.*, 2001) on half-strength (½) Murashige and Skoog (MS) medium (Duchefa Biochemie; http://www.duchefa.com/), 1% (w/v) sucrose, 0.7% (w/v) agar, pH 5.7 at 21°C and under a 16-h light/8-h dark photoperiod, 150 μmol $m^{-2}s^{-1}$ light intensity and 50% relative humidity. The HL treatment was done according to experimental details described by Vanderauwera *et al.* (2011). For the salt stress experiment, plants were grown for two weeks on regular medium or on medium containing 50 mM NaCl. For the cold stress treatment, 3-week-old plants were transferred to 4°C in a controlled environment chamber (Weiss technik; http://www.weiss-gallenkamp.com/) and a pool of ten plants was harvested at each time point, whereas for the heat stress experiment, plants were transferred to a thermostat cabinet (Lovibond; http://www.lovibond.com/) at 37°C and three pools of 35 plants were harvested at each time point. For the BTH treatment, plants were sprayed with 350 μM BTH (BION® 50 WG, a gift from Syngenta Agro S.A. Spain) or with water (mock), whereas for the MeJA treatment, plants were sprayed with 100 μM MeJA containing 0.001% (v/v) Triton X-100 or with 0.001% (v/v) Triton X-100 in water (mock). A pool of 32 plants was harvested at each time point for each treatment. Two independent experiments were carried out for all treatments (independent sets of plants sown and treated on different dates).

5' rapid amplification of cDNA ends (RACE)

Total RNA was extracted from wild-type plants with TRI Reagent (Molecular Research Center; http://www.mrcgene.com/). 5' RACE-ready cDNA was made with the supplied Smart II oligo and Powerscript reverse-transcriptase (BD SMART™ RACE cDNA Amplification Kit; BD Biosciences; http://www.bdbiosciences.com/) and the reaction was run with the gene-specific primers (Table S1) and the supplied universal primer mix. Nested PCR reaction products were gel-purified with the Nucleospin gel extraction kit (Macherey and Nagel; http://www.mn-net.com/) and sequenced after cloning into the pENTR/D-TOPO vector (Invitrogen; http://www.invitrogen.com/).

Production of transgenic lines

Full-length ORFs (with and without stop codon) were PCR-amplified from first-strand cDNA of wild-type plants with the high-fidelity Phusion DNA polymerase (Finnzymes OY; http://www.finnzymes.fi/) with gene-specific primers extended with *attB* sites for subsequent Gateway cloning into pDONR221 (Invitrogen; Table S1). *GFP* fusions were constructed within the binary destination vector pK7FWG2

(Karimi *et al.*, 2007), resulting in a C-terminal *GFP* fusion under the control of the CaMV35S promoter. Overexpression clones were generated within the binary destination vector pK7WG2 (Karimi *et al.*, 2007). To obtain promoter-*GUS* fusion constructs, the intergenic regions of *ARACIN1* (1343 bp) and *ARACIN2* (841 bp) were PCR-amplified from genomic DNA with promoter-specific primers extended with *attB* sites for subsequent Gateway cloning (Table S1). PCR fragments were cloned into Gateway entry vectors and subcloned into the binary destination vector pKGWFS7 (Karimi *et al.*, 2007). All constructs were transformed to the *A. tumefaciens* strain C58C1 harboring the virulence plasmid MP90. Arabidopsis wild-type plants were transformed via *A. tumefaciens* floral dip (Clough and Bent, 1998). Homozygous lines with a single T-DNA locus were selected via segregation analysis and transgene expression was monitored via Northern analysis and qRT-PCR analysis for the overexpression lines, GFP fluorescence for the *GFP* fusion lines or GUS staining for the promoter-*GUS* lines.

Fluorescence microscopy

For fluorescence microscopy, a confocal microscope 100M with software package LSM 510 version 3.2 was used (Zeiss; http://www.zeiss.com/), equipped with a 63x water-corrected objective (numerical aperture 1.2) to scan the leaf epidermis and underlying cell layers. GFP fluorescence was imaged in a single channel setting with 488 nm for GFP excitation.

Promoter GUS analyses

Transgenic 2-week-old seedlings grown *in vitro* on ½ MS plates or organs from mature plants grown in soil were harvested and incubated overnight in 90% acetone at 4°C. Acetone was removed and samples were washed with NT buffer (100 mM Tris, 50 mM NaCl and pH 7.0). Next, the NT buffer was replaced with a ferricyanide solution (0.2 mM ferricyanide in NT buffer) and samples were incubated in the dark at 37°C for at least 1 h. Afterwards, the ferricyanide solution was replaced with the GUS-staining solution containing 0.02 mM 5-bromo-4-chloro-3-indolyl-D-glucuronide in ferricyanide solution. Samples were placed in the dark at 37°C and incubated for 6 h or overnight and were stored in 100% lactic acid. Samples were photographed with a stereomicroscope (Stemi SV11; Zeiss) or with a Nomarski differential interference contrast microscope BX51 (Olympus; http://www.olympus.com/).

qRT-PCR analyses

For the abiotic stress expression analyses, RNA isolation, cDNA synthesis and qRT-PCR analyses were carried out as described in Vanderauwera *et al.*, 2007 with gene-specific primers (Table S1). For *ARACIN1* and *ARACIN2*, gene-specific primers were designed with the Beacon Designer™ software (PremierBiosoft; http://www.premierbiosoft.com/; Table S1). For the genes *PR-1*, *PR-5*, *PDF1.2a*,

THI2.1, *THI2.2* and *ARP7*, primers were designed with the Universal ProbeLibrary Assay Design center ProbeFinder software (Roche; https://www.roche-applied-science.com/; Table S1). *ARP7* was used as a reference gene. For the qRT-PCR analyses on *B. cinerea*-infected leaves, RNA extraction, DNase treatment, cDNA synthesis and qRT-PCR experiments were done as described by Mirouze *et al.*, 2006. *EF1-a* was used as a reference gene.

Protein extraction and western blot analyses

Total protein extracts were prepared by grinding leaf material (100 mg) in 200 µL extraction buffer (100 mM HEPES (pH 7.5), 1 mM EDTA, 10 mM β-mercaptoethanol and 1 mM phenylmethanesulfonylfluoride) and a protease inhibitor cocktail (COMPLETE; Roche). Insoluble debris was removed by centrifugation at 20800 x g for 15 min at 4°C. Protein concentrations were determined with the Bradford method (Zor and Selinger, 1996). Proteins (10 µg) were separated on a 12.5% SDS PAGE gel, transferred to a P membrane (Millipore, http://www.millipore.com/) and immunodetected with the Living Colors A.v. Monoclonal antibody (JL-8; Clontech Laboratories; http://www.clontech.com/) by means of the Western Lightning kit (GE-Healthcare; http://gehealthcare.com/).

Disease assays

Mutant and wild-type Arabidopsis plants were grown in soil (DCM "Zaai- en stekgrond"; De Ceuster Meststoffen N.V.; http://www.dcm.com/) in a growth chamber with at 21°C/18°C day/night time temperature, 75% relative humidity under a 12 h light/12 h dark photoperiod with a light intensity of approximately 120 µmol m^2s^{-1}. 4-week-old plants were inoculated with *A. brassicicola* strain MUCL20297 (Mycothèque Université Catholique de Louvain, Louvain-la-neuve, Belgium) or *B. cinerea* B05-10. To this end, a $2x10^7$ spores mL^{-1} solution of the pathogen was diluted in ½ (12 g L^{-1}) potato dextrose broth (PDB) in water to a final concentration of $5x10^5$ spores mL^{-1}. After spotting 5 µL of the diluted spore solution on two leaves per plant, the plants were placed in a humid chamber.

For the Botrytis infection expression analyes, eight leaves from noninoculated plants (control) and eight leaves from systemical or local infected leaves of inoculated plants were collected 48 h post infection. For each treatment, four replicas were harvested and frozen in liquid nitrogen.

For the disease assay, symptoms were scored by measuring and calculating the average diameters of the necrotic lesions on various days after pathogen inoculation (dpi). This disease assay was repeated twice with an average of 220 plants per assay. For each assay, the average lesion diameter on leaves of wild-type and mutant plants were compared with a Student's *t*-test.

In vitro antifungal activity assays

Chemically synthesized proARACIN1, mARACIN1, proARACIN2, mARACIN2 peptides were purchased (>98% purity) from Genscript (http://www.genscript.com/). Stock solutions of $2x10^7$ spores mL^{-1} of *A. brassicicola*, *B. cinerea* B05-10 and *B. cinerea* Korea were diluted in ½ PDB to a final concentration of $2x10^4$ spores mL^{-1}. After addition of 196-µL aliquots of these spore dilutions to 4 µL of 2-fold dilution series of proARACIN1, mARACIN1, proARACIN2 and mARACIN2 in DMSO (starting from a 100 µg mL^{-1} stock solution) in microtiter plates, the plates were incubated at 23°C for 48 h. DMSO was used as a negative control. Fungal growth was evaluated both microscopically and by measuring the OD_{600}. Each fungus was tested in duplicate in the microtiter plates and each assay was repeated twice. For each assay, the average background corrected OD_{600} of each dilution and the DMSO control were compared with a Student's *t*-test. Dose-response curves were calculated to obtain IC_{50} values. To this end, average background-corrected ODs were converted to percent inhibition, whereas doses were log transformed. Then, either the four parameter logistic model or a simple linear model was fitted to the data using the drc package in R (R Development Core Team, 2011). The choice of the model was determined by the shape of the dose-response curve.

ACKNOWLEDGEMENTS

We thank Dr. Martine De Cock and Dr. Annick Bleys for help in preparing the manuscript. We thank Dr. Cindy Martens for the comparative analysis in *B. rapa*. This work was supported by Ghent University (Multidisciplinary Research Partnership 'Ghent Bio-Economy' project no. 01MRB510Z), the Research Foundation-Flanders (G.0414.09N) and the Katholieke Universiteit Leuven (GOA research funding, project no. GOA/2008/11). A.I is a predoctoral fellow of the Research Foundation-Flanders.

SUPPLEMENTARY MATERIAL

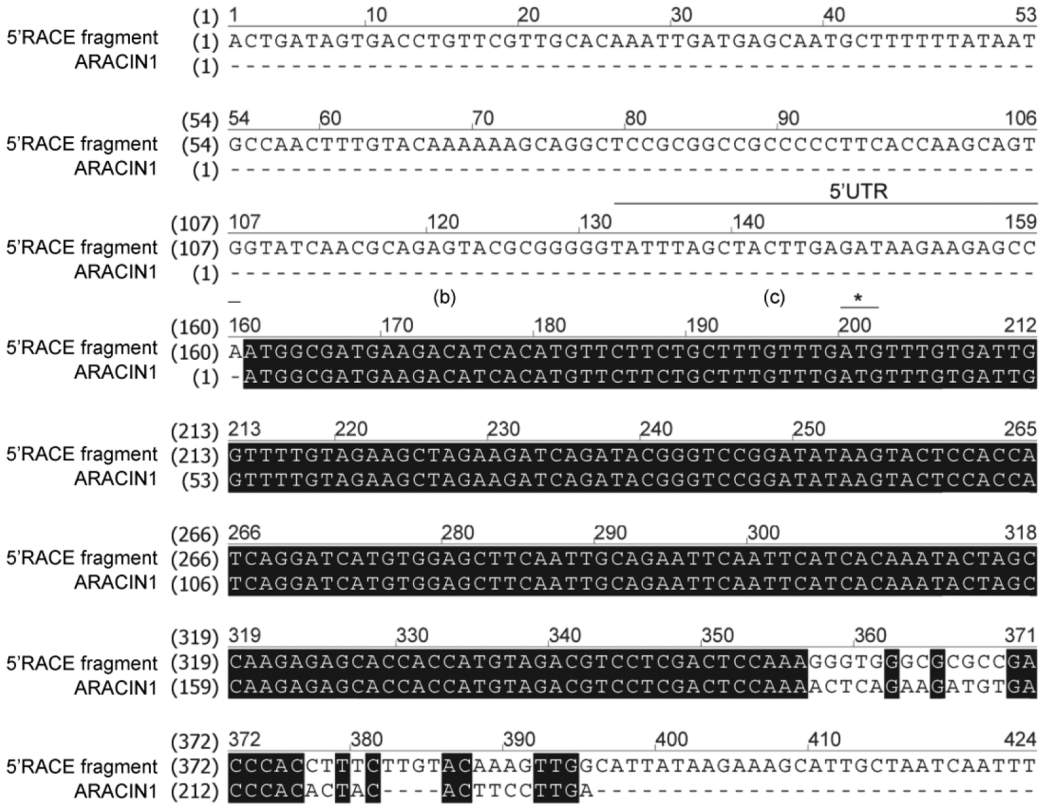

Figure S1. Alignment of the CDS of *ARACIN1* with a representative fragment obtained by 5' RACE analysis.

The CDS of *ARACIN1* extends up to 54 nucleotides at the 5' side of the start codon annotated by TAIR10 (indicated by an asterisk). The 5' UTR obtained by 5'RACE is 29 nucleotides long. Similar results were obtained with several independent 5' RACE fragments. CDS, coding sequence; RACE, Rapid Amplification of cDNA ends; UTR, untranslated region.

(a) Presence in *Arabidopsis lyrata*

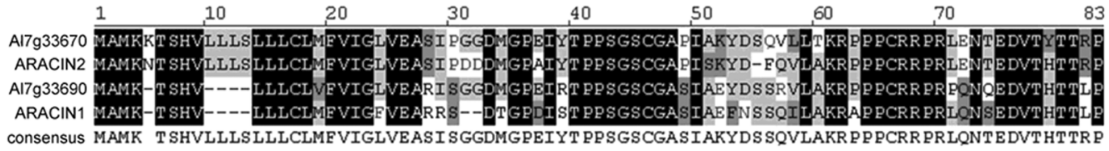

(b) Presence in *Brassica rapa*

```
Query= ARACIN2 full length CDS
       (249 nt)

>Scaffold000258 2010-07-14
          Length = 46842

 Score = 81.3 bits (171), Expect(2) = 4e-17
 Identities = 34/50 (68%), Positives = 37/50 (74%)
 Frame = +1 / +1


Query: 100   MGPAIYTPPSGSCGAPISKYDFQVLAKRPPPCRRPRLENTEDVTHTTRP* 249
          M P I TPPSGSCGA I+K D      R PPCRRPRL+N+EDVTHTT P*
Sbjct: 13072 MVPEISTPPSGSCGAAIAKDDSPQTLARRPPCRRPRLQNSEDVTHTTLP* 13221

>Scaffold000104 2010-07-14
          Length = 773703

 Score = 43.2 bits (88), Expect(3) = 1e-09
 Identities = 17/28 (60%), Positives = 21/28 (75%)
 Frame = +1 / -1


Query: 166  QVLAKRPPPCRRPRLENTEDVTHTTRP* 249
           +VLA+R PPCRRPRL+N    +H T P*
Sbjct: 9096 EVLARRSPPCRRPRLQNP*YTSHATVP* 9013


Query= ARACIN1 full length CDS
       (231 nt)

>Scaffold000258 2010-07-14
          Length = 46842

 Score = 57.0 bits (118), Expect(2) = 9e-18
 Identities = 22/23 (95%), Positives = 22/23 (95%)
 Frame = +1 / +1


Query: 163   RAPPCRRPRLQNSEDVTHTTLP* 231
          R PPCRRPRLQNSEDVTHTTLP*
Sbjct: 13153 RRPPCRRPRLQNSEDVTHTTLP* 13221

>Scaffold000104 2010-07-14
          Length = 773703

 Score = 82.6 bits (174), Expect(2) = 9e-17
 Identities = 33/54 (61%), Positives = 42/54 (77%)
 Frame = +1 / -1


Query: 70   RSDTGPDISTPPSGSCGASIAEFNSSQILAKRAPPCRRPRLQNSEDVTHTTLP* 231
           R +TGP I TPPSGSC   IA+ +SS++LA+R+PPCRRPRLQN    +H T+P*
Sbjct: 9174 RYETGPYIHTPPSGSCRGGIAKQDSSEVLARRSPPCRRPRLQNP*YTSHATVP* 9013
```

Figure S2. Presence of *ARACIN1* and *ARACIN2* in other members of the Brassicaceae family.

(a) Multiple protein sequence alignment of ARACIN1 and ARACIN2 with the *A. lyrata* orthologs (Al7g33690 and Al7g33670, respectively) identified with the PLAZA comparative genomics tool (Proost *et al.*, 2009). Identical and similar residues are shaded black and grey, respectively.

(b) Multiple sequence alignments of *ARACIN1* and *ARACIN2* with the *B. rapa* orthologs identified using the Brassica Database (BRAD; http://brassicadb.org/brad/index.php/).

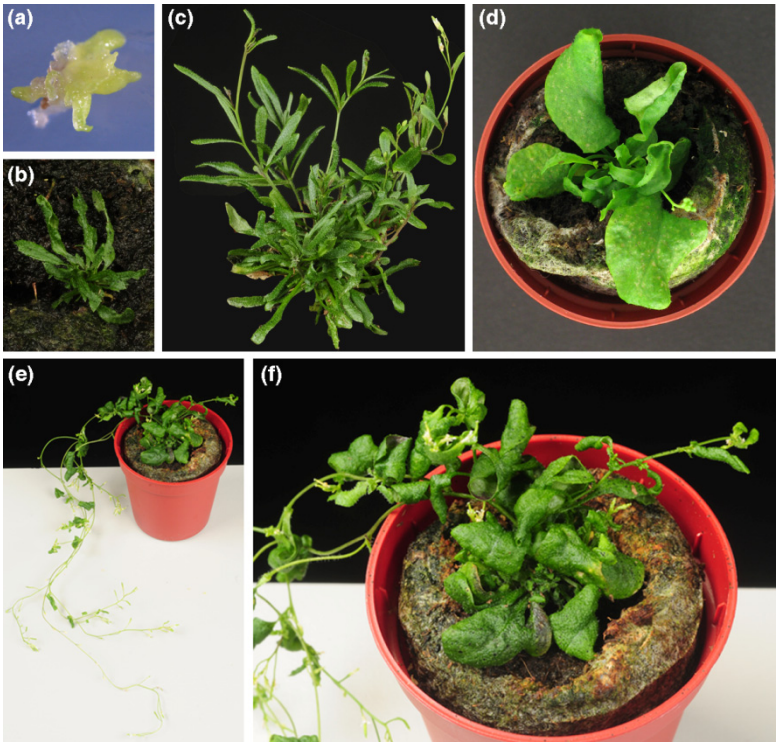

Figure S3. Several independent GFP-positive transgenic lines that constitutively express *GFP-Δ ARACIN1* or *ARACIN2-GFP* and displayed severe abnormal morphologies.

(a) 2-week-old primary *GFP-Δ ARACIN1*^{OE} transformant with a callus-like morphology.

(b,c) primary *GFP-Δ ARACIN1*^{OE} transformant (b, 50-day-old; c, 94-day-old) with bushy stature, thick contorted leaves and seedless siliques.

(c) 3-week-old primary *GFP- Δ ARACIN1*^{OE} line displaying a loss in apical dominance and curled leaves.

(e,f) Unique GFP-positive *ARACIN2-GFP*^{OE} plant with severe developmental defects.

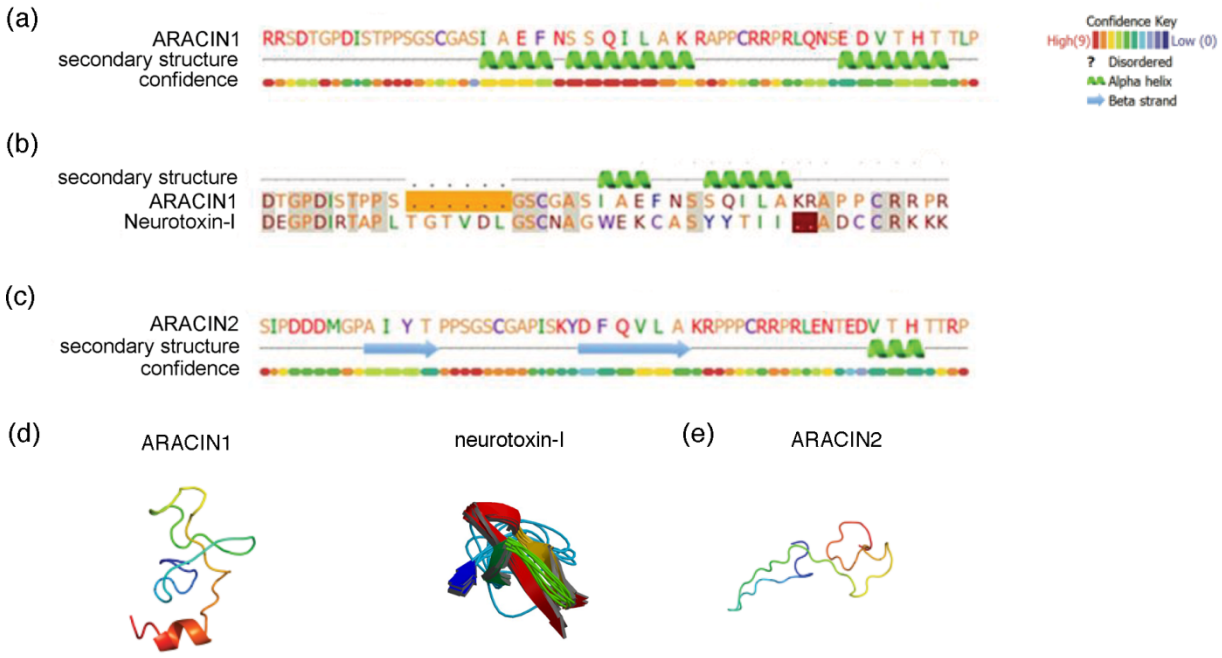

Figure S4. Secondary and tertiary structure predictions of ARACIN peptides.

(a) Secondary structure prediction of ARACIN1 by PHYRE (Protein Homology/analogY Recognition Engine; Bennet-Lovsey *et al.*, 2008; Kelley and Sternberg, 2009).

(b) Alignment of ARACIN1 and the 48 amino acid residue neurotoxin-I from *Stichodactyla heliantus* (Fogh *et al.*, 1990; Wilcox *et al.*, 1993).

(c) PHYRE secondary structure prediction of ARACIN2.

(d) Tertiary structure *ab initio* model of ARACIN1 predicted by PHYRE 2.0 (intensive mode). The experimental determined tertiary structure of neurotoxin-I is depicted (Protein Data Bank (PDB) code 2SH1; Fogh *et al.*, 1990; Wilcox *et al.*, 1993).

(e) Tertiary structure *ab initio* model of ARACIN2.

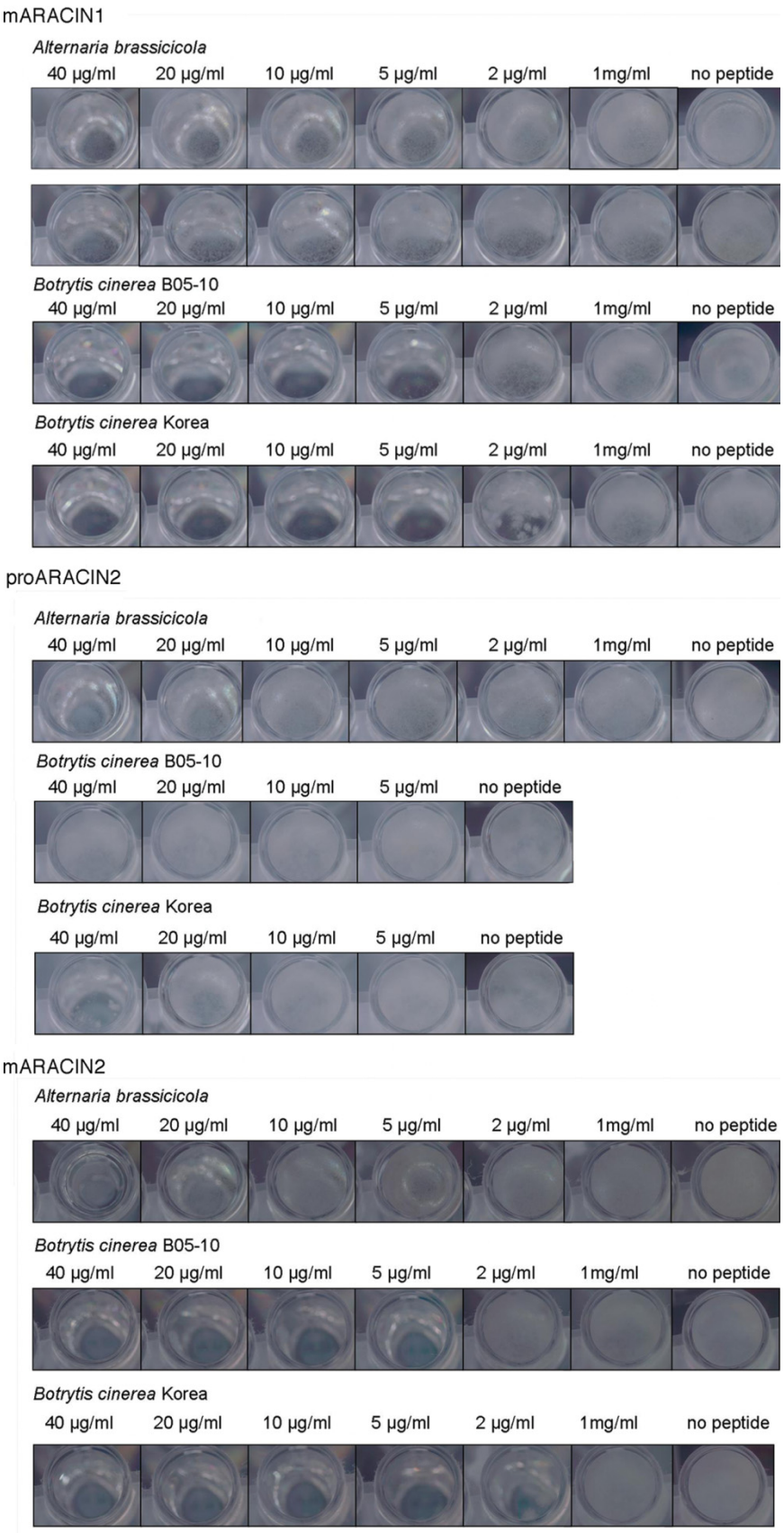

Figure S5. Antifungal activities of mARACIN1, proARACIN2 and mARACIN2 against *A. brassicicola*, *B. cinerea* B05-10 and *B. cinerea* Korea.

Pictures were taken 3 dpi.

Table S1. PCR primers used

Primer	Sequence
At5g36925-TAIR-FW	GGGGACAAGTTTGTACAAAAAAGCAGGCTCCATGTTTGTGATTGGTTTTGTAGAAGCTAG
At5g36925-RV	GGGGACCACTTTGTACAAGAAAGCTGGGTCTCAAGGAAGTGTAGTGTGGGTCAC
At5g36925-NO-STOP-RV	GGGGACCACTTTGTACAAGAAAGCTGGGTCAGGAAGTGTAGTGTGGGTCACATCTTC
PAt5g36925-FW	GGGGACAAGTTTGTACAAAAAAGCAGGCTTCTAACTTATTTGCAGGGAAC
PAt5g36925-RV	GGGGACCACTTTGTACAAGAAAGCTGGGTCCAAACAAAGCAGAAGAAC
PAt5g36925-SIM-RV	GGGGACCACTTTGTACAAGAAAGCTGGGTCTGGCTCTTCTTATCTCAAG
PAt5g36920-FW	GGGGACAAGTTTGTACAAAAAAGCAGGCTTCAAACTAGAAATGTTTCAAGAAG
PAt5g36920-RV	GGGGACCACTTTGTACAAGAAAGCTGGGTCTGGCTCTTCTATCTTAAATAAC
At5g36925-5UTR-FW	GGGGACAAGTTTGTACAAAAAAGCAGGCTTCATGGCGATGAAGACATCAC
At5g36920-FW	GGGGACAAGTTTGTACAAAAAAGCAGGCTTCATGGCGATGAAGAATACATCAC
At5g36920-RV	GGGGACCACTTTGTACAAGAAAGCTGGGTCTCAAGGTCGTGTAGTATGGGTC
At5g36920-NO-STOP-RV	GGGGACCACTTTGTACAAGAAAGCTGGGTCAGGTCGTGTAGTATGGGTCAC
At5g36925-FW-SyBr	GTAGAAGCTAGAAGATCAGATAC
At5g36925-RV-SyBr	TCAAGGAAGTGTAGTGTGG
At5g36920-FW-SyBr	CTAAGTCTTCTGCTTTGCCTGATG
At5g36920-RV-SyBr	CGTCTACATGGTGGTGGTCTC
PR-1-At2g14610-PL-FW	TGATCCTCGTGGGAATTATGT
PR-1-At2g14610-PL-RV	TGCATGATCACATCATTACTTCAT
PR-5-At1g75040-PL-FW	GACTGTGGCGGTCTAAGATGT
PR-5-At1g75040-PL-RV	TGAATTCAGCCAGAGTGACG
THI2.1-At1g72260-PL-FW	CTGGTCATGGCACAAGTTCA
THI2.1-At1g72260-PL-RV	GCCATTTCTAGCTTGGTTGG
THI2.2-At5g36910-PL-FW	TGACCACTCTCCAAAACTTTGAC
THI2.2-At5g36910-PL-RV	CTTTTAACTGCGGCGGTAGA
PDF1.2-At5g44420-PL-FW	GTTCTCTTTGCTGCTTTCGAC
PDF1.2-At5g44420-PL-RV	GCAAACCCCTGACCATGT
At5g36925-GSP1	TCAAGGAAGTGTAGTGTGGGTCACATCT
At5g36925-NGSP1	TCTGAGTTTTGGAGTCGAGGACGTC
At5g36925-GSP2	CAGGATCATGTGGAGCTTCAATTGC
At5g36925-NGSP2	CAATTCATCACAAATACTAGCCAAGAGAGC
NUP-TOPO	CACCAAGCAGTGGTATCAACGCAGAGT
EF1-α-At1g07920-FW	TGAGCACGCTCTTCTTGCTTTCA
EF1-α-At1g07920-RV	GGTGGTGGCATCCATCTTGTTACA

REFERENCES

Aerts, A.M., Francois, I.E.J.A., Cammue, B.P.A. and Thevissen, K. (2008) The mode of antifungal action of plant, insect and human defensins. *Cell. Mol. Life Sci.*, **65**, 2069-2079.

Altschmied, J., Delfgaauw, J., Wilde, B., Duschl, J., Bouneau, L., Volff, J.-N. and Schartl, M. (2002) Subfunctionalization of duplicate *mitf* genes associated with differential degeneration of alternative exons in fish. *Genetics*, **161**, 259-267.

Apel, K. and Hirt, H. (2004) Reactive oxygen species: metabolism, oxidative stress, and signal transduction. *Annu. Rev. Plant Biol.*, **55**, 373-399.

Bennett-Lovsey, R.M., Herbert, A.D., Sternberg, M.J.E. and Kelley, L.A. (2008) Exploring the extremes of sequence/structure space with ensemble fold recognition in the program Phyre. *Proteins*, **70**, 611-625.

Bolton, M.D. (2009) Primary metabolism and plant defense - fuel for the fire. *Mol. Plant Microbe Interact.*, **22**, 487-497.

Boman, H.G. (2003) Antibacterial peptides: basic facts and emerging concepts. *J. Intern. Med.*, **254**, 197-215.

Boyes, D.C., Zayed, A.M., Ascenzi, R., McCaskill, A.J., Hoffman, N.E., Davis, K.R. and Görlach, J. (2001) Growth stage-based phenotypic analysis of *Arabidopsis*: a model for high throughput functional genomics in plants. *Plant Cell*, **13**, 1499-1510.

Braverman, S.W. (1971) Reaction of broccoli and cauliflower introductions to *Alternaria brassicicola*. *Plant Dis. Rep.*, **55**, 454-457.

Broekaert, W.F., Cammue, B.P.A., DeBolle, M.F.C., Thevissen, K., DeSamblanx, G.W. and Osborn, R.W. (1997) Antimicrobial peptides from plants. *Crit. Rev. Plant Sci.*, **16**, 297-323.

Broekaert, W.F., Terras, F.R.G. and Cammue, B.P.A. (2000) Induced and preformed antimicrobial proteins. In *Mechanisms of Resistance to Plant Diseases* (Slusarenko, A.J., Fraser, R.S.S. and van Loon, L.C. eds). Dordrecht: Kluwer Academic Publishers, pp. 371-478.

Broekaert, W.F., Terras, F.R.G., Cammue, B.P.A. and Osborn, R.W. (1995) Plant defensins: novel antimicrobial peptides as components of the host defense system. *Plant Physiol.*, **108**, 1353-1358.

Bulet, P., Stöcklin, R. and Menin, L. (2004) Anti-microbial peptides: from invertebrates to vertebrates. *Immunol. Rev.*, **198**, 169-184.

Clough, S.J. and Bent, A.F. (1998) Floral dip: a simplified method for *Agrobacterium*-mediated transformation of *Arabidopsis thaliana*. *Plant J.*, **16**, 735-743.

Coca, M.A., Damsz, B., Yun, D.-J., Hasegawa, P.M., Bressan, R.A. and Narasimhan, M.L. (2000) Heterotrimeric G-proteins of a filamentous fungus regulate cell wall composition and susceptibility to a plant PR-5 protein. *Plant J.*, **22**, 61-69.

Cordts, S., Bantin, J., Wittich, P.E., Kranz, E., Lörz, H. and Dresselhaus, T. (2001) *ZmES* genes encode peptides with structural homology to defensins and are specifically expressed in the female gametophyte of maize. *Plant J.*, **25**, 103-114.

Ditt, R.F., Kerr, K.F., de Figueiredo, P., Delrow, J., Comai, L. and Nester, E.W. (2006) The *Arabidopsis thaliana* transcriptome in response to *Agrobacterium tumefaciens*. *Mol. Plant Microbe Interact.*, **19**, 665-681.

Donoghue, M.T.A., Keshavaiah, C., Swamidatta, S.H. and Spillane, C. (2011) Evolutionary origins of Brassicaceae specific genes in *Arabidopsis thaliana*. *BMC Evol. Biol.*, **11**, 47.

Eckardt, N.A. (2007) Positive and negative feedback coordinate regulation of disease resistance gene expression. *Plant Cell*, **19**, 2700-2702.

Emanuelsson, O., Brunak, S., von Heijne, G. and Nielsen, H. (2007) Locating proteins in the cell using TargetP, SignalP and related tools. *Nature Protoc.*, **2**, 953-971.

Fogh, R.H., Kem, W.R. and Norton, R.S. (1990) Solution structure of neurotoxin I from the sea anemone *Stichodactyla helianthus*. *J. Biol. Chem.*, **265**, 13016-13028.

Force, A., Lynch, M., Pickett, F.B., Amores, A., Yan, Y.-l. and Postlethwait, J. (1999) Preservation of duplicate genes by complementary, degenerative mutations. *Genetics*, **151**, 1531-1545.

François, I.E.J.A., De Bolle, M.F.C., Dwyer, G., Goderis, I.J.W.M., Woutors, P.F.J., Verhaert, P.D., Proost, P., Schaaper, W.M.M., Cammue, B.P.A. and Broekaert, W.F. (2002) Transgenic expression in *Arabidopsis* of a polyprotein construct leading to production of two different antimicrobial proteins. *Plant Physiol.*, **128**, 1346-1358.

François, I.E.J.A., Van Hemelrijck, W., Aerts, A.M., Wouters, P.F.J., Proost, P., Broekaert, W.F. and Cammue, B.P.A. (2004) Processing in *Arabidopsis thaliana* of a heterologous polyprotein resulting in differential targeting of the individual plant defensins. *Plant Sci.*, **166**, 113-121.

Fritig, B., Heitz, T. and Legrand, M. (1998) Antimicrobial proteins in induced plant defense. *Curr. Opin. Immunol.*, **10**, 16-22.

Fujita, M., Fujita, Y., Noutoshi, Y., Takahashi, F., Narusaka, Y., Yamaguchi-Shinozaki, K. and Shinozaki, K. (2006) Crosstalk between abiotic and biotic stress responses: a current view from the points of convergence in the stress signaling networks. *Curr. Opin. Plant Biol.*, **9**, 436-442.

Gadjev, I., Vanderauwera, S., Gechev, T.S., Laloi, C., Minkov, I.N., Shulaev, V., Apel, K., Inzé, D., Mittler, R. and Van Breusegem, F. (2006) Transcriptomic footprints disclose specificity of reactive oxygen species signaling in *Arabidopsis*. *Plant Physiol.*, **141**, 436-445.

Gao, A.-G., Hakimi, S.M., Mittanck, C.A., Wu, Y., Woerner, B.M., Stark, D.M., Shah, D.M., Liang, J. and Rommens, C.M.T. (2000) Fungal pathogen protection in potato by expression of a plant defensin peptide. *Nat. Biotechnol.*, **18**, 1307-1310.

García-Olmedo, F., Molina, A., Alamillo, J.M. and Rodríguez-Palenzuéla, P. (1998) Plant defense peptides. *Biopolymers*, **47**, 479-491.

Gaudet, D.A., Laroche, A. and Yoshida, M. (1999) Low temperature-wheat-fungal interactions: a carbohydrate connection. *Physiol. Plant.*, **106**, 437-444.

Hanada, K., Zou, C., Lehti-Shiu, M.D., Shinozaki, K. and Shiu, S.-H. (2008) Importance of lineage-specific expansion of plant tandem duplicates in the adaptive response to environmental stimuli. *Plant Physiol.*, **148**, 993-1003.

Hon, W.-C., Griffith, M., Mlynarz, A., Kwok, Y.C. and Yang, D.S.C. (1995) Antifreeze proteins in winter rye are similar to pathogenesis-related proteins. *Plant Physiol.*, **109**, 879-889.

Huang, G.-J., Lai, H.-C., Chang, Y.-S., Sheu, M.-J., Lu, T.-L., Huang, S.-S. and Lin, Y.-H. (2008) Antimicrobial, dehydroascorbate reductase, and monodehydroascorbate reductase activities of defensin from sweet potato [*Ipomoea batatas* (L.) Lam. 'Tainong 57'] storage roots. *J. Agric. Food Chem.*, **56**, 2989-2995.

Inzé, A., Vanderauwera, S., Hoeberichts, F.A., Vandorpe, M., Van Gaever, T. and Van Breusegem, F. (2012) A subcellular localization compendium of hydrogen peroxide-induced proteins. *Plant Cell Environ.*, **35**, 308-320.

Jones-Rhoades, M.W., Borevitz, J.O. and Preuss, D. (2007) Genome-wide expression profiling of the *Arabidopsis* female gametophyte identifies families of small, secreted proteins. *PLoS Genet.*, **3**, 1848-1861.

Karimi, M., Bleys, A., Vanderhaeghen, R. and Hilson, P. (2007) Building blocks for plant gene assembly. *Plant Physiol.*, **145**, 1183-1191.

Kelley, L.A. and Sternberg, M.J.E. (2009) Protein structure prediction on the web: a case study using the Phyre server. *Nature Protoc.*, **4**, 363-371.

Kim, J.-Y., Park, S.-C., Hwang, I., Cheong, H., Nah, J.-W., Hahm, K.-S. and Park, Y. (2009) Protease inhibitors from plants with antimicrobial activity. *Int. J. Mol. Sci.*, **10**, 2860-2872.

Kushmerick, C., de Souza Castro, M., Santos Cruz, J., Bloch, C., Jr. and Beirão, P.S.L. (1998) Functional and structural features of γ-zeathionins, a new class of sodium channel blockers. *FEBS Lett.*, **440**, 302-306.

Lawrence, C.B., Mitchell, T.K., Craven, K.D., Cho, Y., Cramer, R.A., Jr. and Kim, K.-H. (2008) At death's door: *Alternaria* pathogenicity mechanisms. *Plant Pathol. J.*, **24**, 101-111.

Lawton, K.A., Friedrich, L., Hunt, M., Weymann, K., Delaney, T., Kessmann, H., Staub, T. and Ryals, J. (1996) Benzothiadiazole induces disease resistance in *Arabidopsis* by activation of the systemic acquired resistance signal transduction pathway. *Plant J.*, **10**, 71-82.

Lay, F.T. and Anderson, M.A. (2005) Defensins - Components of the innate immune system in plants. *Curr. Protein Pept. Sci.*, **6**, 85-101.

Lee, S.C. and Hwang, B.K. (2009) Functional roles of the pepper antimicrobial protein gene, *CaAMP1*, in abscisic acid signaling, and salt and drought tolerance in *Arabidopsis*. *Planta*, **229**, 383-391.

Lee, S.C., Hwang, I.S., Choi, H.W. and Hwang, B.K. (2008) Involvement of the pepper antimicrobial protein *CaAMP1* gene in broad spectrum disease resistance. *Plant Physiol.*, **148**, 1004-1020.

Lorenzo, O., Chico, J.M., Sánchez-Serrano, J.J. and Solano, R. (2004) *JASMONATE-INSENSITIVE1* encodes a MYC transcription factor essential to discriminate between different jasmonate-regulated defense responses in *Arabidopsis*. *Plant Cell*, **16**, 1938-1950.

Marcos, J.F., Muñoz, A., Pérez-Payá, E., Misra, S. and Lopéz-García, B. (2008) Identification and rational design of novel antimicrobial peptides for plant protection. *Annu. Rev. Phytopathol.*, **46**, 273-301.

McHale, L., Tan, X., Koehl, P. and Michelmore, R.W. (2006) Plant NBS-LRR proteins: adaptable guards. *Genome Biol.*, **7**, 212.

Mirouze, M., Sels, J., Richard, O., Czernic, P., Loubet, S., Jacquier, A., François, I.E.J.A., Cammue, B.P.A., Lebrun, M., Berthomieu, P. and Marquès, L. (2006) A putative novel role for plant defensins: a defensin from the zinc hyper-accumulating plant, *Arabidopsis halleri*, confers zinc tolerance. *Plant J.*, **47**, 329-342.

Mittler, R., Vanderauwera, S., Suzuki, N., Miller, G., Tognetti, V.B., Vandepoele, K., Gollery, M., Shulaev, V. and Van Breusegem, F. (2011) ROS signaling: the new wave? *Trends Plant Sci.*, **16**, 300-309.

Nafisi, M., Goregaoker, S., Botanga, C.J., Glawischnig, E., Olsen, C.E., Halkier, B.A. and Glazebrook, J. (2007) *Arabidopsis* cytochrome P450 monooxygenase 71A13 catalyzes the conversion of indole-3-acetaldoxime in camalexin synthesis. *Plant Cell*, **19**, 2039-2052.

Nakajima, T. and Abe, J. (1996) Environmental factors affecting expression of resistance to pink snow mold caused by *Microdochium nivale* in winter wheat. *Can. J. Bot.*, **74**, 1783-1788.

Neergaard, P. and Andersen, H. (1945) *Danish species of Alternaria and Stemphylium; taxonomy, parasitism, economical significance* Copenhagen: E. Munksgaard.

Oh, I.S., Park, A.R., Bae, M.S., Kwon, S.J., Kim, Y.S., Lee, J.E., Kang, N.Y., Lee, S., Cheong, H. and Park, O.K. (2005) Secretome analysis reveals an *Arabidopsis* lipase involved in defense against *Alternaria brassicicola*. *Plant Cell*, **17**, 2832-2847.

Okuda, S., Tsutsui, H., Shiina, K., Sprunck, S., Takeuchi, H., Yui, R., Kasahara, R.D., Hamamura, Y., Mizukami, A., Susaki, D., Kawano, N., Sakakibara, T., Namiki, S., Itoh, K., Otsuka, K., Matsuzaki, M., Nozaki, H.,

Kuroiwa, T., Nakano, A., Kanaoka, M.M., Dresselhaus, T., Sasaki, N. and Higashiyama, T. (2009) Defensin-like polypeptide LUREs are pollen tube attractants secreted from synergid cells. *Nature*, **458**, 357-361.

Pandey, S.P. and Somssich, I.E. (2009) The role of WRKY transcription factors in plant immunity. *Plant Physiol.*, **150**, 1648-1655.

Penninckx, I.A., Eggermont, K., Terras, F.R.G., Thomma, B.P.H.J., De Samblanx, G.W., Buchala, A., Métraux, J.-P., Manners, J.M. and Broekaert, W.F. (1996) Pathogen-induced systemic activation of a plant defensin gene in *Arabidopsis* follows a salicylic acid-independent pathway. *Plant Cell*, **8**, 2309-2323.

Prince, V.E. and Pickett, F.B. (2002) Splitting pairs: the diverging fates of duplicated genes. *Nat. Rev. Genet.*, **3**, 827-837.

Proost, S., Van Bel, M., Sterck, L., Billiau, K., Van Parys, T., Van de Peer, Y. and Vandepoele, K. (2009) PLAZA: A comparative genomics resource to study gene and genome evolution in plants. *Plant Cell*, **21**, 3718-3731.

Punwani, J.A., Rabiger, D.S. and Drews, G.N. (2007) MYB98 positively regulates a battery of synergid-expressed genes encoding filiform apparatus-localized proteins. *Plant Cell*, **19**, 2557-2568.

Ryan, C.A. (1990) Protease inhibitors in plants: genes for improving defenses against insects and pathogens. *Annu. Rev. Phytopathol.*, **28**, 425-449.

Ryan, C.A., Huffaker, A. and Yamaguchi, Y. (2007) New insights into innate immunity in *Arabidopsis*. *Cell. Microbiol.*, **9**, 1902-1908.

Schenk, P.M., Kazan, K., Manners, J.M., Anderson, J.P., Simpson, R.S., Wilson, I.W., Somerville, S.C. and Maclean, D.J. (2003) Systemic gene expression in *Arabidopsis* during an incompatible interaction with *Alternaria brassicicola*. *Plant Physiol.*, **132**, 999-1010.

Schuhegger, R., Nafisi, M., Mansourova, M., Petersen, B.L., Olsen, C.E., Svatoš, A., Halkier, B.A. and Glawischnig, E. (2006) CYP71B15 (PAD3) catalyzes the final step in camalexin biosynthesis. *Plant Physiol.*, **141**, 1248-1254.

Sels, J., Mathys, J., De Coninck, B.M.A., Cammue, B.P.A. and De Bolle, M.F.C. (2008) Plant pathogenesis-related (PR) proteins: a focus on PR peptides. *Plant Physiol. Biochem.*, **46**, 941-950.

Seo, P.J., Lee, A.-K., Xiang, F. and Park, C.-M. (2008) Molecular and functional profiling of *Arabidopsis pathogenesis-related* genes: insights into their roles in salt response of seed germination. *Plant Cell Physiol.*, **49**, 334-344.

Shai, Y. (2002) Mode of action of membrane active antimicrobial peptides. *Biopolymers*, **66**, 236-248.

Shatters, R.G., Jr., Boykin, L.M., Lapointe, S.L., Hunter, W.B. and Weathersbee, A.A., 3rd (2006) Phylogenetic and structural relationships of the PR5 gene family reveal an ancient multigene family conserved in plants and select animal taxa. *J. Mol. Evol.*, **63**, 12-29.

Silverstein, K.A.T., Graham, M.A., Paape, T.D. and VandenBosch, K.A. (2005) Genome organization of more than 300 defensin-like genes in *Arabidopsis*. *Plant Physiol.*, **138**, 600-610.

Spelbrink, R.G., Dilmac, N., Allen, A., Smith, T.J., Shah, D.M. and Hockerman, G.H. (2004) Differential antifungal and calcium channel-blocking activity among structurally related plant defensins. *Plant Physiol.*, **135**, 2055-2067.

Stotz, H.U., Spence, B. and Wang, Y. (2009) A defensin from tomato with dual function in defense and development. *Plant Mol. Biol.*, **71**, 131-143.

Takayama, S., Shimosato, H., Shiba, H., Funato, M., Che, F.-S., Watanabe, M., Iwano, M. and Isogai, A. (2001) Direct ligand-receptor complex interaction controls *Brassica* self-incompatibility. *Nature*, **413**, 534-538.

Terras, F.R.G., Eggermont, K., Kovaleva, V., Raikhel, N.V., Osborn, R.W., Kester, A., Rees, S.B., Torrekens, S., Van Leuven, F., Vanderleyden, J., Cammue, B.P.A. and Broekaert, W.F. (1995) Small cysteine-rich antifungal proteins from radish: their role in host defense. *Plant Cell*, **7**, 573-588.

Theis, T. and Stahl, U. (2004) Antifungal proteins: targets, mechanisms and prospective applications. *Cell. Mol. Life Sci.*, **61**, 437-455.

Thevissen, K., Ferket, K.K.A., Francois, I.E.J.A. and Cammue, B.P.A. (2003) Interactions of antifungal plant defensins with fungal membrane components. *Peptides*, **24**, 1705-1712.

Thomma, B.P.H.J., Nelissen, I., Eggermont, K. and Broekaert, W.F. (1999) Deficiency in phytoalexin production causes enhanced susceptibility of *Arabidopsis thaliana* to the fungus *Alternaria brassicicola*. *Plant J.*, **19**, 163-171.

Tiffin, P. and Moeller, D.A. (2006) Molecular evolution of plant immune system genes. *Trends Genet.*, **22**, 662-670.

Torres, M.A. and Dangl, J.L. (2005) Functions of the respiratory burst oxidase in biotic interactions, abiotic stress and development. *Curr. Opin. Plant Biol.*, **8**, 397-403.

Torres, M.A., Jones, J.D.G. and Dangl, J.L. (2006) Reactive oxygen species signaling in response to pathogens. *Plant Physiol.*, **141**, 373-378.

Van Breusegem, F., Bailey-Serres, J. and Mittler, R. (2008) Unraveling the tapestry of networks involving reactive oxygen species in plants. *Plant Physiol.*, **147**, 978-984.

Van Breusegem, F. and Dat, J.F. (2006) Reactive oxygen species in plant cell death. *Plant Physiol.*, **141**, 384-390.

van Loon, L.C., Rep, M. and Pieterse, C.M.J. (2006) Significance of inducible defense-related proteins in infected plants. *Annu. Rev. Phytopathol.*, **44**, 135-162.

Vanderauwera, S., De Block, M., Van de Steene, N., van de Cotte, B., Metzlaff, M. and Van Breusegem, F. (2007) Silencing of poly(ADP-ribose) polymerase in plants alters abiotic stress signal transduction. *Proc. Natl. Acad. Sci. U.S.A.*, **104**, 15150-15155.

Vanderauwera, S., Suzuki, N., Miller, G., van de Cotte, B., Morsa, S., Ravanat, J.-L., Hegie, A., Triantaphylidès, C., Shulaev, V., Van Montagu, M.C.E., Van Breusegem, F. and Mittler, R. (2011) Extranuclear protection of chromosomal DNA from oxidative stress. *Proc. Natl. Acad. Sci. USA*, **108**, 1711-1716.

Vanderauwera, S., Zimmermann, P., Rombauts, S., Vandenabeele, S., Langebartels, C., Gruissem, W., Inzé, D. and Van Breusegem, F. (2005) Genome-wide analysis of hydrogen peroxide-regulated gene expression in *Arabidopsis* reveals a high light-induced transcriptional cluster involved in anthocyanin biosynthesis. *Plant Physiol.*, **139**, 806-821.

Wang, Z. and Wang, G. (2004) APD: the Antimicrobial Peptide Database. *Nucleic Acids Res.*, **32**, 590-592.

Wilcox, G.R., Fogh, R.H. and Norton, R.S. (1993) Refined structure in solution of the sea anemone neurotoxin ShI. *J. Biol. Chem.*, **268**, 24707-24719.

Wilmes, M., Cammue, B.P.A., Sahl, H.-G. and Thevissen, K. (2011) Antibiotic activities of host defense peptides: more to it than lipid bilayer perturbation. *Nat. Prod. Rep.*, **28**, 1350-1358.

Zasloff, M. (2002) Antimicrobial peptides of multicellular organisms. *Nature*, **415**, 389-395.

Zeier, J., Pink, B., Mueller, M.J. and Berger, S. (2004) Light conditions influence specific defence responses in incompatible plant-pathogen interactions: uncoupling systemic resistance from salicylic acid and *PR-1* accumulation. *Planta*, **219**, 673-683.

Zeller, G., Henz, S.R., Widmer, C.K., Sachsenberg, T., Rätsch, G., Weigel, D. and Laubinger, S. (2009) Stress-induced changes in the *Arabidopsis thaliana* transcriptome analyzed using whole-genome tiling arrays. *Plant J.*, **58**, 1068-1082.

Zor, T. and Selinger, Z. (1996) Linearization of the Bradford protein assay increases its sensitivity: theoretical and experimental studies. *Anal. Biochem.*, **236**, 302-308.

Part III

Conclusions and Perspectives

6

Conclusions and Perspectives

PART I: Protein subcellular trafficking during the oxidative stress response in plants

Oxidative stress-triggered relocalizations, an effective strategy to initiate a fast stress response

Although significant progress has been made in the description of oxidative stress-dependent gene expression (Desikan *et al.*, 2001; op den Camp *et al.*, 2003; Vandenabeele *et al.*, 2003; Vandenabeele *et al.*, 2004; Vanderauwera *et al.*, 2005; Gadjev *et al.*, 2006; Vanderauwera *et al.*, 2011), we are currently facing the challenge to unwire the complex network of ROS signal transduction mechanisms (Mittler *et al.*, 2011; Suzuki *et al.*, 2011). The accumulation of ROS leads to an upregulation of genes encoding proteins involved in transcription and translation, proteolysis, enzyme reactions such as oxidation and reduction and the defense response against abiotic and biotic factors. The functional analysis of proteins encoded by genes that rapidly respond to ROS, in particular genes encoding for transcription factors, can provide novel insights into the early signaling steps triggered by a sudden rise in intracellular ROS.

Protein activation and trafficking are important in rendering signal transduction highly dynamic over time and space and are actively influenced by diverse environmental stimuli to rapidly initiate an appropriate defense response. A central event during environmental stress conditions is the accumulation of ROS that is commonly referred to as oxidative stress. Several mechanisms have been described for oxidative stress-induced protein relocalizations, such as redox-based relocalizations, phosphorylation-dependent trafficking by ROS-activated kinases, stress-induced release of membrane-anchored transcription factors, sequestration and stress-triggered release, and relocalizations mediated by a nuclear retention factor. Specifically for temperature stresses, salinity and hypoxia, several subcellular dynamic protein distributions have been identified that often involved membrane-anchored protein release and nucleocytoplasmic partitioning. Together with the insights in the tight spatiotemporal control of ROS homeostasis, the identification and characterization of stress-triggered relocalizations of signal transduction components will therefore provide a better understanding of signaling mechanisms that allow plants to cope with adverse environmental conditions.

Comparison of several genome-wide hydrogen peroxide (H_2O_2)-dependent gene expression studies in *Arabidopsis thaliana* enabled us to build a comprehensive inventory of 783 H_2O_2-induced genes from which 85 candidate genes were selected for further functional analyses. In this work, a subcellular localization map of 49 H_2O_2-induced proteins was built by using a medium-throughput *in vivo* localization assay. In a first screen using a transient expression system in *Nicotiana benthamiana,* the functionality and subcellular localization of a substantial amount of protein GFP fusion constructs were determined. Eight GFP-tagged proteins were exclusively localized in the nucleus, whereas 23 resided in

both the nucleus and cytosol. Nuclear proteins were, as expected, nearly all transcription factors or nucleic acid-binding proteins, while nucleocytosolic proteins involved both transcription factors and proteins of unknown function. For two small HSPs, an exclusively cytosolic localization was observed. Three proteins displayed a chloroplastic localization, including unexpectedly a NAC transcription factor (see further). Of six proteins present in the endomembrane compartment, two displayed distinct plasma membrane localizations. To subsequently verify the findings of the transient expression assay, stably transformed transgenic *Arabidopsis* plants for 30 of the 49 proteins were generated and examined. Except for two proteins (HSP17.6BCI and HRE2), all tobacco subcellular localizations of the GFP fusion proteins were confirmed in Arabidopsis.

Because abiotic stress-triggered relocalizations can be directly assessed *in situ* in stable transgenic plants, the obtained transgenic Arabidopsis plants harboring the GFP fusion reporters provided us immediately the tools for such analyses. Moreover, H_2O_2-induced protein trafficking can be studied by direct addition of H_2O_2 to Arabidopsis mesophyll protoplasts that are derived from these stable transgenic plants. Arabidopsis protoplasts are particularly suited for relocalization experiments as they allow quantitative and simultaneous testing of different concentrations and stimuli. In addition, the overall impact of overproduction of the GFP fusion proteins on plant development and the performance towards environmental stimuli could also be assessed in the transgenic plants: for eleven proteins, overexpression substantially affected normal growth and development.

The identification of proteins that relocalize upon oxidative stress is experimentally demanding and often requires a detailed understanding of the physicochemical properties of the protein of interest, its subcellular localization during non-stressed conditions, the potential interactors, the spatiotemporal dynamics of both the protein of interest and ROS, and the involved abiotic stress pathway. Interesting candidates for studying relocalizations are the nucleocytosolic-localized transcription factors, such as ANAC013, ANAC053 and ANAC087 that might be regulated by nucleocytoplasmic partitioning during stress. Furthermore, both ANAC013 and ANAC053 were previously designated as putative membrane-associated NAC transcription factors (NTL1 and NTL4, respectively), which are known to be activated and released by proteolytic cleavage in response to incoming stimuli (Kim *et al.*, 2007). Whereas NTL4 displayed a vesicular localization pattern, NTL1 appeared to be associated with ER membranes. Interestingly, our results demonstrate that GFP-NTL1 overexpression leads to proteolytic processing, possibly explaining its nucleocytosolic localization. Besides the nucleocytosolic-localized transcription factors, ANAC102 that localized exclusively to the chloroplasts is another interesting candidate to study stress-induced relocalization (see further).

Besides our focus on proteins with a subcellular localization that was not expected from their putative function (e.g. a transcription factor with nuclear target genes that is localized in chloroplasts),

we also analyzed some proteins for which the localizations differed in *N. benthamiana* and Arabidopsis. For instance AtDjC68, a DnaJ heat shock N-terminal domain-containing protein localized in nuclear speckles in tobacco. In Arabidopsis mesophyll protoplasts, AtDjC68 displayed a nucleocytosolic localization that upon H_2O_2 addition resulted in an exclusively nuclear localization in ~15% of the protoplasts.

Because H_2O_2-induced gene expression might be the result from the action of proteins that change their localization upon oxidative stress, one could argue that the selected H_2O_2-induced genes are not ideal candidates for identifying stress-dependent relocalizations. However, our results show that starting from ROS transcriptome datasets, proteins with a dynamic relocalization during oxidative stress can be identified. In fact, genes that are rapidly induced by stresses often play a role in stress signaling, presumably by mediating a positive feedback loop (Yamaguchi-Shinozaki and Shinozaki, 2006). The redox status of proteins can be reversibly or irreversibly modified by intracellular ROS that, in turn, can dynamically affect the subcellular localization and function of the protein. The identification of signal transducers with a dynamic localization after modification by ROS might be important candidates for ROS perception. However, proteomic studies of ROS-modified proteins remain scarce and are often gel-based, lack sensitivity and do not reflect the whole proteome. The recent advent of shotgun-oriented proteomics, that are able capture and quantify large portions of the proteome with high sensitivity, will greatly enhance the identification of ROS-modified proteins. Subsequent, integration of ROS-dependent transcriptome, proteome and (re)localisome datasets will provide a systems biology view on the complex regulation of the ROS signaling network. In turn, the integrated knowledge of the underlying molecular mechanisms of ROS signaling can be exploited to genetically engineer and improve stress tolerance in plants.

The oxidative stress-induced chloroplast-to-nucleus relocalization of ANAC102: a novel mechanism in chloroplast retrograde signaling?

During fluctuating environmental conditions, caused by for example variation in light intensity and quality, temperature, salinity, low nutrient status and water availability, the homeostasis of the photosynthetic machinery is rapidly perturbed leading to the enhanced production of ROS. Therefore, chloroplasts are considered sensors of adverse environmental conditions that communicate back to the nucleus to initiate an appropriate response. Although chloroplast retrograde signaling has been extensively studied for many years, the process still remains poorly understood (Pfannschmidt, 2010). Because several transcription factors that regulate nuclear gene expression are found in chloroplasts, the question was raised whether these factors are effectively released upon chloroplast dysfunction to

control nuclear gene expression. Our work provides evidence for the first chloroplast-to-nucleus relocalization of a NAC transcription factor (ANAC102) during chloroplast-derived oxidative stress conditions. Under non-stressed conditions, ANAC102 is localized in the chloroplasts. However, perturbation of the chloroplastic redox balance by methyl viologen (MV) provoked the intercompartimental relocalization of ANAC102 from the chloroplast to the nucleus where it regulates several oxidative stress-related genes. Moreover, transgenic plants with perturbed *ANAC102* expression displayed an altered growth response upon oxidative stress, indicating that ANAC102 might play an important role during chloroplast retrograde signaling by tightly controlling the stress response.

Because the existence of interorganellar protein relocalizations in plants is highly debated and controversial in the field of retrograde signaling, more experimental work is needed to support the occurrence of chloroplast-to-nucleus protein trafficking. At first, the relocalization should be confirmed and quantified by independent techniques. Intracellular protein dynamics can be followed by tracking a photoactivatable (PA) variant of GFP (PA-GFP; Patterson and Lippincott-Schwartz, 2002). Photoactivation of chloroplastic ANAC102-PA-GFP protein fusions prior to MV treatment will allow determining whether, after MV treatment, the nuclear-localized ANAC102 GFP fusions originate from the chloroplasts. In addition, transgenic lines expressing fusion proteins with smaller epitope tags should be produced to confirm the relocalization in isolated nuclei and chloroplasts before and after MV treatment. To exclude potential effects of the tags on protein localization, antibodies that specifically recognize ANAC102 will be required to prove whether ANAC102 is proteolytically processed during its relocalization. Furthermore, truncated versions of ANAC102 will determine which sequences/domains are necessary for chloroplast import, relocalization and transcriptional activity. In-depth chloroplast fractionation experiments together with *in vitro* chloroplast import assays will clarify the exact localization of ANAC102. Also the potential ROS modification of the two closely positioned cysteines of ANAC102 and the effect it might have on the relocalization is worthwhile to investigate further. To understand the ANAC102 relocalization mechanism, it might be crucial to identify its interacting partners. Unfortunately, tandem affinity purification (TAP) experiments in which ANAC102 was expressed with a C-terminal double affinity tag (TAP tag) in a light-grown Arabidopsis cell suspension culture failed. Therefore, several strategies to increase the success rate of the TAP experiments should be employed, such as repositioning of the TAP-tag and optimizing relocalization conditions by addition of MV to the cell cultures.

Although ANAC102 was shown to bind several promoter regions of oxidative stress-related genes in the nucleus, the demonstration of the transcriptional activity of ANAC102 *in planta* is currently lacking. Because only a few targets of ANAC102 are known, the use of inducible *ANAC102* overexpression constructs as well as chromatin immunoprecipitation experiments combined with next-

generation sequencing (ChIP-Seq) could identify additional *in vivo* target genes of ANAC102. Furthermore, transient expression assays using Arabidopsis mesophyll protoplasts will indicate whether ANAC102 could transcriptionally repress a reporter gene driven by the promoter fragments identified in the ChIP assay.

Additional experiments are prerequisite to critically assess whether ANAC102 can be positioned in the chloroplast retrograde signaling pathway. If ANAC102 functions as a true plastidial retrograde signal, it should repress nuclear-encoded photosynthetic genes when plastid function is impaired. Accordingly, the expression of genes encoding the light-harvesting chlorophyll a/b binding proteins 1.1 and 2.4 is down-regulated in *ANAC102* overexpression plants (Christianson *et al.*, 2009). Because *Lhcb* genes, considered as marker transcripts for chloroplast-retrograde signaling, are frequently repressed in photo-oxidized plants (Fey *et al.*, 2005), it is necessary to demonstrate that nuclear accumulation of ANAC102 correlates with changes in *Lhcb* expression during genetic defects or treatments that impair plastid function. Integration of relocalization experiments, gene expression analysis and chemical treatments with norflurazon that causes strong photo-oxidation in the chloroplasts (Reiß *et al.*, 1983; Oelmüller *et al.*, 1986), DCMU (3-(3',4'-dichlorophenyl) 1, 1'-dimethyl urea) and DBMIB (2,5-dibromo-3-methyl-6-isopropyl-*p*-benzoquinone) that inhibit photosynthetic electron transport (Escoubas *et al.*, 1995), together with the *genome uncoupled* (*gun*) mutants that constitutively express *Lhcb* genes even during chloroplast dysfunction (Susek *et al.*, 1993) and the conditional *flu* mutant which can be used to specifically induce the accumulation of singlet oxygen ($^1O_2$) within the plastids (op den Camp *et al.*, 2003), will clarify the origin of the redox signal that triggers the relocalization of ANAC102.

Taken together, our results provide the first evidence for the possible intercompartimental retrograde relocalization of ANAC102 from the chloroplast to the nucleus where it regulates the expression of oxidative stress-responsive genes. However, further extensive experimental evidence is needed to support the current hypothesis that ANAC102 functions in chloroplast retrograde signaling.

PART II: Identification of two novel hydrogen peroxide-induced peptides involved in innate immunity

Due to their sessile nature, plants are continuously exposed to various environmental stress conditions and therefore have developed a variety of defense mechanisms. One of the most important responses in plant defense against pathogens is the rapid and transient production of ROS, including H_2O_2, that is termed the oxidative burst (Torres, 2010). Several functions have been assigned to the pathogen-induced production of ROS, such as the direct toxic effect on pathogens due to their high reactivity, cell wall cross-linking and a signaling function by mediating defense gene activation through interacting with redox-sensitive transcription factors and other defense signaling components such as phosphorylation cascades (Kovtun *et al.*, 2000; Mou *et al.*, 2003) or by generating lipid derivatives (Montillet *et al.*, 2005) and phytoalexins (Thoma *et al.*, 2003). Furthermore, ROS play an important role in the hypersensitive response in which cells undergo programmed cell death to limit the spread of the pathogen (Lam *et al.*, 2001; Greenberg and Yao, 2004).

It is becoming increasingly clear that there is extensive crosstalk between biotic and abiotic stress signaling in which ROS and hormone signaling pathways play key roles (Fujita *et al.*, 2006). Previous transcriptome analyses revealed an important enrichment of ROS-responsive genes during biotic and abiotic stresses, including many pathogen defense-related genes, such as the pathogenesis-related (PR) genes (Broekaert *et al.*, 2000; Apel and Hirt, 2004; Torres and Dangl, 2005; Torres *et al.*, 2006; van Loon *et al.*, 2006). Amongst them, antimicrobial peptides (AMPs) are an evolutionary conserved component of innate immune systems found throughout all kingdoms ranging from bacteria, invertebrates, plants and vertebrates (Broekaert *et al.*, 1997; Ganz and Lehrer, 1998; García-Olmedo *et al.*, 1998; Otvos, 2000; Zasloff, 2002). Although AMPs are hallmarked for their broad-spectrum antimicrobial activity and are considered to play a key role during plant defense by acting as both permanent and inducible defense barriers, evidence is increasing that plant AMPs also play a role in the abiotic stress response.

Our work identified two novel Arabidopsis H_2O_2-induced peptides, designated ARACIN1 and ARACIN2, that are transcriptionally regulated by both biotic and abiotic stress conditions and share many characteristics with AMPs but are structurally unrelated to known plant AMPs. ARACIN1 and ARACIN2 are lineage-specific to the Brassicaceae family and are active against the necrotrophic fungi *Alternaria brassicicola* and *Botrytis cinerea* both *in vitro* and *in planta*. As many AMPs, ARACIN1 and ARACIN2 are potentially expressed as prepropeptides in which the N-terminal propeptide functions as a signal peptide for targeting to the secretory pathway, the propeptide acts as a neutralizing domain and the mature domain is necessary for antimicrobial activity. The validate this hypothesis, the exact nature

of the different domains needs to be determined by for instance amino acid sequencing of the GFP-tagged processed forms of ARACIN1 and ARACIN2. In addition, overexpression of deletion constructs can give more insights in the minimal domain necessary for antimicrobial activity. To further demonstrate their role in plant defense, it is crucial to determine the activity spectra of ARACIN1 and ARACIN2 against biotrophic and necrotrophic fungal, bacterial and viral pathogens. Moreover, gene expression analysis of both *ARACIN1* and *ARACIN2* in hormone signaling mutants will identify by which signaling pathways their expression is regulated. To determine the *in planta* concentration of the different forms of ARACIN1 and ARACIN2 before and during pathogen infection, the development of peptide-specific antibodies will be essential.

In-depth functional characterization of both ARACINS will open perspectives to use them as an alternative strategy to improve disease resistance. In collaboration with the group of Dr. Van Lijsebettens, transgenic corn (*Zea mays*) lines overexpressing *ARACIN1* are currently generated by the in-house maize transformation platform. Once available, these transgenic lines will first be tested against the pathogenic corn smut fungus (*Ustilago maydis*) in collaboration with the laboratorium of Prof. Dr. Cammue. As ARACINS are Brassicaceae-specific, the potential to improve resistance in the agronomical important oilseed rape (*Brassica napus*) will be assessed. Alternatively, ARACIN peptides could be expressed in biocontrol organisms to combat postharvest diseases.

REFERENCES

Apel, K. and Hirt, H. (2004) Reactive oxygen species: metabolism, oxidative stress, and signal transduction. *Annu. Rev. Plant Biol.*, **55**, 373-399.

Broekaert, W.F., Cammue, B.P.A., De Bolle, M.F., Thevissen, K., De Samblanx, G.W. and Osborn, R.W. (1997) Antimicrobial peptides from plants. *Crit. Rev. Plant Sci.*, **16**, 297-323.

Broekaert, W.F., Terras, F.R.G. and Cammue, B.P.A. (2000) Induced and preformed antimicrobial proteins. In *Mechanisms of Resistance to Plant Diseases* (Slusarenko, A.J., Fraser, R.S.S. and van Loon, L.C. eds). Dordrecht: Kluwer Academic Publishers, pp. 371-478.

Desikan, R., A.-H.-Mackerness, S., Hancock, J.T. and Neill, S.J. (2001) Regulation of the *Arabidopsis* transcriptome by oxidative stress. *Plant Physiol.*, **127**, 159-172.

Escoubas, J.M., Lomas, M., LaRoche, J. and Falkowski, P.G. (1995) Light intensity regulation of *cab* gene transcription is signaled by the redox state of the plastoquinone pool. *Proc. Natl. Acad. Sci. USA*, **92**, 10237-10241.

Fujita, M., Fujita, Y., Noutoshi, Y., Takahashi, F., Narusaka, Y., Yamaguchi-Shinozaki, K. and Shinozaki, K. (2006) Crosstalk between abiotic and biotic stress responses: a current view from the points of convergence in the stress signaling networks. *Curr. Opin. Plant Biol.*, **9**, 436-442.

Gadjev, I., Vanderauwera, S., Gechev, T.S., Laloi, C., Minkov, I.N., Shulaev, V., Apel, K., Inzé, D., Mittler, R. and Van Breusegem, F. (2006) Transcriptomic footprints disclose specificity of reactive oxygen species signaling in *Arabidopsis*. *Plant Physiol.*, **141**, 436-445.

Ganz, T. and Lehrer, R.I. (1998) Antimicrobial peptides of vertebrates. *Curr. Opin. Immunol.*, **10**, 41-44.

García-Olmedo, F., Molina, A., Alamillo, J.M. and Rodríguez-Palenzuela, P. (1998) Plant defense peptides. *Biopolymers*, **47**, 479-491.

Greenberg, J.T. and Yao, N. (2004) The role and regulation of programmed cell death in plant–pathogen interactions. *Cell. Microbiol.*, **6**, 201-211.

Kim, S.-Y., Kim, S.-G., Kim, Y.-S., Seo, P.J., Bae, M., Yoon, H.-K. and Park, C.-M. (2007) Exploring membrane-associated NAC transcription factors in *Arabidopsis*: implications for membrane biology in genome regulation. *Nucleic Acids Res.*, **35**, 203-213.

Kovtun, Y., Chiu, W.-L., Tena, G. and Sheen, J. (2000) Functional analysis of oxidative stress-activated mitogen-activated protein kinase cascade in plants. *Proc. Natl. Acad. Sci. USA*, **97**, 2940-2945.

Lam, E., Kato, N. and Lawton, M. (2001) Programmed cell death, mitochondria and the plant hypersensitive response. *Nature*, **411**, 848-853.

Mittler, R., Vanderauwera, S., Suzuki, N., Miller, G., Tognetti, V.B., Vandepoele, K., Gollery, M., Shulaev, V. and Van Breusegem, F. (2011) ROS signaling: the new wave? *Trends Plant Sci.*, **16**, 300-309.

Montillet, J.-L., Chamnongpol, S., Rustérucci, C., Dat, J., van de Cotte, B., Agnel, J.-P., Battesti, C., Inzé, D., Van Breusegem, F. and Triantaphylidès, C. (2005) Fatty acid hydroperoxides and H_2O_2 in the execution of hypersensitive cell death in tobacco leaves. *Plant Physiol.*, **138**, 1516-1526.

Mou, Z., Fan, W. and Dong, X. (2003) Inducers of plant systemic acquired resistance regulate NPR1 function through redox changes. *Cell*, **113**, 935-944.

Oelmüller, R., Levitan, I., Bergfeld, R., Rajasekhar, V.K. and Mohr, H. (1986) Expression of nuclear genes as affected by treatments acting on the plastids. *Planta*, **168**, 482-492.

op den Camp, R.G.L., Przybyla, D., Ochsenbein, C., Laloi, C., Kim, C., Danon, A., Wagner, D., Hideg, É., Göbel, C., Feussner, I., Nater, M. and Apel, K. (2003) Rapid induction of distinct stress responses after the release of singlet oxygen in *Arabidopsis*. *Plant Cell*, **15**, 2320-2332.

Otvos, J.L. (2000) Antibacterial peptides isolated from insects. *J. Pept. Sci.*, **6**, 497-511.

Patterson, G.H. and Lippincott-Schwartz, J. (2002) A photoactivatable GFP for selective photolabeling of proteins and cells. *Science*, **297**, 1873-1877.

Pfannschmidt, T. (2010) Plastidial retrograde signalling - a true "plastid factor" or just metabolite signatures? *Trends Plant Sci.*, **15**, 427-435.

Reiß, T., Bergfeld, R., Link, G., Thien, W. and Mohr, H. (1983) Photooxidative destruction of chloroplasts and its consequences for cytosolic enzyme levels and plant development. *Planta*, **159**, 518-528.

Susek, R.E., Ausubel, F.M. and Chory, J. (1993) Signal transduction mutants of *Arabidopsis* uncouple nuclear *CAB* and *RBCS* gene expression from chloroplast development. *Cell*, **74**, 787-799.

Suzuki, N., Koussevitzky, S., Mittler, R.O.N. and Miller, G.A.D. (2011) ROS and redox signalling in the response of plants to abiotic stress. *Plant Cell Environ.*, doi: 10.1111/j.1365-3040.2011.02336.x.

Thoma, I., Loeffler, C., Sinha, A.K., Gupta, M., Krischke, M., Steffan, B., Roitsch, T. and Mueller, M.J. (2003) Cyclopentenone isoprostanes induced by reactive oxygen species trigger defense gene activation and phytoalexin accumulation in plants. *Plant J.*, **34**, 363-375.

Torres, M.A. (2010) ROS in biotic interactions. *Physiol. Plant*, **138**, 414-429.

Torres, M.A. and Dangl, J.L. (2005) Functions of the respiratory burst oxidase in biotic interactions, abiotic stress and development. *Curr. Opin. Plant Biol.*, **8**, 397-403.

Torres, M.A., Jones, J.D.G. and Dangl, J.L. (2006) Reactive oxygen species signaling in response to pathogens. *Plant Physiol.*, **141**, 373-378.

van Loon, L.C., Rep, M. and Pieterse, C.M.J. (2006) Significance of inducible defense-related proteins in infected plants. *Annu. Rev. Phytopathol.*, **44**, 135-162.

Vandenabeele, S., Van Der Kelen, K., Dat, J., Gadjev, I., Boonefaes, T., Morsa, S., Rottiers, P., Slooten, L., Van Montagu, M., Zabeau, M., Inzé, D. and Van Breusegem, F. (2003) A comprehensive analysis of hydrogen peroxide-induced gene expression in tobacco. *Proc. Natl. Acad. Sci. USA*, **100**, 16113-16118.

Vandenabeele, S., Vanderauwera, S., Vuylsteke, M., Rombauts, S., Langebartels, C., Seidlitz, H.K., Zabeau, M., Van Montagu, M., Inzé, D. and Van Breusegem, F. (2004) Catalase deficiency drastically affects gene expression induced by high light in *Arabidopsis thaliana*. *Plant J.*, **39**, 45-58.

Vanderauwera, S., Suzuki, N., Miller, G., van de Cotte, B., Morsa, S., Ravanat, J.-L., Hegie, A., Triantaphylidès, C., Shulaev, V., Van Montagu, M.C.E., Van Breusegem, F. and Mittler, R. (2011) Extranuclear protection of chromosomal DNA from oxidative stress. *Proc. Natl. Acad. Sci. USA*, **108**, 1711-1716.

Vanderauwera, S., Zimmermann, P., Rombauts, S., Vandenabeele, S., Langebartels, C., Gruissem, W., Inzé, D. and Van Breusegem, F. (2005) Genome-wide analysis of hydrogen peroxide-regulated gene expression in *Arabidopsis* reveals a high light-induced transcriptional cluster involved in anthocyanin biosynthesis. *Plant Physiol.*, **139**, 806-821.

Yamaguchi-Shinozaki, K. and Shinozaki, K. (2006) Transcriptional regulatory networks in cellular responses and tolerance to dehydratation and cold stresses. *Annu. Rev. Plant Biol.*, **57**, 781-803.

Zasloff, M. (2002) Antimicrobial peptides of multicellular organisms. *Nature*, **415**, 389-395.

SUMMARY

Although reactive oxygen species (ROS) were initially considered as toxic byproducts of aerobic metabolism, it is now generally accepted that ROS also act as key signaling molecules. Over the last years, significant progress has been made in the description of oxidative stress-dependent gene expression and the current challenge is to unravel the complex network of ROS signal transduction mechanisms. The functional analysis of proteins encoded by genes that rapidly respond to ROS can therefore provide novel insights into the early signaling steps triggered by a sudden increase of intracellular ROS. In this aspect, the dynamic trafficking of proteins during stress is an important regulatory mechanism to render ROS signaling highly flexible to initiate a fast defense response. Hitherto, several mechanisms are known of oxidative stress-triggered protein dynamic trafficking (**Chapter 1**), such as redox-based relocalizations, phosphorylation-dependent trafficking by ROS-activated kinases, stress-induced release of membrane-anchored transcription factors, sequestration and stress-triggered release, and relocalizations mediated by a nuclear retention factor. Several protein relocalizations during abiotic stress conditions have been reported, in particular as a consequence of low and high temperature stresses, high salinity stress and hypoxia. An important aspect of oxidative-stress triggered relocalizations is the subcellular compartment where the stress is initially sensed. Different types of abiotic stresses seem to affect certain subcellular compartments more which, in turn, produce compartment-specific ROS. Thus, the mechanism of an abiotic stress-induced relocalization is often correlated with the type of abiotic stress and the subcellular compartment. Together with the insights in the tight spatiotemporal control of ROS homeostasis, the identification and characterization of stress-triggered relocalizations of signal transduction components will therefore provide a better understanding of signaling mechanisms that allow plants to cope with adverse environmental conditions (**Chapter 1**).

The aim of this project was to identify and characterize proteins that relocalize during oxidative stress. Therefore, we first made a comprehensive list of 783 hydrogen peroxide (H_2O_2)-induced proteins by comparing three available microarray data sets that profiled the Arabidopsis transcriptome during elevated photorespiratory H_2O_2 levels (**Chapter 2**). In these independent studies, the transcriptome of catalase-deficient plants exposed to high light stress was assessed. Catalase is the major H_2O_2 scavenging enzyme and a reduction of catalase activity renders plants hypersensitive to excess photorespiratory H_2O_2 produced by high light exposure. From this inventory, a well-considered selection of 85 H_2O_2-induced genes for further functional studies was made by implementing consecutive selection criteria such as a rapid induction towards photorespiratory H_2O_2, the *in silico* subcellular prediction, the functional category and the responsiveness towards abiotic stresses. In **chapter 2**, a subcellular localization map of 49 H_2O_2-induced proteins was built by using a medium-throughput *in vivo*

localization assay. In a first screen using a transient expression system in *Nicotiana benthamiana* (tobacco), the functionality and subcellular localization of a substantial amount of protein GFP fusion constructs was determined. Eight GFP-tagged proteins were exclusively localized in the nucleus, whereas 23 resided in both the nucleus and cytosol. Nuclear proteins were, as expected, nearly all transcription factors or nucleic acid-binding proteins, while nucleocytosolic proteins included both transcription factors and proteins of unknown function. For two small HSPs, an exclusively cytosolic localization was observed. Three proteins displayed a chloroplastic localization, including unexpectedly a NAC transcription factor. Of the six proteins present in the endomembrane compartment, two displayed distinct plasma membrane localizations. To subsequently verify the findings of the transient expression assay, stably transformed transgenic *Arabidopsis* plants for 30 of the 49 proteins were generated and examined. Except for two proteins, all subcellular localizations of the GFP fusion proteins originally observed in tobacco were confirmed in Arabidopsis. Abiotic stress-triggered relocalizations could be directly assessed *in situ* in stable transgenic plants harboring the GFP fusion reporters In addition, the overall impact of overproduction of the GFP fusion proteins on plant development and the performance towards environmental stimuli could also be assessed in the transgenic plants: for eleven proteins, overexpression substantially affected normal growth and development.

In **chapter 2**, interesting candidates for studying relocalizations were found of which most are nucleocytosolic-localized transcription factors, such as ANAC013, ANAC053 and ANAC087 that might be regulated by nucleocytoplasmic partitioning during stress. Furthermore, both ANAC013 and ANAC053 were previously designated as putative membrane-associated NAC transcription factors (NTL1 and NTL4, respectively), which are known to be activated and released by proteolytic cleavage in response to incoming stimuli. Besides their nucleocytosolic localization, the localization of NTL4 displayed a vesicular pattern and NTL1 appeared to be associated with ER membranes. Interestingly, our results demonstrate that GFP-NTL1 overexpression leads to proteolytic processing, possibly explaining its nucleocytosolic localization. Proteins for which the localizations differed in *N. benthamiana* and Arabidopsis were also analyzed. For instance AtDjC68, a DnaJ heat shock N-terminal domain-containing protein localized in nuclear speckles in tobacco. In Arabidopsis mesophyll protoplasts, AtDjC68 displayed a nucleocytosolic localization that upon H_2O_2 addition resulted in an exclusively nuclear localization in ~15% of the protoplasts.

Another interesting candidate for relocalization studies was ANAC102, a NAC transcription factor that regulates nuclear gene expression and was found in the chloroplasts. In **chapter 3**, we assessed whether ANAC102 is effectively released during oxidative stress to control nuclear gene expression. During adverse environmental conditions, the homeostasis of the photosynthetic machinery is rapidly perturbed leading to the enhanced production of ROS. Therefore, chloroplasts are considered

as sensors of adverse environmental conditions that communicate back to the nucleus to initiate an appropriate response. By using methyl viologen, a redox active compound that induces ROS in the chloroplasts, we could provoke the intercompartimental relocalization of ANAC102 from the chloroplasts to the nucleus where it regulates several oxidative stress-related genes. Moreover, transgenic plants with perturbed *ANAC102* expression displayed an altered growth response upon oxidative stress, indicating that ANAC102 might play an important role during chloroplast retrograde signaling by tightly controlling the stress response. Because the existence of interorganellar protein relocalizations in plants is highly debated and controversial in the field of retrograde signaling, more experimental work is needed to support the occurrence of the chloroplast-to-nucleus protein trafficking of ANAC102.

Because there is extensive crosstalk between biotic and abiotic stress signaling in which ROS, together with hormones, play a key role, many ROS-responsive genes are common for biotic and abiotic stresses, including many pathogen defense-related genes, such as the pathogenesis-related (PR) genes. In **chapter 5**, we identified two novel Arabidopsis peptides, designated ARACIN1 and ARACIN2, that are induced by photorespiratory H_2O_2 and are transcriptionally regulated by both biotic and abiotic stresses. These peptides share many characteristics with antimicrobial peptides (AMPs) but are structurally unrelated to known AMPs. ARACIN1 and ARACIN2 are lineage-specific to the Brassicaceae family with members in *Arabidopsis thaliana*, *A. lyrata* and *Brassica rapa*. In collaboration with the laboratory of Prof. Dr. Cammue, we demonstrated their role as antifungal peptides by performing both in soil disease assays on transgenic *ARACIN1* overexpression plants and *in vitro* antifungal bioassays. These results demonstrated that overexpression of *ARACIN1* significantly enhances resistance against the necrotrophic fungi *Botrytis cinerea* and *Alternaria brassicicola* and that chemically synthesized ARACIN peptides show *in vitro* antifungal activity against these pathogens. Moreover, we could demonstrate that these peptides are expressed as prepropeptides in which the predomain functions as a signal peptide and the acidic prodomain functions in neutralizing the cationic mature domain. In-depth functional characterization of both ARACINS will open perspectives to use them as an alternative strategy to improve disease resistance. In collaboration with the group of Dr. Van Lijsebettens, transgenic corn (*Zea mays*) lines overexpressing *ARACIN1* are currently generated by the in-house maize transformation platform. Once available, these transgenic lines will first be tested against the pathogenic corn smut fungus (*Ustilago maydis*) in collaboration with the laboratory of Prof. Dr. Cammue.

AMPs are a highly diverse class of peptides and are considered as an evolutionary conserved component of innate immune systems found throughout all kingdoms ranging from bacteria, invertebrates, plants and vertebrates. In **chapter 4**, we focus on the classification and the biological roles of AMPs in plants. Besides the antimicrobial activity, AMPs can have other role in plants such as protein inhibition, redox regulation, ion channel inhibition, metal physiology, development and roles in abiotic

stress tolerance. AMPs are also promising candidates for novel applications in plant disease control through genetic engineering of crops or expressing them in biocontrol agents to combat postharvest diseases.

SAMENVATTING

Hoewel vrije zuurstof radicalen (VZR) jarenlang beschouwd werden als schadelijke nevenproducten van het aeroob metabolisme, is hun signaalfunctie tijdens diverse biologische ontwikkelingsprocessen en omgevingsstimuli nu algemeen geaccepteerd. De laatste jaren is er grote vooruitgang geboekt in het identificeren van genen met een differentiële expressie tijdens oxidatieve stress. De uitdaging is momenteel om het complexe netwerk van de signaaltransductie mechanismen van de oxidatieve stress respons te ontrafelen. De functionele analyse van eiwitten die gecodeerd worden door genen die een vroege respons vertonen bij verhoogde VZR niveaus, kunnen nieuwe inzichten verschaffen in de vroege signalisatie mechanismen die aangezet worden door een plotse accumulatie van intracellulaire VZR. Een belangrijk regulatorisch mechanisme om een flexibele VZR signalisatie en dus een snelle transcriptionele respons te verzekeren, zijn eiwitten die tijdens stress een dynamische subcellulaire lokalisatie vertonen. Tot op heden zijn er verschillende mechanismen gekend van oxidatieve stress-geïnduceerde eiwit relokalisaties (**Hoofdstuk 1**), zoals redox-afhankelijke relokalisaties, fosforylatie-afhankelijke relokalisaties gemedieerd door VZR-geactiveerde kinasen, stress-geïnduceerde vrijstelling van membraanverankerde transcriptiefactoren, retentie en stress-geïnduceerde vrijlating, en translocaties gemedieerd door nucleaire retentiefactoren. Verscheidene abiotische stress-geïnduceerde eiwit relokalisaties zijn reeds beschreven, in bijzonder als gevolg van koude- of hittestress, zoutstress en hypoxia. Een belangrijk aspect van oxidatieve stress-geïnduceerde relokalisaties is het subcellulair compartiment waarin deze stress initieel waargenomen wordt. Verschillende types van abiotische stress lijken bepaalde subcellulaire compartimenten meer te treffen wat vervolgens resulteert in een verhoogde productie van VZR in deze specifieke subcellulaire compartimenten. Het mechanisme van een abiotische stress-geïnduceerde relokalisatie is bijgevolg frequent gecorreleerd met het type van abiotische stress en het subcellulair compartiment. De kennis van stress-geïnduceerde relokalisaties van signaaltransductie componenten zullen samen met de inzichten in de strikte ruimtelijk-temporele controle van VZR homeostase nieuwe inzichten verschaffen in de signalisatie mechanismen van de stress respons in planten (**Hoofdstuk 1**).

Het doel van dit project was de identificatie en karakterisatie van eiwitten die gedurende oxidatieve stress relokaliseren. Hiervoor werd eerst een uitgebreide inventaris van 783 waterstofperoxide (H_2O_2)-geïnduceerde eiwitten samengesteld door een vergelijkende studie te maken van drie beschikbare genoomwijde genexpressie studies die het Arabidopsis transcriptoom gedurende verhoogde niveaus van H_2O_2 profileerden. In deze studies werd het transcriptoom geanalyseerd van catalase-deficiënte planten die geëxposeerd werden aan hoge lichtintensiteit. Catalase is het voornaamste H_2O_2 antioxidant enzym dat fotorespiratorische H_2O_2 verwijdert. Verlaagde niveaus van catalase-activiteit gecombineerd met

hoog licht behandeling resulteert door de accumulatie van fotorespiratorisch H_2O_2 in overgevoelige planten. Voor verdere functionele analyse hebben we vervolgens uit deze inventaris van H_2O_2-geïnduceerde genen een goed overwogen selectie gemaakt van 85 genen op basis van volgende criteria: vroege inductie door fotorespiratorisch H_2O_2, de *in silico* voorspelde subcellulaire lokalisatie, de functionele categorie en de responsiviteit bij verscheidene abiotische stress condities. In **hoofdstuk 2** werd vervolgens een subcellulaire lokalisatie map opgebouwd van 49 H_2O_2-geïnduceerde eiwitten door gebruik te maken van een medium-throughput *in vivo* lokalisatie assay. Vooreerst werd door middel van een transiënt expressiesysteem in *Nicotiana benthamiana* (tabak) de functionaliteit en de subcellulaire lokalisatie bepaald van een substantieel aantal 'green fluorescent protein' (GFP) fusieconstructen. Terwijl acht fusies een exclusieve nucleaire lokalisatie vertoonden, lokaliseerden 23 eiwitten zowel in de nucleus als in het cytosol. Zoals verwacht waren bijna alle nucleaire eiwitten transcriptiefactoren of nucleïnezuurbindende eiwitten, terwijl zowel transcriptiefactoren als eiwitten met een ongekende functie behoorden tot de nucleocytosolische eiwitten. Een exclusieve cytosolische lokalisatie werd enkel waargenomen voor twee kleine hitteschok-eiwitten (sHSP's). Drie eiwitten lokaliseerden in de chloroplast waaronder onverwacht een NAC transcriptiefactor. In het endomembraan compartiment werden zes H_2O_2-geïnduceerde eiwitten gevonden waarvan twee een plasmamembraan lokalisatie vertoonden. Om de resultaten van het transiënt expressiesysteem in tabak te verifiëren werd voor 30 van de 49 eiwitten stabiel getransformeerde transgene Arabidopsis lijnen gegenereerd en bestudeerd. Alle in tabak bepaalde subcellulaire lokalisaties werden met uitzondering van twee eiwitten herbevestigd in Arabidopsis. Abiotische stress-geïnduceerde relokalisaties kunnen vervolgens in deze transgene lijnen nagegaan worden. Daarenboven kan de globale impact van overproductie van de GFP fusie eiwitten worden bepaald in deze lijnen: in het geval van 11 eiwitten werd de normale groei en ontwikkeling substantieel beïnvloed door de overexpressie van het fusieconstruct.

In **hoofdstuk 2** werden verscheidene interessante kandidaat eiwitten geïdentificeerd die mogelijks betrokken zijn in stress-geïnduceerde relokalisaties waaronder voornamelijk de nucleocytosolische gelokaliseerde transcriptiefactoren ANAC013, ANAC053 en ANAC087. Bovendien werden ANAC013 en ANAC053 reeds geïdentificeerd als mogelijke membraangeassocieerde NAC transcriptiefactoren (respectievelijk NTL1 en NTL4 genaamd) die gekend zijn om geactiveerd te worden door stimulus-geïnduceerde intramembranaire proteolyse. Terwijl de lokalisatie van NTL4 een vesiculair patroon vertoonde, bleek NTL1 vermoedelijk geassocieerd te zijn met het endoplasmatisch reticulum (ER). GFP-NTL1 overexpressielijnen vertoonden bovendien een vroegtijdig proteolytische verknipping van NTL1 wat vermoedelijk de nucleocytosolische lokalisatie verklaart. Eiwitten met een verschillende lokalisatie in tabak en Arabidopsis werden eveneens in meer detail bestudeerd. Bijvoorbeeld AtDjC68, een DnaJ hitteschok N-terminaal domeinbevattend eiwit, lokaliseerde in tabak in zogenaamde nucleaire

'speckles'. Daartegenover vertoonde AtDjC68 in Arabidopsis mesofiel protoplasten een nucleocytosolische lokalisatie dat door toevoeging van H_2O_2 in een exclusieve nucleaire lokalisatie resulteerde bij ongeveer 15% van de protoplasten. Een andere interessante kandidaat voor relokalisatie was ANAC102, een NAC transcriptiefactor die lokaliseert in de chloroplasten en tevens nucleaire genexpressie reguleert (**Hoofdstuk 3**). Tijdens fluctuerende omgevingsstimuli wordt het evenwicht van de componenten van de fotosynthetische elektronentransportketen zeer snel verstoord wat resulteert in een verhoogde productie van VZR in de chloroplasten. Daarom worden chloroplasten beschouwd als sensoren van ongunstige omgevingsomstandigheden die op hun beurt informatie terugsturen naar de nucleus om een geschikte respons te initiëren (retrograde signalisatie). Door behandeling met methylviologeen, een redox-actieve molecule dat VZR induceert in de chloroplasten, konden we de intercompartimentele relokalisatie van ANAC102 van de chloroplast naar de nucleus aantonen. Bovendien vertoonden transgene planten met verstoorde expressieniveaus van *ANAC102* een veranderde groeirespons tijdens oxidatieve stress. Dit toont mogelijks aan dat ANAC102 een belangrijke rol zou kunnen spelen in een chloroplast retrograde signalisatie pathway die betrokken is in de strikte regulatie van de stress respons. Doordat in het onderzoeksgebied van retrograde signalisatie de relokalisatie van een transcriptiefactor van een organel naar de nucleus in planten erg controversieel is, zijn additionele experimenten cruciaal om deze relokalisatie van ANAC102 te bevestigen.

Aangezien er een extensieve interactie is tussen biotische en abiotische signalisatienetwerken en VZR hierbij een belangrijke rol spelen, zijn vele VZR-responsieve genen gemeenschappelijk voor de biotische en abiotische stress respons waaronder vele pathogeen defensie-gerelateerde genen. In **hoofdstuk 5** werden twee Arabidopsis peptiden, genaamd ARACIN1 en ARACIN2, geïdentificeerd die geïnduceerd worden door fotorespiratorisch H_2O_2 alsook door zowel biotische als abiotische stress condities. Hoewel deze peptiden vele karakteristieken gemeenschappelijk hebben met antimicrobiële peptiden (AMP's), vertonen ze geen structurele gelijkenissen met gekende AMP's. ARACIN1 en ARACIN2 behoren specifiek tot de Brassicaceae familie en zijn aanwezig in *Arabidopsis thaliana*, *A. lyrata* en *Brassica rapa*. In samenwerking met het laboratorium van Prof. Dr. Cammue hebben we de antifungale rol van deze peptiden kunnen aantonen zowel *in planta* als *in vitro*. Transgene $ARACIN1^{OE}$ lijnen vertoonden een significant verhoogde resistentie tegen de necrotrofe schimmels *Alternaria brassicicola* en *Botrytis cinerea*. Daarenboven werd een directe antifungale rol van deze ARACIN peptiden tegen beide pathogenen met *in vitro* bioassays aangetoond. Tevens werd bewezen dat deze peptiden geëxpresseerd worden als prepropeptiden waarbij het prodomein als signaalpeptide fungeert en het zure prodomain functioneert in de neutralisatie van het basische matuur domein. Een gedetailleerde functionele karakterisatie van beide ARACINS zal perspectieven openen om deze peptiden te gebruiken om de resistentie van planten tegen ziekten te verbeteren. In samenwerking met de groep van Dr. van

Lijsebettens worden momenteel transgene maïs lijnen ontwikkeld die ARACIN1 tot overexpressie brengen. Zodra deze lijnen beschikbaar zijn, zullen deze in samenwerking met het laboratorium van Prof. Dr. Cammue getest worden tegen de builenbrand (*Ustilago maydis*), een brandschimmel dat maïs aantast.

AMP's zijn een zeer diverse groep van peptiden en worden beschouwd als een evolutionair geconserveerde component van de aangeboren immuniteit in alle levende systemen gaande van bacteriën, invertebraten, planten en vertebraten. In **hoofdstuk 4** bespreken we de classificatie en de biologische rol van AMP's in planten. Naast de antimicrobiële activiteit zijn andere functies van AMP's beschreven zoals eiwitinhibitie, redox-regulatie, inhibitie van ionen transporters, een rol in metaalfysiologie, en in ontwikkelingsprocessen en abiotische stress tolerantie. AMP's zijn veelbelovende kandidaten voor nieuwe toepassingen in de controle van plantenziekten. Deze peptiden kunnen tot expressie gebracht worden in gewassen of biocontrole micro-organismen als alternatieve strategie om plantenziekten te bestrijden.